



Biomarkers and the dawn of animal life

Ilya Bobrovskiy

A thesis for the degree of Doctor of Philosophy

The Australian National University

Research School of Earth Sciences

© Copyright by Ilya Bobrovskiy 2019

All Rights Reserved

DECLARATION

The work presented in this thesis is an accurate account of original research performed during the academic program towards the degree of Doctor of Philosophy at The Australian National University. Except where acknowledged, the material presented in this thesis is, to the best of my knowledge, my original work and has not been submitted in whole or part for a degree in any university. Detailed information can be found in the Statements of Contribution provided for each chapter.

Ilya Bobrovskiy

April 2019

ACKNOWLEDGEMENTS

I would like to thank my supervisor Jochen J. Brocks for his guidance and support during my PhD. He has always provided help and advice in all aspects of my work, from sample processing to discussions of results and writing papers. His enthusiasm for research has always been motivating. He granted me a complete freedom in my research, allowing it to follow my interest and inspiration, and I am immensely grateful to him for that.

Janet Hope has always been there for me when I needed help and advice in the laboratory analyses – without her taking great care of laboratory and equipment, my research would not have been possible.

Researchers from the Borissiak Paleontological Institute RAS, Andrey Ivantsov and Ekaterina Luzhnaya (Serezhnikova), along with Alexey Nagovitsyn from the Russian Geographical Society and Anna Krasnova from the Lomonosov Moscow State University, have helped me in the field and provided valuable advice on my studies. Anna Krasnova, while being a Masters student at the Lomonosov Moscow State University, has also participated in studies on taphonomy of the Ediacara biota. Simon W. Poulton provided his laboratory at the University of Leeds for inorganic geochemistry studies, as well as the most helpful advice on the interpretation of results I obtained there. Benjamin J. Nettersheim and Christian Hallmann contributed a lot to the interpretation of biomarkers from Ediacaran fossils by expanding our knowledge on the lipid composition of modern organisms. Pavel, Vasiliy, Stepan and Taisia Rychkovs, Elena Golubkova, Maria Luzhnaya, Valeria Burmistrova, Ulya Olshanskaya, and Anna Makushkina have helped collecting samples and kept a great company in the field trips to the White Sea area in Russia.

ABSTRACT

The macrofossils of the Ediacara biota (~571-539 Ma) mark the emergence of large, complex organisms in the palaeontological record. Preluding the radiation of modern animal phyla, they may hold important clues to the earliest evolution of animals. However, their phylogeny, ecology and even preservation remain largely unresolved. This thesis explores the questions on the biological origins of Ediacaran organisms based on a new technique, reconstructing their lipid composition using molecular fossils. As major outcomes of this research, my biomarker analysis showed that Ediacaran macrofossil *Beltanelliformis* represents large spherical colonies of cyanobacteria, while *Dickinsonia*, along with other dickinsoniid genera, belong among the oldest animals preserved in the rock record.

Utilising the same technique, the thesis explores the diets of three Ediacaran animals: the tube worm *Calyptrina*, currently interpreted as a relative of extant chemosymbiotic *Siboglinidae*, *Kimberella*, a mollusc-like bilaterian, and *Dickinsonia*. The results indicate that the former two animals shared a diet of green algae and bacteria, contradicting previous suggestions that Ediacaran tube worms were chemosymbiotic. In contrast, no traces of dietary molecules were found in *Dickinsonia*, which indicates that these organisms did not possess a digestive system, and instead fed on microbial mats using external digestion.

A new model for the Ediacara biota preservation is proposed here. The model demonstrates that the preservation was promoted by unusually prolonged conservation of organic matter, coupled with differences in rheological behaviour of the over- and underlying sediments. In contrast to accepted models, cementation of overlying sand was not critical for fossil preservation, which is supported by the absence of cement in unweathered White Sea specimens and observations of soft sediment deformation in both White Sea and South Australian specimens. The rheological model, confirmed by laboratory simulations, implies that Ediacaran fossils do not necessarily reflect the external shape of the organism, but the morphology of a soft external or internal organic 'skeleton'.

The thesis also presents new information on primary producers in the Ediacaran based on biomarker molecules that were extracted from sediments that host Ediacaran macrofossils. High

relative abundances of algal steranes over bacterial hopanes suggest that the Ediacara biota inhabited nutrient replete environments with an abundance of algal food sources comparable to Phanerozoic ecosystems. Thus, in contrast to earlier predictions, organisms of the Ediacara biota inhabited nutrient-rich environments akin to those that later fuelled the Cambrian explosion.

Finally, the thesis explores the preservation of palaeoecological biomarker parameters in relation to the interpretation of the ancient biomarker record, including the controls on biomarker distributions in deposits that host the Ediacara biota. Based on biomarker correlations and network analysis, the study shows that core biomarker parameters such as the sterane/hopane ratio and sterane pseudohomolog distributions can be altered by microbial degradation to the extent that ecological information is nearly obliterated, and provides new methodological approaches for biomarker analysis.

In summary, this thesis presents a compilation of advances in different aspects of Ediacara biota studies and biomarker analysis. It provides new baselines for further interpretations of complex morphologies of Ediacaran macrofossils, as well as new methodologies and constraints on the interpretations of the biomarker record.

TABLE OF CONTENTS

Declaration.....	3
Acknowledgements	4
Abstract.....	5
Table of Contents.....	7
Introduction	8
Thesis structure.....	10
Publications.....	11
Chapter 1. Molecular fossils from organically preserved Ediacara Biota reveal cyanobacterial origin for <i>Beltanelliformis</i>	17
Chapter 2. Ancient steroids establish the Ediacaran fossil <i>Dickinsonia</i> as one of the earliest animals	50
Chapter 3. Biomarker evidence for guts, gut contents, and feeding strategies of Ediacaran animals	82
Chapter 4. Simple sediment rheology explains the Ediacara biota preservation	116
Chapter 5. Food sources for the Ediacara biota	148
Chapter 6. Reconsidering the use of molecular fossils for palaeoecological reconstructions	170
Conclusions	201
References	203

INTRODUCTION

For the first four billion years of its history, planet Earth was inhabited by microscopic life. This changed quite suddenly around 539 million years ago, when modern animal phyla appeared in the fossil record – the event that is now called the Cambrian Explosion. However, large enigmatic organisms of the Ediacara biota predated the Cambrian Explosion by ~30 million years. Diverse Ediacaran fossils were first found in the 1940s in South Australia and later all around the globe. These first large organisms may hold the key to the understanding of the origin of animals and the evolution of complex multicellular life on Earth. Yet, exactly what these Ediacaran organisms were and how they lived remains largely obscure.

The path of deciphering and understanding the Ediacaran fossils has been paved with controversy for over 70 years since publication of the landmark paper by Sprigg (1947) describing the Ediacara biota from the Ediacara Hills in South Australia. Members of the Ediacara biota were initially described as animals (Glaessner, 1984; Sprigg, 1947), however, as collections grew, it became apparent that Ediacaran fossils and their body plans are difficult to compare with modern phyla (Narbonne, 2004; Xiao and Laflamme, 2009). A major complication for the study of Ediacaran organisms is their soft-bodied nature and unique mode of preservation, rarely found in younger fossils. Thus, the interpretation of various members of the Ediacara biota has crossed several Kingdoms and Domains, ranging from bacterial colonies (Steiner and Reitner, 2001), marine fungi (Peterson et al., 2003), lichens (Retallack, 2013) and giant protists (Seilacher, 2007; Zhuravlev, 1993) to stem-group animals and crown-group Eumetazoa (Narbonne, 2005; Xiao and Laflamme, 2009). The recent general consensus is that these fossils are polyphyletic (Erwin et al., 2011; Grazhdankin, 2011): at least some members of the Ediacara biota are almost unanimously interpreted as bilaterian animals (*Kimberella*) (Fedonkin and Waggoner, 1997; Ivantsov, 2013), while others can be confidently ascribed to giant protozoa (*Palaeopascichnus*) (Antcliffe et al., 2011; Kolesnikov et al., 2018). The affinity of most other Ediacaran macrofossils, however, remains controversial even at the Kingdom level (Xiao and Laflamme, 2009).

A principal step in unravelling the nature and palaeoecology of the Ediacara biota is to understand their preservation mechanism, and thus to separate features reflecting morphology and palaeoecology of the Ediacaran organisms from those that result from preservational processes (Brasier and Antcliffe, 2008; Droser et al., 2006). Current consensus on the

preservation of the soft-bodied Ediacaran macroorganisms is that the preservation happened via early diagenetic cementation of sediments enclosing the fossils, though different taphonomic models suggest different cementation agents (Callow and Brasier, 2009; Gehling, 1999; Gibson et al., 2018; Liu, 2016; Serezhnikova, 2011; Tarhan et al., 2016).

The late Cryogenian to early Ediacaran is the time when algae became abundant in the oceans after billions of years of bacterial dominance (Brocks et al., 2017). This should have changed availability and quality of primary producers as a food source, and has been hypothesised to trigger the proliferation of eumetazoan animals (Brocks, 2018; Brocks et al., 2017). Yet, it has also been suggested that the Ediacara biota, which remains our best window into the early animal evolution, preferentially inhabited bacteria-dominated environments, used bacteria as their main energy source, as either food or through symbiosis (Kaufman, 2018; Pehr et al., 2018; Sperling and Stockey, 2018). However, knowledge about the composition of primary producer communities in Ediacara biota localities is sparse or absent.

The White Sea Area in the northern part of the East European platform in Russia provides unique opportunities for studies on the Ediacara biota: while other Ediacara biota localities are strongly weathered and/or metamorphosed, White Sea area Ediacaran deposits are unweathered and extremely immature. Consequently, the White Sea area retains nearly intact information about early diagenesis of these sediments, in addition to extremely well preserved biomarkers (molecular fossils). This makes this site an ideal place to test existing hypothesis about phylogeny, ecology and taphonomy of Ediacaran fossils, and develop novel approaches that would bring us closer to the understanding of their nature. Thus, this thesis focuses on four questions: (1) what were the organisms of the Ediacara biota?; (2) how did the Ediacara biota get preserved?; (3) what was the composition of primary producers in the environments inhabited by the Ediacara biota, and what did these organism eat? Biomarker analyses used to answer these questions led to a whole new set of queries: (4) how reliable are biomarker analyses for palaeoecological reconstructions, and how can we disentangle ecological information from taphonomic artefacts?

THESIS STRUCTURE

Chapters 1-3 are devoted to questions about the nature of Ediacaran macrofossils, established based on the study of biomarkers from individual fossils. Chapter 1 discusses the origin of *Beltanelliformis*, Chapter 2 discusses biomarkers detected in *Dickinsonia*, *Andiva* and their morphological relatives, and Chapter 3 explores the lipid composition of *Kimberella*, *Calyptrina* and *Dickinsonia*, focusing on dietary lipids of these organisms.

Chapter 4 presents a new taphonomic model for the Ediacara biota, based on detailed sedimentological, mineralogical and palaeontological analyses of Ediacaran macrofossils from the White Sea Area in Russia and South Australia.

Chapter 5 describes biomarker analyses of sediments enclosing Ediacaran macrofossils, focusing on potential food sources available to Ediacaran macroorganisms.

Chapter 6 takes a more general look at the use of biomarkers; it focuses on alteration of palaeoecological biomarker parameters during microbial degradation, develops constraints on the application of biomarkers in palaeoecological studies, and offers a roadmap towards unravelling ecological and taphonomic influences on biomarker parameters.

PUBLICATIONS

Publications, which did not become a part of this thesis:

Nettersheim, B. J., Brocks, J. J., Schwelm, A., Hope, J. M., Not, F., Lomas, M., Schmidt, C., Schiebel, R., Nowack, E. C. M., De Deckker, P., Pawlowski, J., Bowser, S. S., **Bobrovskiy, I.**, Zonneveld, K., Kucera, M., Stuhr, M., Hallmann, C. (2019). Putative sponge biomarkers in unicellular *Rhizaria* question an early rise of animals. *Nature Ecology & Evolution*, 3, 577-581.

Goryl, M., Marynowski, L., Brocks, J. J., **Bobrovskiy, I.**, Derkowski, A. (2018). Exceptional preservation of hopanoid and steroid biomarkers in Ediacaran sedimentary rocks of the East European Craton. *Precambrian Research*, 316, 38-47.

Conference publications:

Bobrovskiy, I., Hope, J. M., Ivantsov, A., Nettersheim, B. J., Hallmann, C., Brocks, J. J., 2018. Ancient cholesteroloids confirm the Ediacaran fossils *Dickinsonia* and *Andiva* as animals. Australian Organic Geochemistry Conference 2018, Canberra (Australia), 3-7 December 2018.

Bobrovskiy, I., Hope, J. M., Ivantsov, A., Nettersheim, B. J., Hallmann, C., Brocks, J. J., 2018. Ancient steroids establish the Ediacaran fossil *Dickinsonia* as one of the earliest animals. In International Conference on Ediacaran and Cambrian Sciences 2018, Xi'an (China), 12-16 August 2018.

Bobrovskiy, I., Hope, J. M., Ivantsov, A., Nettersheim, B. J., Hallmann, C., Brocks, J. J., 2018. Determining phylogenetic position of Ediacaran macrofossils *Dickinsonia* and *Andiva* using biomarkers. In 5th International Palaeontological Congress, Paris (France), 9-13 July 2018, p. 283.

Bobrovskiy, I., Hope, J.M., Brocks, J.J., 2017. Biomarker analysis of the Ediacaran macrofossil *Beltanelliformis*. In Goldschmidt2017, Paris (France), 13-18 August 2017.

Bobrovskiy, I., Hope, J.M., Brocks, J.J., 2017. Biomarkers from the organically preserved Ediacaran macrofossil *Beltanelliformis*. In D. McIlroy (ed.), ISECT2017, St. Johns (Canada), 15-29 June 2017, p. 15

Bobrovskiy, I., Hope, J.M., Brocks, J.J., 2017. Biomarker analysis of the Ediacaran macrofossil *Beltanelliformis*. In 1st Geobiology Society Conference, 11-14 June 2017.

Krasnova, A., **Bobrovskiy, I.**, 2017. Sedimentology of the fossiliferous layers of the South-East White Sea Region as a key to understanding the mechanism of preservation of the Ediacara biota. In Materials of International forum of Young Scientists «Lomonosov 2017» [in Russian]

Krasnova, A., **Bobrovskiy, I.**, 2017. Preservation of Vendian macrofossils of the South-East White Sea Region. In Materials of the LXIII session of the Paleontological Society RAS (3-7 April 2017, Saint Petersburg, Russia), Saint Petersburg, 2017, 246 p. [in Russian]

Krasnova, A., **Bobrovskiy, I.**, 2017. Taphonomy of the Ediacara biota from the White Sea Region. In Alekseev, A.S. (Ed.), PALEOSTRAT-2017. Program and Abstracts, Moscow, PIN RAS [in Russian]

Bobrovskiy, I., Hope, J.M., Liyanage, T.M., Brocks, J.J., 2016. Biomarkers from the Ediacaran macrofossil *Beltanelliformis*. In 19th Australian Organic Geochemistry Conference, 4-7 December 2016, Fremantle (Australia), pp. 50-51.

Bobrovskiy, I., Krasnova, A., Brocks, J.J., 2016. New data on the habitat of the Ediacara biota: evidence from the Zimmie Gory locality, White Sea region. In Laurie, J.R., Kruse, P.D., Garcia-Bellido, D.C. and Holmes, J.D. (eds.), Palaeo Down Under 2, Adelaide, July 2016. Geological Society of Australia Abstracts 117, p. 19.

Bobrovskiy, I., Krasnova, A., Brocks, J.J., 2016. Depositional environments of the Ediacaran succession in the Zimmie Gory, White Sea region: new insights into the habitat of the Ediacara biota. In 32nd IAS International Meeting of Sedimentology, 23rd - 25th May 2016, Marrakech (Morocco).

Bobrovskiy, I., Krasnova, A., Nagovitsyn, A., Ivantsov, A., Serezhnikova, E., 2015. New sedimentological and paleontological data from the lowermost part of the Upper Vendian succession of the South-East White Sea Region. In Alekseev, A.S. (Ed.), PALEOSTRAT-2015. Program and Abstracts, Moscow, PIN RAS, pp. 18-19 [in Russian]

APPLICATION TO SUBMIT PHD/MPHIL THESIS BY COMPILATION

Part 1: Student Details

U ID: 5709643 _____ Surname: Bobrovskiy _____ First Name: Ilya _____

School and/or Department: Research School of Earth Sciences _____ PhD or MPhil: PhD _____

Intended Submission Date: 25 April 2019 _____

Part 2: Publication List (Please use additional sheets, if necessary)

1. Title and authors: Bobrovskiy, I., Hope, J.M., Krasnova, A., Ivantsov, A., Brocks, J.J. Molecular fossils from organically preserved Ediacara biota reveal cyanobacterial origin for *Beltanelliformis*.

Current status of paper (circle as appropriate): Planned/In Preparation/Submitted/Under Revision/Accepted/**Published** _____

Date paper accepted for publication or anticipated date of publication: 04 December 2017 _____

Name of journal: Nature Ecology & Evolution _____

Extent to which research is your own: High _____

Your contribution to writing the paper: I wrote the paper _____

If paper not yet accepted, has the paper been rejected by any journals: _____

Comments: Contributions: I.B. conceived the study and performed the analyses. I.B. and A.K. collected the samples. J.M.H. helped with the methodology. A.I. provided palaeontological advice. I.B. and J.J.B. interpreted the results and wrote the paper.

2. Title and authors: Bobrovskiy, I., Hope, J.M., Ivantsov, A., Nettersheim, B.J., Hallmann, C., Brocks, J.J. Ancient steroids establish the Ediacaran fossil *Dickinsonia* as one of the earliest animals.

Current status of paper (circle as appropriate): Planned/In Preparation/Submitted/Under Revision/Accepted/**Published** _____

Date paper accepted for publication or anticipated date of publication: 6 August 2018 _____

Name of journal: Science _____

Extent to which research is your own: High _____

Your contribution to writing the paper: I wrote the paper _____

If paper not yet accepted, has the paper been rejected by any journals: _____

Comments: Author contributions: I.B. designed the study and analyzed biomarkers from Ediacaran fossils; J.M.H. helped with biomarker analysis; I.B. and A.I. collected fossils; B.J.N., C.H., J.M.H., and J.J.B. analyzed modern Rhizaria; and I.B. and J.J.B. interpreted data and wrote the manuscript, with contributions from all authors.

3. Title and authors: Bobrovskiy, I., Krasnova, A., Ivantsov, A., Luzhnaya, E., Brocks, J. J. Simple sediment rheology explains the Ediacara biota preservation.
Current status of paper (circle as appropriate): Planned/In Preparation/Submitted/Under Revision/Accepted/**Published** _____
Date paper accepted for publication or anticipated date of publication: 21 January 2019
Name of journal: Nature Ecology & Evolution
Extent to which research is your own: High
Your contribution to writing the paper: I wrote the paper
If paper not yet accepted, has the paper been rejected by any journals: _____
Comments: Contributions: I.B. designed the study, studied the collections and developed the model. A.K. and I.B. performed the thin-section and scanning electron microscopy analyses. I.B., A.K., A.I. and E.L. participated in the field expeditions. A.I. and E.L. provided samples from the Borissiak Paleontological Institute (RAS) collections. I.B. and J.J.B. designed the taphonomic laboratory experiments. I.B. and J.J.B. wrote the paper with contributions from all authors.
4. Title and authors: Bobrovskiy, I., Nagovitsyn, A., Hope, J.M., Luzhnaya, E., Brocks, J. J. Biomarker evidence for guts, gut contents, and feeding strategies of Ediacaran animals.
Current status of paper (circle as appropriate): Planned/In Preparation/**Submitted**/Under Revision/Accepted/Published _____
Date paper accepted for publication or anticipated date of publication: unknown
Name of journal: Science
Extent to which research is your own: High
Your contribution to writing the paper: I wrote the paper
If paper not yet accepted, has the paper been rejected by any journals: No
Comments: Author contributions: I.B. designed the study, analyzed biomarkers from Ediacaran fossils and interpreted the data; J.M.H. helped with biomarker analysis; I.B., A.N. and E.L. collected fossils; A.N. contributed palaeontological description, I.B. and J.J.B. wrote the manuscript, with contributions from all authors.
5. Title and authors: Bobrovskiy, I., Hope, J. M., Golubkova, E., Brocks, J. J. Food sources for the Ediacara biota communities.
Current status of paper (circle as appropriate): Planned/In Preparation/**Submitted**/Under Revision/Accepted/Published _____
Date paper accepted for publication or anticipated date of publication: unknown
Name of journal: Nature Communications
Extent to which research is your own: High
Your contribution to writing the paper: I wrote the paper
If paper not yet accepted, has the paper been rejected by any journals: No
Comments: Author contributions: I.B. designed the study, analyzed biomarkers and interpreted the data; J.M.H. helped with biomarker analysis; I.B. and E.G. collected samples; I.B. and J.J.B. wrote the manuscript, with contributions from all authors.

6. Title and authors: Bobrovskiy, I., Poulton, S., Hope, J. M., Brocks, J. J. Reconsidering the use of steroids and hopanoids as a palaeoecological indicator

Current status of paper (circle as appropriate): Planned/**In Preparation**/Submitted/Under Revision/Accepted/Published _____

Date paper accepted for publication or anticipated date of publication: unknown _____

Name of journal: Science Advances _____

Extent to which research is your own: High _____

Your contribution to writing the paper: I wrote the paper _____

If paper not yet accepted, has the paper been rejected by any journals: No _____

Comments: Author contributions: I.B. conceived the study, collected samples, did experiments and analyses, and interpreted the data; S.P. provided facilities for inorganic geochemistry analyses and advise on interpretations, J.M.H. helped with biomarker analysis; I.B. wrote the manuscript, with contributions from all authors. _____

Part 3: Comments – Chair of Supervisory Panel

The author contribution comments are taken directly from the author contribution statements in the published/submitted papers and are true and agreed among all co-authors. Ilya is an exceptionally independent PhD candidate ~~who worked~~. I strongly support this thesis by compilation.

Part 4: Comments and Conditions– Delegated Authority

Part 5: Approval

<p>Ilya Bobrovskiy Student – Print Name</p>	<p> Signature</p>	<p>09/04/2019 Date</p>
<p>Jocelyn Brooks Chair of Supervisory Panel – Print Name</p>	<p> Signature</p>	<p>9/4/2019 Date</p>
<p>Head of Department – Print Name Stewart Falla Delegated Authority – Print Name</p>	<p>Signature  Signature</p>	<p>Date 9/4/2019 Date</p>

Students: Please return completed form to your HDR Coordinator, who will obtain the necessary approvals.

Please note that the Statement of Contribution in your thesis must be endorsed by the Delegated Authority before submission.

CHAPTER 1. MOLECULAR FOSSILS FROM ORGANICALLY PRESERVED EDIACARA BIOTA REVEAL CYANOBACTERIAL ORIGIN FOR *BELTANELIFORMIS*

Most Ediacara biota fossils have evaded taxonomic classification even at Kingdom level. Some Ediacaran fossils are too simple, thus evading classification, while others are complex but do not correspond to any bodyplan known from extant or Phanerozoic organisms. This chapter presents a technique of analysing biomarkers from individual fossils, opening a new dimension in the study of the enigmatic Ediacara fossils. Biomarkers represent skeletons of biomolecules produced by all living organisms, including the remains of lipids. As different groups of organisms possess different lipids, biomarkers can be used to unravel biological origins at a broad taxonomic level. The first results on applying this method to organically preserved Ediacaran fossils showed that *Beltanelliformis* represent large spherical colonies of cyanobacteria.



Australian
National
University

Statement of Contribution

This thesis is submitted as a Thesis by Compilation in accordance with https://policies.anu.edu.au/ppl/document/ANUP_003405

I declare that the research presented in this Thesis represents original work that I carried out during my candidature at the Australian National University, except for contributions to multi-author papers incorporated in the Thesis where my contributions are specified in this Statement of Contribution.

Title and authors: Bobrovskiy, I., Hope, J.M., Krasnova, A., Ivantsov, A., Brocks, J.J. Molecular fossils from organically preserved Ediacara biota reveal cyanobacterial origin for *Beltanelliformis*.

Current status of paper: Not Yet Submitted/Submitted/Under Revision/Accepted/**Published**

Contribution to paper: I.B. conceived the study and performed the analyses. I.B. and A.K. collected the samples. J.M.H. helped with the methodology. A.I. provided palaeontological advice. I.B. and J.J.B. interpreted the results and wrote the paper

Senior author or collaborating authors endorsement: _____

Ilya Bobrovskiy

Candidate – Print Name

Signature

18/04/2019

Date

Endorsed

Jochen Brocks

Chair of Supervisory Panel – Print Name

Signature

18/04/2019

Date

Stewart Fallon

Delegated Authority – Print Name

Signature

29/04/2019

Date

This is the author's version of the work. It is provided here according to the *Nature Research* guidelines for personal use, not for redistribution. The definitive version was published in *Nature Ecology & Evolution*, 2, 437–440 (2018), doi: <https://doi.org/10.1038/s41559-017-0438-6>

Molecular fossils from organically preserved Ediacara Biota reveal cyanobacterial origin for *Beltanelliformis*

Ilya Bobrovskiy¹, Janet M. Hope¹, Anna Krasnova^{2,3}, Andrey Ivantsov², Jochen J. Brocks^{1*}

¹Research School of Earth Sciences, Australian National University, Canberra, ACT 2601, Australia

²Borissiak Paleontological Institute, Russian Academy of Sciences, Moscow 117997, Russia

³Faculty of Geology, Lomonosov Moscow State University, Moscow 119991, Russia

*Correspondence to: jochen.brocks@anu.edu.au

The microfossils of the Ediacara biota (~575-541 million years, Ma) mark the emergence of large, complex organisms in the palaeontological record. Preluding the radiation of modern animal phyla, they may hold important clues to the earliest evolution of Metazoa. However, their phylogenetic relationship, even at the domain level, remains controversial. We present the discovery of indigenous molecular fossils (biomarkers) from an organically preserved Ediacaran macrofossil *Beltanelliformis*. The biomarker composition demonstrates that *Beltanelliformis* represent large spherical colonies of cyanobacteria. The conservation of molecular remains in organically preserved Ediacaran organisms opens a new path for unravelling the natures of the Ediacara biota.

Beltanelliformis is one of the most revisited Ediacaran macrofossils. It is comprising *Nemiana* and *Beltanelloides* taphonomic forms: *Nemiana* is commonly preserved at the base of sandstone lenses as circular, convex tubercles with or without concentric folds, while *Beltanelloides* are found within clay or carbonate as low-relief circular imprints with concentric folds near the edges¹. *Nemiana* were initially described as abiological structures or compared with jellyfish bodies². Later, *Nemiana* were interpreted as the internal sand skeletons of corals³ or benthic demosponges that agglutinated sand to support their bodies

4. *Beltanelloides* were described as benthic⁵ or planktonic⁴ eukaryotic algae or as fungal colonies with concentric folds caused by non-uniform growth⁶. Some studies regarded both taphonomic forms of *Beltanelliformis* as cnidarian resting traces based on their similarity to Devonian anemone burrows *Alpertia santacrucensis*, interpreting the concentric folds as musculature traces⁷. By contrast, some other studies found that *Beltanelliformis* do not show any characters typical of cnidarians and lack the typical structures of algae and should, thus, be interpreted as colonial prokaryotes⁸⁻¹⁰. Others found that interpretation of *Beltanelliformis* as fluid-filled vesicles with a firm and flexible organic wall is inconsistent with both cnidarian and prokaryotic interpretations, and that these characters point to benthic green algal gametophytes instead^{11,12}.

Specimens of *Beltanelliformis* studied here were collected in ~558 Ma old Ediacaran deposits at the Lyamtsa locality, White Sea, Russia that formed in shallow-marine environments within the photic zone¹³. *Beltanelliformis* are preserved within clay as low-relief, slightly convex, circular imprints up to 1.5 cm in diameter with concentric folds at the edges and covered by a thin, translucent film of organic matter (Fig. 1b, Supplementary Fig. 1). The organic film is restricted to *Beltanelliformis* surfaces and is not found beyond and between the fossils. Thus, it does not represent a film that covered the entire sediment surface. Thicker, brown-coloured organic matter most probably comprised of macroalgae (see Supplementary Information) is preserved on the same surface next to *Beltanelliformis* (Fig. 1a). We were able to detach the organic matter of *Beltanelliformis* and macroalgae from the rock surface and extract hydrocarbon biomarkers under strict exclusion of contamination. Biomarkers were analysed by gas chromatography-mass spectrometry (see Methods), and were found to represent the best preserved molecular remains of Precambrian age to date).

The organic films of *Beltanelliformis* and macroalgae, preserved adjacent to each other on the same clay surface, must have experienced similar diagenetic and burial conditions and comparable degrees of microbial reworking. Differences in the molecular content of these films can, thus, largely be ascribed to the source organisms. In the macroalgal organic matter, steranes (S), the molecular fossils of eukaryotic membrane sterols, dramatically dominate over bacterial hopanes (H) (H/S = 0.061; Table 1; Fig. 1c), confirming the eukaryotic origin of the film. Steranes exhibit a very high C₂₉ predominance (C₂₇:C₂₈:C₂₉ = 8%:5%:87%), which is typical of Chlorophyta (green algae) and diagnostic for bitumens of Ediacaran age¹⁴, confirming the indigenous nature of the hydrocarbons. The distribution of *n*-alkanes in the macroalgal film is unique for the Precambrian (Fig. 1e). The short-chain *n*-alkanes (C₁₈₋₂₂) exhibit a slight odd-over-even carbon number predominance (Odd-to-even predominance index OEP₁₈₋₂₂ = 1.30; Table 1) but their abundances are insignificant relative to long-chain homologues (C₂₃₋₃₃). The long-chain alkanes do not possess any carbon number preference (OEP₂₅₋₂₉ = 0.98) and are probably the diagenetic products of functionalized biomolecules such as long-chain fatty acids or alcohols¹⁵. Suitable precursors are well known from

microalgae^{16,17}, although their presence in macroalgae is less well constrained¹⁸. Long-chain fatty acids might have accumulated in the algal film due to preferential bacterial degradation of the short chain homologues¹⁶, or might have been protected from degradation as part of a cuticle layer or biopolymer such as algaenan, which is widespread amongst chlorophytes¹⁹.

The biomarkers extracted from organically preserved *Beltanelliformis* are remarkably distinct from the macroalgae despite the close physical association (Fig. 1, Table 1). The hopane to sterane ratio is 60 times higher than in the algal film (H/S = 3.6), indicating that the source is largely bacterial. To our knowledge, such a robust contrast in bacterial and eukaryotic marker abundances in adjacent samples has never been observed before. Steranes are present in the *Beltanelliformis* extract but show the same unusual C₂₉ predominance as the adjacent macroalgal film, pointing to minor physical overlap of *Beltanelliformis* and algal organic matter (e.g. Fig. 1a).

The main source of hopanoids, the biogenic precursors of hopanes, are aerobic alphaproteobacteria and oxygenic cyanobacteria²⁰. Some anaerobes and microaerophiles also have the capacity to biosynthesize hopanols, including sulphate-reducing bacteria and methyloproteobacteria²¹, and these may have contributed hopanes during microbial degradation of *Beltanelliformis*. However, the low content of hopanes relative to steranes in the macroalgal film indicates that this heterotrophic contribution must have been minor. Evidence of oxic bottom waters in the Ediacaran sea in the Lyamtsa locality comes from abundant benthic macroalgae, trace fossils and burrows²², which makes aerobic colonies of heterotrophic or phototrophic bacteria the most likely candidates for *Beltanelliformis*.

Further evidence about the nature of *Beltanelliformis* comes from the distribution of *n*-alkanes. In contrast to the algal film, *Beltanelliformis* exhibits *n*-alkanes with OEP at all chain lengths (OEP₁₈₋₂₂ = 1.40, OEP₂₅₋₂₉ = 1.21, Table 1), and short and long-chained homologues are nearly equally abundant (Fig. 1f). The preservation of such a distinct OEP strongly suggests that the precursors included biological long-chain *n*-alkanes or *n*-alkenes, i.e. biosynthetic hydrocarbons without additional functional groups¹⁵. Among bacteria, only cyanobacteria are known to produce such long-chain hydrocarbons with OEP^{16,23-25}, which makes a strong case that *Beltanelliformis* represent colonial structures of cyanobacteria. This conclusion is also supported by the distribution of hopane homologs in the *Beltanelliformis* extract (Supplementary Information).

Based on morphology, *Beltanelliformis* can be compared with modern spherical cyanobacterial freshwater colonies of the genus *Nostoc* that possess degradation resistant outer envelopes (Supplementary Fig. 4)⁹. *Beltanelliformis* may be an early marine representative of such Nostoclean colonies, but it may also belong to an extinct taxon.

Amongst modern organisms, long-chain fatty acids and *n*-alkanes with OEP are abundantly produced by higher plants, where they occur as part of a protective desiccation-resistant cuticle membrane. In some microalgae, long-chain fatty acids were also found to be involved in the formation of the outer cell walls along with aliphatic biopolymers, displaying great similarities with the cuticle layer of higher plants, probably having the same biosynthetic pathway and the same function^{17,26}. Interestingly, among modern cyanobacteria, only non-marine forms appear to produce long-chain hydrocarbons²³⁻²⁵. It opens the possibility that macroalgae and *Beltanelliformis* cyanobacterial colonies from the Ediacaran deposits in the White Sea were partially desiccation resistant and able to survive intermittent subaerial exposure.

Due to the simple morphology of most members of the Ediacara biota and lack of modern analogs for others, there are many controversies about the nature of the Ediacara biota, and the range of interpretations is extremely broad, varying from animals and giant protists to lichen colonies growing on land²⁷. Biomarkers add a new dimension to the study of the Ediacara biota, showing here that *Beltanelliformis* were benthic colonial cyanobacteria.

Acknowledgments

The study was funded by Australian Research Council grants DP160100607 and DP170100556. The authors are grateful to E. Luzhnaya, A. Nagovitsyn, M. Luzhnaya, P. Rychkov and V. Rychkov for their help in the field, L. Zaytseva and E. Luzhnaya for the SEM imaging of organic matter and J.K. Volkman, S. Xiao, N.J. Butterfield and R.E. Summons for their helpful comments on an earlier version of this manuscript.

Author contributions

I.B. conceived the study and performed analyses, I.B. and A.K. collected samples, J.M.H. helped with the methodology, A.I. provided palaeontological advice, I.B. and J.J.B. interpreted results and wrote the paper.

Data availability

Biomarker raw data is available from the corresponding author on reasonable request.

References

- 1 Narbonne, G. M. & Hofmann, H. J. *Palaeontology* **30**, 647-676, (1987).
- 2 Zaika Novatsky, V. & Palij, V. *Paleontol. Sb.* **11**, 59–65, (1974).
- 3 Seilacher, A. *J. Geol. Soc.* **149**, 607-613, (1992).
- 4 Leonov, M. V. *Geol. Soc. Spec. Publ.* **286**, 259-267, (2007).
- 5 Gnilovskaya, M., Ishchenko, Kolesnikov, C., Korenchuk, L. & Udaltsov, A. (Nauka, 1988).
- 6 Aseeva, E. A. in *Biostratigraphy and Paleogeographic Reconstructions of the Precambrian of Ukraine* (eds V.A. Ryabenko, E.A. Aseeva, & V.V. Furtes) 81-92 (Naukova Dumka, 1988).
- 7 Runnegar, B. & Fedonkin, M. in *The Proterozoic biosphere: a multidisciplinary study* (eds J.W. Schopf & C. Klein) 369-388 (Cambridge University Press, 1992).
- 8 Steiner, M. & Reitner, J. *Geology* **29**, 1119-1122, (2001).
- 9 Steiner, M. *Acta Univ. Carol., Geol.* **40**, 645-665, (1996).
- 10 Ivantsov, A. Y., Gritsenko, V. P., Konstantinenko, L. I. & Zakrevskaya, M. A. *Paleontol. J.* **48**, 1415-1440, (2014).
- 11 Xiao, S. & Dong, L. in *Neoproterozoic Geobiology and Paleobiology* (eds Shuhai Xiao & Alan J. Kaufman) 57-90 (Springer Netherlands, 2006).
- 12 Xiao, S., Yuan, X., Steiner, M. & Knoll, A. H. *J. Paleontol.* **76**, 347-376, (2002).
- 13 Grazhdankin, D. *Stratigr. Geol. Correl.* **11**, 313-331, (2003).
- 14 Kodner, R. B., Pearson, A., Summons, R. E. & Knoll, A. H. *Geobiology* **6**, 411-420, (2008).
- 15 Alexander, R., Berwick, L. & Pierce, K. *Org. Geochem.* **42**, 540-547, (2011).
- 16 Volkman, J. K. *et al. Org. Geochem.* **29**, 1163-1179, (1998).
- 17 Allard, B. & Templier, J. *Phytochemistry* **57**, 459-467, (2001).
- 18 Shaw, D. G. & Wiggs, J. N. *Phytochemistry* **18**, 2025-2027, (1979).
- 19 Versteegh, G. J. M. & Blokker, P. *Phycol. Res.* **52**, 325-339, (2004).
- 20 Ricci, J. N., Morton, R., Kulkarni, G., Summers, M. L. & Newman, D. K. *Geobiology* **15**, 173-183, (2016).
- 21 Blumenberg, M. *et al. Environmental Microbiology* **8**, 1220-1227, (2006).
- 22 Nagovitsyn, A. in *PALEOSTRAT-2015* (ed A. S. Alekseev) 57-58 (PIN RAS, Moscow, 2015).
- 23 Jones, J. G. *Microbiology* **59**, 145-152, (1969).
- 24 Gelpi, E., Oró, J., Schneider, H. J. & Bennett, E. O. *Science* **161**, 700-701, (1968).
- 25 Matsumoto, G. I., Yamada, S., Ohtani, S., Broady, P. A. & Nagashima, H. in *Proceedings of the NIPR Symposium on Polar Biology.* 275-282.
- 26 Schouten, S. *et al. Geochim. Cosmochim. Acta* **62**, 1397-1406, (1998).
- 27 Xiao, S. & Laflamme, M. *Trends Ecol. Evol.* **24**, 31-40, (2009).

Methods

Samples were collected in a pre-baked aluminium foil (300°C, 9h) and packed in calico bags under strict avoidance of contamination. Organic matter was removed from the clay surface using a solvent-cleaned scalpel, and tweezers. For biomarker analysis, organic matter of *Beltanelliformis* was collected from around 300 specimens from one surface and combined to get the best possible signal-to-noise ratio. It was also studied for microstructure on scanning electron microscope (SEM) Zeiss EVO50 with microanalyser Oxford INCA (Energy 350). Hydrocarbons were extracted from the organic matter via ultrasonication (methanol 1 h, dichloromethane (DCM) for 15 min (x 2), DCM : *n*-hexane 1 : 1 for 15 min). All solvents were 99.9% grade (UltimAR®; Mallinckrodt Chemicals, St. Louis, MO, USA).

Extracts from organic films were fractionated into saturated+aromatic and polar fractions. An internal standard, 18-MEAME (18-methyleicosanoic acid methylester; Chiron Laboratories AS), was added to the saturated and aromatic fractions, while D4 (d4-C₂₉-ααα-ethylcholestane; Chiron Laboratories AS) was added to the saturated hydrocarbon fractions only. The samples were analysed and quantified by GC–MS. A comprehensive, accumulatory system blank was performed covering all analytical steps. For more specific information about the methods see Supplementary Methods.

Figures and Tables

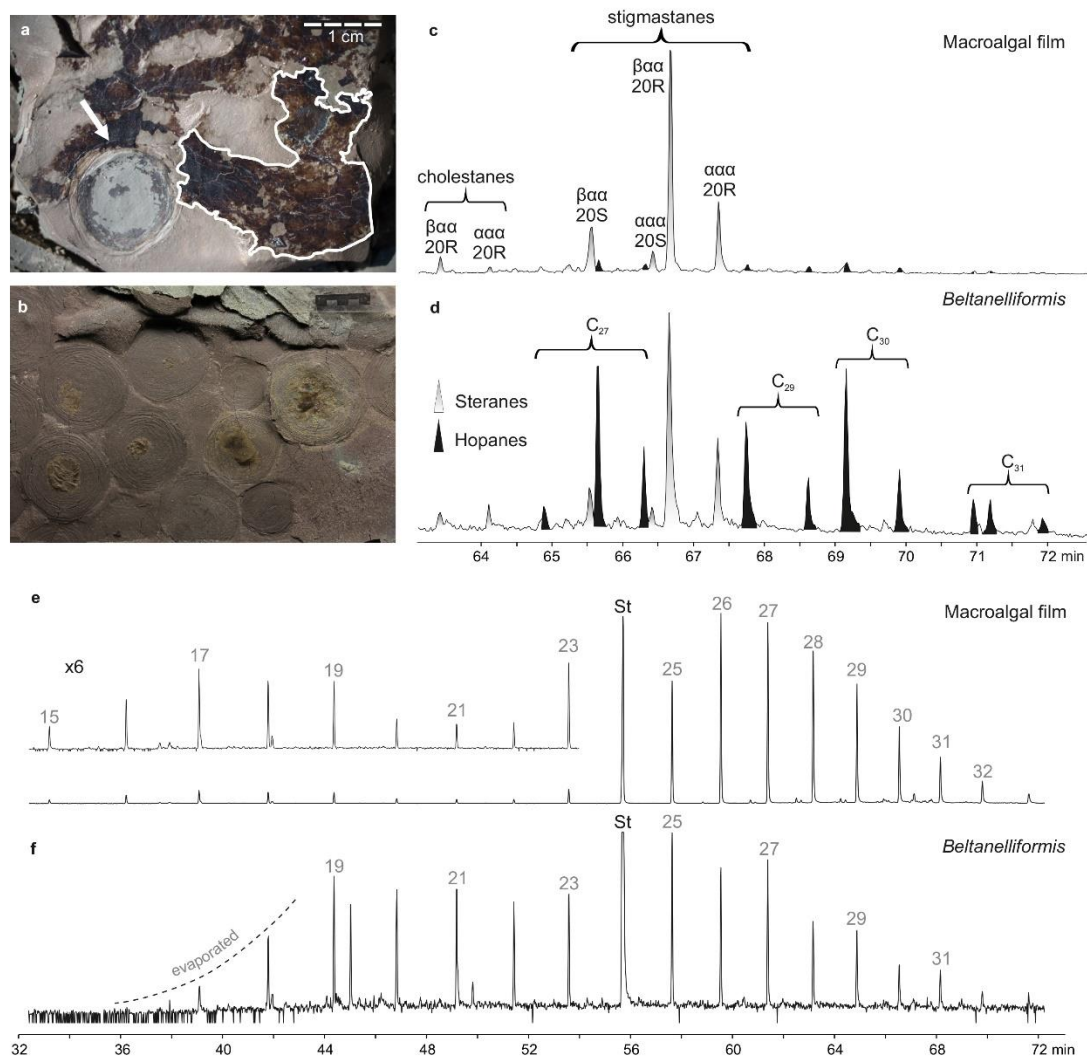


Figure 1 | Distribution of steranes, hopanes and *n*-alkanes in the extracts of a macroalgal film and *Beltanelliformis*. **a**, macroalgal film preserved next to *Beltanelliformis*; the white arrow points at an overlap between *Beltanelliformis* and the macroalgal film, the white outline highlights the extracted algal surface; **b**, organically-preserved *Beltanelliformis*, each scale unit is 1 mm (photo by S. Bagirov); **c**, metastable reaction monitoring (MRM) chromatogram showing the sum of C₂₇₋₃₁ hopane and C₂₇₋₂₉ sterane traces of the macroalgal film extract; **d**, MRM chromatogram showing the sum of C₂₇₋₃₁ hopane and C₂₇₋₂₉ sterane traces of the *Beltanelliformis* extract. C_x denotes the carbon number of hopanes (for isomer identification see Fig. S5); ααα = 5α(H),14α(H),17α(H) and βαα = 5β(H),14α(H),17α(H) sterane isomers; **e**, distribution of *n*-alkanes in the macroalgal film extract on the *m/z* 85 trace; **f**, distribution of *n*-alkanes in the *Beltanelliformis* extracts on the *m/z* 85 trace. Numbers on the Figure indicate the carbon number of *n*-alkanes; x6 in the inset of **e** signifies 6 times magnification of the chromatogram; St – 18-MEAME internal standard.

Table 1 | Biomarker ratios for organic film and clay extracts

	<i>Beltanelliformis</i>	Macroalgal film	<i>Vendotaenides</i>	Clay	Cv
H/S*	3.6	0.061	0.69	4.7	0.86%
C ₂₇ :C ₂₈ :C ₂₉ steranes	7% : 5% : 88%	8% : 4% : 88%	13% : 3% : 84%	11% : 8% : 81%	3.02% : 3.93% : 0.43%
β α /α α C ₂₉ steranes	3.0	3.7	2.0	0.47	6.97%
β α /(β α + α β) C ₃₀ hopanes	0.26	0.26	0.25	0.25	1.39%
Ts/(Ts+Tm) C ₂₇ hopanes	0.082	0.071	0.079	0.080	2.45%
C ₃₀ /C ₃₁ hopanes [†]	2.56	3.06	2.66	1.51	3.89%
C ₂₉ /C ₃₀ hopanes [†]	0.70	0.87	0.86	0.73	3.84%
2-MHI [‡]	0.85%	1.28%	n.d. [¶]	0.68%	5.4%
OEP ₁₈₋₂₂ [§]	1.40	1.30	1.27	1.10	1.88%
OEP ₂₅₋₂₉ [§]	1.21	0.98	0.99	1.35	0.84%

*H/S = $\Sigma(C_{27-35} \text{ hopanes}) / \Sigma(C_{27-29} \text{ steranes})$, hopanes: C₂₇ = $\Sigma(\text{Ts, Tm, } \beta)$, C₂₉ = $\Sigma(\alpha\beta, \text{Ts, } \beta\alpha)$, C₃₀ = $\Sigma(\alpha\beta, \beta\alpha)$, C₃₁₋₃₅ = $\Sigma(\alpha\beta-22(\text{S+R}), \beta\alpha)$, $\alpha\beta = 17\alpha(\text{H})21\beta(\text{H})$, $\beta\alpha = 17\beta(\text{H})21\alpha(\text{H})$; steranes: C₂₇ = $\Sigma(\beta\alpha-20(\text{S+R})\text{-diacholestane, } \alpha\alpha\alpha\text{- and } \beta\alpha\alpha\text{-}20(\text{S+R})\text{-cholestane})$, C₂₈ = $\Sigma(\beta\alpha-20(\text{S+R})\text{-diaergostane, } \alpha\alpha\alpha\text{- and } \beta\alpha\alpha\text{-}20(\text{S+R})\text{-ergostane})$, C₂₉ = $\Sigma(\beta\alpha-20(\text{S+R})\text{-diastigmastane, } \alpha\alpha\alpha\text{- and } \beta\alpha\alpha\text{-}20(\text{S+R})\text{-stigmastane})$, $\alpha\alpha\alpha = 5\alpha(\text{H}), 14\alpha(\text{H}), 17\alpha(\text{H})$, $\beta\alpha\alpha = 5\beta(\text{H}), 14\alpha(\text{H}), 17\alpha(\text{H})$; [†]C₂₉ = $\Sigma(\alpha\beta, \text{Ts, } \beta\alpha)$, C₃₀ hopane = $\Sigma(\alpha\beta, \beta\alpha)$, C₃₁ = $\Sigma(\alpha\beta-22(\text{S+R}), \beta\alpha)$; [‡]2-methylhopane index, 2-MHI (%) = $100 * (\Sigma C_{31} \text{ } 2\alpha+2\beta\text{-methylhopane}) / (\Sigma C_{31} \text{ } 2\alpha+2\beta\text{-methylhopane} + \Sigma(\alpha\beta-22(\text{S+R}), \beta\alpha) \text{ C}_{30} \text{ hopane})$; [§]Odd-to-even predominance index for *n*-alkanes in the carbon number range 18 to 22 and 25 to 29 respectively: OEP₁₈₋₂₂ = $(4C_{19} + 4C_{21}) / (C_{18} + 6C_{20} + C_{22})$; OEP₂₅₋₂₉ = $(C_{25} + 6C_{27} + C_{29}) / (4C_{26} + 4C_{28})$; ^{||}coefficient of variation (%); [¶]n.d. – components not detected.

Molecular fossils from organically preserved Ediacara Biota reveal cyanobacterial origin for *Beltanelliformis*

Supplementary Information

Ilya Bobrovskiy¹, Janet M. Hope¹, Anna Krasnova^{2,3}, Andrey Ivantsov², Jochen J. Brocks^{1*}

¹Research School of Earth Sciences, Australian National University, Canberra, ACT 2601, Australia

²Borissiak Paleontological Institute, Russian Academy of Sciences, Moscow 117997, Russia

³Faculty of Geology, Lomonosov Moscow State University, Moscow 119991, Russia

*Correspondence to: jochen.brocks@anu.edu.au

METHODS

Sample collection

Biomarker analyses were conducted on samples that include organically preserved *Beltanelliformis* (Fig. 1b; Supplementary Fig. 1), a macroalgal film adjacent on the same clay surface (Fig. 1a), clay directly underlying *Beltanelliformis*, and a separate carbonaceous fossil of the macroalga ex gr. *Vendotaenides*, collected 1 m higher in the section (Supplementary Fig. 2b). The fossils were collected during fieldwork in the Lyamtsa locality of the Ediacara Biota in the White Sea Region (Russia) in 2015 and 2016 specifically for biomarker analysis. They come from the lower part of the Lyamtsa Beds (Ust-Pinega Formation, Redkino Regional Stage), exposed to the south of Lyamtsa Village. Samples were collected avoiding weathered zones and cracks and were immediately wrapped in pre-baked aluminium foil (300°C, 9h) and packed in calico bags under strict avoidance of contamination. *Beltanelliformis* fossils were transported in closed rock and opened along the fossiliferous bedding plane under clean laboratory conditions. Organic matter of *Beltanelliformis* was studied for microstructure on scanning electron microscope (SEM) Zeiss EVO50 with microanalyser Oxford INCA (Energy 350).

Sample preparation and extraction

Samples were prepared in an ultra-clean facility dedicated to trace biomarker analysis at the Australian National University. Organic matter of *Beltanelliformis* was removed from the clay surface using a solvent-cleaned scalpel, and macroalgal film with a surface area of ~8 cm² was peeled from the rock surface using solvent-cleaned tweezers. Organically preserved *Beltanelliformis* that are large enough for sufficient biomarker extraction are known only from one surface in the White Sea Region, and for biomarker analysis, organic matter of *Beltanelliformis* was collected from around 300 specimens from this surface and combined to get the best possible signal-to-noise ratio. Hydrocarbons were extracted from the organic matter via ultrasonication (methanol 1 h, dichloromethane (DCM) for 15 min (x 2), DCM : *n*-hexane 1 : 1 for 15 min). All solvents were 99.9% grade (UltimAR®; Mallinckrodt Chemicals, St. Louis, MO, USA). Glassware was cleaned by combustion at 300°C for 9 h.

To identify and eliminate any surficial trace contaminants, the clay was analysed using the so-called Exterior-Interior protocol described in detail elsewhere¹⁻³. Briefly, exterior ('E') 3-4 mm of the clay sample were removed using a micro drill (Dremel® 400 Series Digital, Mexico) with a solvent cleaned saw nozzle. Analysis of the last saw-blade solvent rinse confirmed that it was free of detectable contaminants. The exterior (21.7 g) and the interior (23.1 g) portions of the clay sample were ground to powder (>240 mesh) using a steel puck mill (Rocklabs Ltd., Onehunga, New Zealand). The mill was cleaned using dichloromethane and methanol, and by grinding combusted (600°C, 9 h) quartz sand.

Bitumen was extracted from rock powder using an Accelerated Solvent Extractor (ASE 200, Dionex, USA) with DCM : methanol (9:1), reduced to 100 µl under a stream of nitrogen gas, and then fractionated into saturated, aromatic and polar fractions using micro-column chromatography over annealed (300°C; 12 h) and dry packed silica gel (Silica Gel 60; 230– 600 mesh; EM Science). Saturated hydrocarbons were eluted with 1 dead volume (DV) of *n*-hexane, aromatic hydrocarbons with 4.5 DV of *n*-hexane : DCM (1 : 1) and the polar fraction with 3 ml DCM : methanol (1 : 1). Extracts from organic films were only fractionated into saturated+aromatic and polar fractions to reduce the probability of contamination. An internal standard, 18-MEAME (18-methyleicosanoic acid methylester; Chiron Laboratories AS), was added to the saturated and aromatic fractions, while D4 (d4-C₂₉-αα-

ethylcholestane; Chiron Laboratories AS) was added to the saturated and saturated+aromatic hydrocarbon fractions only. The samples were analysed and quantified by GC–MS.

Gas chromatography–mass spectrometry (GC-MS)

GC-MS analyses were carried out on an Agilent 6890 gas chromatograph coupled to a Micromass Autospec Premier double sector mass spectrometer (Waters Corporation, Milford, MA, USA). The GC was equipped with a 60 m DB-5 MS capillary column (0.25 mm i.d., 0.25 μm film thickness; Agilent JW Scientific, Agilent Technologies, Santa Clara, CA, USA), and helium was used as the carrier gas at a constant flow of 1 mL min⁻¹. Samples were injected in splitless mode into a Gerstel PTV injector at 60°C (held for 0.1 min) and heated at 260°C min⁻¹ to 300°C. For full-scan, selected ion recording (SIR) and metastable reaction monitoring (MRM) analyses, the GC oven was programmed from 60°C (held for 4 min) to 315°C at 4°C min⁻¹, with total run time of 100 min. All samples were injected in *n*-hexane to avoid deterioration of chromatographic signals by FeCl₂ build-up in the MS ion source through use of halogenated solvents⁴. *n*-Alkanes were quantified in full-scan or SIR mode in *m/z* 85 traces relative to the 18-MEAME internal standard (*m/z* 340). Steranes were quantified in MRM mode in M⁺ → 217 and hopanes in M⁺ → 191 transitions relative to the D4 internal standard (404 → 221). Peak areas are uncorrected for differences in GC-MS response. For calculation of the coefficient of variation, clay extract has been injected 5 times, and all the peaks of interest were independently integrated for each run.

Laboratory system blanks

A comprehensive, accumulatory system blank was performed covering all analytical steps from rock surface removal, extraction, fractionation to instrumental analysis. For this purpose, the exterior surfaces of a combusted (600°C, 9 h) clay brick were separated, ground to powder and extracted using the methodologies and identical tools described above.

SUPPLEMENTARY INFORMATION

Hopanes

All extracts exhibit typical immature hopane distributions with low $T_s/(T_s+T_m)$ and $S/(S+R)$ ratios, high $\beta\alpha/\alpha\beta$ ratios and high relative abundances of C_{27} , C_{29} and C_{30} homologs relative to the extended C_{31} to C_{35} homohopanes (Supplementary Fig. 5, Table 1). However, there are also significant differences in homolog distributions between extracts. Most notably, the biofilm extracts demonstrate elevated C_{30}/C_{31} hopane ratios (*Beltanelliformis* $C_{30}/C_{31} = 2.57$; *Vendotaenides* $C_{30}/C_{31} = 2.66$; macroalgal film $C_{30}/C_{31} = 3.06$) in comparison to the clay extract ($C_{30}/C_{31} = 1.51$). As these samples had identical thermal histories, the differences can be attributed to variations in biological sources and/or diagenesis.

Compared to other groups of bacteria, cyanobacteria tend to produce larger proportions of biological C_{30} hopanoids such as diploptene and diplopterol (on average 2 fold)⁵, and this may have contributed to the elevated C_{30} hopane abundances in *Beltanelliformis*. The distinct C_{30}/C_{31} hopane ratio in *Beltanelliformis* ($C_{30}/C_{31} = 2.57$) and clay ($C_{30}/C_{31} = 1.51$) may also point to different modes of functionalization in the precursor biohopanoid side chain. During laboratory periodic acid/sodium borohydride treatment, which is believed to reproduce chemical diagenesis of sedimentary hopanoids, tetrafunctionalised hopanoids produce bishomohopanol (C_{32}), pentafunctionalised hopanoids produce homohopanol (C_{31}) and hexafunctionalised hopanoids – hopanol (C_{30})^{6,7}. After oxidation and subsequent decarboxylation, these compounds eventually produce C_{31} , C_{30} and C_{29} hopanes respectively, which has been used for distinguishing source rock depositional environments of petroleum⁸. Tetrafunctionalised hopanoids are widespread in nature and are produced by a large variety of bacteria, but the only known major sources of pentafunctionalised hopanoids are cyanobacteria of the genus *Nostoc* and microaerophilic Type II methanotrophic bacteria^{9,10}. Thus, in the light of oxic bottom water conditions in the Lyamtsa locality¹¹, the distinctly elevated C_{30}/C_{31} hopane ratio in *Beltanelliformis* may point to increased abundances of pentafunctionalised hopanoids and/or biogenic C_{30} hopanoids, consistent with a cyanobacterial origin of *Beltanelliformis*. It is quite plausible that cyanobacteria were also a source for the low proportions of hopanes detected in *Vendotaenides* and the macroalgal film extracts, either as epiphytes on the surface of the

living macroalgae or, more likely, as a planktonic contribution to the sediment surface. However, alternative explanations for the diverging hopane patterns, particularly differential clay catalysis and redox conditions during early diagenesis, cannot be excluded because too little is known about the influence of hopanol side-chain functionalization, clay catalysis and oxygen exposure on the diagenetic fate of biohopanols. Thus, it is currently not possible to extract reliable information about biological sources from the hopane homolog patterns.

Methylhopanes

3 β -methylhopanes were detected in small amounts in the samples and might reflect a minor contribution of methanotrophic bacteria to the organic matter of the samples¹². The 2-methylhopane index (2-MHI) measures the abundance of C₃₁ 2-methylhopane relative to C₃₀ hopane. 2-MHI is similar in all analysed samples (2-MHI = 0.68-1.28%) except *Vendotaenides* where 2-methylhopanes are below the detection limit (Table 1). Elevated 2-MHI have been interpreted as an indicator for significant cyanobacterial contribution to sedimentary organic matter¹³. However, only a minority of cyanobacteria have the ability to produce 2-methylhopanoids¹⁴, and their content in cyanobacteria significantly depends on growth conditions. Under different cultivation conditions, 2-methylhopanoids may constitute the majority of hopanoids or might be entirely absent even in the same species⁵. Apart from cyanobacteria, 2-methylhopanoids can also be produced by many other oxygenic and anaerobic bacteria including alphaproteobacteria and an acidobacterium¹⁴. Thus, in light of the unspecific taxonomic distribution of 2-methylhopanoids, and environmental control on their biosynthesis^{14,15}, the 2-MHI values in *Beltanelliformis* do not yield any further insights about biological origins.

Biomarkers from the *Vendotaenides* macroalgal fossil in comparison to the macroalgal film adjacent to *Beltanelliformis*

Extraction of the separated organic film of the macroalga *Vendotaenides* (Supplementary Fig. 2b) yielded a strong predominance of C₂₉ steranes (C₂₇:C₂₈:C₂₉ = 13%:3%:84%), low relative hopane abundances (H/S = 0.69) and high abundances of long-

chain relative to short-chain *n*-alkanes with no carbon number preference ($OEP_{25-29} = 0.99$). This signal is very similar to the hydrocarbon distribution in the macroalgal film adjacent to *Beltanelliformis* (Table 1). The similarity of the *n*-alkane distribution and strong C₂₉ sterane predominance suggests that both brown-coloured organic films represent the remains of primary endosymbiotic macroalgae, probably chlorophytes¹⁶.

Biomarkers from clay in comparison with *Beltanelliformis* and macroalgae

Before assigning the bacterial lipids to *Beltanelliformis*, we must consider whether the hydrocarbons may have migrated or diffused into the fossil from the surrounding clay. Migration of a liquid petroleum phase can be excluded as organic matter in the Lyamtsa sediments is highly immature and never generated liquid hydrocarbons. This is shown by the preservation of thermally labile $\beta\alpha\alpha$ -steranes and high ratios of $\beta\alpha$ - over $\alpha\beta$ -hopanes (Table 1). Despite the low thermal maturity, over 558 million years it is likely that some hydrocarbons diffused into the organic film. This effect, however, is minor. Based on very significant differences in biomarker distributions between clay, macroalgae and *Beltanelliformis* (Supplementary Fig. 3; Table 1), it was possible to determine that almost 90% of hopanes detected in the *Beltanelliformis* extract derive directly from *Beltanelliformis*.

Unlike the films of organic matter analysed in this study, which represent specimens of fossils, biomarkers extracted from clay reflect an averaged signal accumulated over long periods of time from different biological sources. It is therefore expected that the distribution of molecules in the clay is different from *Beltanelliformis*, the surrounding macroalgal film and *Vendotaenides*. While the distribution of steranes in the latter three samples is nearly identical, reflecting the same or a similar macroalgal source, the clay shows a somewhat diminished C₂₉ predominance (81%) and two-fold elevated C₂₈ steranes (ergostanes) (Table 1), implying other eukaryotes contributed to the clay biomarker signal as well.

The high ratio of hopanes to steranes in the clay ($H/S = 4.7$) indicates that bacteria played an important role as a source of organic matter while eukaryotic source input was less important. This may be due to the presence of abundant degraded *Beltanelliformis* or cyanobacterial biofilms within the clay. Alternatively or additionally, the high H/S ratio may

reflect advanced bacterial degradation of primary organic matter including consumption of algal biomass by heterotrophic bacteria. This is in stark contrast to the low hopane to sterane ratio in the macroalga adjacent to *Beltanelliformis* (H/S = 0.061). This exceptionally high relative abundance of steranes – values of this magnitude are rarely observed¹² – points to minimal bacterial degradation of the alga, evidently aided by favourable taphonomic conditions. Exclusion of excessive bacterial reworking in the bedding plane of the macroalgae and *Beltanelliformis* may also explain the unusual organic preservation of fossils of the Ediacara biota.

The *n*-alkane distribution in the C₂₅-C₃₁ range in the clay extract is similar to *Beltanelliformis* (Supplementary Fig. 6), and it is possible that remains of *Beltanelliformis*, complete or physically degraded, are present in the underlying clay. The overall distribution of *n*-alkanes, however, is different: C₂₁ and C₂₃ are the most abundant *n*-alkanes in clay, while *Beltanelliformis* clearly demonstrates a bimodal distribution with maxima at C₁₉ (or possibly C₁₇ that may have evaporated from the surface of the exposed biofilm) and C₂₅. Thus, other organisms likely contributed to the *n*-alkane signal in the clay. In light of the odd-over-even predominance (OEP), plausible sources of these *n*-alkanes include other cyanobacteria and microalgae¹⁷. Terrestrial fungi and lichen, which also produce long-chain *n*-alkanes and -alkenes with OEP, are less likely due to the still very low content of C₂₈ steranes (Table 1). Moreover, land plants, which are known to contribute OEP *n*-alkanes in the C₂₇ to C₃₃ range in late Palaeozoic to Cenozoic oils and bitumens, can evidently be excluded as they had not evolved by the Ediacaran.

Other saturated and aromatic hydrocarbons

The majority of biomarkers extracted from the analysed samples is represented by *n*-alkanes, steranes and hopanes, while aromatic compounds in *Beltanelliformis*, *Vendotaenides* and macroalgal film extracts are barely detectable. In *Beltanelliformis*, methylalkanes are below the detection limit. In *Vendotaenides* and the macroalgal film C₁₇ 2-, 3- and 4-methylalkanes, and C₂₆₋₂₉ 2- and 3-methylalkanes and C₃₀₋₃₂ 2-, 3-, 4- and 5-methylalkanes are present. The clay extract demonstrates a full range of mono- and dimethylalkanes that clearly

represent diagenetic products of *n*-alkanes formed due to clay catalysis¹⁸. Apart from clearly detectable pristane and phytane, only traces of C₁₈ to C₂₁ regular isoprenoids were detected in all samples. As pristane and phytane abundances relative to *n*-alkanes are extremely low, it is not possible to obtain reliable values for the pristane/phytane ratio. No other isoprenoids, saturated or aromatic carotenoids or their breakdown products were found in any of the samples. Polycyclic aromatic hydrocarbons are present in small amounts and are represented by typical parent and alkylated phenanthrenes and naphthalenes found in most bitumens and oils. In the clay, the Methylphenanthrene Index (MPI-1 = 0.18) is consistent with the generally immature biomarker distribution¹². Monoaromatic (MAS) and triaromatic (TAS) steroids were also detected in the clay and show homolog distributions similar to the measured saturated cholesterol : ergosteroid : stigmasteroid abundances (MAS = 11%:4%:85%, TAS = 11%:9%:80%).

Syngeneity of biomarkers

GC-MS MRM and SIR analyses of the comprehensive accumulatory laboratory system blank confirmed that the detected hydrocarbons were not introduced by laboratory processes. Monitoring of the blank yielded only trace amounts of *n*-alkanes (comprising < 4% of the *n*-alkane level in the clay sample), while sensitive GC-MS MRM technology only detected < 2% hopanes relative to samples and no detectable steranes (Supplementary Fig. 7). The only other contaminants that were detected in the blank and are most visible in the *Beltanelliformis* extract are phthalates - plasticizers present everywhere in small amounts (Fig. 1e, Supplementary Fig. 6).

To detect hydrocarbons that may have accumulated on surfaces or in cracks in outcrop, e.g. through subsurface biota or groundwater flow, and to eliminate the possibility of contamination during sampling, transportation and storage, an Exterior/Interior (E/I) experiment was carried out on the clay immediately underlying *Beltanelliformis*. In this method, several millimeters of exterior surfaces were removed from the clay, and their hydrocarbon content was compared with the clay interior. E/I >> 1 signifies surficial contamination, while E/I ~1 commonly indicate indigenous hydrocarbons. E/I > 1 and up to 3

are still typical for indigenous compounds and probably caused by the migration or diffusion of indigenous hydrocarbons towards natural joints. Moreover, escalating E/I values with increasing molecular weight indicate diffusion of contaminants into the rock^{1,3}. To illustrate the principle, the dotted line in Figure 8b shows the E/I values of *n*-alkanes of a White Sea clay sample that was not protected against contamination during transport as it was wrapped in paper rather than combusted aluminium foil. The E/I values range from 2.5 to 7.7 with particularly elevated values from *n*-C₁₇ to *n*-C₂₃, a pattern typical for surficial contamination with anthropogenic petroleum distillation cuts¹⁹. In contrast, the results for the Lyamtsa sample that contained *Beltanelliformis* and was protected by aluminium foil shows nearly identical concentrations of all biomarkers in exterior and interior rock portions with E/I = 1.09 to 1.53 for *n*-alkanes and E/I = 0.93 to 1.05 for hopanes and steranes (Supplementary Table 1). Moreover, a plot of E/I with increasing *n*-alkane carbon numbers (Supplementary Fig. 8) does not display any increase from C₁₇ to C₃₁, indicating that no contaminants diffused into the rock interior. The results show that the precombusted aluminium foil and clean calico bag prevented contamination of the *Beltanelliformis* sample during transportation and storage and confirm that all detected compounds are indigenous.

Although application of the E/I protocol to the thin organic films of macroalgae and *Beltanelliformis* was evidently not possible, there is additional evidence that the extracted hydrocarbons are indigenous. All samples yielded a strong C₂₉ predominance among steranes (C₂₉% = 81 to 88%; Table 1), an unusual and extreme pattern typical of the Ediacaran but not observed in Phanerozoic petroleum products, even those with strong input of plant-derived C₂₉ steranes. This is corroborated by the absence of diagnostic plant markers such as oleanane and bicadinanes. Moreover, convincing additional evidence for the Ediacaran age of the hydrocarbons comes from the presence of 24-isopropylcholestane (24-ipc) in the clay extract and the simultaneous absence of 24-*n*-propylcholestane. This 24-ipc predominance pattern is believed to derive from early demosponges and has only been observed in Cryogenian, Ediacaran and earliest Palaeozoic oils and bitumens^{20,21}, thus excluding virtually all important sources of anthropogenic petroleum contaminants.

A third line of evidence against contamination is the low thermal maturity of the extracted bitumens. The extremely high $\beta\alpha/(\beta\alpha + \alpha\beta)$ and low Ts/(Ts + Tm) hopane isomer

ratios, virtual absence of $\alpha\beta\beta$ sterane isomers and presence of $\beta\alpha\alpha$ steranes (Table 1, Fig. 1), which are only found in the most immature sediments, demonstrate that the hydrocarbons are significantly below the so-called oil-generative window, i.e. the kerogen in the Lyamtsa clays never thermally generated and expelled liquid hydrocarbons. Such a low thermal maturity is never observed in contaminant petroleum products and migrated oils which, by their very nature, must have a maturity within the oil generative window. Thus, contamination of the samples by petroleum products or by migrated hydrocarbons did evidently not occur.

Finally, marked differences in biomarker homolog and isomer distributions between *Beltanelliformis* and the adjacent macroalgal film, and reproducibility of the macroalgal signal based on the second algal sample collected during a different field season, imply that the obtained data reflect indigenous distributions of biomarkers.

Alternative origins of the *Beltanelliformis* biomarker signal

There are a number of potential explanations for the biomarker signal of the *Beltanelliformis* extract that are more complex and involve mixed bacterial and eukaryotic sources. Although these scenarios are more derived and less likely, they need to be discussed.

Beltanelliformis may have been a multicellular eukaryote that was severely degraded by heterotrophic bacteria, and the original eukaryotic lipid content was largely replaced by bacterial biomass. The extremely well preserved original lipid content in the macroalgal film adjacent to *Beltanelliformis* may be used as an argument against strong bacterial degradation. Yet, colonization by heterotrophic bacteria can be substrate-selective or substrate-specific, potentially causing selective removal of lipids from *Beltanelliformis*. In such a case, the elevated H/S ratio and unusual *n*-alkane distribution in *Beltanelliformis* would belong to heterotrophic bacteria. However, as discussed in the main text, among all bacteria, OEP of long-chain *n*-alkanes has never been detected in heterotrophic bacteria but is a typical signature of some cyanobacteria, such as certain Nostocales^{17,22-24}. Therefore a heterotrophic origin of the lipid content of *Beltanelliformis* is highly unlikely.

Gelatinous lichens with cyanobacterial symbionts, one of the interpretations of *Beltanelliformis*²⁵, may produce a similar *n*-alkane signal. However, lichens also produce large proportions of C₂₈ steroids²⁶, which are virtually absent in the *Beltanelliformis* extract. *Beltanelliformis* could also represent a stem or crown group animal (e.g. sponge, coral polyp or jellyfish²⁷⁻³⁰) that harboured symbiotic or epiphytic cyanobacteria. The sterane distributions in *Beltanelliformis* and adjacent macroalgae are nearly identical, thus this scenario requires that any steroid signal coming directly from *Beltanelliformis* is entirely concealed by sterane signals from overlapping algae. Therefore, if *Beltanelliformis* was a metazoan, it produced extremely low amounts of steroids. However, let us assume an extreme scenario where all cholestane in the *Beltanelliformis* extract was actually produced by *Beltanelliformis*. In this case, the concentration of cholestane in *Beltanelliformis* is 0.001 ng/cm², whereas the concentration of hopanes is 0.05 ng/cm², corresponding to 52 times higher abundances of hopanes than steranes. As the concentration of hopanoids in bacterial cell membranes is generally similar to the concentration of steroids in eukaryotic membranes⁵, this scenario requires that cyanobacterial symbionts or epiphytes produced one to two orders of magnitude more biomass than their animal host. However, this is extremely unlikely because even sponges with the highest known contents of symbionts only harbour up to 40%, rarely up to 60%, of bacterial biomass³¹. Moreover, the estimate H/S = 52 represents an absolute minimum as it assigns all cholestane quantitatively to *Beltanelliformis* (rather than overlapping algae). Thus, the extremely high ratio of hopanes over cholestane makes animal / symbiont models unrealistic.

More difficult to exclude is the possibility that *Beltanelliformis* were spherical macroalgae or algal gametophytes^{32,33} selectively targeted by cyanobacterial epiphytes. In that case, the steranes could belong to the host algae instead of being a result of physical overlap with the adjacent film. This would require the spherical macroalgae to have produced exactly the same C₂₇:C₂₈:C₂₉ steroid distribution as the adjacent macroalgae. From the difference in H/S ratio, it is also necessary that the macroalgal balls were overgrown with at least 60 times more cyanobacterial epiphytes than the adjacent macroalgae. From the S/H ratio in *Beltanelliformis* (H/S = 3.6), these cyanobacteria should also have had a higher biomass than the algae they were growing on, which would be lethal for a photosynthetic host organism. In the view of these unlikely assumptions, a cyanobacterial origin of

Beltanelliformis is most likely. The steranes in the *Beltanelliformis* extract likely come from overlapping macroalgal organic matter, which was estimated to be $\sim 0.8 \text{ mm}^2$ (or 0.03% of the surface area of analysed *Beltanelliformis*).

The discussion above firmly suggests that *Beltanelliformis* are not eukaryotic but represent bacterial structures. There are currently no known diagnostic lipid biomarkers for cyanobacteria. However, based on the hopane composition and *n*-alkane homolog distribution, a cyanobacterial origin is most likely.

The OEP among long-chain *n*-alkanes observed in *Beltanelliformis* may also belong to a now extinct (or poorly known) group of non-cyanobacterial bacteria. Generally, the consideration of extinct groups as the source of molecular fossils is largely intractable and the best interpretation will necessarily follow uniformitarian principles. With this caveat, we consider it unlikely that a fossils with a morphology and molecular composition similar to *Nostoc* is not a cyanobacterial colony.

Applications for studying other Ediacaran macrofossils

Current major interpretations of the Ediacara biota include such groups as animals³⁴, giant protists³⁵ and lichen²⁵. Other phylogenetic interpretations of some members of the Ediacara biota included prokaryotic or eukaryotic microbial colonies^{36,37}, marine fungi³⁸ and sponges³⁹. Although most scientists will reject lichen as a reasonable interpretation for the Ediacara biota⁴⁰, we think it is still crucial to provide unambiguous evidence for such or any other interpretation. This manuscript shows that it is possible to distinguish bacteria from eukaryotes. Using steranes and other biomarkers, it is in principle possible to differentiate between sponges, eumetazoans, most protists, algae, fungi and lichen. For example, eumetazoan animals mainly produce cholesterol or other C_{27} sterols^{41,42}, sponges may contain 24-isopropylcholesteroids, foraminifera may produce 24-*n*-propylcholesterol⁴³ and lichens ergosterol⁴⁴. Mapping individual members of the Ediacara biota on the phylogenetic tree even on such scale would be an important achievement in the study of these enigmatic fossils. While other localities with fossils of the Ediacara Biota may be weathered or thermally too

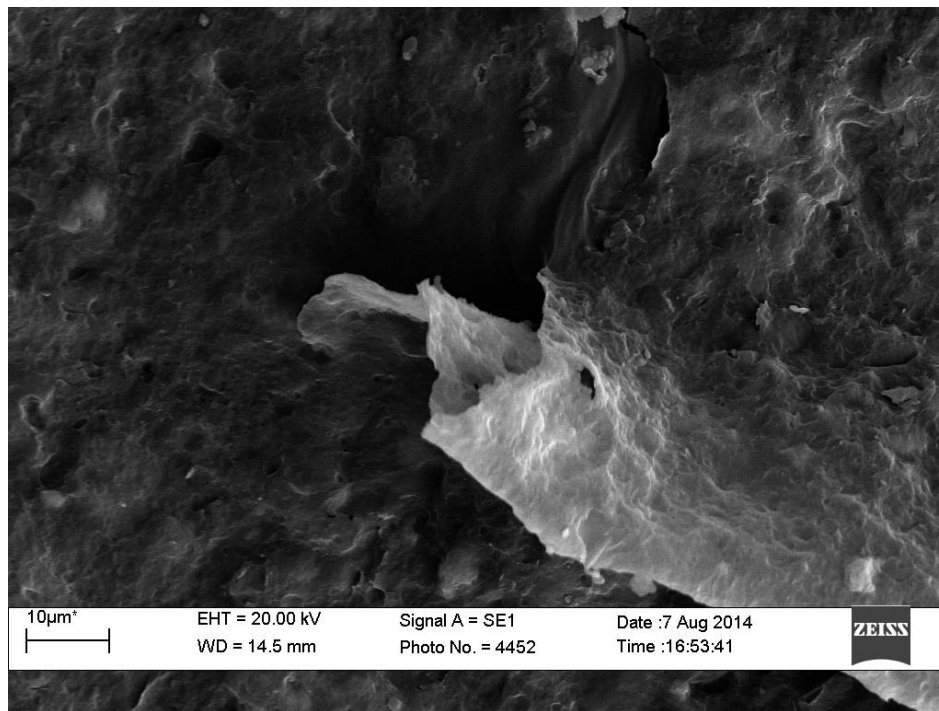
mature to preserve biomarkers, the White Sea section harbours organically preserved specimens of enigmatic Ediacaran microfossils suitable for biomarker analysis³⁷.

REFERENCES

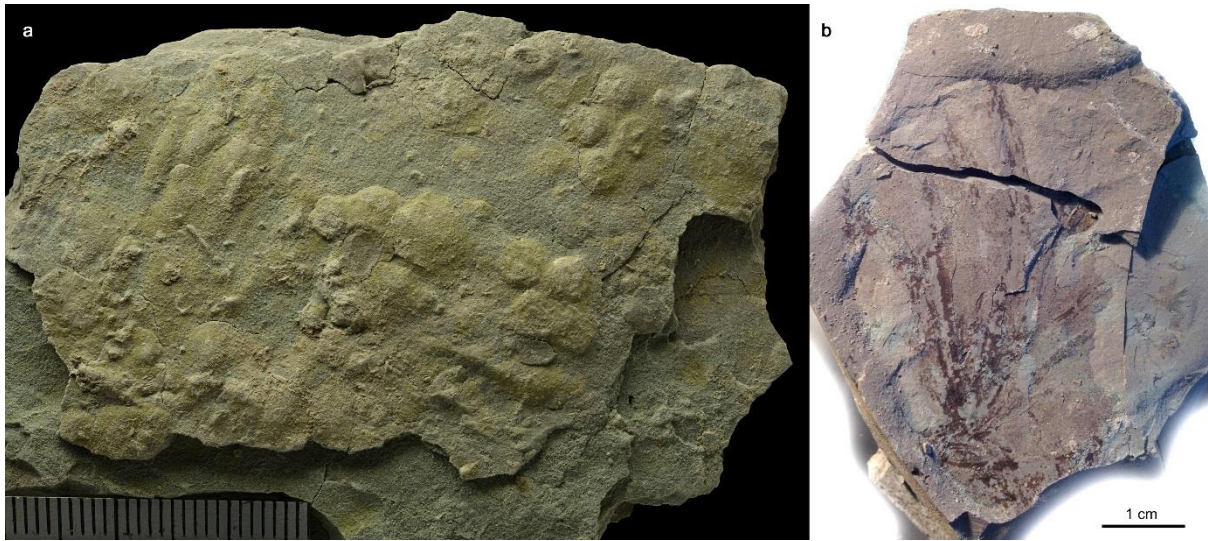
- 1 Brocks, J. J., Grosjean, E. & Logan, G. A. *Geochim. Cosmochim. Acta* **72**, 871-888, (2008).
- 2 Schinteie, R. & Brocks, J. J. *Org. Geochem.* **72**, 46-58, (2014).
- 3 Jarrett, A. J. M., Schinteie, R., Hope, J. M. & Brocks, J. J. *Org. Geochem.* **61**, 57-65, (2013).
- 4 Brocks, J. J. & Hope, J. M. *Journal of Chromatographic Science* **52**, 471-475, (2014).
- 5 Rohmer, M., Bouvier-Nave, P. & Ourisson, G. *Microbiology* **130**, 1137-1150, (1984).
- 6 Zundel, M. & Rohmer, M. *FEMS Microbiol. Lett.* **28**, 61-64, (1985).
- 7 Innes, H. E., Bishop, A. N., Fox, P. A., Head, I. M. & Farrimond, P. *Organic Geochemistry* **29**, 1285-1295, (1998).
- 8 Knoll, A. H., Summons, R. E., Waldbauer, J. R. & Zumberge, J. E. in *Evolution of Primary Producers in the Sea* (eds P. Falkowski & A. H. Knoll) 133-163 (Academic Press, 2007).
- 9 Zhao, N. *et al. Tetrahedron* **52**, 2777-2788, (1996).
- 10 Talbot, H. M. *et al. Organic Geochemistry* **39**, 232-263, (2008).
- 11 Nagovitsyn, A. in *PALEOSTRAT-2015* (ed A. S. Alekseev) (PIN RAS, Moscow, 2015).
- 12 Peters, K., Walters, C. & Moldowan, J. 2nd edn, (Cambridge University Press, 2005).
- 13 Summons, R. E., Jahnke, L. L., Hope, J. M. & Logan, G. A. *Nature* **400**, 554-557, (1999).
- 14 Welander, P. V., Coleman, M. L., Sessions, A. L., Summons, R. E. & Newman, D. K. *Proceedings of the National Academy of Sciences* **107**, 8537-8542, (2010).
- 15 Ricci, J. N. *et al. ISME J* **8**, 675-684, (2014).
- 16 Kodner, R. B., Pearson, A., Summons, R. E. & Knoll, A. H. *Geobiology* **6**, 411-420, (2008).
- 17 Volkman, J. K. *et al. Org. Geochem.* **29**, 1163-1179, (1998).
- 18 Kissin, Y. V. *Geochimica et Cosmochimica Acta* **51**, 2445-2457, (1987).
- 19 Brocks, J. J., Buick, R., Logan, G. A. & Summons, R. E. *Geochim. Cosmochim. Acta* **67**, 4289-4319, (2003).
- 20 McCaffrey, M. A. *et al. Geochimica et Cosmochimica Acta* **58**, 529-532, (1994).
- 21 Love, G. D. *et al. Nature* **457**, 718-721, (2009).
- 22 Jones, J. G. *Microbiology* **59**, 145-152, (1969).
- 23 Gelpi, E., Oró, J., Schneider, H. J. & Bennett, E. O. *Science* **161**, 700-701, (1968).
- 24 Matsumoto, G. I., Yamada, S., Ohtani, S., Broady, P. A. & NAGASHIMA, H. in *Proceedings of the NIPR Symposium on Polar Biology*. 275-282.
- 25 Retallack, G. J. *Alcheringa: An Australasian Journal of Palaeontology* **40**, 583-600, (2016).
- 26 Safe, S., Safe, L. M. & Maass, W. S. G. *Phytochemistry* **14**, 1821-1823, (1975).
- 27 Leonov, M. V. *Geol. Soc. Spec. Publ.* **286**, 259-267, (2007).
- 28 Runnegar, B. & Fedonkin, M. in *The Proterozoic biosphere: a multidisciplinary study* (eds J.W. Schopf & C. Klein) 369-388 (Cambridge University Press, 1992).
- 29 Seilacher, A. *J. Geol. Soc.* **149**, 607-613, (1992).
- 30 Zaika Novatsky, V. & Palij, V. *Paleontol. Sb.* **11**, 59-65, (1974).
- 31 Taylor, M. W., Radax, R., Steger, D. & Wagner, M. *Microbiol. Mol. Biol. Rev.* **71**, 295-347, (2007).
- 32 Xiao, S. & Dong, L. in *Neoproterozoic Geobiology and Paleobiology* (eds Shuhai Xiao & Alan J. Kaufman) 57-90 (Springer Netherlands, 2006).
- 33 Xiao, S., Yuan, X., Steiner, M. & Knoll, A. H. *J. Paleontol.* **76**, 347-376, (2002).

- 34 Fedonkin, M., Ivantsov, A. Y., Leonov, M. & Serezhnikova, E. in *The rise and fall of the Vendian (Ediacaran) biota. Origin of the modern biosphere. Transact. Int. Conf. on the IGCP project.* 6-9.
- 35 Seilacher, A., Grazhdankin, D. & Legouta, A. *Paleontol. Res.* **7**, 43-54, (2003).
- 36 Grazhdankin, D. & Gerdes, G. *Lethaia* **40**, 201-210, (2007).
- 37 Steiner, M. & Reitner, J. *Geology* **29**, 1119-1122, (2001).
- 38 Peterson, K. J., Waggoner, B. & Hagadorn, J. W. *Integr. Comp. Biol.* **43**, 127-136, (2003).
- 39 Gehling, J. G. & Rigby, J. K. *J. Paleontol.* **70**, 185-195, (2016).
- 40 Xiao, S. & Knauth, L. P. *Nature* **493**, 28-29, (2013).
- 41 Kanazawa, A. *Fish. Sci.* **67**, 997-1007, (2001).
- 42 Kerr, R. G. & Baker, B. J. *Natural Product Reports* **8**, 465-497, (1991).
- 43 Grabenstatter, J. *et al. Org. Geochem.* **63**, 145-151, (2013).
- 44 Weete, J. D., Abril, M. & Blackwell, M. *PLoS One* **5**, e10899, (2010).

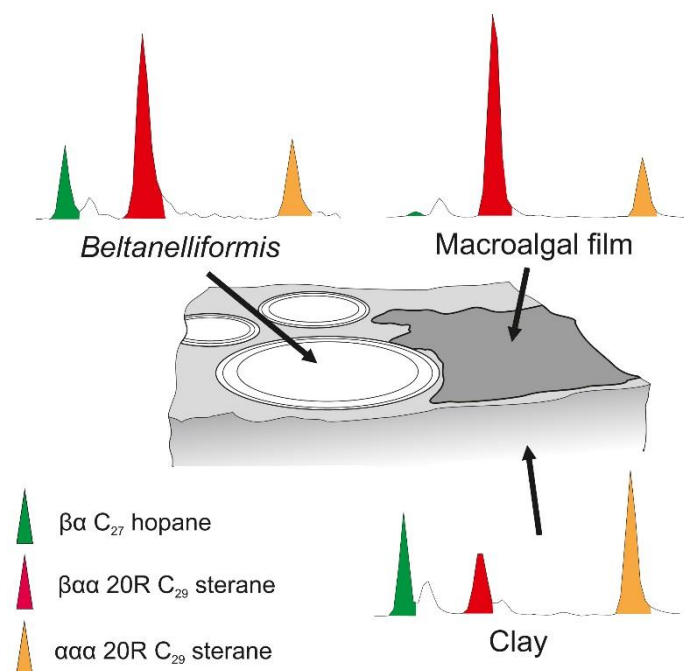
SUPPLEMENTARY FIGURES



Supplementary Figure 1 | SEM image of the organic matter of *Beltanelliformis*. The organic film is extremely thin (less than 1 μm), single-layered and does not preserve any visible structure.



Supplementary Figure 2 | Fossils from the Lyamtsa locality. a, *Nemiana* taphonomic form of *Beltanelliformis*, replacing organically preserved *Beltanelloides* where the surface with the fossils is cut by a siltstone lens, each scale unit is 1 mm; b, carbonaceous fossil of the macroalga ex gr. *Vendotaenides*.

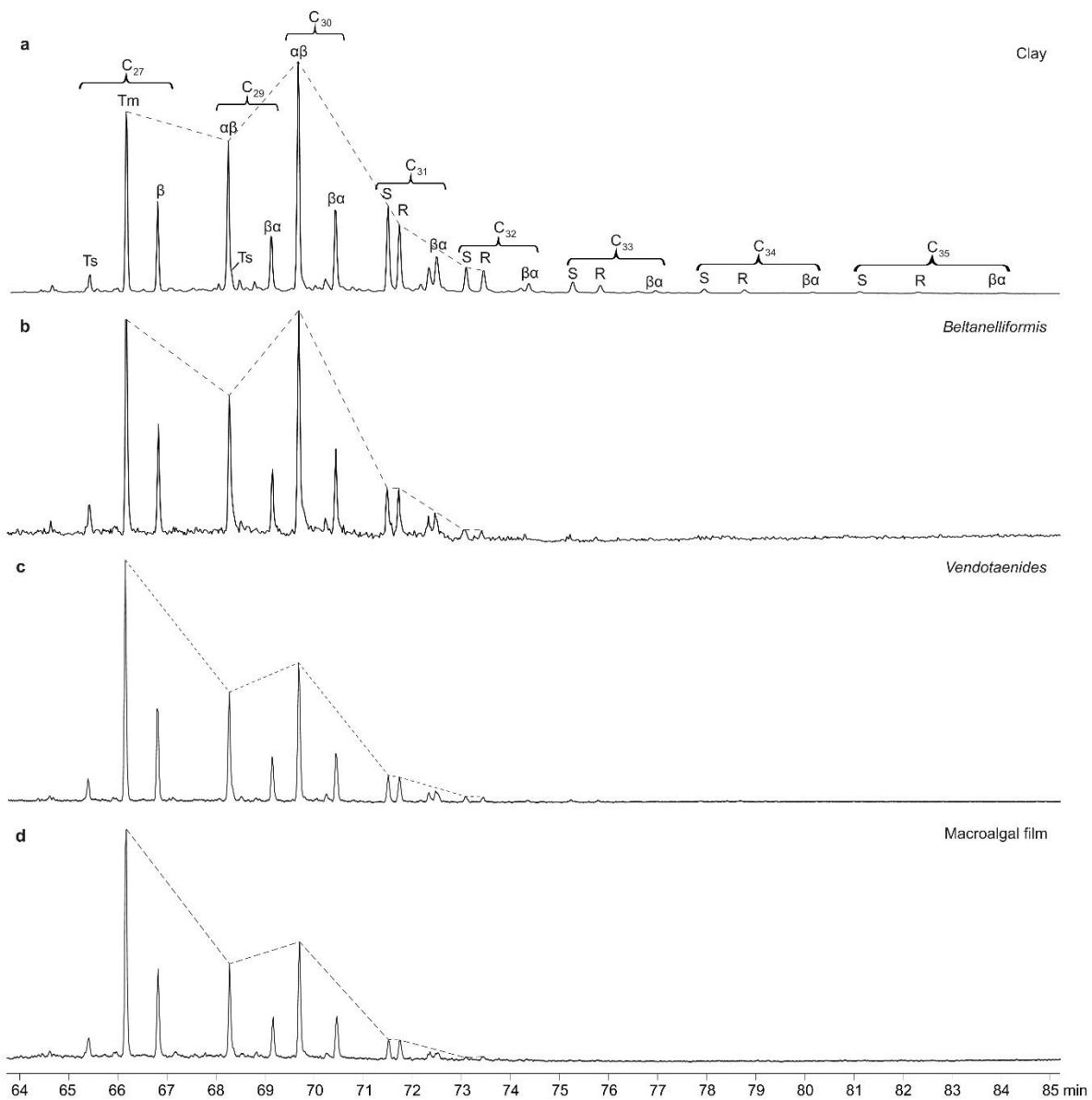


Supplementary Figure 3 | Relative distribution of molecular fossils in the extracts of

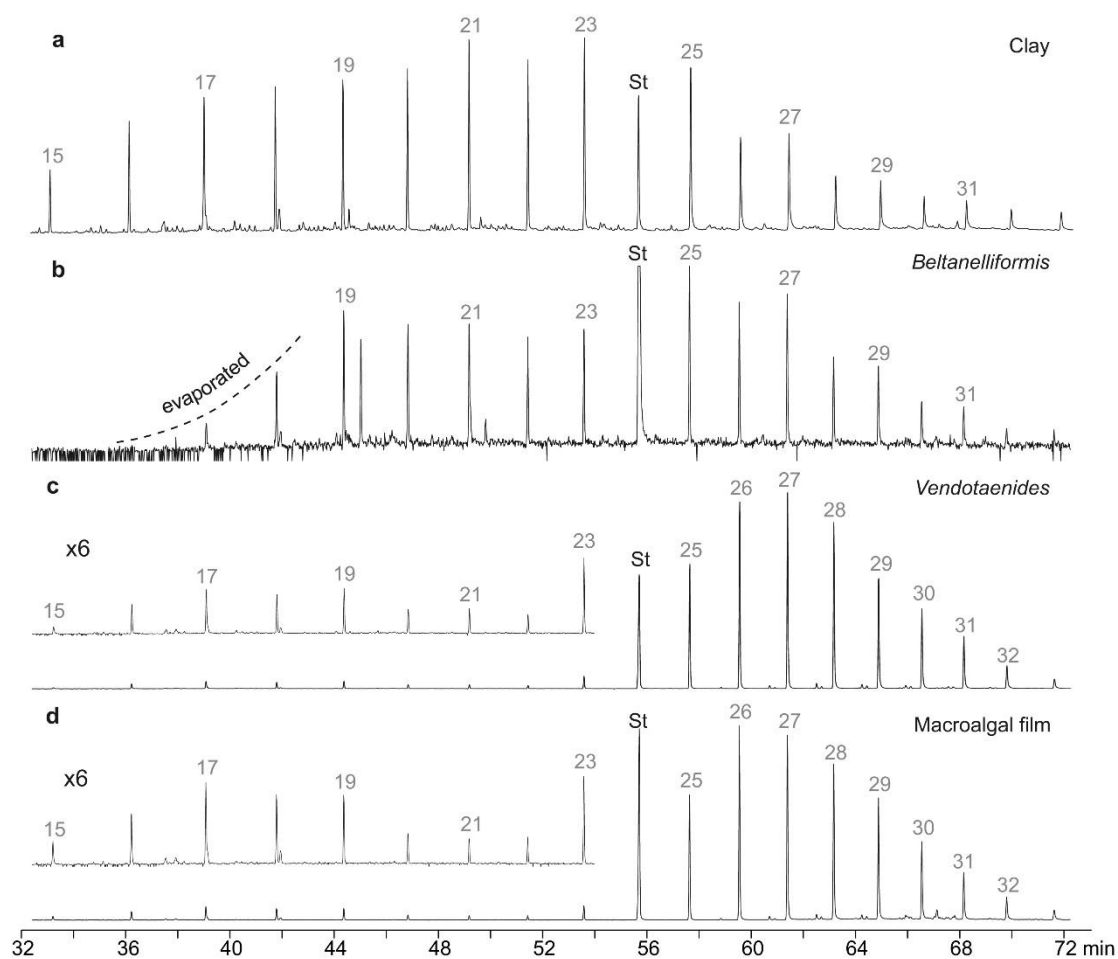
***Beltanelliformis*, macroalgal film and clay.** Note distinct relative abundances of hopanes over steranes, and of $\beta\alpha$ - over $\alpha\alpha$ -steranes in the three samples. Based on the low $\beta\alpha/\alpha\alpha$ sterane ratio (0.47) in the clay in comparison to *Beltanelliformis* (3.0) and alga (3.7) (Table 1) in these samples, we can apply a two component mixing scenario to determine the proportion of steranes and hopanes that were introduced into the *Beltanelliformis* extract from the clay and from the macroalgal film. Assuming that the original sterane content of *Beltanelliformis* was zero, a maximum of 32% of the sterane and hopane mixture in *Beltanelliformis* may have diffused into the fossil from the surrounding clay and/or is derived from residual clay particles attached to the isolated organic film of *Beltanelliformis* (see Supplementary File 'Mixing simulation'). A mixture consisting of 32% clay- and 68% macroalga-derived hydrocarbons would have a H/S ratio of 0.43. However, the actual H/S of the *Beltanelliformis* extract is 3.8, demonstrating that $1 - 0.43/3.8 \approx 89\%$ of the hopanes must come from the fossil itself and the remainder largely from the surrounding clay. The sterane content of the *Beltanelliformis* extract can be explained by a small contribution of extremely sterane-rich macroalgal debris underlying the fossils (0.03% by surface area).



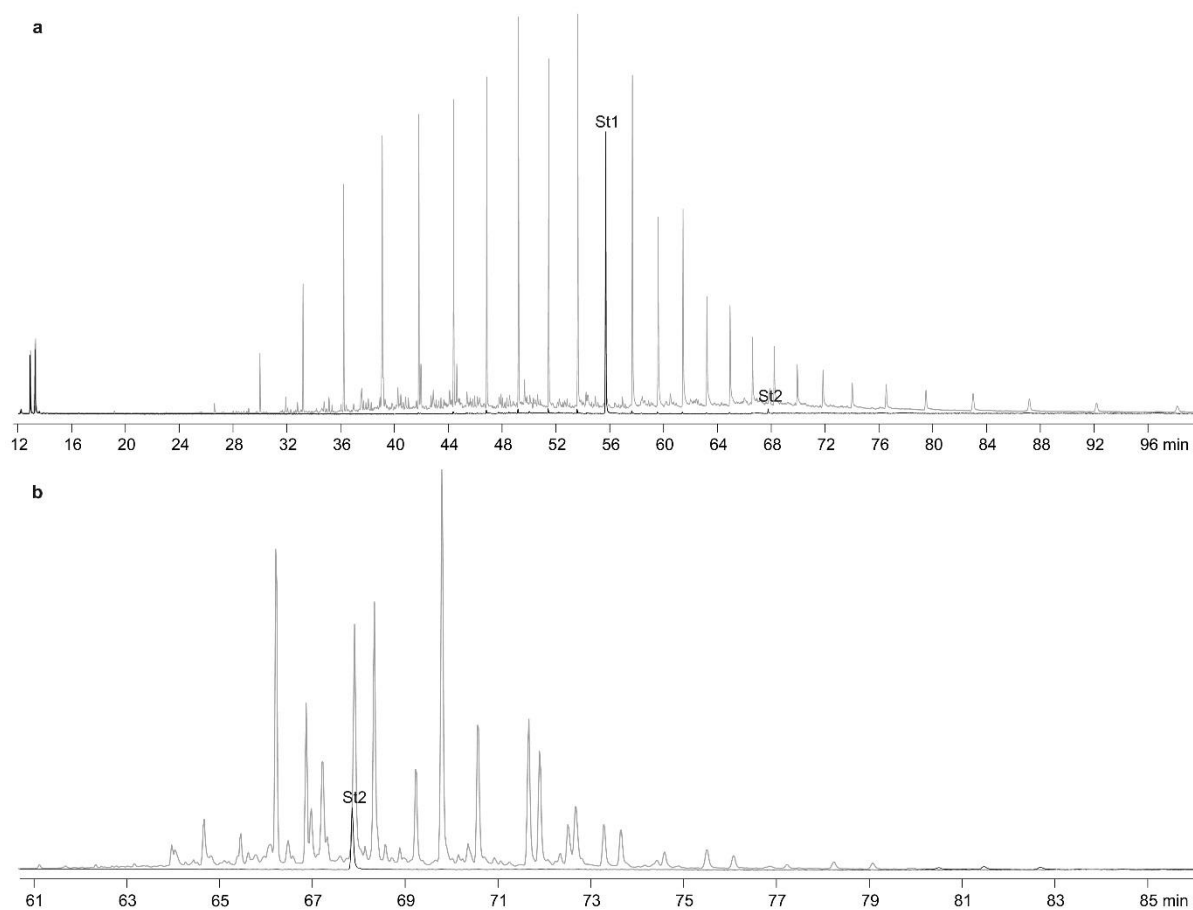
Supplementary Figure 4 | Modern cyanobacterial colonies *Nostoc communis*. Such structures represent a modern analogue for cyanobacterial colonies that produced *Beltanelliformis*. The photo was taken at Gait Barrows National Nature Reserve in North Lancashire, UK, in 2005 by R. Petley-Jones.



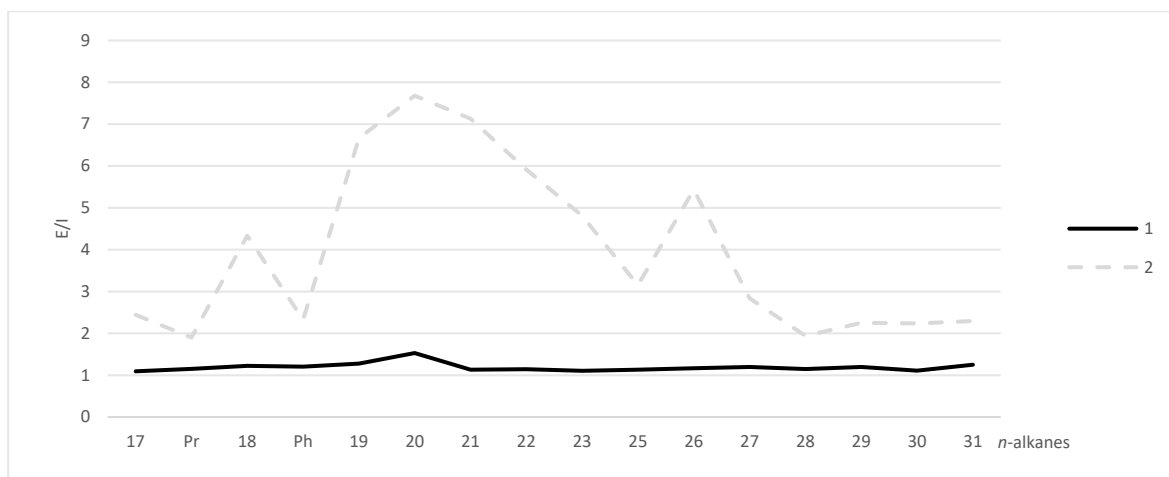
Supplementary Figure 5 | Metastable reaction monitoring (MRM) chromatograms highlighting differences of C₂₇₋₃₅ hopane distributions. a, clay; b, *Beltanelliformis*; c, *Vendotaenides*; d, macroalgal film.



Supplementary Figure 6 | Distribution of *n*-alkanes (m/z 85) of a, clay; b, *Beltanelliformis*; c, *Vendotaenides*; d, macroalgal film. Numbers on chromatographic signals indicate the carbon number of *n*-alkanes; x6 in the inset of c and d signifies 6 times magnification of the chromatogram; St – 18-MEAME internal standard.



Supplementary Figure 7 | GC-MS analysis of the comprehensive accumulatory laboratory system (black line) in comparison to the clay extract (grey line). a, full-scan chromatogram, m/z 85 trace; b, metastable reaction monitoring (MRM) chromatogram: $\Sigma(C_{27-35}$ hopanes, C_{27-29} steranes and D4 standard); St1 – 18-MEAME internal standard, St2 - D4 internal standard.



Supplementary Figure 8 | Results of Exterior/Interior experiments for *n*-alkanes from clay samples (1) wrapped in precombusted aluminium foil, and (2) wrapped in paper. Pr – pristane, Ph – phytane. Clay sample wrapped in clean aluminium foil (1) demonstrates E/I ratios around 1 indicating that no contamination was introduced. Clay sample wrapped in paper (2) shows E/I values up to 7.7 with particularly elevated values from *n*-C₁₇ to *n*-C₂₃, a pattern typical for surficial contamination with anthropogenic petroleum distillation cuts (see Supplementary Information).

Supplementary Table 1 | Results of Exterior/Interior experiment on the clay sample.

<i>n</i> -alkanes													
C ₁₇	C ₁₈	C ₁₉	C ₂₀	C ₂₁	C ₂₂	C ₂₃	C ₂₅	C ₂₆	C ₂₇	C ₂₈	C ₂₉	C ₃₀	C ₃₁
1.09	1.22	1.28	1.53	1.13	1.15	1.10	1.13	1.17	1.20	1.15	1.20	1.11	1.25

Steranes		
C ₂₇	C ₂₈	C ₂₉
1.05	1.04	1.05

Hopanes				
C ₂₇	C ₂₉	C ₃₀	C ₃₁	C ₃₂
0.93	0.99	0.94	0.94	0.94

Exterior/Interior reflects the compound concentration in the exterior portion of a sample relative to the concentration of the same compound in the interior (see Supplementary Information); steranes: C₂₇ = $\Sigma(\alpha\alpha\alpha\text{- and } \beta\alpha\alpha\text{-}20(\text{S+R})\text{-cholestane})$, C₂₈ = $\Sigma(\alpha\alpha\alpha\text{- and } \beta\alpha\alpha\text{-}20(\text{S+R})\text{-ergostane})$, C₂₉ = $\Sigma(\alpha\alpha\alpha\text{- and } \beta\alpha\alpha\text{-}20(\text{S+R})\text{-stigmastane})$; hopanes: C₂₇ = $\Sigma(\text{Ts, Tm, } \beta)$, C₂₉ = $\Sigma(\alpha\beta, \text{Ts, } \beta\alpha)$, C₃₀ = $\Sigma(\alpha\beta, \beta\alpha)$, C₃₁₋₃₂ = $\Sigma(22\text{S, } 22\text{R, } \beta\alpha)$.

CHAPTER 2. ANCIENT STEROIDS ESTABLISH THE EDIACARAN FOSSIL

DICKINSONIA AS ONE OF THE EARLIEST ANIMALS

Successful application of biomarkers to constrain the biological origin of *Beltanelliformis* allowed to expand this method to other Ediacaran fossils. *Dickinsonia* is one of the most famous Ediacaran organisms. Next to *Kimberella*, it has been considered as one of the strongest Ediacaran candidates for an animal among Ediacaran fossils, but other interpretations, such as unicellular protists and lichens, have not been entirely refuted. This chapter presents a reconstruction of the lipid composition of *Dickinsonia* and morphologically similar fossils, showing they indeed were animals.

Statement of Contribution

This thesis is submitted as a Thesis by Compilation in accordance with https://policies.anu.edu.au/ppl/document/ANUP_003405

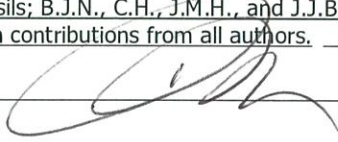
I declare that the research presented in this Thesis represents original work that I carried out during my candidature at the Australian National University, except for contributions to multi-author papers incorporated in the Thesis where my contributions are specified in this Statement of Contribution.

Title and authors: Bobrovskiy, I., Hope, J.M., Ivantsov, A., Nettersheim, B.J., Hallmann, C., Brocks, J.J. Ancient steroids establish the Ediacaran fossil *Dickinsonia* as one of the earliest animals.

Current status of paper: Not Yet Submitted/Submitted/Under Revision/Accepted/**Published**

Contribution to paper: I.B. designed the study and analyzed biomarkers from Ediacaran fossils; J.M.H. helped with biomarker analysis; I.B. and A.I. collected fossils; B.J.N., C.H., J.M.H., and J.J.B. analyzed modern Rhizaria; and I.B. and J.J.B. interpreted data and wrote the manuscript, with contributions from all authors.

Senior author or collaborating authors endorsement: _____



Ilya Bobrovskiy

Candidate – Print Name



Signature

18/04/2019

Date

Endorsed

Jochen Brocks

Chair of Supervisory Panel – Print Name



Signature

18/04/2019

Date

Stewart Falk

Delegated Authority – Print Name



Signature

29/04/2019

Date

Ancient steroids establish the Ediacaran fossil *Dickinsonia* as one of the earliest animals

**Ilya Bobrovskiy^{1*}, Janet M. Hope¹, Andrey Ivantsov², Benjamin J. Nettersheim³,
Christian Hallmann^{3,4}, Jochen J. Brocks^{1*}**

¹Research School of Earth Sciences, Australian National University, Canberra, ACT 2601, Australia

²Borissiak Paleontological Institute, Russian Academy of Sciences, Moscow 117997, Russia

³Max Planck Institute for Biogeochemistry, Jena 07745, Germany

⁴MARUM—Center for Marine Environmental Sciences, University of Bremen, Bremen 28359, Germany

*Correspondence to: ilya.bobrovskiy@anu.edu.au, jochen.brocks@anu.edu.au

The enigmatic Ediacara biota (575 to 541 My) represents the first macroscopic complex organisms in the geological record and may hold the key to our understanding of the origin of animals. Ediacaran macrofossils are “strange as life on another planet” and have evaded taxonomic classification, with interpretations ranging from marine animals or giant single-celled protists to terrestrial lichens. Here we show that lipid biomarkers extracted from organically preserved Ediacaran macrofossils unambiguously clarify their phylogeny. *Dickinsonia* and its relatives solely produced cholesteroloids, a hallmark of animals. Our results make these iconic members of the Ediacara biota the oldest confirmed macroscopic animals in the rock record, indicating that the appearance of the Ediacara biota was indeed a prelude to the Cambrian explosion of animal life.

One Sentence Summary: Lipid biomarkers constrain the nature of enigmatic fossil *Dickinsonia* and its morphological relatives, expanding the record of earliest animals.

The Ediacara biota remains one of the greatest mysteries in palaeontology. Members of this assemblage were initially described as animals (1, 2), however, as collections grew, it became apparent that Ediacaran fossils and their body plans are difficult to compare with modern phyla (3, 4). A major complication for the study of Ediacaran organisms is their soft-bodied nature and unique mode of preservation, rarely found in younger fossils. Thus, the interpretation of various members of the Ediacara biota has crossed several Kingdoms and

Domains, ranging from bacterial colonies (5), marine fungi (6), lichens (7) and giant protists (8, 9) to stem-group animals and crown-group Eumetazoa (4, 10, 11). The recent general consensus is that these fossils are polyphyletic (12, 13): at least some members of the Ediacara biota are almost unanimously interpreted as bilaterian animals (*Kimberella*) (14, 15), while others are confidently ascribed to giant protozoa (*Palaeopascichnus*) (16). *Beltanelliformis*, although previously interpreted as bacteria, benthic and planktonic algae, as well as different animals, is now recognized as a spherical colony of cyanobacteria based on their biomarker content (17). The affinity of most other Ediacarans however remains controversial even at the Kingdom level (4). Most recently, arguments surrounding these fossils have centred on lichens, giant protists and stem- or crown group Metazoa.

While the lichen hypothesis (7) requires an implausible re-interpretation of the habitat of the Ediacara biota from a marine to a continental depositional environment (18), for many Ediacaran fossils, including dickinsoniids, it currently seems impossible to distinguish between giant protist and metazoan origins (4, 19). Some Ediacaran fossils, such as *Palaeopascichnus*, were likely giant unicellular eukaryotes (protists) (16), which means that, in contrast to modern ecosystems, these organisms were present, and sometimes extremely abundant, in shallow-water Ediacaran habitats (20). Features of dickinsoniids such as ‘quilting’ patterns, the inferred absence of dorso-ventral differentiation, and putative external digestion mode were found to be compatible with modern giant protists and hard to reconcile with metazoans (8, 20). Some modern giant protists can be up to 25 cm in size (21). In the absence of metazoan competition they may have become even larger, thereby possibly providing an explanation for the size range of Ediacaran protistan fossils (8). Some giant protists even have a motile lifestyle, compatible with Ediacaran trace fossils (22) and dickinsoniid ‘footprints’ (15). For dickinsoniids, the absence of evidence for a mouth and gut, perceived absence of bilateral symmetry and possible external digestion are all consistent with a protistan origin. However, all of the above characteristics are also compatible with basal Metazoa such as the Placozoa that are situated at the very base of Eumetazoa (23), while rejection of an external digestion mode and acceptance of supposed cephalization (15) may place dickinsoniids even higher on the metazoan tree. The nature of dickinsoniids, and most other Ediacaran fossils, thus remains unresolved.

We applied a novel approach (17) to test the lichen, protist and animal hypotheses by studying biomarkers extracted from organically preserved dickinsoniids. Hydrocarbon biomarkers are the molecular fossils of lipids and other biological compounds. Encased in sedimentary rock, biomarkers may retain information about their biological origins for hundreds of millions of years. For instance, hopanes are the hydrocarbon remains of bacterial hopanepolyols, while saturated steranes and aromatic steroids are diagenetic products of eukaryotic sterols. The most common sterols of Eukarya possess a cholesterol, ergosteroid or stigmasteroid skeleton with 27, 28 or 29 carbon atoms respectively. These C₂₇ to C₂₉ sterols, distinguished by the alkylation pattern at position C-24 in the sterol side chain, function as membrane modifiers and are widely distributed across extant Eukarya, but their relative abundances can give clues about the source organisms (24).

Apart from *Dickinsonia* (Fig. 1B), which is one of the most recognizable Ediacaran fossils, dickinsoniids include *Andiva* (Extended Data Fig. 1C), *Vendia*, *Yorgia* and other flattened Ediacaran organisms with segmented metameric bodies and a median line along the body axes, separating the ‘segments’. The specimens for this study were collected from two surfaces in the Lyamtsa (*Dickinsonia*) and Zinnie Gory (*Andiva*) localities of the Ediacara biota in the White Sea region (Russia). Both *Dickinsonia* and *Andiva* are preserved in negative hyporelief on the sole of sandstones with microbial mat impressions and consist of a thin (up to around 3 μm) film of organic matter. The organic matter was detached from the rock surface (Fig. S1) and extracted for hydrocarbon biomarkers under strict exclusion of contamination (see Methods). Much thinner organic films covering the surfaces around *Andiva* fossils from the Zinnie Gory locality were extracted as well, providing a background signal coming from associated microbial mats. Investigation of biomarker composition of surrounding surfaces and enclosing sedimentary rocks allowed not only to subtract the background signal, but also to make sure that the biomarker signal from the fossils is not contaminated (Supplementary Text) Biomarkers were analysed using gas chromatography-mass spectrometry (see Methods).

The deposits immediately above and below *Dickinsonia* are characterized by a monoaromatic steroid distribution of 10.6–11.9% cholesteroloids, 13.4–16.8% ergosteroids and 71.3–76.0% stigmasteroids, consistent with the general steroid distribution of sediments at the Lyamtsa locality (Fig. 1). The strong stigmasteroid predominance is typical for the Ediacaran period and presumably related to green algae (Chlorophyta) inhabiting benthic mats or the water column (25). In these and all other Ediacaran sediment samples from the White Sea region, the carbon-number distribution of saturated steranes is nearly identical to the distribution of monoaromatic steroid homologues and always dominated by green algal stigmasteroids (Table 1). In stark contrast, biomarkers extracted from the isolated organic matter of the largest *Dickinsonia* specimen had a monoaromatic steroid distribution of 93% cholesteroloids, 1.8% ergosteroids and 5.2% stigmasteroids (Table 1, Fig. 1A). A general trend of increasing monoaromatic cholesteroloid abundance from 84.8% to 93.0% from the smaller to the larger *Dickinsonia* specimens (Fig. 1D), reflects decreasing contribution of the green algal background signal (Fig. S2).

The striking abundance of cholesteroloids in *Dickinsonia* is corroborated by an unusual sterane isomer distribution. In sediments surrounding the fossils in Lyamtsa and Zinnie Gory localities, the ratio of 5β over 5α stereoisomers for all steranes is generally near the equilibrium diagnostic for abiological isomerization (average $5\beta/5\alpha = 0.65 \pm 0.26$, $n = 54$, Figs. 1D,E). By contrast, in the fossils, $5\beta/5\alpha$ of cholestane is markedly elevated, up to 5.5 in *Dickinsonia* (Table 1, Figs. 1C,D,E), values that are generated by strictly anaerobic microbial activity (26, 27) such as during the decay of carcasses. Though gut flora of some mammals are known to produce 5β -stanols (precursors of 5β -steranes) (28), high relative abundance of these molecules in some background sediments (Fig. 1E) and macroalgae (17) from the White Sea contests the otherwise exciting possibility that 5β -steranes originated from *Dickinsonia*’s gut microbiota (see Supplementary Text). Notably, 5β ergostanes and stigmastanes in the *Dickinsonia* extracts are not elevated (Table 1), demonstrating that they are ultimately not derived from dickinsoniids but from the underlying microbial mat or surrounding sediment (Fig. S2). Based on these steroid homologue and isomer patterns, we compute that the sterols

of living *Dickinsonia* consisted of at least 99.7% cholesteroloids (Supplementary Information). Within analytical precision, it is impossible to exclude that *Dickinsonia* produced traces of ergosteroids (up to 0.23%) or stigmasteroids (up to 0.07%). Such steroids, if present, may be derived from the organism itself, but could also represent dietary uptake or contributions from symbionts.

Biomarker signatures of *Andiva* specimens from the Zimmie Gory locality are less well differentiated from the microbial mat background signal and do not display a clear elevation of cholesteroloids relative to the background (Table 1). Yet, even in these fossils, $5\beta/5\alpha$ ratios for cholestanes are significantly higher ($5\beta/5\alpha = 1.02\text{--}1.31$) when compared to ergostanes and stigmastanes from the fossil extract ($5\beta/5\alpha = 0.52\text{--}0.66$) and the surrounding mat ($5\beta/5\alpha = 0.65\text{--}0.81$; Table 1). Based on these values we can compute a conservative minimum C_{27} sterol content of 88.1% for *Andiva* (Supplementary Text).

Using the remarkable steroid patterns of the fossils, it is possible to test the position of dickinsoniids on the phylogenetic tree. Lichen-forming fungi only produce ergosteroids, and even in those that host symbiotic algae, ergosteroids remain the major sterols (29, 30). *Dickinsonia* contained no, or a maximum of only 0.23% ergosteroids, conclusively refuting the lichen hypothesis (7). The groups of rhizarian protists that include gigantic representatives (Gromiidae, Xenophyophorea and other Foraminifera), and their retarian relatives, all produce a complex mixture of sterols, with cholesteroloids comprising 10.3 to 78.2% of the mixture, ergosteroids 4.9 to 43.0% and stigmasteroids 7.2 to 60.1% (Table S4). Moreover, rhizarian protists may produce C_{30} sterols (24*n*-propylcholestane) that can form a significant (up to around 20%) proportion of their total sterol content (31). By contrast, in most *Dickinsonia* and *Andiva* extracts, C_{30} steroids were below detection limits. Thus, the steroid composition of dickinsoniids is markedly distinct from steroid distributions observed in Rhizaria, rendering a protozoan affinity of these fossils extremely unlikely. All animals, with rare exceptions such as some demosponges and bivalve molluscs, are characterised by exclusive production of C_{27} sterols (32, 33). The closest relatives of metazoans, *Choanoflagellata* and *Filasterea*, produce 90–100% and 84–100% of cholesterol, respectively, and contain up to 16% ergosteroids (34–36). While the sterol composition of some choanoflagellates and filastereans falls within the range observed for *Dickinsonia* and *Andiva*, they are unlikely precursor candidates since these groups are only ever represented by microscopic organisms, leaving a stem- or crown-group metazoan affinity as the only plausible phylogenetic position for *Dickinsonia* and its morphological relatives.

Molecular fossils firmly place dickinsoniids within the animal kingdom, establishing *Dickinsonia* as the oldest confirmed macroscopic animals in the fossil record (558 Ma) next to marginally younger *Kimberella* from Zimmie Gory (555 Ma) (37). However alien they looked, the presence of large dickinsoniid animals, reaching 1.4 m in size (38), reveals that the appearance of the Ediacara biota in the fossil record is not an independent experiment in large body size but indeed a prelude to the Cambrian explosion of animal life.

References and Notes

1. R. C. Sprigg, Early Cambrian (?) jellyfishes from the Flinders Ranges, South Australia. *Transactions of the Royal Society of South Australia* **71**, 212-224 (1947).
2. M. F. Glaessner, *The dawn of animal life: a biohistorical study*. (Cambridge University Press, Cambridge, UK, 1984), pp. 244.
3. G. M. Narbonne, Modular Construction of Early Ediacaran Complex Life Forms. *Science* **305**, 1141-1144 (2004).
4. S. Xiao, M. Laflamme, On the eve of animal radiation: phylogeny, ecology and evolution of the Ediacara biota. *Trends Ecol Evol* **24**, 31-40 (2009).
5. M. Steiner, J. Reitner, Evidence of organic structures in Ediacara-type fossils and associated microbial mats. *Geology* **29**, 1119-1122 (2001).
6. K. J. Peterson, B. Waggoner, J. W. Hagadorn, A Fungal Analog for Newfoundland Ediacaran Fossils? *Integrative and Comparative Biology* **43**, 127-136 (2003).
7. G. J. Retallack, Ediacaran life on land. *Nature* **493**, 89-92 (2013).
8. A. Seilacher, The nature of vendobionts. *Geological Society, London, Special Publications* **286**, 387-397 (2007).
9. A. Y. Zhuravlev, Were Ediacaran Vendobionta multicellulars? *Neues Jahrbuch für Geologie und Paläontologie, Abhandlungen* **190**, 299-314 (1993).
10. G. M. Narbonne, THE EDIACARA BIOTA: Neoproterozoic Origin of Animals and Their Ecosystems. *Annual Review of Earth and Planetary Sciences* **33**, 421-442 (2005).
11. S. D. Evans, M. L. Droser, J. G. Gehling, Highly regulated growth and development of the Ediacara macrofossil Dickinsonia costata. *PLOS ONE* **12**, e0176874 (2017).
12. D. Grazhdankin, in *Encyclopedia of Geobiology*, J. Reitner, V. Thiel, Eds. (Springer Netherlands, Dordrecht, 2011), pp. 342-348.
13. D. H. Erwin *et al.*, The Cambrian Conundrum: Early Divergence and Later Ecological Success in the Early History of Animals. *Science* **334**, 1091-1097 (2011).
14. M. A. Fedonkin, B. M. Waggoner, The Late Precambrian fossil Kimberella is a mollusc-like bilaterian organism. *Nature* **388**, 868 (1997).
15. A. Y. Ivantsov, Trace fossils of precambrian metazoans “Vendobionta” and “Mollusks”. *Stratigraphy and Geological Correlation* **21**, 252-264 (2013).
16. J. B. Antcliff, A. J. Gooday, M. D. Brasier, Testing the protozoan hypothesis for Ediacaran fossils: a developmental analysis of Palaeopascichnus. *Palaeontology* **54**, 1157-1175 (2011).
17. I. Bobrovskiy, J. M. Hope, A. Krasnova, A. Ivantsov, J. J. Brocks, Molecular fossils from organically preserved Ediacara biota reveal cyanobacterial origin for *Beltanelliformis*. *Nature Ecology & Evolution*, (2018).
18. S. Xiao *et al.*, Affirming life aquatic for the Ediacara biota in China and Australia. *Geology* **41**, 1095-1098 (2013).
19. M. L. Droser, J. G. Gehling, The advent of animals: The view from the Ediacaran. *Proceedings of the National Academy of Sciences* **112**, 4865-4870 (2015).
20. D. Grazhdankin, Patterns of Evolution of the Ediacaran Soft-Bodied Biota. *Journal of Paleontology* **88**, 269-283 (2014).
21. A. J. Gooday *et al.*, Giant protists (xenophyophores, Foraminifera) are exceptionally diverse in parts of the abyssal eastern Pacific licensed for polymetallic nodule exploration. *Biological Conservation* **207**, 106-116 (2017).

22. M. V. Matz, T. M. Frank, N. J. Marshall, E. A. Widder, S. Johnsen, Giant Deep-Sea Protist Produces Bilaterian-like Traces. *Current Biology* **18**, 1849-1854 (2008).
23. E. A. Sperling, J. Vinther, A placozoan affinity for Dickinsonia and the evolution of late Proterozoic metazoan feeding modes. *Evolution & Development* **12**, 201-209 (2010).
24. J. K. Volkman, Sterols and other triterpenoids: source specificity and evolution of biosynthetic pathways. *Organic Geochemistry* **36**, 139-159 (2005).
25. R. B. Kodner, A. Pearson, R. E. Summons, A. H. Knoll, Sterols in red and green algae: quantification, phylogeny, and relevance for the interpretation of geologic steranes. *Geobiology* **6**, 411-420 (2008).
26. T. M. Peakman, J. W. De Leeuw, W. I. C. Rijpstra, Identification and origin of $\Delta 8(14)5\alpha$ - and $\Delta 14 5\alpha$ -sterenes and related hydrocarbons in an immature bitumen from the Monterey Formation, California. *Geochimica et Cosmochimica Acta* **56**, 1223-1230 (1992).
27. S. J. Gaskell, G. Eglinton, Sterols of a contemporary lacustrine sediment. *Geochimica et Cosmochimica Acta* **40**, 1221-1228 (1976).
28. I. D. Bull, M. J. Lockheart, M. M. Elhmmali, D. J. Roberts, R. P. Evershed, The origin of faeces by means of biomarker detection. *Environment international* **27**, 647-654 (2002).
29. J. D. Weete, M. Abril, M. Blackwell, Phylogenetic distribution of fungal sterols. *PLoS One* **5**, e10899 (2010).
30. S. Safe, L. M. Safe, W. S. G. Maass, Sterols of three lichen species: *Lobaria pulmonaria*, *Lobaria Scrobiculata* and *Usnea Longissima*. *Phytochemistry* **14**, 1821-1823 (1975).
31. J. Grabenstatter *et al.*, Identification of 24-n-propylidenecholesterol in a member of the Foraminifera. *Organic geochemistry* **63**, 145-151 (2013).
32. A. Kanazawa, Sterols in marine invertebrates. *Fisheries Science* **67**, 997-1007 (2001).
33. G. D. Love *et al.*, Fossil steroids record the appearance of Demospongiae during the Cryogenian period. *Nature* **457**, 718-721 (2009).
34. R. B. Kodner, R. E. Summons, A. Pearson, N. King, A. H. Knoll, Sterols in a unicellular relative of the metazoans. *Proc Natl Acad Sci U S A* **105**, 9897-9902 (2008).
35. D. A. Gold *et al.*, Sterol and genomic analyses validate the sponge biomarker hypothesis. *Proceedings of the National Academy of Sciences* **113**, 2684-2689 (2016).
36. S. R. Najle, M. C. Molina, I. Ruiz-Trillo, A. D. Uttaro, Sterol metabolism in the filasterean *Capsaspora owczarzaki* has features that resemble both fungi and animals. *Open Biology* **6**, (2016).
37. D. Grazhdankin, Patterns of distribution in the Ediacaran biotas: facies versus biogeography and evolution. *Paleobiology* **30**, 203-221 (2004).
38. R. Jenkins, Aspects of the geological setting and palaeobiology of the Ediacara assemblage. *Natural history of the flinders ranges* **7**, 33-45 (1996).
39. J. J. Brocks, E. Grosjean, G. A. Logan, Assessing biomarker syngeneity using branched alkanes with quaternary carbon (BAQCs) and other plastic contaminants. *Geochimica et Cosmochimica Acta* **72**, 871-888 (2008).
40. A. J. M. Jarrett, R. Schinteie, J. M. Hope, J. J. Brocks, Micro-ablation, a new technique to remove drilling fluids and other contaminants from fragmented and fissile rock material. *Organic Geochemistry* **61**, 57-65 (2013).

41. J. J. Brocks, J. M. Hope, Tailing of Chromatographic Peaks in GC–MS Caused by Interaction of Halogenated Solvents with the Ion Source. *Journal of Chromatographic Science* **52**, 471-475 (2014).
42. I. Björkhem, J.-Å. Gustafsson, Mechanism of Microbial Transformation of Cholesterol into Coprostanol. *European Journal of Biochemistry* **21**, 428-432 (1971).
43. F. Zollo, E. Finamore, D. Gargiulo, R. Riccio, L. Minale, Marine sterols. Coprostanols and 4 α -methyl sterols from mediterranean tunicates. *Comparative Biochemistry and Physiology Part B: Comparative Biochemistry* **85**, 559-560 (1986).
44. T. S. Milkova, S. S. Popov, N. L. Marekov, S. N. Andreev, Sterols from black sea invertebrates—I. Sterols from Scyphozoa and Anthozoa (Coelenterata). *Comparative Biochemistry and Physiology Part B: Comparative Biochemistry* **67**, 633-638 (1980).
45. S. B. Seidel, J. R. Proudfoot, C. Djerassi, D. Sica, G. Sodano, Minor and trace sterols from marine invertebrates 56. Novel coprostanols from the marine sponge petrosia ficiformis. *Steroids* **47**, 49-62 (1986).
46. R. C. Janaway, S. L. Percival, A. S. Wilson, in *Microbiology and Aging: Clinical Manifestations*, S. L. Percival, Ed. (Humana Press, Totowa, NJ, 2009), pp. 313-334.
47. H. Gill-King, Chemical and ultrastructural aspects of decomposition. *Forensic taphonomy: The postmortem fate of human remains*, 93-108 (1997).
48. A. Y. Ivantsov, Feeding traces of proarticulata—the Vendian metazoa. *Paleontological Journal* **45**, 237-248 (2011).
49. J. N. Ricci, R. Morton, G. Kulkarni, M. L. Summers, D. K. Newman, Hopanoids play a role in stress tolerance and nutrient storage in the cyanobacterium *Nostoc punctiforme*. *Geobiology*, n/a-n/a (2016).
50. R. E. Summons, L. L. Jahnke, J. M. Hope, G. A. Logan, 2-Methylhopanoids as biomarkers for cyanobacterial oxygenic photosynthesis. *Nature* **400**, 554-557 (1999).
51. P. V. Welander, M. L. Coleman, A. L. Sessions, R. E. Summons, D. K. Newman, Identification of a methylase required for 2-methylhopanoid production and implications for the interpretation of sedimentary hopanes. *Proceedings of the National Academy of Sciences* **107**, 8537-8542 (2010).
52. M. Rohmer, P. Bouvier-Nave, G. Ourisson, Distribution of Hopanoid Triterpenes in Prokaryotes. *Microbiology* **130**, 1137-1150 (1984).
53. J. N. Ricci *et al.*, Diverse capacity for 2-methylhopanoid production correlates with a specific ecological niche. *ISME J* **8**, 675-684 (2014).
54. K. Peters, C. Walters, J. Moldowan, *The Biomarker Guide. Volume 2. Biomarkers and Isotopes in Petroleum Systems and Earth History*. (Cambridge University Press, New York, ed. 2nd, 2005), pp. 634.
55. Y. V. Kissin, Catagenesis and composition of petroleum: Origin of n-alkanes and isoalkanes in petroleum crudes. *Geochimica et Cosmochimica Acta* **51**, 2445-2457 (1987).

Acknowledgments: We thank E. Luzhnaya, A. Krasnova, A. Nagovitsyn, P. Rychkov, V. Rychkov and S. Rychkov for their help with collecting Ediacaran fossils, E. Golubkova with organizing one of the field trips, P. Pringle and R. Tarozo for laboratory support, F. Not, C. Schmidt, R. Schiebel, P. De Deckker, S. Eggins, J. Pawlowski, S. S. Bowser and M. Stuhr for rhizarian specimens; **Funding:** The study is funded by Australian Research Council grants DP160100607 and DP170100556 (to J.J.B.), Russian Foundation for Basic Research project

No. 17-05-02212A (A.I. and I.B) and the Max-Planck-Society (C.H.). I.B. gratefully acknowledges an Australian Government Research Training Program stipend scholarship, and B.J.N. a Geobiology fellowship of the Agouron Institute. **Author contributions:** I.B. designed the study and analysed biomarkers from Ediacaran fossils, J.M.H. helped with biomarker analysis, I.B. and A.I. collected fossils, B.J.N., C.H., J.M.H. and J.J.B. analysed modern Rhizaria, I.B. and J.J.B. interpreted data and wrote the manuscript with contributions from all authors; **Competing interests:** Authors declare no competing interests; **Data and materials availability:** All data required to understand and assess the conclusions of this research are available in the main text and supplementary materials.

Supplementary Materials:

Materials and Methods

Supplementary Text

Figs. S1 to S6

Tables S1 to S4

References (39-55)

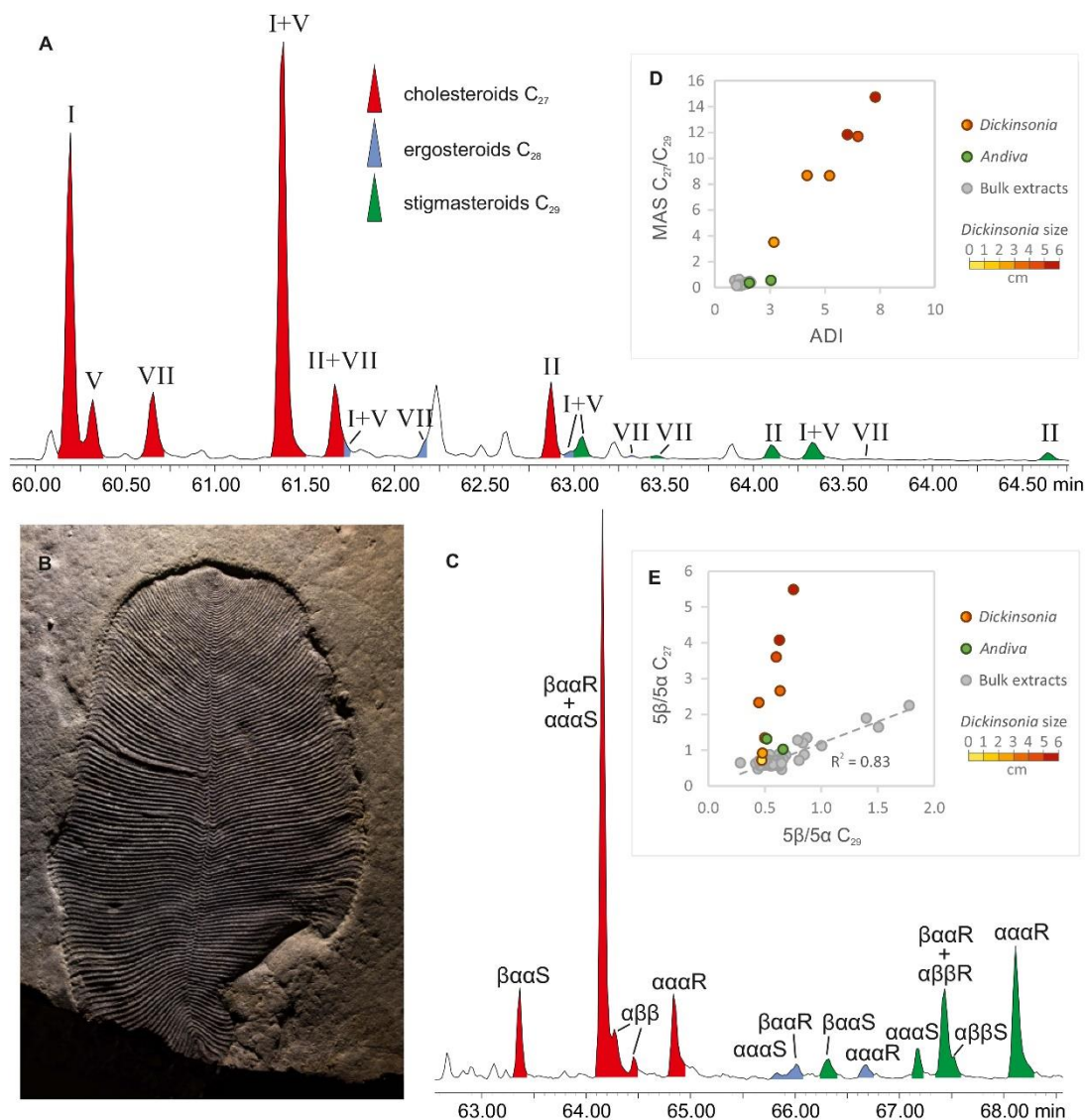


Fig. 1. Biomarkers from organically preserved *Dickinsonia*. (A) m/z 253 selected ion recording (SIR) chromatogram showing the distribution of monoaromatic steroids (MAS) of the solvent extract of a large *Dickinsonia* specimen (*Dickinsonia*-2; 5.5 cm width); (B) organically preserved *Dickinsonia* from the Lyamtsa locality (*Dickinsonia*-2); (C) metastable reaction monitoring (MRM) chromatogram showing the sum of C_{27-29} sterane traces of *Dickinsonia*-2; $\alpha\beta\beta = 5\alpha(H), 14\beta(H), 17\beta(H)$ (and correspondingly for $\alpha\alpha\alpha$ and $\beta\alpha\alpha$), S and R indicates isomerisation at position C-20; (D) relationship between the MAS C_{27}/MAS C_{29} ratio and the Animal Decomposition Index $ADI = (C_{27} 5\beta/5\alpha)/(C_{29} 5\beta/5\alpha)$ in *Dickinsonia* ($n = 6$), *Andiva* ($n = 2$) and bulk rock extracts from the Lyamtsa and Zimmie Gory localities ($n = 32$); only samples with detectable MAS were used in the plot; ADI is a measure of the quantity of sterols that decomposed in the anaerobic microenvironment of an animal carcass relative to normal sterol decomposition within the background sediment. $ADI \approx 1$ indicates that cholesteroids and stigmasteroids underwent alteration in the same diagenetic environment consistent with the absence of animal tissue. $ADI > 1$ indicates contribution of animal steroids to the biomarker signal. (E) Relationship between the $5\beta/5\alpha$ sterane isomer ratio for cholestane (C_{27}) and stigmastane (C_{29}) in *Dickinsonia* ($n = 8$), *Andiva* ($n = 2$) and bulk rock extracts from the Lyamtsa and Zimmie Gory localities ($n = 54$); $5\beta/5\alpha = (\beta\alpha\alpha$

20R+ $\alpha\alpha\alpha$ 20S)/ $\alpha\alpha\alpha$ 20R. MAS structures: I = 5 β (H)10 β (CH₃), II = 5 α (H)10 β (CH₃), V = 5 β (CH₃)10 β (H), VII = 5 α (CH₃)10 α (H).

Sample	Locality	Size (width, cm)	Saturated steranes								Monoaromatic steroids ⁴			
			C ₂₇ %	C ₂₈ %	C ₂₉ %	C ₃₀ % ¹	C ₂₇ 5 β /5 α ²	C ₂₈ 5 β /5 α ²	C ₂₉ 5 β /5 α ²	ADI ³	C ₂₇ %	C ₂₈ %	C ₂₉ %	C ₂₇ /C ₂₉
<i>Dickinsonia-1</i>	Lyamtsa	6.0	48.1 (1.3) ⁵	5.7 (0.2)	45.8 (1.2)	0.4 (0.04)	3.61 (0.21)	0.52 (0.34)	0.60 (0.06)	6.01 (0.67)	92.4 (2.5)	2.1 (0.1)	5.5 (0.3)	11.84 (0.93)
<i>Dickinsonia-2</i>	Lyamtsa	5.5	63.2 (1.5)	4.9 (0.2)	31.9 (0.8)	0 {0.05} ⁶	5.49 (0.28)	0.65 (0.34)	0.75 (0.06)	7.28 (0.65)	93.0 (2.3)	1.8 (0.1)	5.2 (0.3)	14.75 (0.91)
<i>Dickinsonia-3</i>	Lyamtsa	4.5	47.9 (1.5)	6.1 (0.3)	46.0 (1.4)	0 {0.03}	4.08 (0.29)	0.75 (0.34)	0.63 (0.04)	6.50 (0.64)	92.5 (3.2)	2.7 (0.2)	4.8 (0.3)	11.71 (1.41)
<i>Dickinsonia-4</i>	Lyamtsa	4.0	33.4 (2.2)	8.0 (0.7)	58.5 (3.5)	0 {0.08}	2.66 (0.41)	0.97 (0.34)	0.64 (0.08)	4.18 (0.83)	87.9 (6.4)	4.8 (0.7)	7.3 (0.9)	8.67 (1.59)
<i>Dickinsonia-5</i>	Lyamtsa	4.0	44.8 (0.9)	7.6 (0.4)	47.6 (1.0)	0 {0.01}	2.33 (0.10)	0.81 (0.34)	0.45 (0.02)	5.21 (0.32)	91.3 (4.5)	3.6 (0.4)	5.1 (0.5)	8.66 (1.81)
<i>Dickinsonia-6</i>	Lyamtsa	3.5	27.5 (0.7)	9.9 (0.5)	62.6 (1.3)	0 {0.04}	1.34 (0.07)	0.79 (0.34)	0.50 (0.02)	2.67 (0.18)	84.8 (5.7)	3.4 (0.5)	11.8 (1.2)	3.51 (0.80)
<i>Dickinsonia-7</i>	Lyamtsa	1.0	17.2 (1.2)	6.9 (1.2)	75.9 (3.6)	0 {0.18}	0.71 (0.10)	0.22 (0.34)	0.47 (0.05)	1.49 (0.26)	-	-	-	-
<i>Dickinsonia-8</i>	Lyamtsa	2.5	20.5 (1.3)	6.7 (1.2)	72.7 (3.6)	0 {0.10}	0.91 (0.13)	0.26 (0.34)	0.48 (0.05)	1.89 (0.32)	-	-	-	-
<i>Dickinsonia-Sandstone</i>	Lyamtsa	-	11.6 (0.3)	8.9 (0.2)	78.9 (1.2)	0.6 (0.04)	0.64 (0.04)	0.85 (0.34)	0.52 (0.02)	1.23 (0.08)	11.9 (1.0)	16.8 (1.5)	71.3 (4.4)	0.17 (0.01)
<i>Dickinsonia-Clay</i>	Lyamtsa	-	9.7 (0.3)	7.8 (0.2)	82.0 (1.3)	0.5 (0.03)	0.61 (0.03)	0.71 (0.34)	0.59 (0.02)	1.03 (0.07)	10.6 (0.7)	13.4 (0.9)	76.0 (3.3)	0.2 (0.01)
<i>Andiva-1</i>	Zimnie Gory	8.0	24 (0.4)	10.3 (0.3)	64.3 (0.9)	1.3 (0.1)	1.07 (0.04)	0.76 (0.34)	0.68 (0.02)	1.55 (0.07)	21.5 (0.8)	17.5 (0.7)	61.0 (1.9)	0.36 (0.01)
<i>Andiva-2</i>	Zimnie Gory	4.0	24.9 (1.2)	12.2 (1.2)	61.8 (2.7)	1.0 (0.2)	1.31 (0.15)	0.81 (0.34)	0.52 (0.04)	2.54 (0.36)	29.3 (2.6)	12.6 (1.4)	58.1 (4.5)	0.55 (0.05)
<i>Andiva Mat</i>	Zimnie Gory	-	25.8 (1.0)	15.8 (1.0)	57.4 (1.9)	1.0 (0.1)	0.80 (0.07)	0.96 (0.34)	0.65 (0.04)	1.24 (0.13)	18.7 (1.4)	21.4 (1.6)	59.8 (3.5)	0.35 (0.02)
<i>Andiva-Sandstone</i>	Zimnie Gory	-	37.5 (1.0)	10.5 (0.3)	51.6 (1.3)	0.5 (0.04)	0.65 (0.04)	0.91 (0.34)	0.61 (0.03)	1.08 (0.08)	25.6 (1.7)	15.7 (1.2)	58.7 (3.4)	0.43 (0.03)
<i>Andiva-Clay</i>	Zimnie Gory	-	23.1 (0.5)	9.5 (0.3)	65.9 (1.3)	1.5 (0.02)	0.86 (0.04)	0.84 (0.34)	0.68 (0.02)	1.26 (0.07)	19.4 (1.6)	11.2 (1.2)	69.4 (4.7)	0.28 (0.02)

Table 1. Steroid distributions in *Dickinsonia* and *Andiva* extracts.

¹C₃₀ steranes are only represented by 24-isopropylcholestanes; ²5 β /5 α = ($\beta\alpha\alpha$ 20R+ $\alpha\alpha\alpha$ 20S)/ $\alpha\alpha\alpha$ 20R; ³Animal Decomposition Index ADI = (C₂₇ 5 β /5 α)/(C₂₉ 5 β /5 α) (see Figure 1 caption); ⁴only the I and V monoaromatic steroid isomers (see Figure 1 for nomenclature) were used for all computations as they display the least coelution with other peaks on the chromatogram; ⁵numbers in parentheses are standard deviation values; ⁶numbers in braces ‘{ }’ next to zero values represents the detection limit, i.e. the maximum of a given compound that may be present when not detected.



Supplementary Materials for

Ancient steroids establish the Ediacaran fossil *Dickinsonia* as one of the earliest animals

Ilya Bobrovskiy*, Janet M. Hope, Andrey Ivantsov, Benjamin J. Nettersheim, Christian Hallman, Jochen J. Brocks*

*Correspondence to: ilya.bobrovskiy@anu.edu.au, jochen.brocks@anu.edu.au

This PDF file includes:

Materials and Methods
Supplementary Text
Figs. S1 to S6
Tables S1 to S4

Materials and Methods

Sample collection

Biomarker analyses were conducted on organically preserved macrofossils *Dickinsonia* and *Andiva* (Fig. 1; Fig. S1), microbial mats surrounding the fossils, and bulk extracts of sedimentary rocks enclosing the fossils. Samples were collected during fieldwork in the Lyamtsa and Zimmie Gory localities of the Ediacara Biota in the White Sea Region (Russia) in 2015–2017 specifically for biomarker analysis. *Dickinsonia* (8 specimens) come from a surface in the lower part of the Lyamtsa Beds (Ust-Pinega Formation, Redkino Regional Stage), exposed to the south of Lyamtsa Village. The fossils were underlain by clay with mm-thick lenses of siltstone and sandstone, and buried under 30 cm-thick sandstone layer, composed of thinner (5-10 cm) beds with hummocky cross-stratification, separated by microbially induced wrinkle structures. *Andiva* (2 specimens) were collected from a surface in the lower part of the Erga Beds (Mezen Formation, Kotlin Regional Stage). The fossils were also underlain by clay with mm-thick lenses of siltstone and sandstone and covered with 40-60 cm thick lenses of massive sandstone with soft sediment deformations and thick (up to 5 cm thick) load cracks at the bottom. Samples used for determining the background signal ($n=54$) were collected from Lyamtsa and Verkhovka Beds (Ust-Pinega Formation, Redkino Regional Stage) of the Lyamtsa locality and from Vaysitsa, Zimmie Gory (Ust-Pinega Formation, Redkino Regional Stage) and Erga Beds (Mezen Formation, Kotlin Regional Stage) of the Zimmie Gory locality. All samples were collected avoiding weathered zones and cracks and were immediately wrapped in pre-combusted aluminium foil (300°C, 9h) and packed in calico cotton bags under strict avoidance of contamination (17).

Sterol signatures of rhizarian protists were determined on natural specimens. *Sorites* sp. and *Amphistegina lobifera* were collected attached to pebbles by snorkelling in shallow water 1-3 m in Eilat, Israel and subsequently kept under controlled laboratory conditions for four months until they were handpicked again and cleaned with a brush prior to laboratory analyses. The two Foraminifera *Shepherdella* sp. (collected at the Gulf of Eilat) and *Quinqueloculina* sp. (collected at the Mediterranean coast of Tel Aviv, Israel) were extracted shortly after collection in the field after separation and cleaning with tweezers and brushes. Brightly orange *Shepherdella* sp. allogromid Foraminifera were picked from rocks and sea-grass. Collodarian radiolarians were handpicked from the contents of a plankton net collected from surface waters in the Villefranche sur Mer bay (France). *Gromia* sp. were collected by Scuba Divers from the bottom sediments at the McMurdo Station jetty in Antarctica and pickled in ethanol. A bulk *Acantharea* sample was collected using a plankton tow net during a bloom event of *Acantharea* sp. in the shallow Twofold Bay near Eden, SE Australia that is open to the Tasman Sea. After collection, the sample was washed with freshwater and pickled in 100% ethanol, then kept frozen until analysis at the Australian National University.

Fossils characteristics

The thickness of organic matter of *Dickinsonia* was estimated based on a thin section made through one of the fossil specimens. The size of fossil specimens was determined based on their width as most of the analysed specimens were not complete and lacked either of their

ends. These size measurements are estimates as all dickinsoniids were deformed before or during burial.

Sample preparation and extraction

Organic matter of the fossils was separated from the sandstone surface using 5% hydrochloric acid (several drops on the surface of a fossil) and 30% hydrofluoric acid (several drops on the surface of a fossil, followed by drying, repeated two times). Fossils were then placed into a glass beaker filled with water to remove acid, allowing most of organic matter to detach from remaining inorganic components of the fossils. Any remaining organic matter attached to the rock was separated with a scalpel. Combined organic matter was neutralized in deionized (Millipore Elix 3UV, France) water under ultrasonic agitation and subsequently centrifuged (3 times) to remove remaining acids. Hydrocarbons were extracted from the organic matter via ultrasonic agitation in solvents (methanol for 30 min, dichloromethane (DCM) for 15 min (x 2), DCM : *n*-hexane 1 : 1 for 15 min). All solvents were 99.9% grade (UltimAR®; Mallinckrodt Chemicals, St. Louis, MO, USA). Glassware was cleaned by combustion at 300°C for 9 h.

Bulk sedimentary samples (represented by clay, heterolithic interlamination and sandstones) were analysed using the so-called Exterior-Interior protocol described in detail elsewhere (17, 39, 40). Briefly, exterior ('E') 3–4 mm of rock samples were removed using a micro drill (Dremel® 400 Series Digital, Mexico) with a solvent cleaned saw nozzle. Analysis of the last saw-blade solvent rinse confirmed that it was free of detectable contaminants. The exterior and the interior portions of each sample were ground to powder (>240 mesh) using a steel puck mill (Rocklabs Ltd., Onehunga, New Zealand). The mill was cleaned using methanol and dichloromethane, and by grinding combusted (600°C, 9 h) quartz sand.

Bitumen was extracted from rock powder using an Accelerated Solvent Extractor (ASE 200, Dionex, USA) with DCM : methanol (9:1), reduced to 100 µL under a stream of nitrogen gas, and then fractionated into saturated, aromatic and polar fractions using micro-column chromatography over annealed (300°C; 12 h) and dry packed silica gel (Silica Gel 60; 230–600 mesh; EM Science). Saturated hydrocarbons were eluted with 1 dead volume (DV) of *n*-hexane, aromatic hydrocarbons with 4.5 DV of *n*-hexane : DCM (1 : 1) and the polar fraction with 3 ml DCM : methanol (1 : 1). Extracts from fossils with low hydrocarbon content were only fractionated into saturated+aromatic and polar fractions to reduce the probability of contamination and loss of analytes. An internal standard, 18-MEAME (18-methyleicosanoic acid methylester; Chiron Laboratories AS), was added to the saturated and aromatic fractions, while D4 (*d*₄-C₂₉-αααR-ethylcholestane; Chiron Laboratories AS) was added to saturated and saturated+aromatic hydrocarbon fractions with low biomarker content. The samples were analysed and quantified by GC–MS.

Biomass of rhizarian protists (Extended Data Table 4) was extracted thrice using a modified Bligh and Dyer method (DCM:MeOH:H₂O=1:2:0.4, then 2:2:0.4, then 2:2:1.4) or by ultrasonic agitation in DCM : MeOH (9 : 1). *Gromia* specimens were stored in ethanol after sampling and the ethanol was analysed in the same manner as the other extracts. The total lipid extracts were separated into hydrocarbons (F1), esters and ketones (F2), alcohols (F3) and fatty acids (F4) by small-scale open column chromatography over aminopropyl-substituted silica gel (Chromabond Sorbent NH₂, Macherey-Nagel, Germany; 500 mg in a 6 mL glass SPE

column), where F1 was eluted with 4 mL *n*-hexane, F2 with 6 mL *n*-hexane:DCM (3:1), F3 with 7 mL DCM:acetone (9:1) and F4 with 8 mL DCM containing 2% formic acid. F3 was hydrogenated by bubbling a gentle stream of hydrogen gas into a 4 mL vial filled with *n*-hexane, F3 lipids and platinum (IV) oxide (ca. 7 mg) under stirring for >4h. Converted steranes were purified by eluting with an excess of *n*-hexane over a small chromatographic column filled with activated silica gel. Blank hydrogenations were run before and after samples to assess contamination. *Acantharea* sp. lipids were extracted with a similar modified Bligh and Dyer method, and saponified with 5 % KOH in MeOH : H₂O (8 : 2) and neutral lipids were recovered by addition of H₂O and the same amount of Hex : DCM (4:1), pyrolysed at 320 °C for 21 h in an evacuated glass tube and hydrogenated with PtO₂ overnight.

Gas chromatography–mass spectrometry (GC-MS)

GC-MS analyses of Ediacaran and *Acantharea* extracts were carried out on an Agilent 6890 gas chromatograph coupled to a Micromass Autospec Premier double sector mass spectrometer (Waters Corporation, Milford, MA, USA) at the Australian National University. The GC was equipped with a 60 m DB-5 MS capillary column (0.25 mm i.d., 0.25 µm film thickness; Agilent JW Scientific, Agilent Technologies, Santa Clara, CA, USA), and helium was used as the carrier gas at a constant flow of 1 mL min⁻¹. Samples were injected in splitless mode into a Gerstel PTV injector at 60°C (held for 0.1 min) and heated at 260°C min⁻¹ to 300°C. For full-scan, selected ion recording (SIR) and metastable reaction monitoring (MRM) analyses, the GC oven was programmed from 60°C (held for 4 min) to 315°C at 4°C min⁻¹, with total run time of 100 min. All samples were injected in *n*-hexane to avoid deterioration of chromatographic signals by FeCl₂ build-up in the MS ion source through use of halogenated solvents (41). *n*-Alkanes were quantified in full-scan mode in *m/z* 85 trace, and $\alpha\alpha\alpha$ 20R-stigmastane – in *m/z* 217 trace, relative to the 18-MEAME internal standard (*m/z* 340). Steranes and hopanes were quantified in MRM mode in M⁺ → 217 and M⁺ → 191 transitions respectively relative to $\alpha\alpha\alpha$ 20R-stigmastane. Monoaromatic steroids were quantified in SIR mode using the *m/z* 253 base ion. Peak areas are uncorrected for differences in GC-MS response.

Hydrogenated rhizarian steroids were analysed on a Thermo Quantum XLS Ultra triple quadrupole MS coupled to a Thermo Trace GC at the University of Bremen. The GC was fitted with a VF-1 ms (40m; 0.15 µm; 0.15 mm), DB-XLB (60 m; 0.25 mm; 0.25 µm) or DB-35 ms (60 m; 0.25 mm; 0.25 µm) capillary column and operated under a constant flow (1.3 mL/min.) of helium (99.999% pure, Westfalen AG). Samples were injected in splitless mode using a Thermo PTV injector, while the oven was ramped from 60°C (5 mins. isothermal) to 325°C at 4°/min. and held at final temperature for 25 mins. Electron impact ionization was achieved at 70 eV and 250°C with an emission current of 50 mA. The MS was operated in 0.7 Da resolution (Q1 and Q3) with a cycle time of 0.5 sec, while Q2 was operated with Argon (99.999% pure; Westfalen AG) at a pressure of 1.1 mtorr and varying collision voltages. Analytes were identified in comparison to the NSO-1 oil standard and quantified on characteristic parent-to-daughter ion mass transitions (*m/z* 372, 386, 400 and 414 fragmenting to 217) without correcting for differences in response. Ediacaran biomarker peaks were identified based on relative retention time in comparison with AGSO industrial standard (a standard mixture of oils of different ages) and literature data. Identification of $\beta\alpha\alpha$ sterane isomers was additionally confirmed by mass spectra obtained in full-scan mode.

Error quantification

As repeat injections of fossil extracts were not possible due to the limited abundance of valuable sample material, standard deviations for the concentration of each biomarker were externally determined using the AGSO industrial standard. The main sources of quantification error in extracts are low signal to noise ratios of molecular peaks in mass chromatograms. We explored the relationships between signal/noise ratio and coefficient of variation for our specific GC-MS system for each quantified compound using five repeat injections of the AGSO Standard. MRM signal areas of steranes, hopanes, cheilanthanes and the D4 internal standard were integrated for each repeat run and plotted against the coefficient of variation C_v for the five repeats (Fig. S3; C_v was computed for the ratio of compound signal relative to the highest biomarker peak, $C_{30} 17\alpha(H)21\beta(H)$ hopane). The plot yields a relationship described by the formula $C_v = 186.18x^{-0.31}$ ($R^2 = 0.82$), where x is the integrated peak area. The standard deviation for each GC-MS signal in sample extracts used in this study was calculated based on this relationship ($STD = C_v * \text{signal area}$). For biomarker ratios, error propagation followed standard root mean square error propagation formulae. As an estimate of the maximum content of compounds that were below detection limits, the smallest visible peak in corresponding chromatograms was integrated.

As $\beta\alpha\alpha$ 20R-ergostane (5β) coelutes with two other compounds, $\alpha\alpha\alpha$ 20S-ergostane and an unknown sterane (tentatively identified as a $\beta\alpha\alpha$ 20R-27-nor-sterane), its integration error should be expected to be much higher than the error for peaks that are not coeluting and are mainly controlled by signal/noise ratio. Therefore, we estimated an error by comparing measured and computed values for 5β 20R-ergostane. In bulk extracts, $5\beta/5\alpha$ ratios should theoretically be identical for all three sterane pseudohomologues, i.e. for cholestanes, ergostanes and stigmastanes (26). We thus measured the $5\beta/5\alpha$ ratios of cholestanes and stigmastanes in bulk sediment extracts (Fig. 1E) and used the average of $5\beta/5\alpha$ of cholestanes and stigmastanes in each individual sample to predict a theoretical $5\beta/5\alpha$ value for ergostanes. The average deviation of calculated and measured values across 54 samples was used as the standard deviation for this ratio.

Laboratory system blanks

A comprehensive, accumulatory system blank was performed covering all analytical steps from rock surface removal, extraction, fractionation to instrumental analysis. For this purpose, combusted (600°C, 9 h) sand was used to monitor background contamination during grinding, extraction, and fractionation processes.

Supplementary Text

Biomarker composition of dickinsoniids

5 β /5 α sterane isomers ratio

The elevated 5 β /5 α ratio of cholestane (up to 5.5) detected in all dickinsoniid fossils (Table 1, Figs. 1C,D,E) is rarely observed in nature and the geological record. Yet more unusual, in the dickinsoniids only cholestane 5 β /5 α is elevated while the corresponding ergostane and stigmastane ratios show the typical sedimentary background value 5 β /5 α \approx 0.6. Such a discrepancy between sterane pseudohomologues has, to our knowledge, never been observed before in the fossil record. Under usual sedimentary conditions, the 5 β isomer is generated by hydrogenation of Δ^5 sterenes (sterenes with a double bond in position 5 of the ring system), while 5 α is formed from Δ^4 sterenes. The biological configuration of most biological sterols is Δ^5 . However, due to double bond isomerisation between the Δ^5 and Δ^4 positions, the equilibrium ratio between the 5 β and 5 α sterane isomers in an abiological thermodynamically driven system is $\Delta^5 \rightarrow 5\beta : \Delta^4 \rightarrow 5\alpha = 39:61$, resulting in 5 β /5 α = 0.64 (26). This proportion is characteristic of bulk rock extracts from the White Sea Area (average 5 β /5 α = 0.64 \pm 0.26, n = 54), but is much lower than 5 β /5 α cholestane ratios in all dickinsoniid fossils. An origin of such elevated 5 β /5 α sterane ratios as observed in *Dickinsonia* can be explained by microbial or dietary hydrogenation of unsaturated sterols to 5 β -stanols, common under strictly anaerobic conditions, and their further dehydration to Δ^3 5 β -sterenes and subsequent reduction to 5 β -steranes (26, 27, 42). These processes, when occurring within sediment, affect all steroid pseudohomologs equally, regardless of side chain methylation (26). In order to create the elevated 5 β /5 α cholestane ratio observed in the dickinsoniid extracts, only C₂₇ sterols could have been subject to this mode of decay in a strongly anaerobic microenvironment. Sterols from the surroundings of the fossils were degraded under different taphonomic conditions, allowing us to discern the signal of fossils and background.

In principle, the elevated 5 β /5 α cholestane ratios and the strong aromatization of cholesteroloids (Table 1) in dickinsoniids may arise from the presence of an unusual C₂₇ steroid, e.g. possessing multiple unsaturations. Additionally, the gut microbiota of some mammals, including humans, transforms cholesterol to coprostanol (5 β -cholestanol) (28), resulting in the formation of 5 β -steranes during diagenesis. Thus, it is tempting to speculate that dickinsoniids possessed a gut or other digestive systems, and also microbiota responsible for this process. However, elevated 5 β /5 α ratios were also detected for C₂₇ to C₂₉ steranes in some sediment extracts (5 β /5 α = up to 2.3; Fig. 1E) and in Ediacaran macroalgae from the White Sea with 5 β /5 α as high as 3.7 for cholestane, ergostane and stigmastane (Fig. S4) (17). The data show that elevated 5 β /5 α ratios form in sedimentary environments during decomposition of organic matter, and that these processes are not restricted to Ediacaran microfossils.

The elevated 5 β /5 α cholestane ratio in dickinsoniid fossil extracts is consistent with an origin from decomposing animal tissues. The occurrence of 5 β -stanols has been recorded even in freshly collected marine animals on initial stages of decomposition (43, 44). In such cases, formation of 5 β -stanols can be connected with microbial transformation of animal tissue, independent of the structure of the precursor sterol. For instance, in decaying sponges, unusual sponge sterols were also found to be affected by this process, resulting in formation of 5 β -

dihydro stanols (45). Anaerobic degradation of lipids via hydrogenation also dominates in human remains, which is well studied in forensic taphonomy (46, 47).

Determination of exact sterol composition of Dickinsonia

Dickinsoniids inhabited a sea floor covered by microbial mats (Fig. 1B, Figs. S1,S2). Such microbial mats presumably developed over weeks, months or even years, accumulating senescent biomass of mat inhabitants and plankton. After burial by mud or sand, the organic matter of mats, plankton and dickinsoniids fused (Figs. S2A,B,C), making it impossible to physically separate the biomass. Thus, to determine the molecular composition of dickinsoniids, the molecular signal from the underlying mat needs to be separately determined and subtracted.

The determination of the background signal coming from the mat is a technical challenge. Measurement of the molecular signal of the mat directly surrounding the fossils (e.g. Fig. S1A) yielded extracts with extremely low signal/noise ratios (Table 1) and thus intolerably high propagated errors, or did not yield any detectable biomarkers. Moreover, it was unclear whether decaying and liquefied biomass from dickinsoniids would spill along the bedding plane, creating a halo around the carcass and affecting the taphonomy of molecules that do not belong to the organism. Furthermore, dickinsoniid fossils may contain dietary organic matter ('gut content', if dickinsoniids had a gut (48)), and this organic matter would be transformed in similar microenvironments as indigenous dickinsoniid tissue, complicating the signal further.

Variations in steroid composition of the extracts of different *Dickinsonia* specimens can be described by a two-component mixing system curve as a result of mixing between the steroids of the background signal and steroids directly derived from *Dickinsonia* (Fig. S2D). The mixing scenario is generally described by $x = n \cdot x_1 + (1-n) \cdot x_2$ where x is the concentration of a compound in the mixture, and x_1 and x_2 are the concentrations of that compound in the two components. In Figure S2D, the steroid composition for the background was taken as the average of sediment directly under- and overlying *Dickinsonia* (Table 1), and the concentrations of steranes and MAS in *Dickinsonia* were adjusted to best describe the data. The resulting relationship between sterane C₂₇ (%) and MAS C₂₇ (%) allows to estimate that *Dickinsonia* largely or exclusively produced C₂₇ sterol (~95–100%) and that aromatisation of sterols during the decay of *Dickinsonia* was more pronounced than in the background (Fig. S2D). The extrapolation, however, is not precise enough to discern whether living *Dickinsonia* contained small quantities of indigenous C₂₈ and C₂₉ sterols.

We were able to obtain a more precise sterol composition of *Dickinsonia* by quantifying bacterial hopanes in several *Dickinsonia* specimens. Hopanes are largely derived from aerobic bacteria; they are extremely uncommon in anaerobes (49). As *Dickinsonia* was degraded under largely anaerobic conditions (see above), the hopanes in the fossil extracts must be largely derived from the underlying mat or the surrounding sediment. Thus, the hopane content in individual *Dickinsonia* extracts is a measure for the magnitude of the background signal. To subtract the background and to estimate the relative proportion of cholesteroloids, ergosteroids and stigmasteroids of living *Dickinsonia* we used the three largest specimens with the best signal/noise ratios (Table 1). First we quantified the variance of the three eukaryotic monoaromatic steroids relative to hopanes between the *Dickinsonia* extracts (Table S1). The steroid/hopane ratio of steroids that are solely derived from the background should stay

constant, while the ratio for steroids produced by *Dickinsonia* as well as the background should vary with a varying *Dickinsonia*/background biomass ratio. To determine this mathematically, for each of the MAS/H ratios we used a standard MS Office Excel variance VAR.S formula $VAR.S = \sum(x - \bar{x})^2 / (n - 1)$, where x is a MAS/H value for each MAS homolog in an extract, \bar{x} is a mean value between the extracts and n is the number of samples ($n = 3$).

The ratios of ergosteroids and stigmasteroids over hopanes remained nearly constant across the three fossil extracts with very small variances ($0.076 \cdot 10^{-4}$ for ergosteroids and $0.024 \cdot 10^{-4}$ for stigmasteroids; Table S1). By contrast, the content of cholesteroloids relative to hopanes changed with a three order of magnitude higher variance ($33 \cdot 10^{-4}$). These data indicate that the bulk of cholesteroloids must come from the dickinsoniids while almost all of the ergosteroids and stigmasteroids, together with the bacterial hopanes, represent a constant background signal, presumably coming from the underlying microbial mat containing biomass of bacteria and algae. Based on the computed variances, the proportion of each steroid variability can be estimated in % relative to the total variability (sum of all three steroid/hopane ratios). Such quantification of *Dickinsonia* steroid composition is based on the assumption that the background has no variability in steroid homolog proportions or relative hopane abundances. This is a conservative assumption because if the steroid/hopane ratios of the background were not constant, then ergosteroid and stigmasteroid variability would increase and their estimated content in dickinsoniids would go up. Based on these assumptions, we compute a minimum cholesteroloid content of *Dickinsonia* of 99.7%, while the maximum ergosteroid content is 0.23% and stigmateroids 0.07% (Table S1).

Similar computations can be made based on variability of $5\beta/5\alpha$ sterane ratios in *Dickinsonia* extracts. Unfortunately, an assumption that the background signal is invariable, necessary for this computation, does not fully apply to $5\beta/5\alpha$ sterane background ratios (an average $5\beta/5\alpha$ value between all background signals is 0.65, ranging however from 0.28 to 1.78, $n = 54$; Fig. 1C). In our computations, this variability in the background signal, which is likely due to natural variations in diagenesis (see above), would artificially elevate the ergosteroid and stigmasteroid proportion of *Dickinsonia*. However, even based on this imperfect data, the computation yields a conservative minimum C_{27} steroid content for *Dickinsonia* of 98.4%, while the maximum proportions of ergosteroids and stigmasteroids are 1.1% and 0.54% respectively (Table S1).

Estimation of the sterol composition of Andiva

Andiva specimens for this study were exclusively recovered from the Zinnie Gory locality. At Zinnie Gory, the proportion of sedimentary background signal in fossil extracts was far higher than at the Lyamtsa locality, where *Dickinsonia* was recovered. Thus, for *Andiva* it is more difficult to separate the dickinsoniid signal from the background. Moreover, the methodology employed for *Dickinsonia*, i.e. computation of the variance of MAS/hopane ratios, was not possible for *Andiva* because the background MAS signal is too high. However, a rough estimate of the sterol composition of *Andiva* was possible based on $5\beta/5\alpha$ sterane ratios the same way as for *Dickinsonia*, but in this case using variability in $5\beta/5\alpha$ ratios for each sterane between the analysed *Andiva* extracts and an extract of surrounding microbial mat. With the assumptions discussed above, the most conservative estimate for the minimum C_{27} steroid content of *Andiva* is 88.1%, while the maximum proportions of ergosteroids and stigmasteroids are 1.2% and 10.7% respectively (Table S2).

Other biomarkers

Hopanes

All extracts exhibit typical immature hopane distributions with low $T_s/(T_s+T_m)$ and $S/(S+R)$ ratios, high $\beta\alpha/(\beta\alpha+\alpha\beta)$ ratios and high relative abundances of C_{27} , C_{29} and C_{30} homologs relative to the extended C_{31} to C_{35} homohopanes (Table S3, Figs. S5C,D). An unusual elevated proportion of C_{27} – C_{30} hopanes in *Dickinsonia* and *Andiva* extracts, relative to bulk extracts from the Zimmie Gory and Lyamtsa localities, might indicate relatively large proportions of cyanobacteria among hopanoid-producing bacteria in the underlying microbial mats when compared to bulk organic matter. However, the unusual hopane pattern may also be the result of differences in the diagenesis of hopanoids between organic films and bulk samples (17).

Methylhopanes

The 2-methylhopane index (2-MHI) measures the abundance of C_{31} 2-methylhopane relative to C_{30} hopane (Table S3). 2-MHI is low and similar in all analysed fossils where 2-methylhopanes were detected (2-MHI = 0.8–1.8%). Elevated 2-MHI have been interpreted as an indicator for significant cyanobacterial contribution to sedimentary organic matter (50). However, only a minority of cyanobacteria have the ability to produce 2-methylhopanoids (51), and their content in cyanobacteria significantly depends on growth conditions (52). Apart from cyanobacteria, 2-methylhopanoids can also be produced by other oxygenic and anaerobic bacteria including alphaproteobacteria and an acidobacterium (51). Thus, in light of the unspecific taxonomic distribution of 2-methylhopanoids, and environmental control on their biosynthesis (51, 53), the 2-MHI values in the fossils do not yield any further insights about biological origins. 3 β -methylhopanes were detected in small amounts in the samples (Table S3) and might reflect a minor contribution of methanotrophic bacteria to the organic matter of the samples (the 3-methylhopane index values 3-MHI = 1.1–2.6%) (54).

n-Alkanes and methylalkanes

Bulk extracts of background sediment from the Zimmie Gory and Lyamtsa localities demonstrate odd-over-even predominance among *n*-alkanes at all chain lengths and, unusually for the Precambrian, a relatively large proportion of long-chain *n*-alkanes with odd-over-even predominance (Figs. S5A,B). Such a distribution might indicate that a large proportion of *n*-alkanes is derived from cyanobacteria or green algae (17). All *Andiva* and the leanest *Dickinsonia* extracts do not provide sufficient signal for *n*-alkane analysis. The richest *Dickinsonia* extracts demonstrate the same *n*-alkane pattern as the background, however the fossil extracts additionally contain large proportions of short-chain (up to C_{19}) *n*-alkanes with no odd-over-even predominance (Fig. S5A). These *n*-alkanes are presumably directly derived from *Dickinsonia* or from degrading bacteria. However, such compounds are widely distributed

in nature and do not provide any further phylogenetic information. All samples demonstrate only low amounts of methylalkanes, which likely represent diagenetic products of *n*-alkanes formed through clay mediated catalysis (55).

Other saturated and aromatic hydrocarbons

The majority of hydrocarbons extracted from the analysed samples are represented by *n*-alkanes, steranes and hopanes, with minor amounts of cheilanthanes, which are ubiquitous molecules of unknown origin. Aromatic compounds, apart from MAS and triaromatic steroids (TAS), include polycyclic aromatic hydrocarbons represented by typical parent and alkylated phenanthrenes and naphthalenes found in most bitumens and oils. TAS follow the patterns of distribution of MAS, demonstrating slightly lower relative content of cholesteroloids (e.g. in the richest *Dickinsonia*, cholesteroloid : ergosteroid : stigmasteroid abundances = 86% : 5% : 9%).

Syngeneity of biomarkers

GC-MS MRM, SIR and full-scan analyses of the comprehensive accumulatory laboratory system blank confirmed that the detected hydrocarbons were not introduced by laboratory processes. Monitoring of the blank yielded no *n*-alkanes, hopanes or steranes, even when measured using the most sensitive GC-MS MRM methods (Fig. S6). The only contaminants detected in the blank are trace amounts of phthalates—plasticizers present in small amounts in solvents used for extraction of biomarkers.

The results of Exterior/Interior (E/I) experiment, as well as a detailed discussion of biomarkers syngeneity of the samples from the White Sea that were collected, transported and stored in the same way as samples used in this study are presented elsewhere (17). The results show nearly identical concentrations of all biomarkers in exterior and interior rock portions with E/I = 1.09 to 1.53 for *n*-alkanes and E/I = 0.93 to 1.05 for hopanes and steranes, which indicates that the precombusted aluminium foil and clean calico bags prevented contamination of samples during transportation and storage, and confirm that all detected compounds are indigenous (17).

Dickinsoniid extracts demonstrate the same exceptionally low thermal maturity as *Beltanelliformis* and organically preserved macroalgae from the Lyamtsa locality (17). The high $\beta\alpha/(\beta\alpha + \alpha\beta)$ and low $Ts/(Ts + Tm)$ hopane isomer ratios, virtual absence of diasteranes and $\alpha\beta\beta$ sterane isomers, and presence of $\beta\alpha\alpha$ steranes (Fig. 1C; Table S3), which are only found in the most immature sediments, demonstrate that the hydrocarbons are significantly below the so-called oil-generative window, i.e. the kerogen never thermally generated and expelled liquid hydrocarbons (54). Such a low thermal maturity is never observed in contaminant petroleum products and migrated oils, which by their very nature must have a maturity within the oil generative window. Thus, contamination of the samples by petroleum products or by migrated hydrocarbons did evidently not occur.

Supplementary Figures

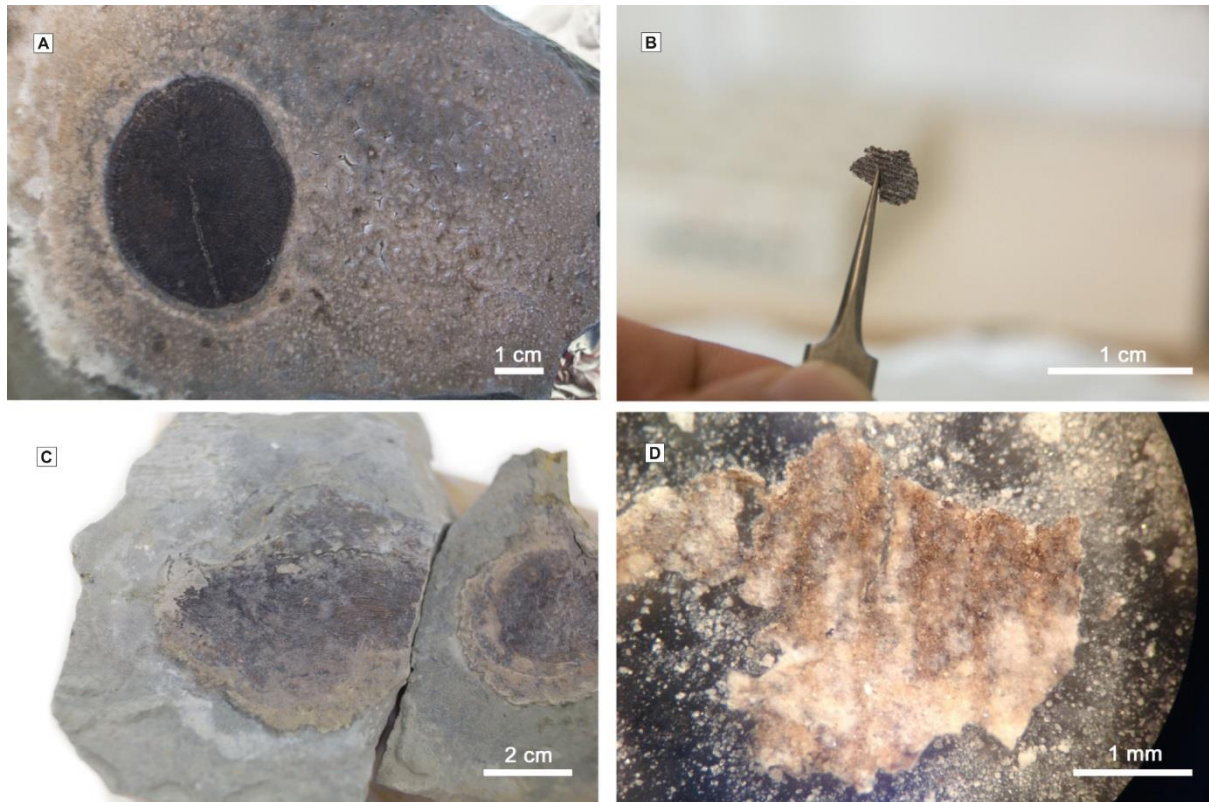


Fig. S1. Separation of organic matter from dickinsoniids. (A) Organically preserved *Dickinsonia* (specimen 4) after treatment with hydrochloric and hydrofluoric acids. Note the thin film of organic matter covering the surface with microbial mat impression surrounding the fossil; (B) a piece of organic matter of *Dickinsonia*-3 separated from the specimen with tweezers; (C) organically preserved *Andiva* (specimen *Andiva*-1) after treatment with hydrochloric and hydrofluoric acids, the organic matter is more visible as it starts separating from the rock surface where the acids were applied; (D) organic matter of *Andiva*-1 suspended in water after separation from the specimen showing preservation of *Andiva*'s fine structure.

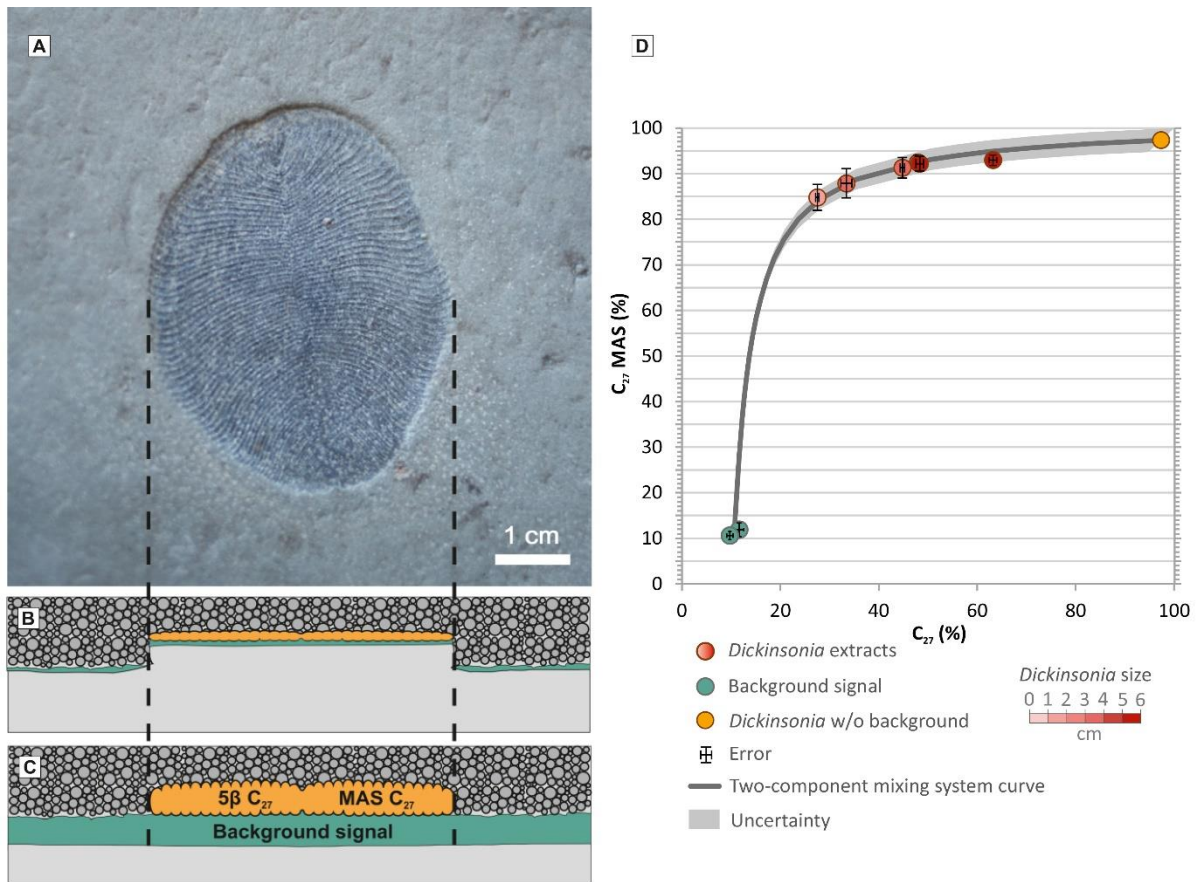


Fig. S2. Explanation of the origin of different biomarker signals of dickinsoniid extracts.

(A) Organically preserved *Dickinsonia* fossil (specimen 4) and surrounding impression of microbial mat; (B) schematic cross-section of the fossil, showing the position of organic matter of the microbial mat (green) and *Dickinsonia* (orange); (C) cross-section reconstructing the position of microbial mat and *Dickinsonia* immediately after burial beneath sand, highlighting the origin of the background signal in dickinsoniid extracts and explaining its variable influence depending on the size of a *Dickinsonia* specimen; (D) plot showing relationship between relative proportion of cholesteroloids among steranes (C_{27} (%)) and monoaromatic steroids (C_{27} MAS (%)); the dark-grey curve represents a numerically solved two component mixing scenario, and the light-grey area represent uncertainty of this curve (Supplementary Text).

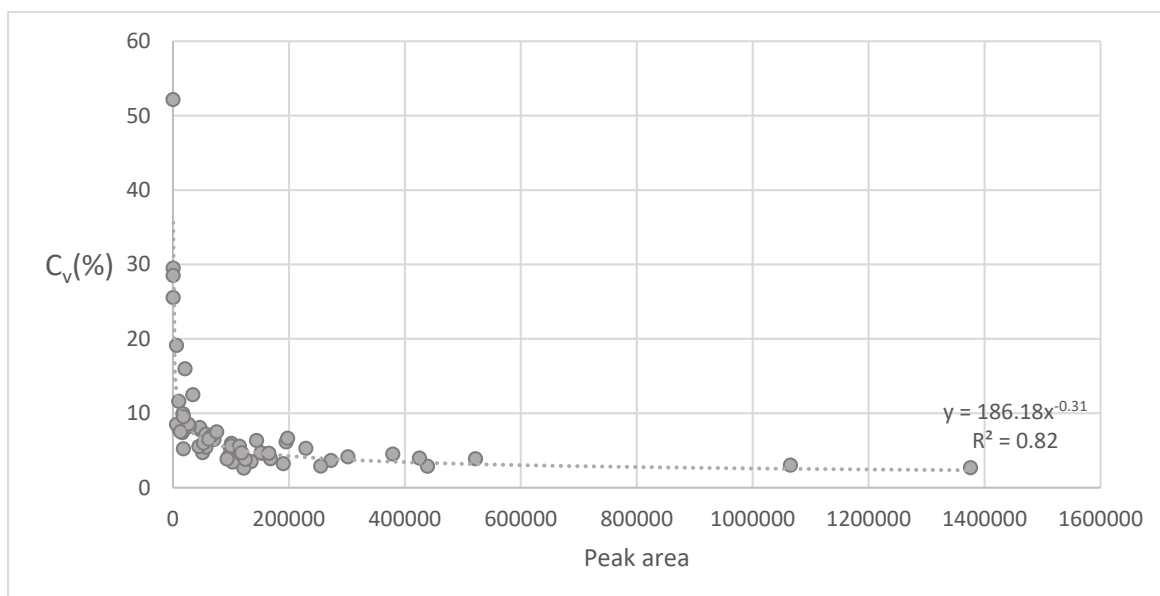


Fig. S3. Relationship between measured biomarker peak area and coefficient of variation (C_v). Each data point represents a different sterane or hopane in the AGSO-II industrial standard oil mixture, and the peak area is the dimensionless Metastable Reaction Monitoring (MRM) chromatographic signal area of the average of five repeat injections. C_v was computed for the ratio of compound signal area normalized to $C_{30} 17\alpha(H)21\beta(H)$ hopane, which represents the highest signal in the MRM chromatograms. In the formula describing the relationship between measured biomarker peak area and C_v ($y = 186.18x^{-0.31}$), $y = C_v$, $x =$ peak area.

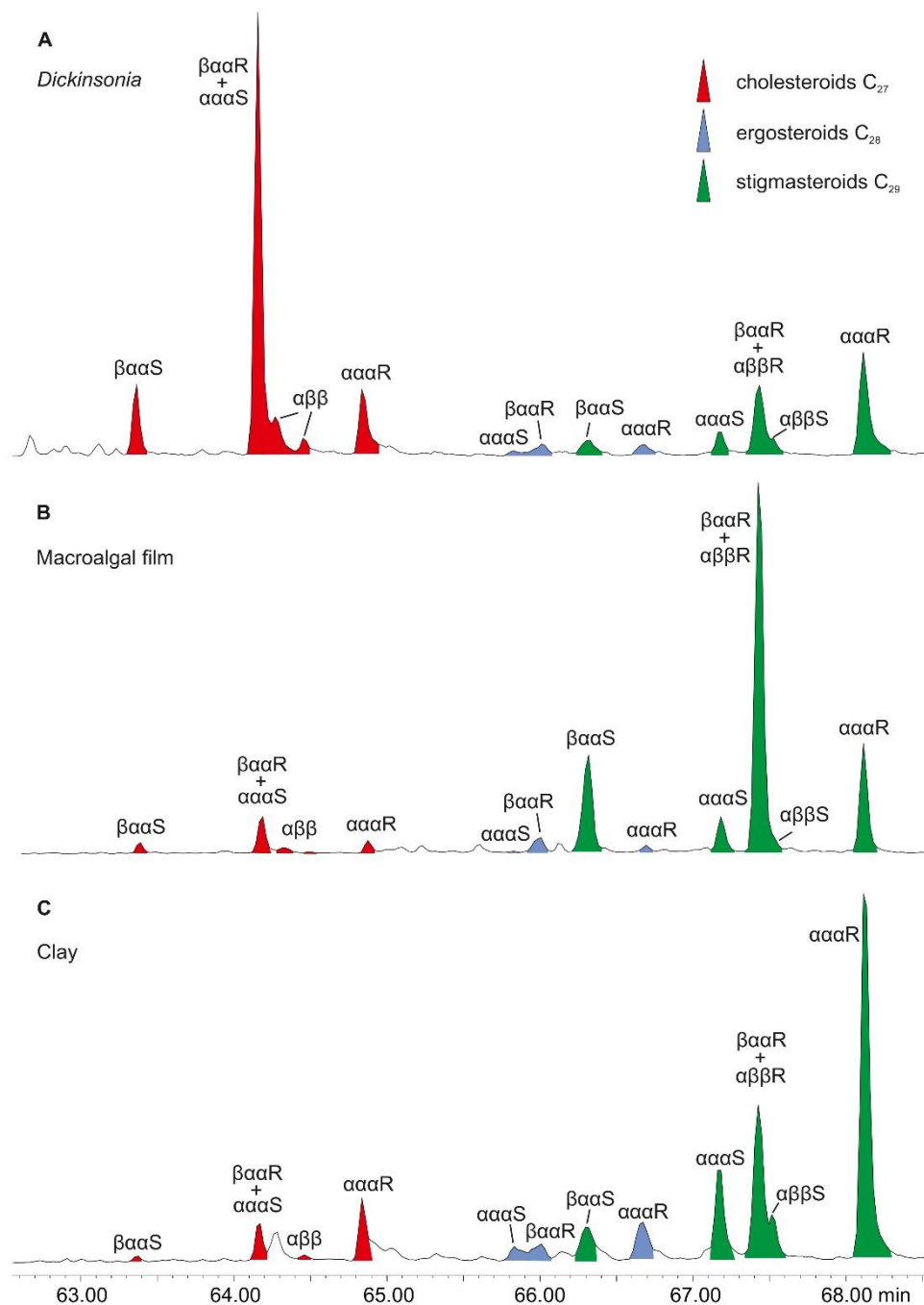


Fig. S4. Comparison of the sterane composition of *Dickinsonia-2* macroalgal film and background sediments from the Lyamtsa locality. (A) *Dickinsonia-2* displays elevated $5\beta/5\alpha = 5.5$ for cholestane only, while it is ~ 0.7 for ergostane and stigmasterane; (B) the macroalgal film extract demonstrates elevated $5\beta/5\alpha$ ratios for all three steranes with $5\beta/5\alpha = 3.7$; (C) clay immediately underlying the level with *Dickinsonia* demonstrates typical background $5\beta/5\alpha$ ratio values of 0.64 for all three steranes. The elevated $5\beta/5\alpha$ ratios in the alga demonstrate that 5β steranes can form in sedimentary environments during decomposition of organic matter and that the process is not restricted to microbial activity within the digestive system of animals (28) and is not caused by a specific nature of cholesteroloid in *Dickinsonia* and *Andiva*.

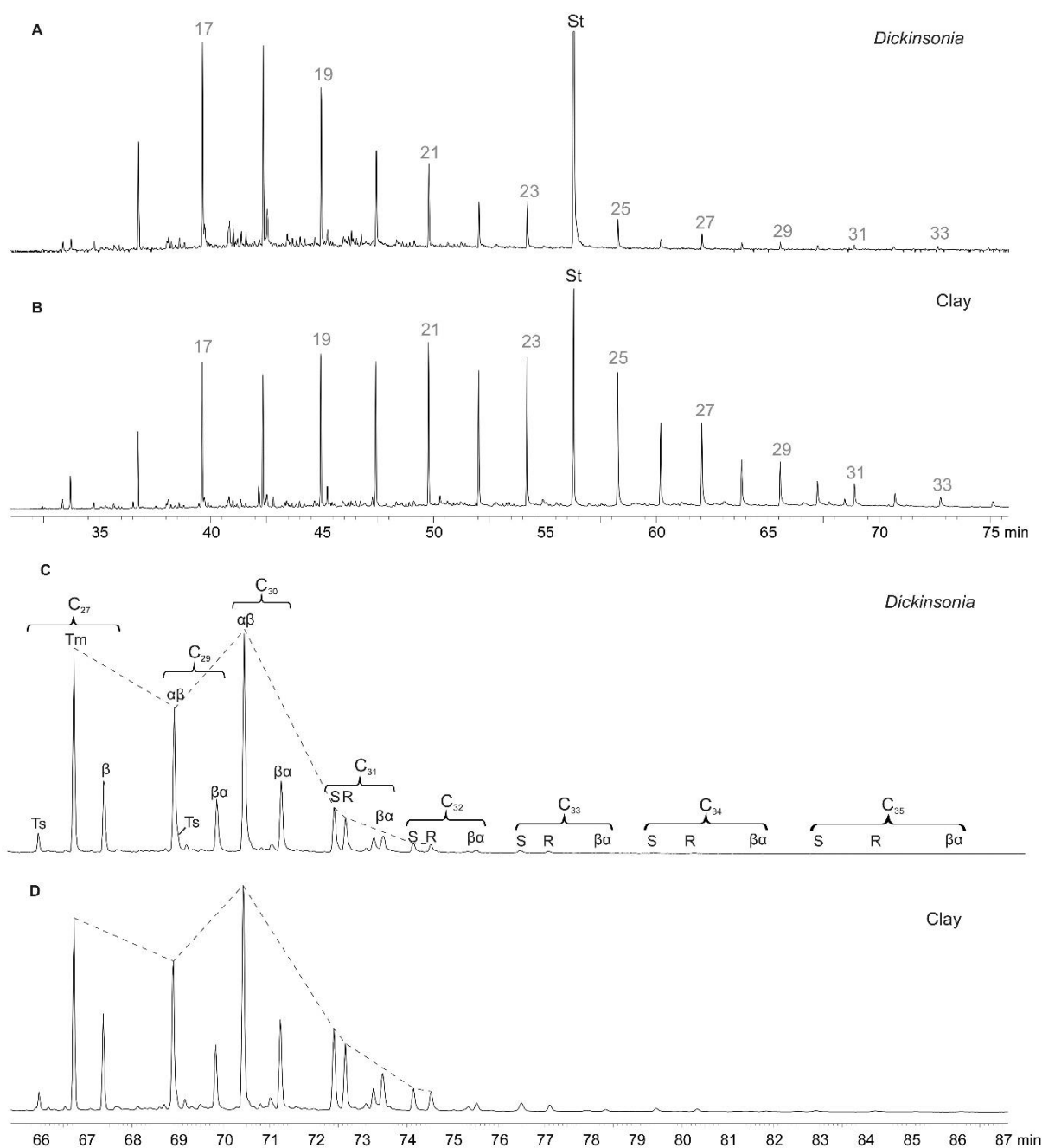


Fig. S5. Distribution of *n*-alkanes and hopanes in *Dickinsonia-2* and the underlying clay extracts. (A) Full-scan chromatogram, m/z 85 trace of *Dickinsonia-2* extract showing the distribution of *n*-alkanes; (B) full-scan chromatogram, m/z 85 trace of clay extract underneath *Dickinsonia* showing the distribution of *n*-alkanes; (C) Metastable Reaction Monitoring (MRM) chromatogram showing the sum of C₂₇–35 hopane traces of *Dickinsonia-2* extract; (D) MRM chromatogram showing the sum of C₂₇–35 hopane traces of clay extract. Numbers on chromatographic signals in (A) and (B) indicate the carbon number of *n*-alkanes, St = internal standard 18-MEAME. The dotted line in (C) and (D) highlights the difference in hopane (C₂₇–30) and homohopane (C₃₁–35) relative abundances between *Dickinsonia* and clay extracts. Hopane structures: $\alpha\beta$ = 17 α (H)21 β (H), $\beta\alpha$ = 17 β (H)21 α (H), S and R indicates stereochemistry at the C-22 position.

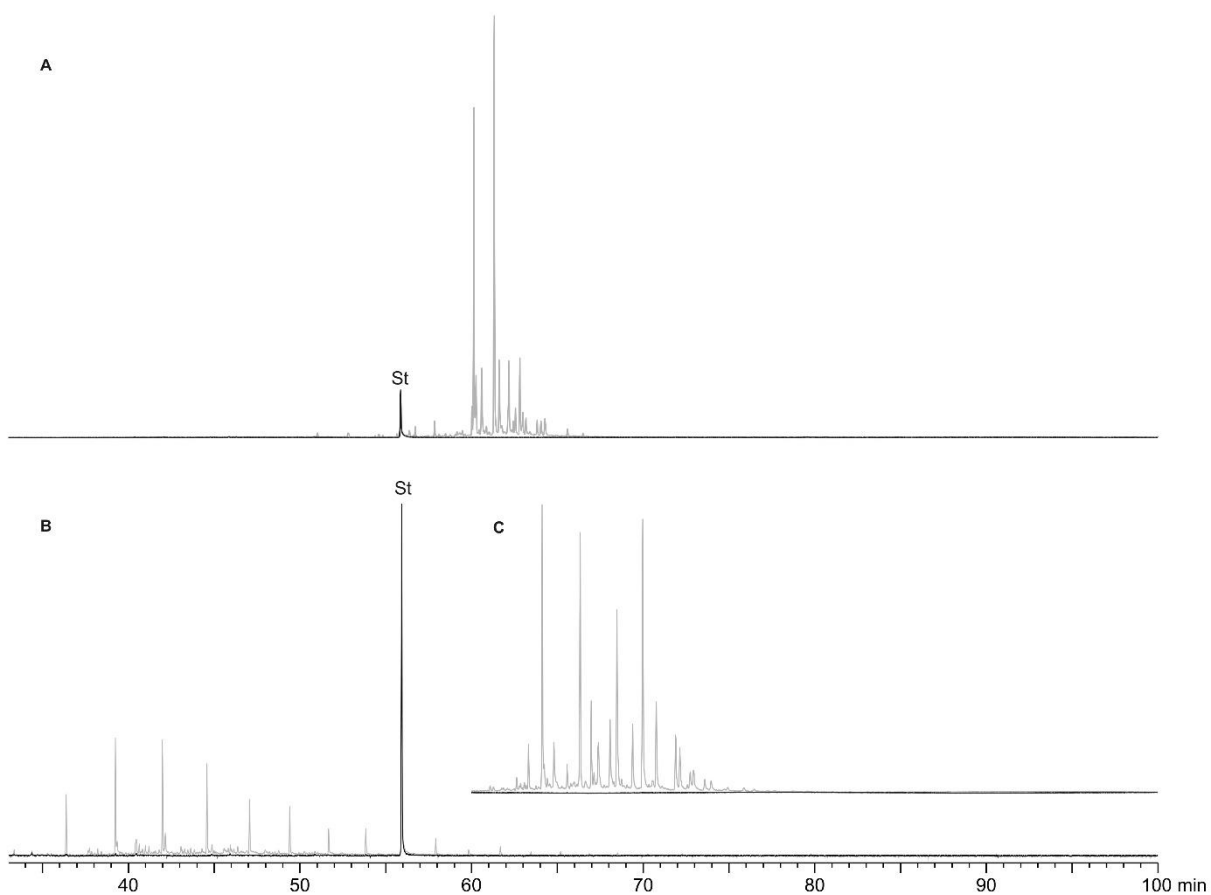


Fig. S6 | GC-MS chromatograms of a comprehensive accumulatory laboratory system blank (black line) in comparison to a *Dickinsonia-2* extract (grey line). (A) Selected Ion Recording (SIR) chromatogram showing monoaromatic steroids on mass trace m/z 253 ; (B) full-scan chromatogram m/z 85 trace (n -alkanes and methylalkanes); (C) Metastable Reaction Monitoring (MRM) chromatogram: $\Sigma(C_{27-35}$ hopanes, C_{27-29} steranes); St: 18-MEAME internal standard.

	MAS _y /H ¹			5β/5α ²		
	C ₂₇	C ₂₈	C ₂₉	C ₂₇	C ₂₈	C ₂₉
<i>Dickinsonia</i> -1	0.155 (0.004) ⁵	0.022 (0.001)	0.147 (0.003)	3.606 (0.207)	0.519 (0.324)	0.600 (0.057)
<i>Dickinsonia</i> -2	0.254 (0.005)	0.028 (0.001)	0.145 (0.004)	5.490 (0.28)	0.652 (0.231)	0.754 (0.056)
<i>Dickinsonia</i> -3	0.156 (0.004)	0.025 (0.001)	0.148 (0.004)	4.079 (0.29)	0.749 (0.265)	0.628 (0.043)
<i>Dickinsonia</i> -4	-	-	-	2.656 (0.408)	0.972 (0.344)	0.635 (0.08)
<i>Dickinsonia</i> -5	-	-	-	2.329 (0.102)	0.814 (0.288)	0.447 (0.019)
<i>Dickinsonia</i> -6	-	-	-	1.337 (0.071)	0.788 (0.279)	0.500 (0.022)
Variance (*10⁻⁴)³	32.617 (0.007)	0.076 (0.001)	0.024 (0.005)	21379 (4.4)	235 (5.038)	117 (0.878)
<i>Dickinsonia</i> sterol composition ⁴	99.70% (0.33)	0.23% (0.04)	0.07% (0.16)	98.38% (0.04)	1.08% (0.02)	0.54% (0.004)

Table S1. Estimation of the sterol composition of *Dickinsonia*.

¹ Concentration of C₂₇, C₂₈ and C₂₉ monoaromatic steroid (MAS) homologs (sum of isomers I and V) relative to total hopanes (sum of C₂₇–C₃₅ hopanes) in *Dickinsonia* extracts; hopanes: C₂₇ = Σ(Ts, Tm, β), C₂₉ = Σ(αβ, Ts, βα), C₃₀ = Σ(αβ, βα), C_{31–35} = Σ(αβ-22(S+R), βα), αβ = 17α(H)21β(H), βα = 17β(H)21α(H); y indicates carbon number of monoaromatic steroids; ²5β/5α = (βαα20R+ααα20S)/ααα20R; ³Variance = Σ(x - \bar{x})²/(n - 1), where x is C_y/H value, \bar{x} is a mean C_y/H value between the samples and n is the number of samples (n = 3); ⁴C_y% = 100%*(C_y variance)/(sum of variances for each of three steroids), y indicates carbon number of monoaromatic steroids; ⁵numbers in parentheses are standard deviation values.

	C ₂₇	C ₂₈	C ₂₉
<i>Andiva-1</i> 5 β /5 α ¹	1.072 (0.036) ⁴	0.758 (0.268)	0.685 (0.017)
<i>Andiva-2</i> 5 β /5 α ¹	1.315 (0.150)	0.811 (0.287)	0.517 (0.042)
<i>Andiva-Mat</i> 5 β /5 α ¹	0.805 (0.068)	0.761 (0.269)	0.65 (0.041)
Variance (*10 ⁻⁴) ²	651.363 (1.192)	8.938 (3.369)	78.694 (0.432)
<i>Andiva</i> sterol composition ³	88.14% ⁵ (0.46)	1.21% (0.46)	10.65% (0.08)

Table S2. Estimation of sterol composition of *Andiva*.

¹5 β /5 α = ($\beta\alpha\alpha$ 20R + $\alpha\alpha\alpha$ 20S)/ $\alpha\alpha\alpha$ 20R; ²Variance = $\sum(x - \bar{x})^2 / (n - 1)$, where x is C_y/H value, \bar{x} is a mean 5 β /5 α value for each sterane between the samples and n is the number of samples ($n = 3$); ³C_y% = 100%*(C_y variance)/(sum of variances for each of three steroids); ⁴numbers in parentheses are standard deviation values; ⁵conservative minimum estimate of relative cholesterol content (C₂₇%) of *Andiva* (see Supplementary Text).

Sample	Ts/(Ts+Tm) C ₂₇ hopanes	β α /(β α + $\alpha\beta$) C ₃₀ hopanes	22S/22(S+R) C ₃₁ hopanes	C ₂₇₋₃₀ /C ₃₁ hopanes ¹	2-MHI (%) ²	3-MHI (%) ³	S/H ⁴
<i>Dickinsonia-1</i>	0.09 (0.01)	0.24 (0.01)	0.57 (0.01)	0.41 (0.01)	5.22 (0.03)	0.82 (0.08)	1.92 (0.16)
<i>Dickinsonia-2</i>	0.08 (0.00)	0.27 (0.01)	0.55 (0.01)	0.59 (0.01)	6.44 (0.03)	0.91 (0.09)	1.39 (0.13)
<i>Dickinsonia-3</i>	0.09 (0.01)	0.24 (0.01)	0.58 (0.01)	0.38 (0.01)	5.57 (0.03)	0.96 (0.11)	2.57 (0.24)
<i>Dickinsonia-4</i>	0.09 (0.01)	0.27 (0.03)	0.56 (0.03)	0.26 (0.01)	6.32 (0.06)	1.00 (0.22)	1.91 (0.34)
<i>Dickinsonia-5</i>	0.11 (0.01)	0.27 (0.02)	0.55 (0.02)	1.41 (0.04)	6.15 (0.06)	-	-
<i>Dickinsonia-6</i>	0.09 (0.01)	0.27 (0.02)	0.55 (0.02)	0.89 (0.02)	6.22 (0.05)	-	-
<i>Dickinsonia-7</i>	0.08 (0.02)	0.32 (0.06)	0.53 (0.06)	0.73 (0.05)	5.93 (0.12)	-	-
<i>Dickinsonia-8</i>	-	-	-	-	-	-	-
<i>Dickinsonia-Sandstone</i>	0.10 (0.00)	0.25 (0.01)	0.53 (0.01)	0.44 (0.01)	4.48 (0.02)	1.13 (0.07)	2.88 (0.15)
<i>Dickinsonia-Clay</i>	0.07 (0.00)	0.31 (0.01)	0.55 (0.02)	0.27 (0.00)	3.85 (0.87)	1.47 (0.07)	2.89 (0.13)
<i>Andiva-1</i>	0.03 (0.00)	0.31 (0.01)	0.38 (0.01)	0.17 (0.00)	3.82 (0.02)	0.95 (0.08)	1.34 (0.12)
<i>Andiva-2</i>	0.10 (0.01)	0.30 (0.03)	0.40 (0.03)	0.17 (0.01)	3.93 (0.05)	1.76 (0.27)	1.06 (0.21)
<i>Andiva Mat</i>	0.07 (0.01)	0.33 (0.03)	0.37 (0.03)	0.19 (0.01)	3.82 (0.05)	1.11 (0.21)	1.29 (0.26)
<i>Andiva-Sandstone</i>	0.04 (0.00)	0.37 (0.01)	0.39 (0.02)	0.24 (0.00)	5.63 (0.02)	0.80 (0.06)	0.93 (0.08)
<i>Andiva-Clay</i>	0.05 (0.00)	0.33 (0.01)	0.38 (0.01)	0.22 (0.00)	3.03 (0.02)	0.96 (0.05)	0.68 (0.04)

Table S3. Hopane and methylhopane biomarker parameters in extracts of dickinsoniids and surrounding deposits.

¹C₂₇ = Σ (Ts, Tm, β), C₂₉ = Σ ($\alpha\beta$, Ts, $\beta\alpha$), C₃₀ hopane = Σ ($\alpha\beta$, $\beta\alpha$), C₃₁ = Σ ($\alpha\beta$ -22(S+R), $\beta\alpha$);
²2-methylhopane index, 2-MHI (%) = 100*(Σ C₃₁ 2 α +2 β -methylhopane)/ (Σ C₃₁ 2 α +2 β -methylhopane + Σ (C₃₀ $\alpha\beta$ -22(S+R), $\beta\alpha$ hopane);
³3-methylhopane index, 3-MHI (%) = 100*(Σ C₃₁ 3 β -methylhopane)/ (Σ C₃₁ 3 β -methylhopane + Σ ($\alpha\beta$ -22(S+R), $\beta\alpha$ C₃₀ hopane);
⁴S/H = Σ (C₂₇₋₂₉ steranes)/ Σ (C₂₇₋₃₅ hopanes), steranes: C₂₇ = Σ ($\beta\alpha$ -20(S+R)-diacholestane, $\alpha\alpha\alpha$ - and $\beta\alpha\alpha$ -20(S+R)-cholestane), C₂₈ = Σ ($\beta\alpha$ -20(S+R)-diaergostane, $\alpha\alpha\alpha$ - and $\beta\alpha\alpha$ -20(S+R)-ergostane), C₂₉ = Σ ($\beta\alpha$ -20(S+R)-diastigmastane, $\alpha\alpha\alpha$ - and $\beta\alpha\alpha$ -20(S+R)-stigmastane), $\alpha\alpha\alpha$ = 5 α (H),14 α (H),17 α (H), $\beta\alpha\alpha$ = 5 β (H),14 α (H),17 α (H); hopanes: C₂₇ = Σ (Ts, Tm, β), C₂₉ = Σ ($\alpha\beta$, Ts, $\beta\alpha$), C₃₀ = Σ ($\alpha\beta$, $\beta\alpha$), C₃₁₋₃₅ = Σ ($\alpha\beta$ -22(S+R), $\beta\alpha$), $\alpha\beta$ = 17 α (H)21 β (H), $\beta\alpha$ = 17 β (H)21 α (H); ⁵numbers in parentheses are standard deviation values.

Species	Type	Sample Origin	C ₂₇ to C ₂₉ Sterols		
			C ₂₇ %	C ₂₈ %	C ₂₉ %
<i>Collodaria</i> SpB	Polycystinea (Radiolaria)	Mediterranean (Villefranche sur Mer)	75.38	16.10	8.52
<i>Collodaria</i> SpA	Polycystinea (Radiolaria)	Mediterranean (Villefranche sur Mer)	73.82	18.77	7.41
<i>Collodaria</i> SpC	Polycystinea (Radiolaria)	Mediterranean (Villefranche sur Mer)	75.70	15.17	9.13
<i>Collodaria</i> SC2	Polycystinea (Radiolaria)	Mediterranean (Villefranche sur Mer)	60.54	23.30	16.16
<i>Collodaria</i> SC1	Polycystinea (Radiolaria)	Mediterranean (Villefranche sur Mer)	61.86	14.50	23.64
<i>A. lobifera</i>	Foraminifera	Red Sea (Eilat)	13.58	43.16	43.26
<i>Sorites</i> sp.	Foraminifera	Red Sea (Eilat)	30.67	20.06	49.27
<i>Shepherdella</i> sp.	Foraminifera	Red Sea (Eilat)	45.72	16.16	38.12
<i>Quinqueloculina</i> sp.	Foraminifera	Mediterranean (Tel Aviv)	78.15	14.66	7.19
<i>Acantharea</i> sp.	Acantharea	Indian Ocean near Eden	51.98	39.35	8.67
<i>Gromia</i> sp.	Gromiidae	Southern Ocean (McMurdo Sound)	11.77	27.88	60.35
<i>A. laticollaris</i> ¹	Foraminifera	Literature (31)	10.31	26.93	62.76

Table S4. Distribution of C₂₇-C₂₉ sterols in extant Rhizaria (Retaria and Gromiidae)

¹Values for *A. laticollaris* were determined by integrating peak areas of the functionalized sterols in Fig.1a of Grabenstatter et al. (31).

CHAPTER 3. BIOMARKER EVIDENCE FOR GUTS, GUT CONTENTS, AND FEEDING STRATEGIES OF EDIACARAN ANIMALS

This chapter expands biomarker studies of individual Ediacaran fossils to decipher their gut contents and feeding strategies. Using biomarkers, the study reconstructs the diets of Ediacaran animals *Kimberella* and *Calyptrina* and demonstrates that they possessed a gut. Conversely, *Dickinsonia* did not possess an internal digestive system and instead fed on microbial mats using an external digestion mode.



Australian
National
University

Statement of Contribution

This thesis is submitted as a Thesis by Compilation in accordance with https://policies.anu.edu.au/ppl/document/ANUP_003405

I declare that the research presented in this Thesis represents original work that I carried out during my candidature at the Australian National University, except for contributions to multi-author papers incorporated in the Thesis where my contributions are specified in this Statement of Contribution.

Title and authors: : Bobrovskiy, I., Nagovitsyn, A., Hope, J.M., Luzhnaya, E., Brocks, J. J. Biomarker evidence for guts, gut contents, and feeding strategies of Ediacaran animals.

Current status of paper: Not Yet Submitted/**Submitted**/Under Revision/Accepted/Published

Contribution to paper: I.B. designed the study, analyzed biomarkers from Ediacaran fossils and interpreted the data; J.M.H. helped with biomarker analysis; I.B., A.N. and E.L. collected fossils; A.N. contributed palaeontological description, I.B. and J.J.B. wrote the manuscript, with contributions from all authors.

Senior author or collaborating authors endorsement: 

Ilya Bobrovskiy

Candidate – Print Name



Signature

18/04/2019

Date

Endorsed

Jochem Brocks

Chair of Supervisory Panel – Print Name



Signature

18/04/2019

Date

Stewart Fallon

Delegated Authority – Print Name



Signature

29/04/2019

Date

Biomarker evidence for guts, gut contents, and feeding strategies of Ediacaran animals

Ilya Bobrovskiy^{1*}, Alexey Nagovitsyn², Janet M. Hope¹, Ekaterina Luzhnaya (Serezhnikova)³, Jochen J. Brocks^{1*}

¹Research School of Earth Sciences, Australian National University, Canberra, ACT 2601, Australia

²Arkhangelsk Regional Lore Museum, Arkhangelsk 163000, Russia

³Borissiak Paleontological Institute, Russian Academy of Sciences, Moscow 117997, Russia

*Correspondence to: ilya.bobrovskiy@anu.edu.au, jochen.brocks@anu.edu.au

The oldest animals appear in the fossil record among Ediacara biota communities. However, little is known about the phylogeny of these animals, and even less about their diet and feeding behaviour. Here we decipher the gut contents of Ediacaran animals using biomarker molecules. We show that tube worms *Calyptrina* and mollusc-like *Kimberella* shared a diet of green algae and bacteria. Given their feeding ecology, the underground lifestyle of Ediacaran tube worms suggests that predators had started to shape animal evolution by 558 Ma ago already. *Dickinsonia* show no traces of dietary molecules, indicating an external digestion mode analogous to modern Placozoa.

One Sentence Summary: Lipid biomarkers decipher the gut content of Ediacaran macroorganisms, opening a new window into the ecology of early animals.

The Ediacara biota represents the oldest large complex organisms in the fossil record. It precludes animal-dominated ecosystems of the Phanerozoic and may hold clues to the appearance of modern animal phyla in the Cambrian Explosion. However, most Ediacaran fossils display bodyplans that are distinct from modern organisms (1, 2), and are only preserved as impressions that retain minimal information about morphology and biology (3). Particularly little is known about their feeding ecology, knowledge that is crucial if we want to understand what these earliest large organisms were and how they lived. An exception is *Kimberella* (Fig. 1A), for which a fossilized gut, feeding traces and even potential coprolites have been preserved (4, 5). This fossil is considered to be a mollusc-like bilaterian animal that was feeding by scraping microbial mats (5, 6). By contrast, organic-walled tubes, such as *Sabellidites* and *Calyptrina* (Figs. 1C, S1-S3), are thought to belong to tube worms comparable with modern Siboglinidae that have no gut but gain their nutrition from symbiotic bacteria (7, 8). *Dickinsonia* (Fig. 1B), though morphologically distinct from any living organism, is an animal based on its steroid composition (see the discussion of alternative views in the Supplementary Text). *Dickinsonia* and their morphological relatives, dickinsoniids, moved across the sea floor, leaving behind feeding marks on microbial mats (9). However, their feeding style remains unknown. Similar to modern Placozoa, they may have used an external digestion mode, taking up nutrients by osmotrophy (10). Alternatively, they may have possessed an internal digestive

system (9, 11) and collected microbial mats by physically scraping them off (9), a feeding style indicative of more advanced Eumetazoa.

Organically preserved Ediacaran fossils from the White Sea area in Russia (Fig. 1) offer the unique opportunity to study the biology of individual organisms using the hydrocarbon skeletons of lipids (biomarkers) (12, 13). Generally, some of the most abundant biomarkers in sedimentary environments are hopanes originating from bacterial hopanepolyols, and steranes, the alteration products of eukaryotic sterols. Common steranes include cholestane, ergostane and stigmastane with 27, 28 and 29 carbon atoms respectively. Varying proportions of these three steranes can be used to distinguish different eukaryotic sources such as algae and animals (14). Moreover, different structural isomers of steranes may retain information about decay processes. Abiological isomerization of sterols yields 5β and 5α steranes with an equilibrium ratio of $5\beta/5\alpha \sim 0.64$ (15). This proportion is generally characteristic of bulk rock extracts from the White Sea area (average $5\beta/5\alpha = 0.64 \pm 0.26$, $n = 54$) (12). $5\beta/5\alpha$ sterane values that are significantly higher or lower than this can be explained by stereoselective microbial hydrogenation of unsaturated sterols forming saturated 5β or 5α stanols and eventually 5β or 5α steranes (15, 16). These processes affect C_{27} , C_{28} and C_{29} sterols equally, regardless of side chain alkylation (15). Thus, differences in $5\beta/5\alpha$ between C_{27} , C_{28} and C_{29} steranes in a given sample reflect that sterols were degraded in different microenvironments by distinct microbial consortia. For example, C_{27} steranes extracted from *Dickinsonia* specimens have $5\beta/5\alpha$ values up to 5.5, caused by microbial degradation within the decaying animal carcass (12). Conversely, C_{28} and C_{29} steranes in that same extract have $5\beta/5\alpha$ around 0.64, typical of the White Sea area background signal and derived from green algae in the underlying microbial mat.

Using sterane carbon numbers and isomers it is also possible to detect the gut content of Ediacaran animals. The digestive tract is a separate, intensely anaerobic environment with a distinct microbial community and sterols derived from food. Gut contents should thus possess distinct C_{27} to C_{29} sterane abundances and $5\beta/5\alpha$ ratios compared to the rest of a decomposing animal. To search for gut contents, we first studied biomarkers from organically preserved *Kimberella*. Although *Kimberella* is known to possess a gut, visual inspection of the organic matter did not reveal any internal organs (Fig. 1). We thus analysed the biomarker content of an entire *Kimberella* specimen, which had been separated from the overlying sandstone using acids (see Methods), and compared the sterane composition with microbial mat immediately adjacent (within first 2-3 mm) and more distal (within 1 cm) to the fossils, and with the clay and sand immediately under- and overlying the fossil (Fig. 2).

The clay and the distal microbial mat representing the living environment and food source of *Kimberella*, reveal a C_{29} sterane predominance ($C_{29} = 65$ - 66% of total C_{27} to C_{29} steranes, Fig. 2C, Table S1) diagnostic for chlorophyte algae and typical of White Sea area sediments (mean $C_{29} = 76 \pm 9\%$, $n = 59$) (17). Steranes in these extracts possess $5\beta/5\alpha$ values close to 0.6, diagnostic for predominantly abiogenic transformation of steroids (Fig. 2B, Table S1). Moving to the mat and sandstone in the immediate surrounding of *Kimberella* (Fig. 2), the $5\beta/5\alpha$ ratio of cholestane rises to 1, affected by 5β cholesteroids that presumably emanated from the *Kimberella* carcass. This suggests that *Kimberella*, like most animals (18), contained cholesterol as the major membrane sterol, and that cholesterol degradation within the anaerobic carcass caused elevated $5\beta/5\alpha$ values as previously observed in *Dickinsonia* (12).

The biomarker composition of the *Kimberella* specimen itself is remarkably unusual (Fig. 2, Table S1). As in the surrounding mat, steranes demonstrate the typical green algal C₂₉ predominance. Yet, the 5 β /5 α ratio of C₂₈ and C₂₉ steranes is extremely low (0.1), much lower than in the surrounding mat. At the same time, 5 β /5 α of cholestane (C₂₇) is elevated by a factor of six (0.57). The elevated 5 β /5 α of cholestane must be associated with decaying animal tissue, but the low values for C₂₈ and C₂₉ steranes require a separate microenvironment in which algal matter was degraded under distinct conditions. Bacterial hopanes in the *Kimberella* extract reveal additional information about that microenvironment. Hopanes show very low isomerization values, including strongly depleted ratios of $\alpha\beta/\beta\alpha$ -hopanes and T_s/T_m (Fig. 2D, Table S1). These low hopane isomerisation values, together with low 5 β /5 α of C₂₈ and C₂₉ steranes, suggest that C=C double bonds required for isomerization (19, 20) were rapidly removed during early diagenesis in a strongly reducing microenvironment. This anoxic environment was likely the digestive tract of *Kimberella* that contained hydrogenated hopanols and sterols derived from its food – bacterial and algal material from microbial mats or planktonic debris.

Cholestane has an unusually low concentration in the *Kimberella* extract, comprising merely 4% of total steranes, which is even depleted relative to the surrounding mats and sediments containing ~25% cholestane (Fig. 2C, Table S1). Given that *Kimberella* was a bilaterian animal producing cholesterol, the low cholestane levels are, at first sight, counterintuitive. However, as the biomarkers in the *Kimberella* extract are dominated by the gut content due to preferential preservation of gut lipids under instantly reducing conditions, the depleted cholestane signal is expected. Eumetazoan animals require cholesterol and can absorb it directly from their diet. As a result, the cholesterol content in guts and faeces may become strongly depleted relative to other sterols (21). Thus, the sterane and hopane composition of *Kimberella*, in comparison with the surroundings, reveals that the animal consumed an algal and bacterial diet and preferentially absorbed C₂₇ sterol from its food (Supplementary Text). The result demonstrates that gut contents can leave a dominant and distinct signal in Ediacaran fossils.

The Ediacaran worm *Calyptrina* (Fig. 1C, S1-S3) and its relatives lived largely underground with a tube opening to the sediment surface (Supplementary Text). In a world still devoid of predators, it is difficult to explain why these sessile worms lived within sediment. They have thus been compared to extant Siboglinidae (7, 8), tube worms without a gut that are sustained by chemotrophic bacteria deriving sulfide or methane from their anoxic sedimentary environment (22). However, biomarkers extracted from organically preserved *Calyptrina* show a pattern nearly identical to *Kimberella* (Fig. 2, Table S1), revealing that they had a mixed diet of chlorohyte algae and bacteria and a digestive system that preferentially absorbed cholesterol. This refutes the view that they were solely sustained by bacterial symbionts (8, 23) or preferentially fed on bacteria (24). Rather, they implemented a feeding behaviour more similar to modern suspension- or detritus-feeding tube worms (22).

It is generally accepted that both Precambrian and Cambrian burrowing organisms have gone underground to explore new resources rather than hide from predators (25, 26). However, Ediacaran tube worms challenge this hypothesis as they lived within sediment but fed on the

surface. In principle, the burrowing lifestyle of Ediacaran tube worms might reflect a defence against predators (27). The oldest direct evidence for macrophagy, such as bite marks and hunting burrows, belong to the Early Cambrian (28), and likely predation marks were found in terminal Ediacaran skeletal organisms *Cloudina* (29). However, the inferred absence of macrophagy yet earlier in time is only based on negative evidence (23, 30). The lifestyle of Ediacaran tube worms indicates that predation may have started to shape animal evolution at the latest by 558 Ma ago, potentially driving increasing body size, diversification and evolution of complex behaviour within the Ediacara biota. Alternatively, or additionally, the underground lifestyle may have protected tube worms from storms and tides, supporting a sessile lifestyle, and improving their suspension-feeding efficiency.

In contrast to *Calyptrina* and *Kimberella* (Fig. 2, 3A), not one of 13 analysed dickinsoniid specimens of the genera *Dickinsonia*, *Andiva* and *Yorgia* yielded a biomarker pattern diagnostic of a gut signal (Fig. 3B-D, Table S1) (12). Dickinsoniid extracts are strongly dominated by cholesterol alteration products that formed under anaerobic conditions within decaying animal tissue, in mixture with bacterial hopanes and algal steranes derived from the underlying microbial mat (12) (Fig. 3D). If a gut wall was present but did not remain intact during earliest diagenesis, the gut content would have been altered by the same microbial communities that operated in the rest of the carcass (Fig. 3C). In this case it is possible to compute that the gut content could not have exceeded $0.10 \pm 0.23\%$ of the body mass of *Dickinsonia* (Supplementary Text). By contrast, the gut content of extant marine invertebrates commonly constitutes ~10% to >50% of body mass (31), suggesting that dickinsoniids possessed an external, not an internal, digestion mode (Fig. 3D), analogous to modern Placozoa (10).

Gut content analysis is one of the most powerful tools for deciphering trophic structure of ancient ecosystems and ecology of their members (32). Biomarkers provide a new dimension for these studies, expanding this approach to oldest known animals and allowing analysis of gut contents of ancient macroorganisms even if the gut itself it is not fossilized.

References and Notes

1. S. Xiao, M. Laflamme, On the eve of animal radiation: phylogeny, ecology and evolution of the Ediacara biota. *Trends Ecol Evol* **24**, 31-40 (2009).
2. G. E. Budd, S. Jensen, The origin of the animals and a ‘Savannah’ hypothesis for early bilaterian evolution. *Biological Reviews* **92**, 446-473 (2017).
3. I. Bobrovskiy, A. Krasnova, A. Ivantsov, E. Luzhnaya, J. J. Brocks, Simple sediment rheology explains the Ediacara biota preservation. *Nature Ecology & Evolution* **3**, 582-589 (2019).
4. J. G. Gehling, B. N. Runnegar, M. L. Droser, Scratch Traces of Large Ediacara Bilaterian Animals. *Journal of Paleontology* **88**, 284-298 (2014).
5. M. A. Fedonkin, A. Simonetta, A. Y. Ivantsov, New data on *Kimberella*, the Vendian mollusc-like organism (White Sea region, Russia): palaeoecological and evolutionary implications. *Geological Society, London, Special Publications* **286**, 157-179 (2007).
6. M. A. Fedonkin, B. M. Waggoner, The Late Precambrian fossil *Kimberella* is a mollusc-like bilaterian organism. *Nature* **388**, 868 (1997).

7. B. Sokolov, in *Proceedings of the IPU, International Geological Congress*. (1968), vol. 23, pp. 79-86.
8. M. Moczyłowska, F. Westall, F. Foucher, Microstructure and biogeochemistry of the organically preserved Ediacaran metazoan Sabellidites. *Journal of Paleontology* **88**, 224-239 (2014).
9. A. Y. Ivantsov, Trace fossils of precambrian metazoans “Vendobionta” and “Mollusks”. *Stratigraphy and Geological Correlation* **21**, 252-264 (2013).
10. E. A. Sperling, J. Vinther, A placozoan affinity for Dickinsonia and the evolution of late Proterozoic metazoan feeding modes. *Evolution & Development* **12**, 201-209 (2010).
11. J. Dzik, Anatomical information content in the Ediacaran fossils and their possible zoological affinities. *Integrative and Comparative Biology* **43**, 114-126 (2003).
12. I. Bobrovskiy *et al.*, Ancient steroids establish the Ediacaran fossil *Dickinsonia* as one of the earliest animals. *Science* **361**, 1246-1249 (2018).
13. I. Bobrovskiy, J. M. Hope, A. Krasnova, A. Ivantsov, J. J. Brocks, Molecular fossils from organically preserved Ediacara biota reveal cyanobacterial origin for *Beltanelliformis*. *Nature Ecology & Evolution*, (2018).
14. J. K. Volkman, Sterols and other triterpenoids: source specificity and evolution of biosynthetic pathways. *Organic Geochemistry* **36**, 139-159 (2005).
15. T. M. Peakman, J. W. De Leeuw, W. I. C. Rijpstra, Identification and origin of $\Delta 8(14)5\alpha$ - and $\Delta 14 5\alpha$ -sterenes and related hydrocarbons in an immature bitumen from the Monterey Formation, California. *Geochimica et Cosmochimica Acta* **56**, 1223-1230 (1992).
16. S. J. Gaskell, G. Eglinton, Sterols of a contemporary lacustrine sediment. *Geochimica et Cosmochimica Acta* **40**, 1221-1228 (1976).
17. I. Bobrovskiy, J. M. Hope, E. Golubkova, J. J. Brocks, Food sources for the Ediacara biota communities. *Nature Communications*, (in review).
18. A. Kanazawa, Sterols in marine invertebrates. *Fisheries Science* **67**, 997-1007 (2001).
19. H. Ten Haven, J. De Leeuw, T. Peakman, J. Maxwell, Anomalies in steroid and hopanoid maturity indices. *Geochimica et Cosmochimica Acta* **50**, 853-855 (1986).
20. J. M. Moldowan, P. Sundararaman, M. Schoell, Sensitivity of biomarker properties to depositional environment and/or source input in the Lower Toarcian of SW-Germany. *Organic Geochemistry* **10**, 915-926 (1986).
21. S. A. Bradshaw, G. Eglinton, in *Organic Geochemistry: Principles and Applications*, M. H. Engel, S. A. Macko, Eds. (Springer US, Boston, MA, 1993), pp. 225-235.
22. P. A. Jumars, K. M. Dorgan, S. M. Lindsay, Diet of Worms Emended: An Update of Polychaete Feeding Guilds. *Annual Review of Marine Science* **7**, 497-520 (2015).
23. M. A. McMenamin, The Garden of Ediacara. *Palaios*, 178-182 (1986).
24. K. Pehr *et al.*, Ediacara biota flourished in oligotrophic and bacterially dominated marine environments across Baltica. *Nature communications* **9**, 1807 (2018).
25. R. B. MacNaughton, G. M. Narbonne, Evolution and ecology of Neoproterozoic-Lower Cambrian trace fossils, NW Canada. *Palaios*, 97-115 (1999).
26. A. Seilacher, *Trace fossil analysis*. (Springer Berlin Heidelberg, Berlin, 2007), pp. 226.
27. C. E. Kicklighter, M. E. Hay, To avoid or deter: interactions among defensive and escape strategies in sabellid worms. *Oecologia* **151**, 161-173 (2007).
28. S. Bengtson, Origins and early evolution of predation. *The Paleontological Society Papers* **8**, 289-318 (2002).
29. H. Hua, B. R. Pratt, L.-Y. Zhang, Borings in Cloudina shells: complex predator-prey dynamics in the terminal Neoproterozoic. *Palaios* **18**, 454-459 (2003).

30. M. A. Mcmenamin, in *Predator—Prey Interactions in the Fossil Record*. (Springer, 2003), pp. 379-400.
31. C. F. Phleger, P. D. Nichols, P. Virtue, Lipids and trophodynamics of Antarctic zooplankton. *Comparative Biochemistry and Physiology Part B: Biochemistry and Molecular Biology* **120**, 311-323 (1998).
32. J. Vannier, Gut Contents as Direct Indicators for Trophic Relationships in the Cambrian Marine Ecosystem. *PLOS ONE* **7**, e52200 (2012).
33. J. J. Brocks, E. Grosjean, G. A. Logan, Assessing biomarker syngeneity using branched alkanes with quaternary carbon (BAQCs) and other plastic contaminants. *Geochimica et Cosmochimica Acta* **72**, 871-888 (2008).
34. A. J. M. Jarrett, R. Schinteie, J. M. Hope, J. J. Brocks, Micro-ablation, a new technique to remove drilling fluids and other contaminants from fragmented and fissile rock material. *Organic Geochemistry* **61**, 57-65 (2013).
35. J. J. Brocks, J. M. Hope, Tailing of Chromatographic Peaks in GC–MS Caused by Interaction of Halogenated Solvents with the Ion Source. *Journal of Chromatographic Science* **52**, 471-475 (2014).
36. B. Sokolov, The oldest Pogonophora. *Doklady Akademii Nauk SSSR* **177**, 201-204 (1967).
37. B. S. Sokolov, in *Proceedings of All-Union Symposium on Precambrian and Cambrian Paleontology*, B. S. Sokolov, Ed. (Institute of Geology and Geophysics, Siberian Branch, USSR Academy of Sciences, Novosibirsk, USSR, 1965), pp. pp. 78–91.
38. V. G. Chistyakov, N. A. Kalmykova, L. A. Nessonov, G. A. Suslov, On the presence of the Vendian deposits in the mid-stream of Onega River and on the possible existence of tunicates (Tunicata: Chordata) in the Precambrian. *Vestnik Leningradskogo Universiteta* **6**, 11-19 (1984).
39. B. Sokolov, *Essays on the Advent of the Vendian System*. (KMK Scientific, Moscow, 1997).
40. A. L. Ragozina, in *Proceedings of the 2nd International Symposium “Evolution of Life on Earth”*. (Izd. Nauchno-Tekh. Lit-ry, Tomsk, 2001), pp. 133-137.
41. D. Grazhdankin, K. Nagovitsin, A. Maslov, in *Doklady Earth Sciences*. (Springer, 2007), vol. 417, pp. 1183-1187.
42. C. A. Carbone, G. M. Narbonne, F. A. Macdonald, T. H. Boag, New Ediacaran fossils from the uppermost Blueflower Formation, northwest Canada: disentangling biostratigraphy and paleoecology. *Journal of Paleontology* **89**, 281-291 (2015).
43. R. J. Jenkins, The problems and potential of using animal fossils and trace fossils in terminal Proterozoic biostratigraphy. *Precambrian Research* **73**, 51-69 (1995).
44. S. Xiao, X. Yuan, M. Steiner, A. H. Knoll, Macroscopic carbonaceous compressions in a terminal Proterozoic shale: a systematic reassessment of the Miaohu biota, South China. *Journal of Paleontology* **76**, 347-376 (2002).
45. A. Seilacher, L. A. Buatois, M. Gabriela Mángano, Trace fossils in the Ediacaran–Cambrian transition: Behavioral diversification, ecological turnover and environmental shift. *Palaeogeography, Palaeoclimatology, Palaeoecology* **227**, 323-356 (2005).
46. L. A. Buatois, M. G. Mángano, in *The Trace-Fossil Record of Major Evolutionary Events: Volume 1: Precambrian and Paleozoic*, M. G. Mángano, L. A. Buatois, Eds. (Springer Netherlands, Dordrecht, 2016), pp. 27-72.
47. A. Urbanek, G. Mierzejewska, The Fine Structure of Zooidal tubes in Sabellidita and Pogonophora with reference to their affinity. *Acta Palaeontologica Polonica* **22**, 223-240 (1977).

48. S. N. Stampar, A. C. Morandini, L. C. Branco, F. L. Da Silveira, A. E. Migotto, Drifting in the oceans: *Isarachnanthus nocturnus* (Cnidaria, Ceriantharia, Arachnactidae), an anthozoan with an extended planktonic stage. *Marine biology* **162**, 2161-2169 (2015).
49. R. W. Frey, The Lebensspuren of some common marine invertebrates near Beaufort, North Carolina. II. Anemone burrows. *Journal of Paleontology*, 308-311 (1970).
50. P. Jensen, *Cerianthus vogti* Danielssen, 1890 (Anthozoa: Ceriantharia). A species inhabiting an extended tube system deeply buried in deep-sea sediments off Norway. *Sarsia* **77**, 75-80 (1992).
51. M. N. Georgieva *et al.*, Identification of fossil worm tubes from Phanerozoic hydrothermal vents and cold seeps. *Journal of Systematic Palaeontology* **17**, 287-329 (2019).
52. R. C. Vrijenhoek, On the instability and evolutionary age of deep-sea chemosynthetic communities. *Deep Sea Research Part II: Topical Studies in Oceanography* **92**, 189-200 (2013).
53. G. Roeselers, I. L. G. Newton, On the evolutionary ecology of symbioses between chemosynthetic bacteria and bivalves. *Applied Microbiology and Biotechnology* **94**, 1-10 (2012).
54. I. Björkhem, J.-Å. Gustafsson, Mechanism of Microbial Transformation of Cholesterol into Coprostanol. *European Journal of Biochemistry* **21**, 428-432 (1971).
55. S. A. Bradshaw, S. C. M. O'Hara, E. D. S. Cornert, G. Eglinton, Changes in lipids during simulated herbivorous feeding by the marine crustacean *Neomysis integer*. *Journal of the Marine Biological Association of the United Kingdom* **70**, 225-243 (1990).
56. S. A. Bradshaw, S. C. M. O'Hara, E. D. S. Corner, G. Eglinton, Dietary lipid changes during herbivory and coprophagy by the marine invertebrate *Nereis diversicolor*. *Journal of the Marine Biological Association of the United Kingdom* **70**, 771-787 (1990).
57. S. A. Bradshaw, S. C. M. O'Hara, E. D. S. Corner, G. Eglinton, Effects on Dietary Lipids of the Marine Bivalve *Scrobicularia plana* Feeding in Different Modes. *Journal of the Marine Biological Association of the United Kingdom* **71**, 635-653 (1991).
58. S. A. Bradshaw, S. C. O'Hara, E. D. Corner, G. Eglinton, Assimilation of dietary sterols and faecal contribution of lipids by the marine invertebrates *Neomysis integer*, *Scrobicularia plana* and *Nereis diversicolor*. *Journal of the Marine Biological Association of the United Kingdom* **69**, 891-911 (1989).
59. M. J. Hoefs, W. I. C. Rijpstra, J. S. S. Damsté, The influence of oxic degradation on the sedimentary biomarker record I: Evidence from Madeira Abyssal Plain turbidites. *Geochimica et Cosmochimica Acta* **66**, 2719-2735 (2002).
60. M. Nishimura, T. Koyama, The occurrence of stanols in various living organisms and the behavior of sterols in contemporary sediments. *Geochimica et cosmochimica acta* **41**, 379-385 (1977).
61. A. D. Butler, J. A. Cunningham, G. E. Budd, P. C. J. Donoghue, Experimental taphonomy of *Artemia* reveals the role of endogenous microbes in mediating decay and fossilization. *Proceedings of the Royal Society B: Biological Sciences* **282**, (2015).
62. J. N. Ricci, R. Morton, G. Kulkarni, M. L. Summers, D. K. Newman, Hopanoids play a role in stress tolerance and nutrient storage in the cyanobacterium *Nostoc punctiforme*. *Geobiology*, n/a-n/a (2016).
63. K. Fauchald, P. A. Jumars, The diet of worms: a study of polychaete feeding guilds. (1979).

64. E. A. Sperling *et al.*, Oxygen, ecology, and the Cambrian radiation of animals. *Proceedings of the National Academy of Sciences* **110**, 13446-13451 (2013).
65. G. J. Retallack, Interflag sandstone laminae, a novel sedimentary structure, with implications for Ediacaran paleoenvironments. *Sedimentary Geology* **379**, 60-76 (2019).
66. J. D. Weete, M. Abril, M. Blackwell, Phylogenetic distribution of fungal sterols. *PLoS One* **5**, e10899 (2010).
67. J. Fontaine, A. Grandmougin-Ferjani, M.-A. Hartmann, M. Sancholle, Sterol biosynthesis by the arbuscular mycorrhizal fungus *Glomus intraradices*. *Lipids* **36**, 1357-1363 (2001).
68. K. Peters, C. Walters, J. Moldowan, *The Biomarker Guide. Volume 2. Biomarkers and Isotopes in Petroleum Systems and Earth History*. (Cambridge University Press, New York, ed. 2nd, 2005), pp. 634.

Acknowledgments: We thank A. Ivantsov, A. Krasnova, A. Nagovitsyn, P. Rychkov, V. Rychkov, S. Rychkov, T. Rychkova, A. Makushkina for their help with collecting Ediacaran fossils, E. Golubkova for the help with organizing one of the field trips. **Funding:** The study is funded by Australian Research Council grants DP160100607 and DP170100556 (to J.J.B.), Russian Foundation for Basic Research project No. 17-05-02212A (to I.B). I.B. gratefully acknowledges an Australian Government Research Training Program stipend scholarship. **Author contributions:** I.B. designed the study, analyzed biomarkers from Ediacaran fossils and interpreted the data; J.M.H. helped with biomarker analysis; I.B., A.N. and E.L. collected fossils; A.N. contributed palaeontological descriptions, I.B. and J.J.B. wrote the manuscript, with contributions from all authors. **Competing interests:** Authors declare no competing interests; **Data and materials availability:** All data required to understand and assess the conclusions of this research are available in the main text and supplementary materials.

Supplementary Materials:

Materials and Methods

Supplementary Text

Figs. S1 to S3

Tables S1 to S3

References (33-68)

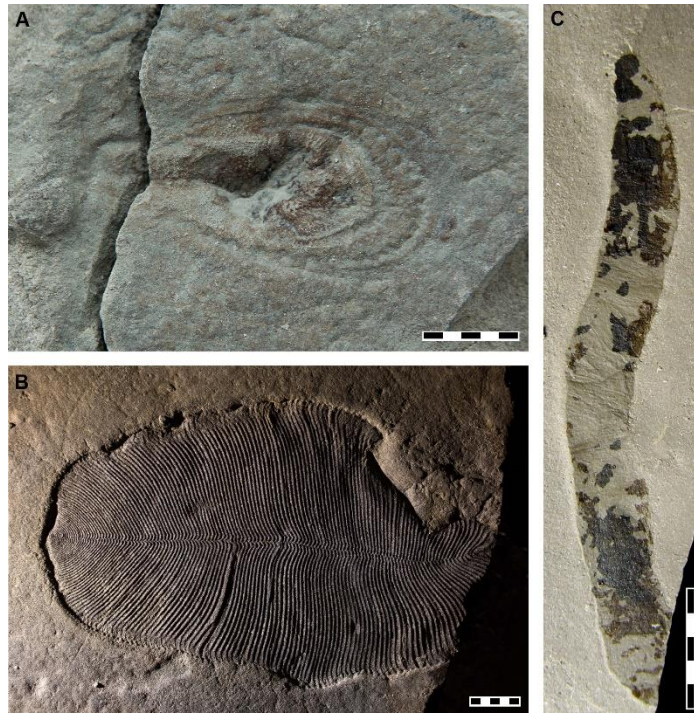


Fig. 1. Organically preserved macrofossils of Ediacaran animals. (A) *Kimberella*, Zimnie Gory locality, scale bar is 5 mm; (B) *Dickinsonia*, Lyamtsa locality, scale bar is 10 mm; (C) *Calyptrina*, Lyamtsa locality, scale bar is 5 mm.

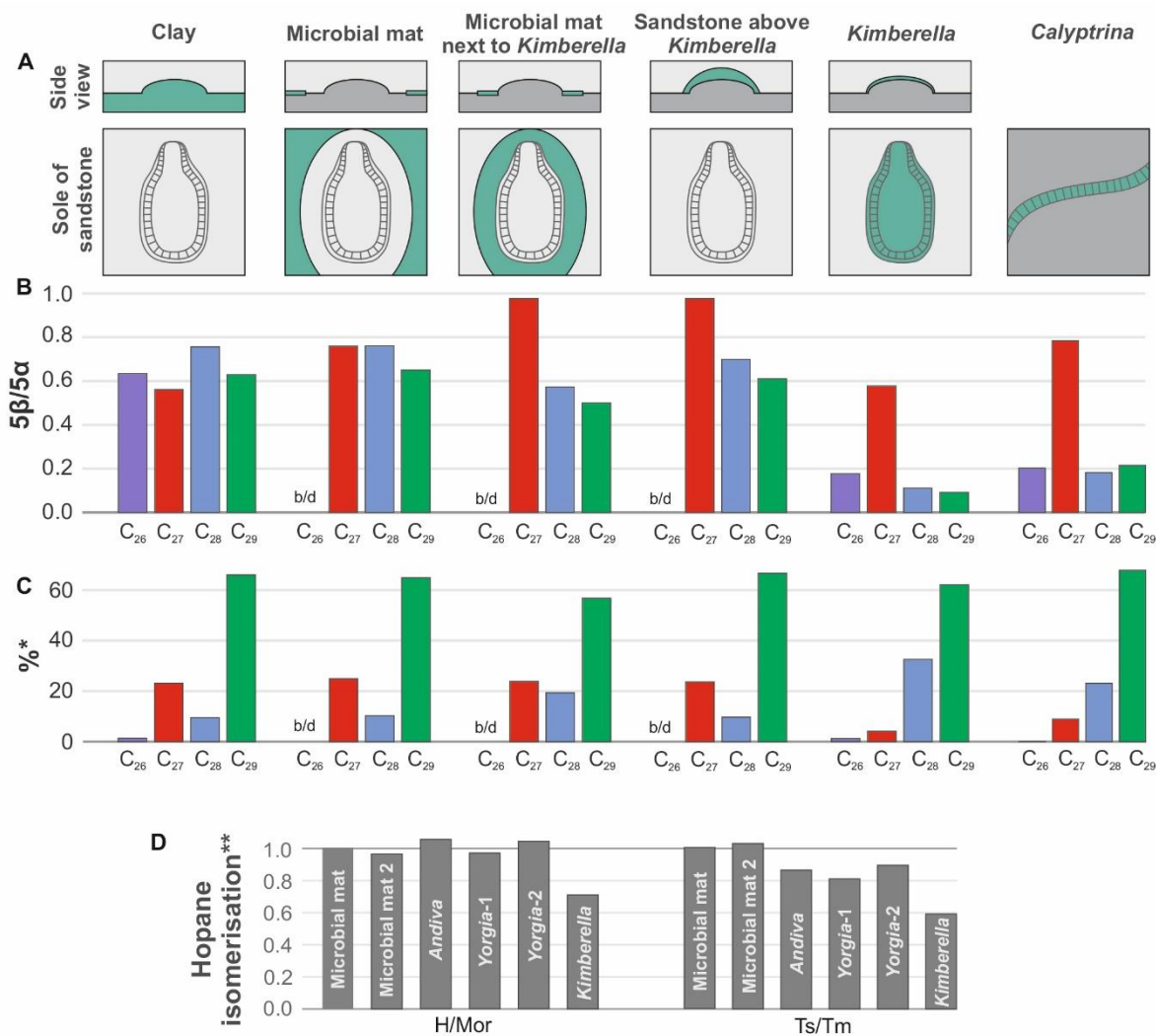


Fig. 2. Biomarker parameters of *Kimberella*, *Calyptrina* and adjacent microbial mats and sediments. (A) A cartoon that highlight the analysed subsamples (highlighted in green); **(B)** 5β/5α ratios for C₂₆-C₂₉ steranes; **(C)** %* - relative proportion of C₂₆-C₂₉ sterane pseudohomologues; **(D)** the extent of hopane isomerisation in the extracts of microbial mats and fossils, to make the data comparable, the panel exclusively compares data that comes from the same surface at the Zimmie Gory locality; **hopane isomerisation parameters are normalised to values in the distant microbial mat extract; b/d– below detection limits.

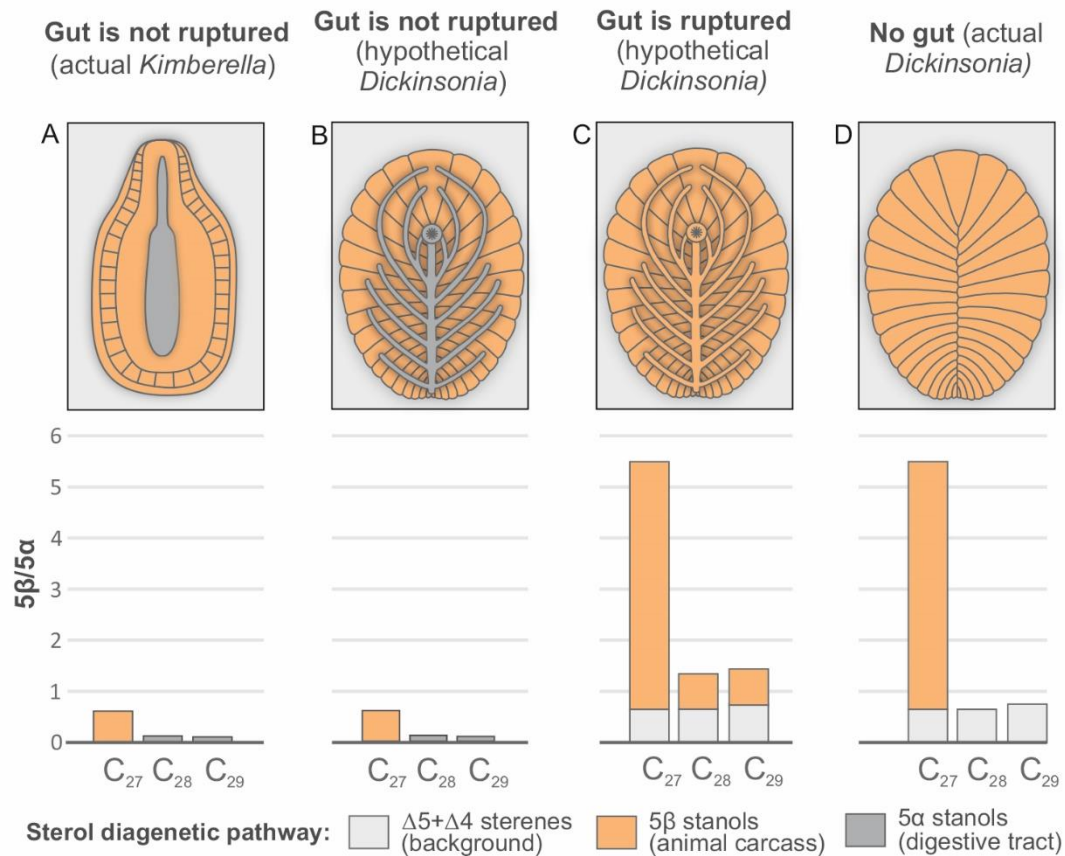


Fig 3. Measured and predicted biomarker signatures of hypothetical *Dickinsonia* with and without guts. (A) Distribution of actual sterane $5\beta/5\alpha$ isomer ratios in *Kimberella* extract; (B) hypothetical sterane isomer distribution of a *Dickinsonia* with an undamaged gut based on sterane data from *Kimberella* extracts assuming a comparable background signal from the mat and comparable diet; hypothetical gut morphology is based on Dzik (11); (C) with a hypothetical damaged gut (based on observations of sterane isomerization in taphonomic experiments on the mollusc *Limax sp.* where gut content and animal tissue became homogenized after rupture of the gut wall; values are computed based on a two component mixing scenario where $5\beta/\alpha = 0.64$ for the mat background (grey area) and a hypothetical gut content comprises 10% of the mass of *Dickinsonia* (Supplementary Text); (D) no gut (actual *Dickinsonia* signal (12)).

Supplementary Materials for

Biomarker evidence for guts, gut contents, and feeding strategies of Ediacaran animals

Ilya Bobrovskiy^{1*}, Alexey Nagovitsyn², Janet M. Hope¹, Ekaterina Luzhnaya (Serezhnikova)³, Jochen J. Brocks^{1*}

¹Research School of Earth Sciences, Australian National University, Canberra, ACT 2601, Australia

²Arkhangelsk Regional Lore Museum, Arkhangelsk 163000, Russia

³Borissiak Paleontological Institute, Russian Academy of Sciences, Moscow 117997, Russia

*Correspondence to: ilya.bobrovskiy@anu.edu.au, jochen.brocks@anu.edu.au

This PDF file includes:

Materials and Methods
Supplementary Text
Figs. S1 to S3
Tables S1 to S3
References (33-68)

Materials and Methods

Sample collection

The palaeontology of *Calyptrina* was studied on collections of the Paleontological Institute of Russian Academy of Sciences and of A. Nagovitsyn coming from the Karakhta, Lyamtsa, Onega, Solza and Zimnie Gory localities of the White Sea area, plus one specimen from Podolia, Ukraine.

Biomarker analyses were conducted on organically preserved macrofossils *Kimberella*, *Calyptrina*, *Dickinsonia*, *Yorgia* and *Andiva*, microbial mats surrounding the fossils, and bulk extracts of sedimentary rocks enclosing the fossils. This data was compared with published biomarker data from *Andiva* and *Dickinsonia* (12). Samples were collected specifically for biomarker analysis during fieldwork in the Lyamtsa and Zimnie Gory localities of the Ediacara Biota in the White Sea Region (Russia) in 2015–2018. The *Calyptrina* specimen analysed for biomarkers comes from a clay layer in the lower part of the Lyamtsa Beds (Ust-Pinega Formation, Redkino Regional Stage), exposed to the south of Lyamtsa Village. All specimens of *Dickinsonia* come from a single surface from the Lyamtsa locality; the surface was underlain by clay with mm-thick lenses of siltstone and sandstone, and overlain with 30 cm-thick sandstone layer with a continuous microbial mat impression at the bottom, composed of thinner (5-10 cm) beds with hummocky cross-stratification, separated by microbially induced wrinkle structures. *Kimberella*, *Yorgia* and *Andiva* were collected from a single surface in the lower part of the Erga Beds (Mezen Formation, Kotlin Regional Stage). The fossils were underlain by clay with mm-thick lenses of siltstone and sandstone and covered with 40-60 cm thick lenses of massive sandstone with soft sediment deformations and thick (up to 5 cm) load cracks and a continuous microbial mat impression at the bottom. All samples were collected avoiding weathered zones and cracks and were immediately wrapped in pre-combusted aluminium foil (300°C, 9h) and packed in calico bags under strict avoidance of contamination (13).

Taphonomic experiments

Two slugs (*Limax sp.*) were fed with avocado for 2 weeks. Subsequently, the *Limax* were euthanized in 50% ethanol solution and then rinsed with sterile water. The first *Limax* was immediately freeze-dried for analysis of its sterol composition. The second was instantly placed into a container filled with natural marine water (collected at the south-eastern coast of Australia, New South Wales), covered with 3 cm of sand and 1 cm clay to create anoxic decomposition conditions; the closed vessel was stored at room temperature in darkness. Anoxic conditions in the sediment were reached within the first week of decomposition, as was evident from the formation of black iron monosulfide, and confirmed with direct measurements (O₂ content < 0.05 µmol/L, measured with PreSens Microx 4 trace fiber optic oxygen meter, PreSens DP-PST7 factory-calibrated dipping probe). The *Limax* was recovered after 5 months of decomposition and freeze-dried for lipid extraction.

Laboratory materials

All solvents were 99.9% grade (UltimAR®; Mallinckrodt Chemicals, St. Louis, MO, USA). The water used in the study was deionized (Millipore Elix 3UV, France). All glassware and aluminium foil were cleaned by combustion at 300°C for 9 h.

Sample preparation and extraction

Organic matter of the *Kimberella*, *Yorgia* and *Andiva* specimens was separated from the sandstone surface using 5% hydrochloric acid (several drops on the surface of a fossil) and 30% hydrofluoric acid (several drops on the surface of a fossil, followed by drying, repeated two times). After acid treatment, the sandstone was placed into a water-filled glass beaker to remove acid. At this stage, most of the organic matter separated itself from the fossils and was collected from the beaker. Any remaining organic matter on the sandstone was separated using a scalpel. Combined organic matter was neutralized in deionized water under ultrasonic agitation, centrifuged (3 times) to separate the solids and then dried. As *Calyptrina* was preserved as a carbonaceous impression within clay, its organic matter could be removed from the rock surface using tweezers. To analyse the sandstone directly above *Kimberella*, after removing the organic matter, 1-1.5 mm of sandstone above the fossil were collected using a micro drill (Dremel® 400 Series Digital, Mexico). Analysis of the last saw-blade solvent rinse confirmed that it was free of detectable contaminants. The drilled powder was collected on combusted aluminium foil. Hydrocarbons were extracted from the organic matter and rock powder via ultrasonic agitation in solvents (methanol for 30 min, dichloromethane (DCM) for 15 min (x 2), DCM : *n*-hexane 1 : 1 for 15 min).

Bulk sedimentary samples surrounding the fossils (represented by clay, heterolithic interlamination and sandstone) were analysed using the so-called Exterior-Interior protocol described in detail elsewhere (13, 33, 34). Briefly, exterior ('E') 3–4 mm of rock samples were removed using a micro drill with a solvent cleaned saw nozzle from all sides of a sample except at the position of the fossil. The exterior and the interior portions of each sample were ground to powder (>240 mesh) using a steel puck mill (Rocklabs Ltd., Onehunga, New Zealand). The mill was cleaned using methanol and dichloromethane, and by grinding combusted (600°C, 9 h) quartz sand.

Bitumen was extracted from rock powder using an Accelerated Solvent Extractor (ASE 200, Dionex, USA) with DCM : methanol (9:1), reduced to 100 µL under a stream of nitrogen gas, and then fractionated into saturated, aromatic and polar fractions using micro-column chromatography over annealed (300°C; 12 h) and dry packed silica gel (Silica Gel 60; 230–600 mesh; EM Science). Saturated hydrocarbons were eluted with 1 dead volume (DV) of *n*-hexane, aromatic hydrocarbons with 4.5 DV of *n*-hexane : DCM (1 : 1) and the polar fraction with 3 ml DCM : methanol (1 : 1). Extracts from fossils with low hydrocarbon content were

only fractionated into saturated+aromatic and polar fractions to reduce the loss of analytes. An internal standard, 18-MEAME (18-methyleicosanoic acid methylester; Chiron Laboratories AS), was added to the saturated and aromatic fractions, while D4 (*d*₄-C₂₉- $\alpha\alpha\alpha$ R-ethylcholestane; Chiron Laboratories AS) was added to saturated and saturated+aromatic hydrocarbon fractions with low biomarker content. The samples were analysed and quantified by GC–MS.

Freeze-dried *Limax* were extracted via ultrasonic agitation in solvents (methanol : dichloromethane (DCM) 3 : 2 for 15 min (x 2), DCM : *n*-hexane 2 : 3 for 15 min). The extract was fractionated into non-polar and polar fractions using micro-column chromatography over annealed and dry packed silica gel. Non-polar molecules were eluted with 1.5 ml of *n*-hexane : DCM (1 : 1) and the polar fraction with 1 ml DCM : methanol (1 : 1). The polar fractions were saponified in 1 ml 5% KOH methanol : water 4 : 1 solution at 50°C overnight, 1 ml of water was added, and the neutral fraction was subsequently extracted by vortexing for 1 min with 1 ml of DCM : *n*-hexane 1 : 4 (x 3). Sterols in the neutral fraction were converted to the trimethylsilyl (TMS) derivatives for gas chromatography–mass spectrometry analysis.

Gas chromatography–mass spectrometry (GC-MS)

GC-MS analyses of biomarker extracts were carried out on an Agilent 6890 gas chromatograph coupled to a Micromass Autospec Premier double sector mass spectrometer (Waters Corporation, Milford, MA, USA) at the Australian National University. The GC was equipped with a 60 m DB-5 MS capillary column (0.25 mm i.d., 0.25 μ m film thickness; Agilent JW Scientific, Agilent Technologies, Santa Clara, CA, USA), and helium was used as the carrier gas at a constant flow of 1 mL min⁻¹. Samples were injected in splitless mode into a Gerstel PTV injector at 60°C (held for 0.1 min) and heated at 260°C min⁻¹ to 300°C. For full-scan, selected ion recording (SIR) and metastable reaction monitoring (MRM) analyses, the GC oven was programmed from 60°C (held for 4 min) to 315°C at 4°C min⁻¹, with total run time of 100 min. All samples were injected in *n*-hexane to avoid deterioration of chromatographic signals by FeCl₂ build-up in the MS ion source through use of halogenated solvents (35). $\alpha\alpha\alpha$ 20R-Stigmastane was quantified in full-scan mode in *m/z* 217 trace, relative to the 18-MEAME internal standard (*m/z* 340). Steranes and hopanes were integrated in MRM mode in M⁺ \rightarrow 217 and M⁺ \rightarrow 191 transitions respectively and quantified relative to the $\alpha\alpha\alpha$ 20R-stigmastane signal obtain during full scan experiments. Monoaromatic steroids were quantified in SIR mode using the *m/z* 253 base ion. Sterol TMS-ethers from *Limax* were quantified in full-scan mode using base peaks (*m/z* 129 for sterols, and *m/z* 370, *m/z* 384 and *m/z* 398 for C₂₇, C₂₈ and C₂₉ stanols respectively) relative to the 18-MEAME internal standard (*m/z* 340); differences in *m/z* response between sterol and stanol integrated areas were corrected based on signal areas of C₂₇ sterols and stanols in full scan total ion current chromatograms. Peak areas for saturated and aromatic molecules are uncorrected for differences in GC-MS response.

Error quantification

As numerous repeat injections of fossil extracts were not possible due to the limited abundance of valuable sample material, standard deviations for the concentration of each biomarker were externally determined based on repeat injections of the AOGC industrial standard biomarker mixture. For repeat GC-MS experiments of the AOGC standard on the AutoSpec Premier, a clear relationship exists between the peak area and its coefficient of variation: $C_v = 186.18x^{-0.31}$ ($R^2 = 0.82$), where x is the integrated peak area (12). The standard deviation was calculated as $STD = C_v * \text{signal area}$. For biomarker ratios, error propagation followed standard root mean square error propagation formulae. As $\beta\alpha\alpha$ 20R-ergostane (5β) coelutes with two minor other compounds, $\alpha\alpha\alpha$ 20S-ergostane and an unknown sterane (tentatively identified as a $\beta\alpha\alpha$ 20R-27-nor-sterane), its integration error is expectedly much higher than the error for sterane isomers that are not coeluting and where the error is mainly controlled by the signal/noise ratio. Thus, an integration error for ergostane $5\beta/5\alpha$ ratios was calculated based on the whole dataset of sediment extracts assuming $5\beta/5\alpha$ is constant among C_{27} to C_{29} sterane pseudohomologs, which was determined to be $C_v = 0.34$ for the Ediacaran White Sea area extracts (12).

Laboratory system blanks

A comprehensive, accumulatory system blank was performed covering all analytical steps from extraction and fractionation to instrumental analysis. For this purpose, combusted (600°C , 9 h) sand was used to monitor background contamination during grinding, extraction, and fractionation processes.

Supplementary Text

Calyptrina palaeontological description

Calyptrina striata has been first described by Sokolov (36) based on a single pyritised specimen from the drillcore Obozerskaya in Russia. Since then, a significant collection of *in situ* preserved *Calyptrina striata* from the White Sea area has been assembled, which allows us to get a more complete picture about morphology and lifestyle of these organisms. Here we provide a short preliminary description of the palaeontological data on *Calyptina striata* from the White Sea area.

Phylum Annelida Lamarck, 1809

Genus *Calyptrina* Sokolov, 1967

Type species. *Calyptrina partita* Sokolov, 1967; Viluy River, Eastern Siberia, Russia; Nemakit-Daldyn Fm., Fortunian Stage, Cambrian.

Composition. Type species and *Calyptrina striata*.

Remarks. B.S. Sokolov introduced the names of the genus and its type species in the symposium abstracts 1965 (37), but the date of their formal erection should be considered 1967, when the specified *C. partita* holotype and its photographs were published (36).

Calyptrina striata Sokolov, 1967

Fig. 1a, Figs. S1-S3

1967 *Calyptrina striata* sp. nov. Sokolov – Sokolov (36), p. 130–131, fig. 2.3.

1984 cf. *Paleolina* sp. – Chistyakov et al. (38), p. 13, figs. 2d–g.

1997 ?*Calyptrina* sp. – Sokolov (39), pl. XII, figs. 4, 5.

1997 *Calyptrina striata* Sokolov – Sokolov (39), pl. XIV, fig. 4.

2001 *Calyptrina* sp. – Ragozina (40), pl. I, figs. 1–3.

2007 *Sinospongia chenjunyuani* Chen – Grazhdankin et al. (41), p. 1185, Fig. 2e

Holotype. Obozerskaya borehole № 1, depth 303.5 m, work settlement Obozersky, Arkhangelsk Region, Russia; lower part of the Verkhovka Beds, Ust-Pinega Formation, Ediacaran (Fig. S3B,C).

Material. Holotype and numerous specimens of various types of preservation from the Karakhta, Lyamtsa, Onega, Solza and Zimnie Gory localities of the Arkhangelsk Region, one specimen from the Podolia, Ukraine. Collections of the Paleontological Institute of RAS and of A. Nagovitsyn.

Original diagnosis. Tube has an irregular funnel-shaped structure without a rim, but with a characteristic transverse annulation, which may be due to a differential degree of chitinization of the tube or compaction of its organic matter (36).

Description. Fossils *C. striata* in the White Sea area are usually mass buried *in situ* within heterolithic interlamination (Figs. S1, S2, S3A-I) or redeposited in channelized sandstone lenses, co-occurring there with *Rangea* and *Ventogyrus* (Fig. S3J,K).

C. striata is a cylindrical, non-branched, flexible, organic-walled tube with fine transverse ridged wrinkles on the external surface (Fig. 1). Tube morphology is variable between different parts of the tube. The anterior part is best preserved at the base of separate sandstone and siltstone beds as negative hyporelief impressions of the external tube surface (Figs. S1A-D, S3D,E,F,H) and casts of its internal cavity if sand has penetrated into the tube (Figs. S1C,E,F, S3A,C). The anterior part is supposedly thick-walled (Fig. S1C,E,F), annulations are created by transverse dense ridges and wrinkles, that are distributed either evenly (Figs. 1A; S1C, S3G,K), or in regular ring-like groups (Fig. S1A,D, S3B-F,J), with fine longitudinal ridges in-between them (Fig. S3B,F). The front-end that is mainly located above the sediment-water interface is vertical, short, and straight. It was flexible enough to be pressed into the sea-bottom by a current, forming scratch circles, and to be buried under a thin layer of sand (Fig. S1A-C). The posterior underground part is best preserved in a thin-bedded clay and in a thinnest alternation of sandstone and shale (Fig. S2). The posterior part has thinner walls and finer transverse ridges and wrinkles, oriented more chaotically (Fig. S2G). It is nearly horizontal, long and irregularly meandering, either sinusoidal or zigzag (geniculate) in form (Fig. S2A-F).

During life, *C. striata* could survive several episodes of sand deposition, separated by sedimentation of clay material. There is often an erosional pocket filled with sediment at the base of the anterior part of a tube (Fig. S1G,H); this pocket likely formed due to the erosion of sediments behind the tube by a current. Such pockets, as well as scratch circles can be seen at the bases of all sand layers the tube goes through. Some tubes terminate earlier than others, indicating different times of death of the individuals during sediment deposition (Fig. S1G).

Evidence that the anterior part of the tube was located at the same spot for long periods of time indicates that the growth in the horizontal plane of the tube happened at its posterior end. The absence of segmentation in the underground part of the tube suggests that the posterior end stayed open throughout the life of the organism.

Dimensions. The tube width is from 1 to 10 mm, usually 4 to 8 mm, for both anterior and posterior parts of the tube. The full maximum length of the tube is unknown, but the longest found specimen of the posterior part is 62 cm (with the width 8 mm, Fig. S2B), and the longest anterior part is 32 mm (with the width 4 mm).

Remarks. Sokolov described *C. striata* based on a single pyritized specimen. =In his diagnosis of the species he mentions ‘funnel-like structures’ (36), however this study does not confirm their presence.

Calyptrina-like cylindrical, organic-walled, annulated tube fossils were described from the Ediacaran age around the world. These include *Annulatubus flexuosus* and *Sekwitubulus annulatus* from Canada (42), “*Taenidium cf. serpentinum*” from Australia (43), “*Sinospongia tubulata* = *Calyptrina striata* from China (44). However, we were unable to reliably compare these findings with the White Sea material solely based on publications.

The underground *C. striata* part resembles South Australian “*Aulozoon*”, a long, horizontal, undermat tubular fossil (45, 46). It is possible that the “*Aulozoon*” belongs to a related species, however it is typically 1.5-3 times wider than *C. striata*.

Affinity. Most of the previous studies on *C. striata* and related Cambrian sabelliditids agreed that these fossils represent tube-dwelling Annelida, probably related to the family Siboglinidae (8, 36, 47). Among extant organisms other than annelids, a number of Anthozoa members dwell in organic-walled underground tubes; however, thick agglutinated walls and branching morphology of the anthozoan tubes makes these organisms unlikely candidates for *C. striata* (48-50). Cylindrical shape of the tubes, the great length and longitudinal ridges of *C. striata* indeed resemble some modern siboglinid and chaetopterid tubes. As most of the *C. striata* tube dwelled within the sediment covered in microbial mats, decomposition of organic matter in the lower layers of the mats and in the sediment could potentially provide methane and hydrogen sulfide for chemosymbiotic nutrition of these worms. However, the morphology of *C. striata* is not unique for Siboglinidae, and allows for other affinities within annelids (51). Additionally, both systematic analysis of siboglinid fossils through time and molecular clock estimates suggest Siboglinidae only appeared in the Mesozoic (51, 52). Presence of a gut and the green algal gut content in *C. striata* suggest that these tube worms were suspension feeders (this study). However, in view of the length of their underground part, it cannot be excluded that they combined suspension feeding with obtaining nutrition from chemosynthetic symbionts, as some extant bivalves do (53).

Distribution. Late Ediacaran, about 563-550 Ma; (1) the Arkhangelsk, Verkhovka, Syuzma, Zimnie Gory Beds of the Ust-Pinega Formation and the Erga Beds of the Mezen Formation, Arkhangelsk Region, Russia; (2) Mohyliv Formation, Mohyliv-Podilskyi Group, Podolia, Ukraine; possible (3) Upper Doushantuo black shales at Miaohu, China.

5 β /5 α sterane isomers ratio

There is a large variation in 5 β /5 α ratios of steranes in the extracts of Ediacaran fossils. Elevated 5 β /5 α values for cholestanes (up to 5.5) were detected in all dickinsoniids, while the corresponding ergostane and stigmastane ratios in these fossils show the typical sedimentary background value 5 β /5 α \approx 0.6 (12); the same pattern is observed in mats and sediments immediately surrounding *Kimberella* (Table S1). C₂₆, C₂₈ and C₂₉ steranes in *Kimberella* and *Calyptrina* are, in contrast, strongly dominated by 5 α isomers (5 β /5 α from 0.09 to 0.21). Both patterns, i.e. strongly elevated and depleted 5 β /5 α ratios, are rarely observed in nature and the geological record. Under usual sedimentary conditions, the 5 β isomer is generated by

hydrogenation of Δ^5 sterenes (sterenes with a double bond in position 5 of the ring system), while 5α is formed from Δ^4 sterenes. The configuration of most biological sterols is Δ^5 . However, due to double bond isomerisation between the Δ^5 and Δ^4 positions, the equilibrium ratio between the 5β and 5α sterane isomers in an abiological thermodynamically driven system is always $\Delta^5 \rightarrow 5\beta : \Delta^4 \rightarrow 5\alpha = 39:61$, resulting in $5\beta/5\alpha = 0.64$ (15). This proportion is generally characteristic of bulk rock extracts from the White Sea Area (average $5\beta/5\alpha = 0.64 \pm 0.26$, $n = 54$) (12). $5\beta/5\alpha$ sterane ratios that are much higher or much lower than this value can be explained by microbial or dietary hydrogenation of unsaturated sterols, depending on the operating microbiological community, to 5β or 5α stanols, and their further dehydration to Δ^3 - 5β or Δ^2 - 5α sterenes and reduction to 5β or 5α steranes (15, 16, 54). These processes, when occurring within sediment, affect all steroid pseudohomologs equally, regardless of side chain alkylation (15). In order to create the elevated $5\beta/5\alpha$ cholestane (C_{27}) ratios observed in dickinsoniid extracts, in combination with equilibrium values for ergostane (C_{28}) and stigmastane (C_{29}), only C_{27} sterols were subject to decay in the strongly anaerobic microenvironment of the decaying carcass. Sterols from the surroundings of the fossils were degraded under different taphonomic conditions, allowing us to disentangle the signals of fossils and background. Similarly, C_{26} , C_{28} and C_{29} steranes in *Kimberella* and *Calyptrina* demonstrate extremely low $5\beta/5\alpha$ values (0.09 to 0.21). This implies that these molecules were predominantly transformed into 5α stanols by a local microbial community restricted to these organisms, and the fact that cholesterol was removed from this process suggests it was happening in their guts (55-58).

Gut content of *Kimberella* and *Calyptrina*

Steroids in the gut of invertebrates often constitute a large proportion of the total steroid content, sometimes in excess of 50% (31). However, the proportion of gut-derived steroids in the extracts of *Kimberella* and *Calyptrina* is much larger yet. There are three possible explanations for this phenomenon. Firstly, based on the halo of animal-derived cholestane surrounding *Kimberella* (Fig. 2), it is evident that some proportion of cholesterol was lost into the surrounding sediments. By contrast, the gut content may have been restrained by the gut wall. Secondly, the chemical state of sterols in the animal tissue and in the gut must have been very distinct at the time of burial. Dietary sterols in the gut were rapidly hydrogenated after death by the gut microbiome, as evident from their isomer distributions, resulting in saturated stanols that are relatively degradation resistant. This is also supported by the distribution of monoaromatic steroids (MAS): they are below detection limit in *Calyptrina*, and solely bear the signature of the background organic matter in *Kimberella* extract (MAS $C_{27} : C_{28} : C_{29} = 23\% : 18\% : 58\%$), indicating that dietary sterols of both *Calyptrina* and *Kimberella* were quantitatively transformed into saturated steranes. By contrast, animal cholesterol possesses an unsaturation in the ring system that constitutes a point of attack for oxygen and other chemicals, presumably causing preferential degradation (59, 60). The difference in the saturation state of sterols in the tissue and in the gut at the point of burial would thus have strongly favoured the

preservation of dietary steroids. Finally, during the critical initial stages of decay, gut walls provide a physical barrier against oxygen and other reagents that may aid decomposition of lipids. As most organic compounds in sediments, including lipids, are remineralized (commonly >99% (59)), even a small difference in the preservation potential of sterols in animal tissues and gut contents may cause order-of-magnitude differences in resulting lipid ratios.

Absence of gut content in dickinsoniids

Absence of the 5α dominated sterane signal in dickinsoniids indicates the lack of a contrasting microbial community as observed in the gut of *Kimberella* and *Calyptrina*. However, this observation by itself does not exclude the presence of a gut microbiome in *Dickinsonia*. Gut walls are often ruptured early during decay (61), and in those cases it is plausible that gut content and animal tissues will be altered by a shared microbiological community operating under relatively homogeneous chemical conditions. To test this proposition, i.e. whether dietary and animal sterols follow the same diagenetic pathway when the gut wall is ruptured, we studied sterol transformations within an animal (the slug *Limax*) after degradation within a layer of sediment under anoxic conditions, mimicking the decay of Ediacaran organisms after burial under a thick layer of fine sand (12). To create a contrast between the cholesterol produced by the animal (C_{27}) and its gut content, *Limax* had been sustained on a diet of avocado, which contains the phytosterols campesterol (C_{28}) and sitosterol (C_{29}). After 5 months of decay under anaerobic conditions, the slug had become completely liquefied and homogenized within its outer cuticle, and its cholesterol was transformed into degradation products overwhelmingly represented by 5β -cholestanol (5β -cholestanol/cholesterol = 3.57; Table S3). In contrast, 5α -cholestanols, the precursors of 5α -cholestanes, were below detection limit. Notably, although the molecular composition and degradability of organic matter of avocado are different from *Limax*, the transformation of the phytosterols resulted in the same proportion of 5β stanols to sterols (5β -ergostanol/campesterol = 3.55; 5β -stigmastanol/sitosterol = 3.69; Table S3). As in case of cholesterol, 5α -phytosterols were below detection limit. These results have two important implications. Firstly, it confirms that the transformation pathway of sterols was not influenced by side chain alkylation, i.e. the C_{27} , C_{28} and C_{29} sterols were degraded in the same way (15). Secondly, sterol transformation does not appear to be influenced by the immediate organic environment (i.e. sterols within animal cell membranes degrade in the same way as phytosterols associated with plant cell walls), but appears to be controlled by the reducing chemical conditions in the rotting carcass/gut mixture and its specific microbial community. Based on the preferential degradation of *Limax*- and gut-sterols to 5β stanols, further degradation of the carcass over geological time would generate a sterane isomer distribution with $5\beta/5\alpha \gg 0.64$, equally for C_{27} , C_{28} and C_{29} pseudohomologs (see section “ $5\beta/5\alpha$ sterane isomers ratio”). By contrast, in *Dickinsonia* extracts, only C_{27} steranes have elevated $5\beta/5\alpha$ ratios (up to 5.5), while C_{28} and

C₂₉ steranes display the equilibrium ratio of ~0.6. These values are thus inconsistent with the presence of significant gut content (see below for a quantitative argument). Furthermore, these values are also inconsistent with significant amounts of sterols from eukaryotic endosymbionts, as their degradation would likewise generate elevated 5 β /5 α ratios.

That dietary lipids and the lipids of an animal follow a shared transformation pathway allows to quantify the potential gut content of *Dickinsonia*. *Dickinsonia* specimens preserved on bedding surfaces were inhabiting microbial mat at the moment of burial, so the organic matter of these organisms became fused with algal and bacterial organic matter in the mat. However, analysis of biomarkers from multiple *Dickinsonia* specimens of different size that all came from the same surface allowed to quantify the original lipid composition of *Dickinsonia* (12). There are three distinct features that make this quantification possible by providing a contrast between *Dickinsonia* and the background biomarker signatures. Firstly, *Dickinsonia* carcasses were degraded in permanently anoxic local microenvironments, which resulted in anomalously high 5 β /5 α cholestane isomer ratios (up to 5.5), which contrasts with 5 β /5 α of ergostane and stigmastane close to 0.64 derived from background sterols transformed abiologically or by different microbial communities (12). Secondly, aromatisation of sterols in the microenvironment within *Dickinsonia* carcasses was more than an order of magnitude higher than in the background, so aromatic steroids provide a yet more distinct difference between *Dickinsonia* and microbial mats than saturated steranes (12). Finally, the anoxic conditions during *Dickinsonia* diagenesis imply that little or no hopanoids were contributed by bacterial degradation (62) because hopanoids are overwhelmingly produced by aerobic bacteria. Thus, the bulk of hopanoids in the *Dickinsonia* extracts must come from the underlying microbial mat. The *Dickinsonia* and the underlying microbial mat comprise a two-component mixing system, which, based on multiple *Dickinsonia* extracts, can be extrapolated to identify the composition of the components. Thus, variability in the relative proportion of 5 β and 5 α isomers of saturated steranes (5 β /5 α) and the proportion of monoaromatic steroids and hopanes (MAS/H) for C₂₇, C₂₈ and C₂₉ steroid homologs between the extracts allowed to quantify that *Dickinsonia* sterols were nearly exclusively represented by cholesterol, with a possible 0.3 \pm 0.33% contribution of other sterols (Table S2) (12). This is the maximum amount of sterols in *Dickinsonia* extracts that could have potentially come from gut content.

We can improve the estimate of a possible gut content in *Dickinsonia* yet further. The above computation is based on the ergosteroid and stigmasteroid content of *Dickinsonia* extracts. However, ergosteroids have a high integration error due to low signal to noise ratios and multiple coeluting peaks on the chromatogram. By contrast, monoaromatic stigmasteroids yield clear and clean chromatographic signals and can be quantified with great precision. We can thus reduce the error by using only stigmasteroids for the computation. Knowing the proportion of stigmasteroids among C₂₇ to C₂₉ sterols in the background signal around *Dickinsonia* (~80%) (12) and the maximal stigmasteroid content in *Dickinsonia* based on the MAS/H variations (0.07 \pm 0.16%, Table S2), the possible contribution of C₂₇ to C₂₉ gut sterols to *Dickinsonia* extracts cannot have exceeded 0.10 \pm 0.23%. As this computation is based on

MAS/H ratios, the lack of variability in C₂₈ MAS/H and C₂₉ MAS/H values also indicates that the hopanoid content in the *Dickinsonia* extracts was constant and at the background level. Based on these low numbers, which represent maxima, it is likely that *Dickinsonia* did not possess an internal digestive system: in contrast to predators, filter and deposit feeders maintain continuous food input and constantly have filled guts (63, 64). Thus, dickinsoniids must have followed a different feeding mode and likely possessed an external digestion system (10).

Could *Dickinsonia* be a lichen?

The sterol composition of *Dickinsonia* was in excess of 99.7% cholesteroloids. Based on this composition, dickinsoniids have been assigned to total-group Metazoa (12). Retallack (65) suggested the alternative view that dickinsoniids are lichenized fungi of the division Glomeromycota as these apparently also produce cholesterol as a principle sterol. However, this suggestion has been made based on misapprehension of the literature. It is correct that Glomeromycota do not produce ergosterol (C₂₈) as most lichens do; yet, they do not contain major concentrations of C₂₇ sterols either (66). Based on the literature cited by Retallack (65), Glomeromycota mainly produce “24-methyl and 24-ethyl cholesterol” (66, 67), compounds that are in fact unrelated to cholesterol, possessing 28 and 29 carbon atoms (C₂₈ and C₂₉ sterols) respectively, compounds that are arguably not produced by dickinsoniids. Thus, the steroid composition of *Dickinsonia* rules out a lichen affinity and narrows down the phylogenetic position of *Dickinsonia* to Metazoa, while their mode of preservation reveals the presence of differentiated tissues that is diagnostic for stem or crown Eumetazoa (3).

Syngeneity of biomarkers

GC-MS MRM, SIR and full-scan analyses of the comprehensive accumulatory laboratory system blank confirmed that the detected hydrocarbons were not introduced by laboratory processes. Monitoring of the blank yielded no *n*-alkanes, hopanes or steranes, even when measured using the most sensitive GC-MS MRM methods. The only contaminants detected in the blank are trace amounts of phthalates—plasticizers present in small amounts in solvents used for extraction of biomarkers.

The results of Exterior/Interior (E/I) experiments, as well as a detailed discussion of biomarker syngeneity of the samples from the White Sea that were collected, transported and stored in the same way as samples used in this study, are presented elsewhere (13). The results show nearly identical concentrations of all biomarkers in exterior and interior rock portions with E/I = 1.09 to 1.53 for *n*-alkanes and E/I = 0.93 to 1.05 for hopanes and steranes, which indicates that the precombusted aluminium foil and clean calico bags prevented contamination of samples during transportation and storage, and confirm that all detected compounds are indigenous (13).

Dickinsoniid extracts demonstrate the same exceptionally low thermal maturity as other fossils from the White Sea area (12, 13). The high $\beta\alpha/(\beta\alpha + \alpha\beta)$ and low $T_s/(T_s + T_m)$ hopane isomer ratios, virtual absence of diasteranes, $\alpha\beta\beta$ and $\alpha\alpha\alpha$ 20S sterane isomers are characteristic of highly immature sediments, which demonstrates that the hydrocarbons are significantly below the so-called oil-generation window, i.e. the kerogen never thermally generated and expelled liquid hydrocarbons (68). Such low thermal maturity is never observed in contaminant petroleum products and migrated oils, which by their very nature must have a maturity within the oil-generation window. Thus, contamination of the samples by petroleum products or by migrated hydrocarbons did evidently not occur.

Supplementary Figures and Tables

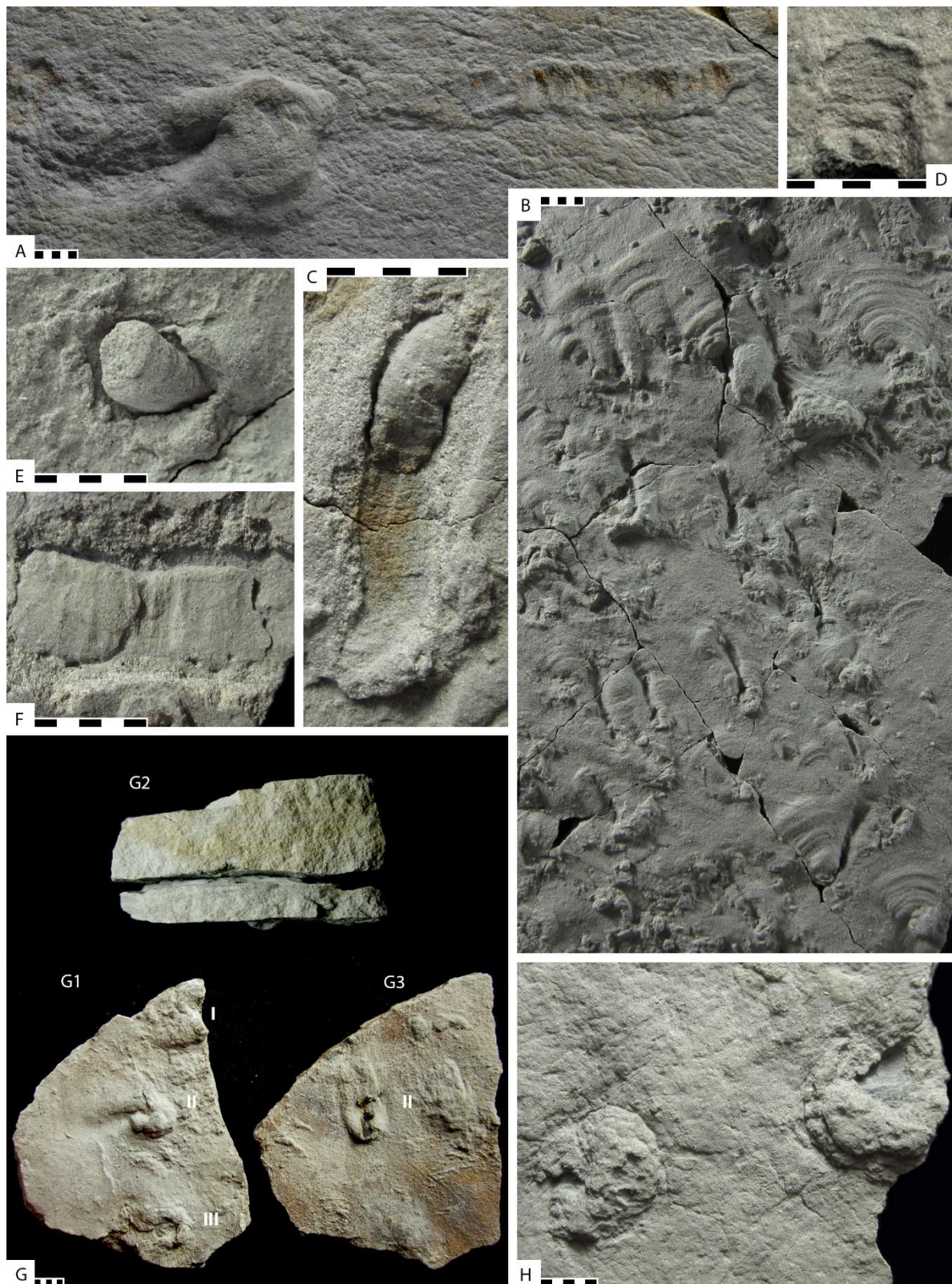


Fig. S1. The anterior part of *Calyptrina striata* and related sedimentary structures, all photographs show the base of sandstone layers that buried the fossils unless specified. (A) an erosional depression with circle scratch marks next to a deformed front end of the tube

(left) and a horizontal underground part of the tube with annulations, preserved ~1.5 mm below the sandstone base; **(B)** circle scratch marks around the negative hyporelief impressions of the tubes; **(C)** composite impression of a tube, partially filled with sand (internal mould) and not filled with sand (negative hyporelief); **(D)** negative hyporelief imprint of the base of a front end of the tube with ring-like annulation; **(E,F)** internal moulds of the tubes; the gap between the internal moulds and the rest of the sandstone might reflect the thickness of the tube wall, though it might have been distorted by sediment deformations and incomplete enclosing of the tube by sand; **(G)** layer-by-layer preservation of the sedimentary structures around the front end of the tube, indicating that it has survived several events of sand sedimentation, G1 – the lower sand bed with three tubes (marked as I-III), G2 – side view of the sample, G3 – the upper sand bed with only tube II remaining; **(H)** – erosion of a microbial mat-covered surface behind the tubes by a current. A – Syuzma Beds, Ust-Pinega Formation, Karakhta River locality, B-H – Syuzma Beds, Ust-Pinega Formation, Solza River locality. Scale bar is 5 mm.

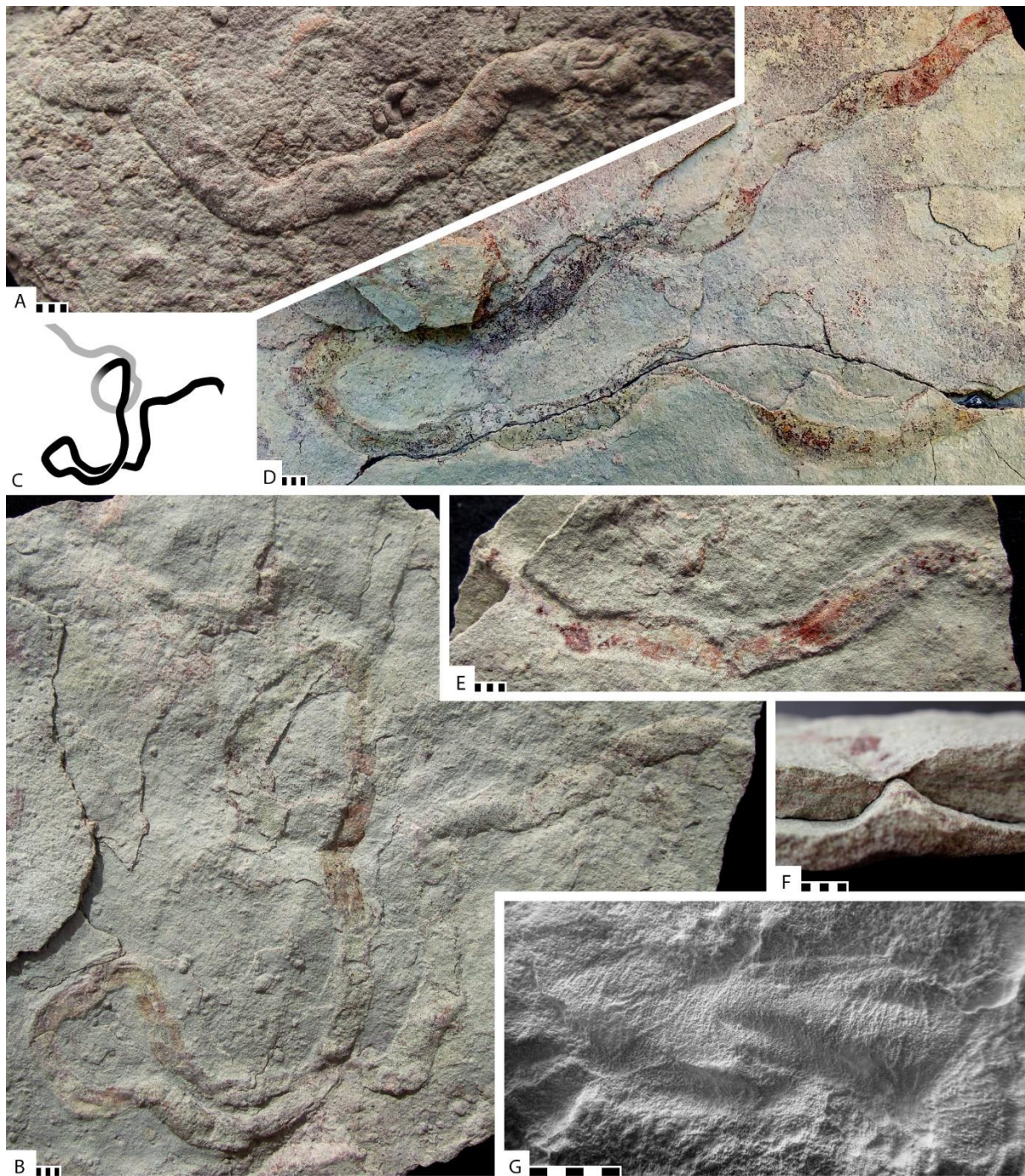


Fig. S2. The posterior part of *Calyptrina striata* within clay and thin heterolithic interlamination. (A) Details of the wrinkles on the underground part of the tube in a latex cast of a negative hyporelief impression; (B) change in hyporelief preservation of the tube between positive and negative depending on its depth below the sediment-water interface; show is the longest tube found in the White Sea area; (C) interpretive drawing of the same specimen; (D) a sinusoidal-shaped underground part of the tube; (E) change in the preservation hyporelief of the tube between negative (left) and positive (right) depending on its depth below the sediment-water interface; (F) side view of the same specimen where the tube has collapsed; (G) a part of the tube that most probably died before it was buried. All

specimens are from the Erga Beds, Mezen Formation, uppermost section of the Zimmie Gory locality. Scale bar is 5 mm.

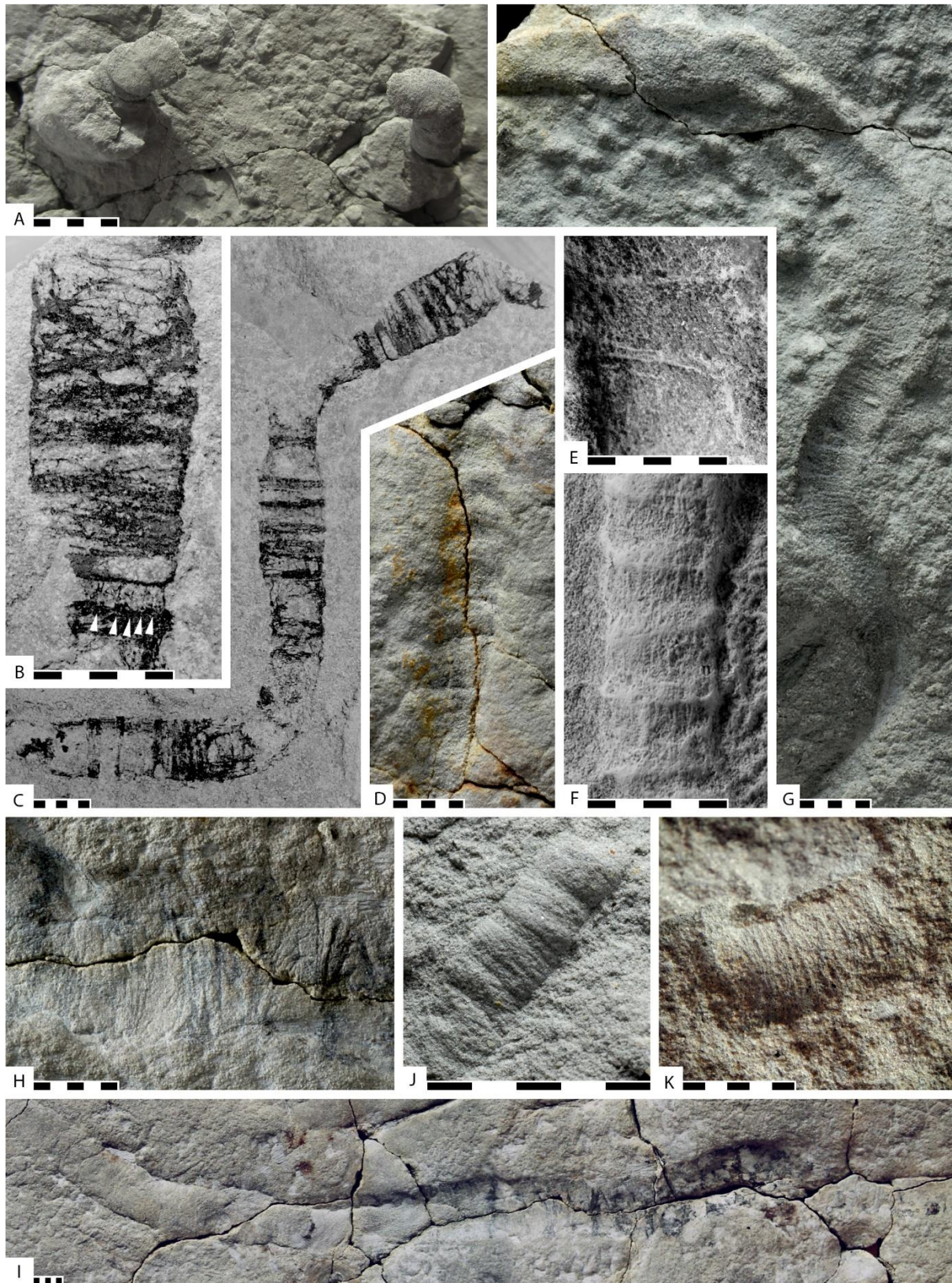


Fig. S3. Details of *Calyptrina striata* tube morphology. (A) internal molds of the anterior parts of the tubes filled with sand, Syuzma Beds, Ust-Pinega Formation, Solza River locality;

(B,C) holotype, a pyritized flat compression in a silty clay, note that the dark transverse rings are not homogeneously distributed, **B** – magnification, showing longitudinal ridges that are marked with white arrows, Verkhovka Beds, Ust-Pinega Formation, Obozerskaya № 1 borehole, depth 303.5 m; **(D)** a tube in negative hyporelief, additional pattern is created by transverse rings, Lower Erga Beds, Mezen Formation, Zimnie Gory locality; **(E)** a tube in negative hyporelief, transverse ridges and wrinkles are distributed in regular ring-like groups, with longitudinal ridges visible in-between, Syuzma Beds, Ust-Pinega Formation, Karakhta River locality; **(F)** a tube in negative hyporelief, transverse ridges and wrinkles are distributed in regular ring-like groups; **(G)** posterior part of a tube in negative hyporelief, with clear transverse wrinkles, Syuzma Beds, Ust-Pinega Formation, Karakhta River locality; **(H)** a tube in negative hyporelief with clear irregular transverse wrinkles, Lower Erga Beds, Mezen Formation, Zimnie Gory locality; **(I)** a tube partially filled with sediment (left), partially preserved in negative hyporelief (right), where it additionally shows transverse wrinkles due to pyritisation, Lower Erga Beds, Mezen Formation, Zimnie Gory locality; **(J)** a cast of a tube fragment preserved within channelized sandstone lenses, imprinting the outer surface of a tube with ring-like annulation, Syuzma Beds, Ust-Pinega Formation, Solza River locality; **(K)** a cast of a tube fragment preserved within channelized sandstone lenses, imprinting the outer surface of a tube with dense even annulation, Erga Beds, Mezen Formation, Zimnie Gory locality. Scale bar is 5 mm.

Sample	Sterane parameters											Hopane parameters		S/H ⁷
	C ₂₆ 5β/5α ¹	C ₂₇ 5β/5α	C ₂₈ 5β/5α	C ₂₉ 5β/5α	ADI ²	C ₂₆ (%)	C ₂₇ (%)	C ₂₈ (%)	C ₂₉ (%)	dia/reg ³	S/R ⁴	Ts/Tm ⁵	H/Mor ⁶	
Sandstone overlying <i>Kimberella</i>	0.51 (0.06)	0.65 (0.04)	0.91 (0.32)	0.61 (0.03)	1.08 (0.08)	3.79 (0.13)	36.3 (1.03)	9.92 (0.33)	49.98 (1.3)	0.09 (0.01)	0.14 (0.03)	0.06 (0.00)	1.69 (0.05)	0.18 (0.00)
Clay underlying <i>Kimberella</i>	0.63 (0.04)	0.56 (0.04)	0.76 (0.30)	0.63 (0.02)	0.89 (0.07)	1.38 (0.07)	23.09 (0.54)	9.5 (0.27)	66.03 (1.27)	0.04 (0.00)	0.06 (0.02)	0.05 (0.00)	1.98 (0.06)	0.21 (0.00)
Microbial mat from the surface with <i>Kimberella</i>	n/d	0.76 (0.07)	0.76 (0.27)	0.65 (0.04)	1.17 (0.07)	n/d	24.89 (0.96)	10.2 (1.04)	64.91 (1.86)	0.08 (0.01)	0.13 (0.04)	0.07 (0.01)	1.86 (0.17)	0.14 (0.00)
Microbial mat next to <i>Kimberella</i>	n/d	0.98 (0.10)	0.57 (0.20)	0.5 (0.03)	1.95 (0.26)	n/d	23.86 (1.07)	19.33 (1.62)	56.8 (2.28)	0.13 (0.01)	0.06 (0.04)	0.07 (0.02)	1.79 (0.27)	0.19 (0.01)
First mm of sandstone above <i>Kimberella</i>	n/d	0.98 (0.30)	0.7 (0.25)	0.62 (0.13)	1.6 (0.60)	n/d	23.63 (3.21)	9.68 (1.80)	66.69 (7.66)	n/d	0.13 (0.11)	n/d	n/d	n/d
<i>Kimberella</i>	0.18 (0.04)	0.58 (0.04)	0.11 (0.04)	0.09 (0.00)	6.3 (0.54)	1.22 (0.10)	4.11 (0.14)	32.55 (1.23)	62.12 (1.31)	0.09 (0.00)	0.02 (0.02)	0.04 (0.01)	1.31 (0.20)	0.62 (0.01)
<i>Calyptrina</i>	0.2 (0.08)	0.78 (0.11)	0.18 (0.06)	0.21 (0.02)	3.65 (0.62)	3.48 (0.53)	8.7 (0.63)	22.28 (2.28)	65.54 (3.34)	0.05 (0.00)	0.05 (0.04)	0.09 (0.03)	2.59 (0.70)	0.62 (0.02)
<i>Andiva-3</i>	0.53 (0.06)	1.07 (0.05)	0.71 (0.25)	0.59 (0.02)	1.82 (0.12)	2.02 (0.11)	33.38 (0.81)	8.28 (0.49)	56.32 (1.27)	0.05 (0.00)	0.11 (0.02)	0.06 (0.01)	1.95 (0.12)	0.38 (0.01)
<i>Yorgia-1</i>	n/d	1.17 (0.07)	0.8 (0.28)	0.71 (0.03)	1.66 (0.12)	n/d	26.77 (0.75)	8.32 (0.55)	64.91 (1.53)	0.06 (0.00)	0.1 (0.03)	0.06 (0.01)	1.80 (0.16)	0.28 (0.01)
<i>Yorgia-2</i>	0.62 (0.15)	1.49 (0.09)	0.56 (0.20)	0.64 (0.03)	2.35 (0.17)	1.61 (0.19)	27.99 (0.79)	11.62 (0.71)	58.79 (1.43)	0.06 (0.00)	0.08 (0.03)	0.06 (0.01)	1.93 (0.11)	n/d

Table S1. Distributions of sterane and hopane biomarker parameters in *Kimberella* and *Calyptrina* extracts, adjacent rocks and microbial mats, and new dickinsoniids from the surface with *Kimberella*. ¹5β/5α = (βαα 20R+ααα 20S)/ααα 20R; ²Animal Decomposition Index ADI = (C₂₇ 5β/5α)/(C₂₉ 5β/5α); ³dia/reg = βα-20(S+R)-diacholestane / Σ(ααα- and βαα-20(S+R)-cholestane); ⁴S/R = ααα20S/ααα20R C₂₉ steranes; ⁵Ts/Tm = Ts/Tm C₂₇ hopanes; ⁶H/Mor = βα/αβ C₃₀ hopane; ⁷S/H = Σ(C₂₇₋₂₉ steranes) / Σ(C₂₇₋₃₅ hopanes).

	MAS _y /H ¹		
	C ₂₇	C ₂₈	C ₂₉
<i>Dickinsonia</i> -1	0.155 (0.004) ⁴	0.022 (0.001)	0.147 (0.003)
<i>Dickinsonia</i> -2	0.254 (0.005)	0.028 (0.001)	0.145 (0.004)
<i>Dickinsonia</i> -3	0.156 (0.004)	0.025 (0.001)	0.148 (0.004)
Variance (*10 ⁻⁴) ²	32.617 (0.007)	0.076 (0.001)	0.024 (0.005)
<i>Dickinsonia</i> sterol composition ³	99.7% (0.33)	0.23% (0.04)	0.07% (0.16)

Table S2. Quantification of the sterol composition of *Dickinsonia* (based on Bobrovskiy et al (12)).

¹ Concentration of C₂₇, C₂₈ and C₂₉ monoaromatic steroid (MAS) homologs (sum of isomers I and V) relative to total hopanes (sum of C₂₇–C₃₅ hopanes) in *Dickinsonia* extracts; hopanes: C₂₇ = Σ(Ts, Tm, β), C₂₉ = Σ(αβ, Ts, βα), C₃₀ = Σ(αβ, βα), C_{31–35} = Σ(αβ-22(S+R), βα), αβ = 17α(H)21β(H), βα = 17β(H)21α(H); y indicates carbon number of monoaromatic steroids; ²Variance = Σ(x – \bar{x})² / (n – 1), where x is C_y/H value, \bar{x} is a mean C_y/H value between the samples and n is the number of samples (n = 3); ³C_y% = 100%*(C_y variance)/(sum of variances for each of three steroids), y indicates carbon number of monoaromatic steroids; ⁴numbers in parentheses are standard deviation values.

	C ₂₇	C ₂₈	C ₂₉
Sterol composition of fresh <i>Limax</i>	95.5%	1.9%	2.7%
Steroid composition of degraded <i>Limax</i>	93.7%	3.4%	2.9%
5β stanol/sterol ratio in degraded <i>Limax</i>	3.57	3.55	3.69

Table S3. Steroid composition of fresh and degraded slugs.

CHAPTER 4. SIMPLE SEDIMENT RHEOLOGY EXPLAINS THE EDIACARA BIOTA

PRESERVATION

Understanding of the preservation mechanism of Ediacaran macrofossils is crucial for the interpretation of their morphologies: it allows to separate features that reflect the morphology of the organisms from those that are caused by taphonomic processes. Previous studies on the Ediacara biota taphonomy agree that the fossils were preserved via cementation of the overlying sediment before the organisms started to decay. These taphonomic hypotheses are only distinguished by the suggested cementation agents (pyrite, silica, carbonates or clay minerals). Based on uniquely well preserved Ediacaran deposits in the White Sea area in Russia, and available fossil collections from both Russia and South Australia, this chapter shows that early diagenetic cementation commonly does not exist and cannot have played a deciding role in fossil preservation. Instead, fossilization of Ediacaran organisms was promoted by unusually prolonged conservation of organic matter, coupled with differences in rheological behaviour of the over- and underlying sediments.

Statement of Contribution

This thesis is submitted as a Thesis by Compilation in accordance with https://policies.anu.edu.au/ppl/document/ANUP_003405

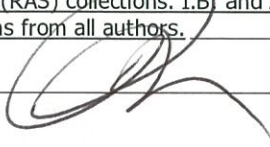
I declare that the research presented in this Thesis represents original work that I carried out during my candidature at the Australian National University, except for contributions to multi-author papers incorporated in the Thesis where my contributions are specified in this Statement of Contribution.

Title and authors: Bobrovskiy, I., Krasnova, A., Ivantsov, A., Luzhnaya, E., Brocks, J. J. Simple sediment rheology explains the Ediacara biota preservation.

Current status of paper: Not Yet Submitted/Submitted/Under Revision/Accepted/**Published**

Contribution to paper: I.B. designed the study, studied the collections and developed the model. A.K. and I.B. performed the thin-section and scanning electron microscopy analyses. I.B., A.K., A.I. and E.L. participated in the field expeditions. A.I. and E.L. provided samples from the Borissiak Paleontological Institute (RAS) collections. I.B. and J.J.B. designed the taphonomic laboratory experiments. I.B. and J.J.B. wrote the paper with contributions from all authors.

Senior author or collaborating authors endorsement: _____



Ilya Bobrovskiy

Candidate – Print Name



Signature

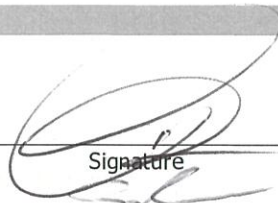
18/04/2019

Date

Endorsed

Jochen Brocks

Chair of Supervisory Panel – Print Name



Signature

18/04/2019

Date

Stewart Fallow

Delegated Authority – Print Name

Signature

29/04/2019

Date

This is the author's version of the work. It is provided here according to the *Nature Research* guidelines for personal use, not for redistribution. The definitive version was published in *Nature Ecology & Evolution*, 3, 582–589 (2019), doi: <https://doi.org/10.1038/s41559-019-0820-7>

Simple sediment rheology explains the Ediacara biota preservation

Ilya Bobrovskiy^{1*}, Anna Krasnova^{2,3}, Andrey Ivantsov², Ekaterina Luzhnaya (Serezhnikova)², Jochen J. Brocks^{1*}

¹Research School of Earth Sciences, Australian National University, Canberra, ACT 2601, Australia

²Borissiak Paleontological Institute, Russian Academy of Sciences, Moscow 117997, Russia

³Faculty of Geology, Lomonosov Moscow State University, Moscow 119991, Russia

*Correspondence to: ilya.bobrovskiy@anu.edu.au, jochen.brocks@anu.edu.au

Abstract

The soft-bodied Ediacara biota (571-541 Ma) represents the oldest complex large organisms in the fossil record, providing a bridge between largely microbial ecosystems of the Precambrian and the animal dominated world of the Phanerozoic, potentially holding clues about the early evolution of Metazoa. However, the nature of most Ediacaran organisms remains unresolved, partly due to their enigmatic non-actualistic preservation. Here we show that Flinders-style fossilization of Ediacaran organisms was promoted by unusually prolonged conservation of organic matter, coupled with differences in rheological behaviour of the over- and underlying sediments. In contrast to accepted models, cementation of overlying sand was not critical for fossil preservation, which is supported by the absence of cement in unweathered White Sea specimens and observations of soft sediment deformation in South Australian specimens. The rheological model, confirmed by laboratory simulations, implies that Ediacaran fossils do not necessarily reflect the external shape of the organism, but the morphology of a soft external or internal organic 'skeleton'. The rheological mechanism provides new constraints on biological interpretations of the Ediacara biota.

While most Cambrian fossils can be recognised as stem or crown group members of extant phyla, most organisms of the Ediacara biota look alien, and their taxonomic position, even at the kingdom level, remains unclear. Few fossils, such as *Kimberella*, leave little doubt about their animal nature, showing not only complex behaviour, but also preserving internal organs and characteristic feeding traces^{1,2}. Others, like *Palaeopascichnus*, are comparable with giant protozoans³⁻⁵, while *Beltanelliformis* represent giant spherical colonies of cyanobacteria^{6,7}. For most Ediacarans, however, the phylogenetic position remains unresolved^{8,9}.

A principal step in unravelling the nature and palaeoecology of the Ediacaran organisms is to understand their taphonomy, and thus to separate features reflecting morphology and palaeoecology of the Ediacaran organisms from those that result from taphonomic processes^{10,11}. For example, it is unclear whether dickinsoniids lacked a gut or mouth¹⁰ or whether these features were not preserved¹². It even remains ambiguous whether the impressions of the Ediacara biota reflect external morphology or some internal structure^{12,13}. Ediacaran macroorganisms, except late biomineralizing forms, were soft-bodied yet globally preserved in a wide range of depositional environments¹⁴⁻¹⁷ – something rarely observed in older or younger geological periods. Thus, their preservation may require unusual non-actualistic conditions and processes.

Fossils of the Ediacara biota are preserved in three principal styles: Conception, Flinders and Nama (Fig. 1)¹⁴. In Conception-style preservation, organisms are cast by rapid cementation of an overlying volcanic ash layer, creating positive epirelief fossils (Fig. 1)¹⁴. Preservation of fossils in other styles is, however, less well-understood. Nama-style preservation unites fossils preserved three-dimensionally within sand, while Flinders-style preserves fossils on bedding planes on the sole of sandstone layers both in positive and negative hyporelief¹⁴ (Fig. 1). Fermeuse-style is a case of Flinders-style preservation referring to holdfasts and trace fossils. Positive hyporelief is attributed to collapse of an organism's carcass or infill with overlying sediment^{18,19}.

The most ambiguous mode of preservation is the Flinders-style negative hyporelief (Fig. 1). It appears counterintuitive that the void created by the decaying organism was not filled with sand from above but with sediment from below. An early model from 1968 suggested

that the underlying sediment was moving up because it was less 'competent' (less viscous) than the overlying sediment due to differences in lithology¹⁸. Newer models, however, unanimously agree that the sediment above the Ediacaran macroorganisms must have been rapidly cemented by mineralization with pyrite¹⁹⁻²², calcite²³, silica²⁴ or clay minerals²⁵ before the carcass of the organism decayed, preventing collapse of the sediment.

Not only members of the Ediacara biota demonstrate exceptional preservation in the Ediacaran successions. Microbially-induced sedimentary structures (MISS) preserve finest details cast in sandstone including even single bacterial filaments and bundles^{25,26}. Such preservation in the Precambrian has been assigned to the absence of vertical burrowing, which otherwise destroys microbial mats and sedimentary structures and enhances circulation of oxidizing fluids within the sediment^{25,27}. Sealing of the sediment surface by mats changes the chemistry of underlying pore waters, creating an anoxic environment that favours preservation of organic tissues²⁵. Thus, diagenetic conditions in Ediacaran sediments were unusual, promoting exceptional preservation of macroorganisms in different depositional environments globally.

The shallow-marine siliciclastic Ediacaran successions of the White Sea region in Russia and South Australia provide diverse and well-preserved fossils of the Ediacara biota. The fossils occur at the base of sandstone (Flinders- and Fermeuse-styles), within sandstone (Nama-style) and within clay⁷. Fossils are commonly associated with exceptionally fine-detailed MISS, such as elephant skin, but some display fine preservation in the absence of microbial mats²⁸. In most localities in the world, such as South Australia, England and Canada, Ediacaran deposits are metamorphosed and/or substantially weathered, making taphonomic studies challenging. By contrast, the White Sea region provides an exceptional opportunity to test existing taphonomic hypotheses in unweathered and thermally immature⁶ fossiliferous deposits. In this study, fossils of *Dickinsonia*, *Andiva*, *Kimberella*, *Aspidella*, *Beltanelliformis*, putative tube worms *Sabellidites* and macroalgae from the White Sea region and South Australia were studied to test taphonomic hypotheses about the preservation of the Ediacara biota.

Results

According to current hypotheses for Flinders-style preservation, the sediment above, and only above, Ediacaran organisms became cemented before the carcass started to decay. To test these hypotheses, fossils from the Lyamtsa and Zimnie Gory localities of the White Sea were closely examined for the presence of diagenetic minerals and cement. Many White Sea fossils contain pyrite, but its distribution is commonly patchy: while some fossils exhibit a crust at the surface, others have only single framboids or contain no pyrite at all (Figs. 6a-d, Supplementary Figs. 3, 4). Where present, pyrite framboids demonstrate perfect preservation without signs of dissolution (Supplementary Fig. 3b). The preservation of pyrite framboids and presence of organic matter (Figs. 6a-d) indicate that lack of pyrite cannot be explained by past weathering processes that secondarily removed a pyrite mask. Likewise, diagenetic quartz overgrowths and dolomite often only occur as single grains, not forming a supportive cement (Supplementary Figs. 3, 4), and the observation that most of the pore space is not empty but filled by detrital clay also eliminates the possibility that early diagenetic silica or carbonate cement was present but removed during later stages of burial²⁹. Authigenic clay involved in fossil preservation is usually distinct as it is monomineral and thus can be recognized even in metamorphic rocks^{30,31}. The absence of such a distinct phase on fossil surfaces also rules out clay cementation (Supplementary Figs. 3,4). In summary, fossils from White Sea localities that do not show any sign of cementation or encrustation are preserved in the same style as those that are heavily encrusted with pyrite²⁸, iron oxides¹⁹ or contain diagenetic quartz²⁴, indicating that early diagenetic cementation was not the driving mechanism for the preservation of Ediacaran macrofossils at the White Sea locality.

Further observations on Ediacaran specimens from the White Sea and other localities confirm that cementation generally did not play a deciding role in fossilization (Fig. 2; Supplementary Fig. 5). *Dickinsonia* and *Kimberella* specimens represent Flinders-style preservation in this study, forming negative hyporelief impressions at the base of sandstone, with a positive epirelief counterpart formed within underlying clay or sand (Fig. 1). Both White Sea and South Australian sites accommodate *Dickinsonia* that display a rim around the fossils that was presumably left by contraction of their bodies – sometimes attributed to putative muscle contraction, postmortal contraction or dehydration^{8,10,32}. Most rims are preserved in

positive hyporelief and probably represent ‘footprints’ (possible feeding traces)^{33,34}, marking the initial position of *Dickinsonia*’s body. Some specimens, however, have a positive hyporelief outer rim and a negative hyporelief inner rim (Fig. 2a). The negative rim and body impression capture an imprint of the organism before and after contraction respectively, after the organism was covered with sand. If late mineralisation was responsible for fossil preservation and formation of external moulds, then only the final position of the body fossil should be imprinted. Conversely, if mineralisation happened very early, then only the position of the body before contraction would be imprinted (Supplementary Fig. 5). Thus, the co-existence of the contraction rim and the final resting stage imply that the sand was malleable when the impressions formed. This observation is supported by some South Australian *Dickinsonia* specimens where a wedge of overlying sand is trapped beneath the organism (*Dickinsonia*’s ‘lift-offs’³⁵). During decomposition and compression of the organism, this wedge moved upwards together with the underlying sediment (Figs. 2b,d; Supplementary Fig. 5), revealing that the sand was not cemented.

It is impossible to exclude that cementation additionally contributed to Flinders-style preservation of Ediacaran organisms not included in this study. However, the observation that Ediacaran fossils of the same type from all localities look nearly identical, with similar relief and details of morphology, implies that they share a common preservation mechanism³⁰. Thus, if at least one fossil demonstrates evidence for absence of early diagenetic cementation, we can be confident that cementation was not crucial for preservation of all fossils. Conversely, if minerals that potentially could play a role in cementation were found in some fossil localities²⁰, it does not necessarily imply that they actually contributed to the preservation of the fossils. Absence of cement in well-preserved fossil specimens from the White Sea and evidence for malleable sand in both White Sea and South Australia specimens demonstrate that early diagenetic cementation did not play a deciding role in preservation of the Ediacara biota. Given that organisms of the Ediacara biota were too soft and flexible to be composed of hard or resistant materials³⁶, as evident, for example, from folded specimens¹⁹ and fossils stretched but not torn by load cracks cutting the fossils²⁸, an alternative explanation for the preservation of the Ediacara biota has to be found.

Rheological model and negative hyporelief preservation

The only existing model that does not require cementation, proposed by Mary Wade in 1968¹⁸, is based on differences in mechanical properties between sediments under- and overlying fossils, and consequent differences in their rheological behaviour. This model can now be tested using new material and taphonomic experiments.

In the White Sea, a layer underlying the fossils is nearly always composed of clay, while the overlying layer is a fine-grained sandstone. Apart from the lower density of clay relative to sand, clay also has very distinct rheological properties. As sand has a stiff, grain-supported structure, it has much higher strength (ability to withstand an applied load without plastic deformation) and viscosity (measure of resistance to gradual deformation) than clay³⁷, meaning that it takes much less force to deform clay than sand. Thus, when an organism is trapped between clay and sand layers and loses its volume due to dehydration and decomposition, the clay is more likely to deform than the sand, flowing upwards to fill the accommodation space. Extracellular polymeric substances released into the pore space of the sand by microorganisms involved in the decomposition of the carcass³⁸ may have increased the viscosity of the overlying sediment yet further. Thus, the formation of negative hyporelief impressions can theoretically be explained by simple rheological properties of the sediments without invoking cementation of the sand.

The rheological model becomes less intuitive when it comes to South Australian fossil specimens where both overlying and underlying layers are represented by sandstone. Yet, Mary Wade¹⁸ already noted that the layer underlying these fossils is usually more fine-grained, well-sorted, composed of more rounded grains and containing less clay matrix when compared to the layer above. She suggested that the underlying finer sand was moving up because it was less 'competent' due to decline of sediment strength and viscosity with decreasing grain size^{37,39}. In cases when specimens are trapped between sandstones with similar grain sizes¹⁹, the clay matrix content and differences in grain roundness and sorting¹⁸, which all substantially modify the mechanical properties of sand^{37,39,40}, can be responsible for the required contrast in rheology.

Taphonomic experiments

To test the rheological hypothesis for negative hyporelief preservation, a series of taphonomic experiments were performed in the laboratory (See Methods; Fig. 3, Supplementary Fig. 1). In these experiments, a melting Death Star cast composed of water ice (Fig. 3a), representing a decomposing organism, was trapped in between two types of sediment under pressure (Fig. 3b). The centre of the ice cast contained a horizontal corrugated cardboard sheet, representing degradation-resistant tissue within the organism (Fig. 3b). In all experiments, the underlying sediment had lower rheological properties (i.e. lower viscosity and strength) than overlying sediment. As the ice cast melted, it was replaced by sediment from below creating a negative hyporelief impression. The cardboard sheet was pushed up to the top of the cast, forming an impression of its corrugations in the overlying sand (Figs. 3c-f; Supplementary Fig. 1).

In the first experiment with clay below and fine sand above the ice cast, and an applied pressure equivalent to an 18 cm thick sand load, clay expanding up from below reached the horizontal cardboard sheet in the middle of the ice cast and stopped there, while the space above the cardboard barrier was filled by sand from above, creating an impression of the corrugated cardboard sheet (Supplementary Figs. 1c,d). In the second experiment with higher applied pressure (equal to a 40 cm thick sand layer), the cardboard was pushed by clay all the way up to the top of the cast, again forming an impression of its corrugations in the overlying sand (Figs. 3c,d). The same happened in the experiment simulating grain sizes of Ediacaran deposits in South Australia, with rounded coarse sand below and angular coarse sand above the ice cast, under pressure equivalent to a 90 cm thick sand layer (Figs. 3e,f). An additional experiment was performed without a sheet of cardboard within the ice cast, producing an impression of the general shape of the cast, but lacking any fine surficial details (Supplementary Fig. 1b).

Our taphonomic experiments produced impressions similar to fossils of the Ediacara biota, confirming that they indeed may form if a shrinking body is located between two rheologically distinct sediment layers (Fig. 3, Supplementary Fig. 6). Formation of negative hyporelief impressions thus requires (a) that an organism is sandwiched between a low-viscosity sediment at the bottom and a higher-viscosity sediment above, which always seems

to be the case for Flinders-style Ediacaran fossils, and (b) that the carcass, or part of the carcass, resists collapse, desiccation or degradation until sufficient sediment has accumulated over the top to induce sediment flow (Fig. 4).

Natural taphonomic experiment

To understand how negative hyporelief impressions form in the absence of early diagenetic cementation, we investigated other sedimentary structures at the White Sea locality preserved in negative hyporelief at the base of sandstone. The processes creating negative hyporelief appear to affect a wide variety of biological and abiological objects, including putative tube worms, macroalgae and clay pebbles (Fig. 2c).

The mechanism of preservation of Ediacaran organisms and formation of negative hyporelief is spectacularly illustrated on a 30 cm thick sandstone layer in the White Sea that bears organically preserved *Dickinsonia* at its sole and clay pebbles up to 9 cm wide within the sand. In the unique situation when a clay pebble is located precisely above an Ediacaran fossil, the entire taphonomic process can be traced (Fig. 5). As the *Dickinsonia* specimen shown in Figure 5 was buried by a layer of sand, one edge of the organism was flipped up and a wedge of sand was deposited beneath (location 1 in Fig. 5a). At the location of sand injection, parallel streaks in the sediment indicate that the wedge of sand was disrupted as the overlying body compacted (location 1 in Fig. 5a). After burial, the clay pebble gradually lost its volume and the centre of the body of *Dickinsonia* was pushed upwards into the forming void, dragging along the edge of the body that was not caught in sand (the upper right on the figure, location 2 in Fig. 5a). As this edge of *Dickinsonia* retracted, the forming accommodation space was filled with clay from below, leaving a vague negative hyporelief impression of the initial body position. During this process, the carcass did not lose its rigidity and did not fall apart. During final decomposition and compression, a second, clearer negative hyporelief impression formed, this time accentuated by a thin layer of organic matter, and in places surrounded by a thin contraction rim (location 3 in Fig. 5a). The latter indicates that even after desiccation and compaction of the clay, which requires considerable time and

pressure, there was still a notable quantity of organic matter preserved, highlighting unusually prolonged organic preservation during diagenesis.

Positive hyporelief preservation

Positive hyporelief preservation of some Ediacaran macrofossils (Fig. 1, 4) can be explained by injection of sand into body cavities, as observed for spherical cyanobacterial colonies *Beltanelliformis* and many Ediacaran holdfasts^{7,41-43}. For others, like *Phyllozoon* or *Palaeopascichnus*, positive hyporelief is attributed to early collapse of body carcasses under the weight of overlying sand, leaving an impression in the underlying microbial mat^{18,19}. Preservation of impressions of Ediacaran organisms and impressions of the mat itself on the base of overlying sand would collapse as soon as the mat started decomposing, and their preservation is currently attributed to early diagenetic cementation^{11,19,20,23-25,29}. The rheological model, however, explains conservation of the finest details of organisms and their traces³³ in positive hyporelief, as well as the remarkable preservation of microbial mat impressions at the base of sandstones^{19,25,26,44}, without invoking cementation. Based on this model, we posit that, as microbial mats desiccated and degraded under the weight of overlying sand, less viscous underlying sediment flowed up, gently and gradually replacing the decaying mat, and pressing the upper surface of the mat firmly into the overlying sand layer, preventing deformation of the sand and preserving the finest details of the impressions (Figs. 3, 4).

Organic preservation

Preservation of organic matter plays an important role in the taphonomy of all fossils from the White Sea localities. A close investigation of dozens of Ediacaran macrofossils, including *Dickinsonia*, *Andiva*, *Kimberella*, *Aspidella*, *Sabelliditides* and *Beltanelliformis* collected from unweathered layers in the White Sea revealed that they all are preserved organically, including those that occur within sandstone or clay (Fig. 6a-d)^{6,7,45}. The *Dickinsonia* preserved beneath the clay pebble (Fig. 5) demonstrates that full collapse of organic matter only occurred after the pebble was completely compressed, indicating that

significant amounts of organic matter survived decomposition. The taphonomic simulation with 'no cuticle' (no cardboard inside the ice cast, see Methods) shows that without a resistant layer no details of an organism's morphology are preserved in negative hyporelief because movement of sediment tends to smear them (Supplementary Fig. 1b). Thus, conservation of physically resistant, relatively rigid organic matter may be crucial for the preservation of fine details in negative-hyporelief Flinders-style fossils.

Preservation of organic matter may be also vital for Nama-style preservation, which unites fossils that are found within uniform sandstone but still reveal finest morphological details. Even when such fossils are pyritised, the pyrite does not create a cement but often only a thin layer, likely replacing a film of residual organic matter (Supplementary Fig. 2c), while other fossils completely lack pyrite. Organic matter on Nama-style fossils has, for instance, been observed on a *Charniodiscus*-like specimen from the White Sea preserved within sandstone⁴⁶. Prolonged preservation of a film of organic matter will prevent interlocking of sand grains during early diagenesis¹⁸ and obstruct their fusion during later cementation, allowing preservation of Nama-style fossils.

DISCUSSION

Our results indicate that Flinders-style preservation of the Ediacara biota, as well as of impressions of microbially induced structures in siliciclastic sediments, was possible due to differences in rheology between under- and overlying sediments (Fig. 4). Fossils were only preserved if the sediment beneath the organism was less viscous than the sediment above. Prolonged conservation of organic matter of Ediacaran macrofossils likely promoted preservation of fine details in Flinders-style preservation, and may also be responsible for preservation of Nama-style macrofossils.

The rheological model has important implications for our understanding of the biology of the Ediacara biota. Ediacaran macrofossils preserved in Nama-style have been hypothesised to capture only details of soft organic 'skeletons'^{12,43} instead of the morphology of the organism itself. However, when it comes to fossils preserved in negative hyporelief, all cementation models^{19,20,24,47} imply that the sandstone imprinted the upper surface of the

organism, otherwise the ‘death mask’ would have captured the organism at different stages of decomposition depending on the timing of cementation, as possibly observed in some Conception-style fossils⁴⁸. By contrast, according to the rheological model, the preserved impression could have been left by a degradation-resistant and relatively more rigid organic structure, such as dorsal or ventral external cuticle or a soft internal ‘skeleton’. The results of our taphonomic experiments show how resistant organic matter located even in the middle of an organism is pressed upwards by underlying sediment to form an imprint in negative hyporelief where the top of the organism used to be (Fig. 3). Thus, we may remain largely oblivious about the external shape of Ediacaran organisms. The mechanism also implies low preservation potential for mouths and guts (unless these are filled with sediment to form a composite impression, which sometimes seems to be the case for *Kimberella*⁴⁹ and potentially for some dickinsoniid specimens⁵⁰) and other soft tissues, making conclusions based on their perceived absence¹⁰ meaningless.

Some specimens of *Dickinsonia*, *Andiva* and *Yorgia*²⁸ have an edge that is flipped up and preserved vertically within the sandstone (Figs. 6c,d; Supplementary Fig. 6a), creating preservational effects that are transitional between Flinders- and Nama-style. The parts of these fossils that are at the base of the sandstone are preserved in usual Flinders-style, forming a negative hyporelief impression. In contrast, the flipped edges are preserved in Nama-style within the sandstone, creating impressions that are continuous with, and identical to, the Flinders-style impressions, both from the general pattern and the relief of their middle ridges, but entirely lacking the overall concave relief of the Flinders-style fragment (Fig. 6c). The counterpart of such Nama-style impression is a simple cast (Fig. 6d). In other words, only one surface is imprinted – and this is always the same surface also found in negative hyporelief on bedding planes. As the enclosing sandstone in Nama-style preservation is isotropic, the anisotropy promoting preservation of only one particular surface of dickinsoniids must reside within the organism itself. Dickinsoniids, including *Dickinsonia*, *Andiva*, *Yorgia* and other flattened Ediacaran organisms made of serially repeated units, must thus have possessed relatively more and less resistant tissue, and it is exclusively the upper surface of the more resistant tissue that became preserved as a fossil (Supplementary Fig. 6c). In *Andiva*, differentiation of tissues is also reflected in their differential preservation in Flinders-style fossils: while the central part of a body is sometimes preserved organically, the

surrounding smooth area is not (Supplementary Fig. 6b). By extension, the presence of a resistant soft 'skeleton'^{12,43} can explain preservation of the conventional Nama-style fossils without invoking mineralisation.

Based on their steroid content, dickinsoniids were animals⁴⁵; in this view our findings indicate that dickinsoniids had tissue-grade organization, which confidently classifies them as the oldest (at least 558 Ma)¹⁶ eumetazoans in the fossil record, next to marginally younger *Kimberella* (555 Ma)¹⁶. Thus, while the global preservation of soft-bodied macroorganisms in the Ediacaran period is a non-actualistic phenomenon, the rheological taphonomic model provides the framework that is required for meaningful biological and ecological interpretations of the Ediacara biota.

Acknowledgments:

The study was funded by Australian Research Council grants DP160100607 and DP170100556 (to J.J.B.) and Russian Foundation for Basic Research project No. 17-05-02212A (to I.B., A.K. and A.I.). I.B. gratefully acknowledges an Australian Government Research Training Program stipend scholarship. The authors are grateful to A. Nagovitsyn, P. Rychkov, V. Rychkov, S. Rychkov, T. Rychkova and A. Makushkina for their help in the field, L. Zaytseva for help with SEM imaging, J.M. Hope, J. Wurtzel, S. Eggins, A. Rummery and R. Kerr for providing materials for taphonomic experiments, M.-A. Binnie and J.G. Gehling for providing access to the South Australian Museum collections, N.J. Butterfield and A.G. Liu for their helpful comments on this study.

Author contributions

I.B. designed the study, studied collections and developed the model, A.K. and I.B. performed thin section and SEM analyses, I.B., A.K., A.I. and E.L. participated in field expeditions, A.I. and E.L. provided samples from the Borissiak Paleontological Institute RAS collections, I.B. and J.J.B. designed taphonomic laboratory experiments, I.B. and J.J.B. wrote the paper with contributions from all authors.

Figures

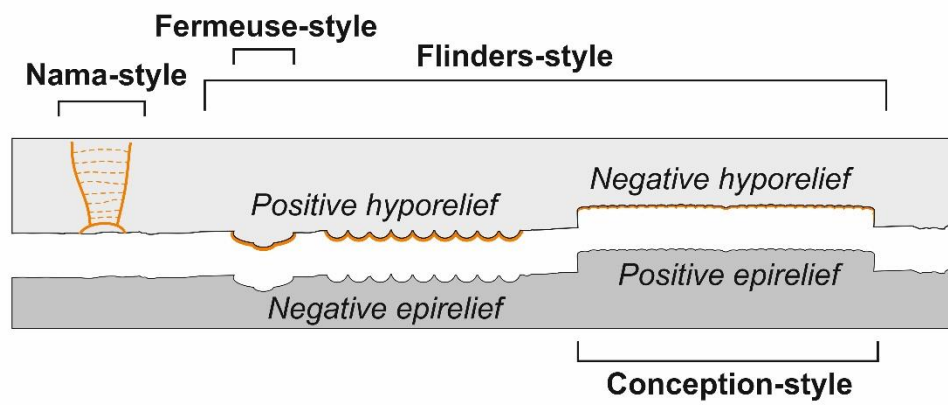


Fig. 1. Styles of preservation of the Ediacara biota fossils (after G. Narbonne¹⁴).

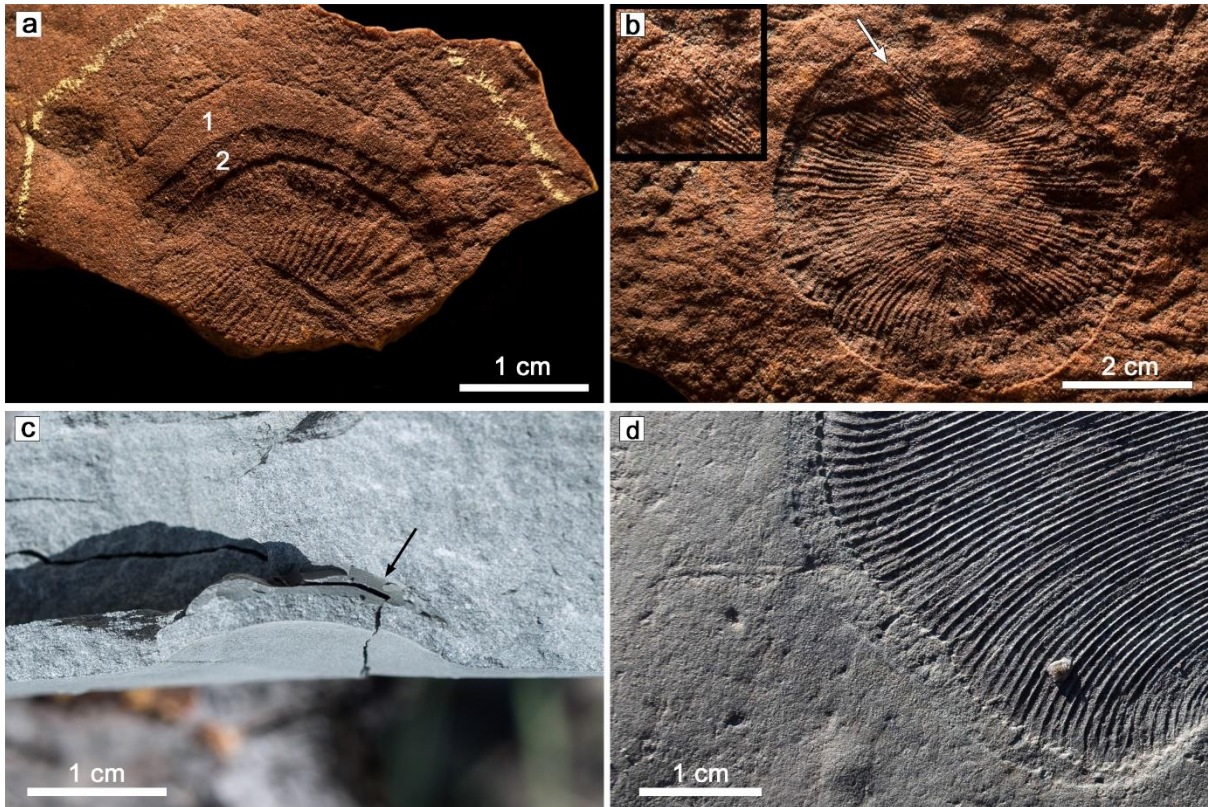


Fig. 2. Evidence for absence of early diagenetic cementation in the White Sea and South Australian Ediacaran sections. **a**, Contraction rims around *Dickinsonia* from South Australia (South Australian Museum, sample P40944); 1 – positive hyporelief outer rim, 2 – negative hyporelief inner rim; note that the disappearance of the fossil in the left lower corner is caused by weathering of the sample; **b**, *Dickinsonia* from South Australia with a thin wedge of sand material intruded beneath its edge (South Australian Museum, sample P12557); arrow points at *Dickinsonia*'s isomers visible through the wedge (also shown in magnification in the insert); **c**, a clay pebble (arrow) within sandstone forming negative hyporelief structure at the base of sandstone; **d**, a fragment of *Dickinsonia* from the Lyamtsa locality in the White Sea Area, an edge of the fossil is hidden under a wedge of sand that also forms a vague negative hyporelief. Light direction is from the upper left on **a**, **b** and **d**. Presented features demonstrate plastic deformation of sand indicating that the sand was not cemented while organisms were decomposing and while the clay pebble compacted.

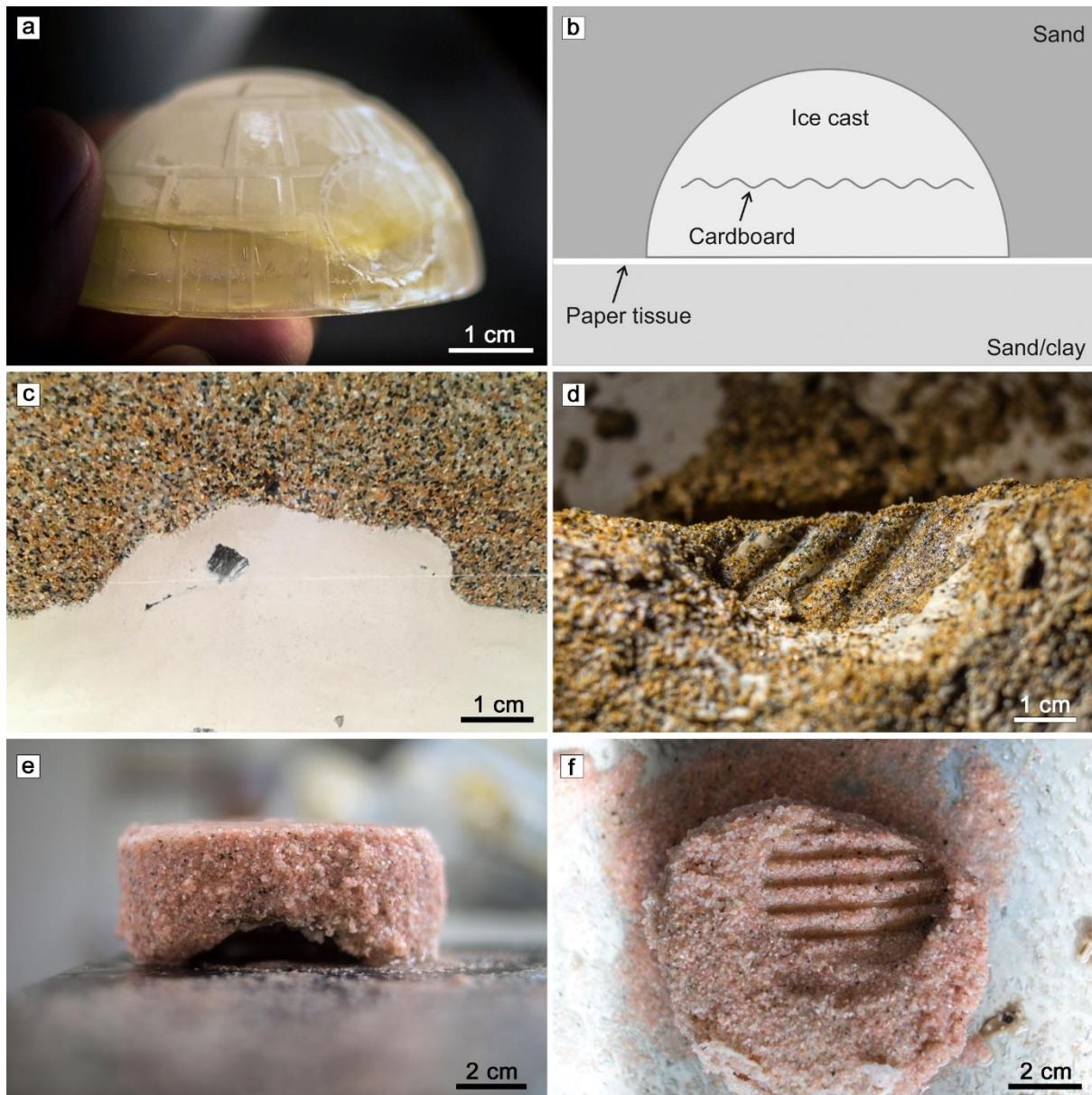


Fig. 3. Taphonomic laboratory experiments testing the Rheological model; **a**, Death Star ice cast used in all four taphonomic experiment; note the deep engineering bay around the superlaser focus lens that provides considerable relief on the surface of the cast; **b**, cartoon illustrating the setup of the experiments; **c-d** – results of the experiments with clay below and fine sand above that generated negative hyporelief impression of the cardboard on sand bases (experiment 2); **c**, side view of experiment 2; **d**, view from below of the sand layer that has been frozen and separated from underlying clay, showing impression of corrugated cardboard sheet; **e-f**, results of the experiment with coarse rounded sand below and coarse angular sand above ('South Australian' scenario, experiment 4), a negative hyporelief impression of the cardboard on the overlying sand base is produced; **e**, side view of upper sand layer after freezing and separation from the lower layer; **f**, view from below of that layer showing impression of corrugated cardboard sheet.

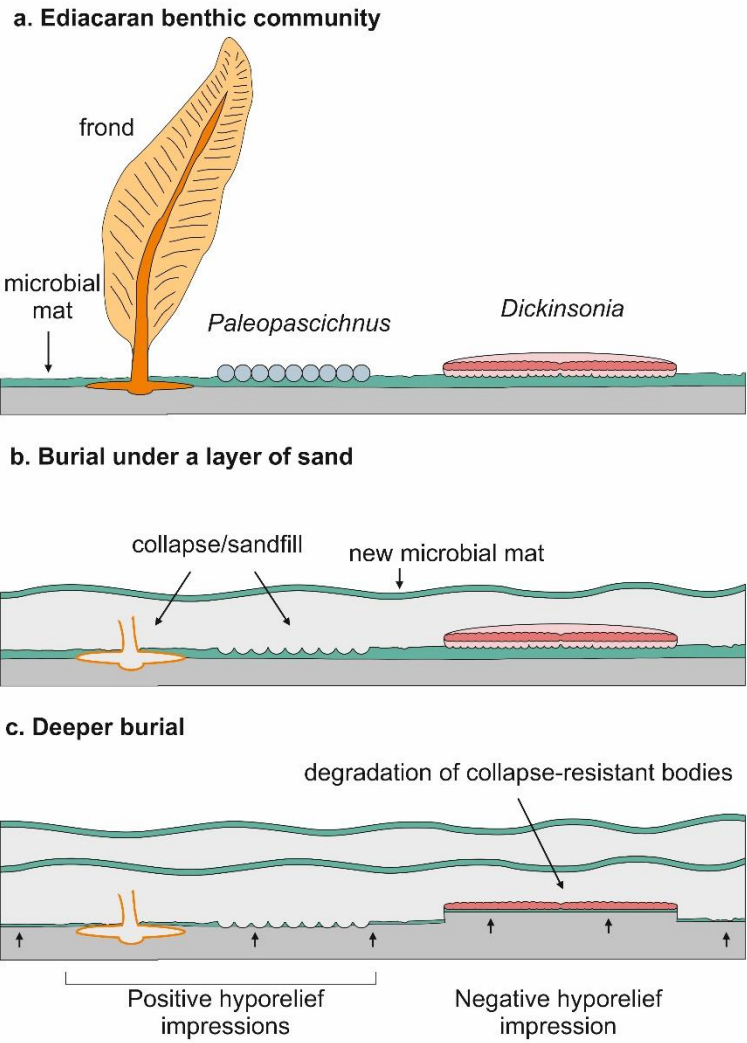


Fig. 4. The Rheological model of preservation of Ediacaran macrofossils.

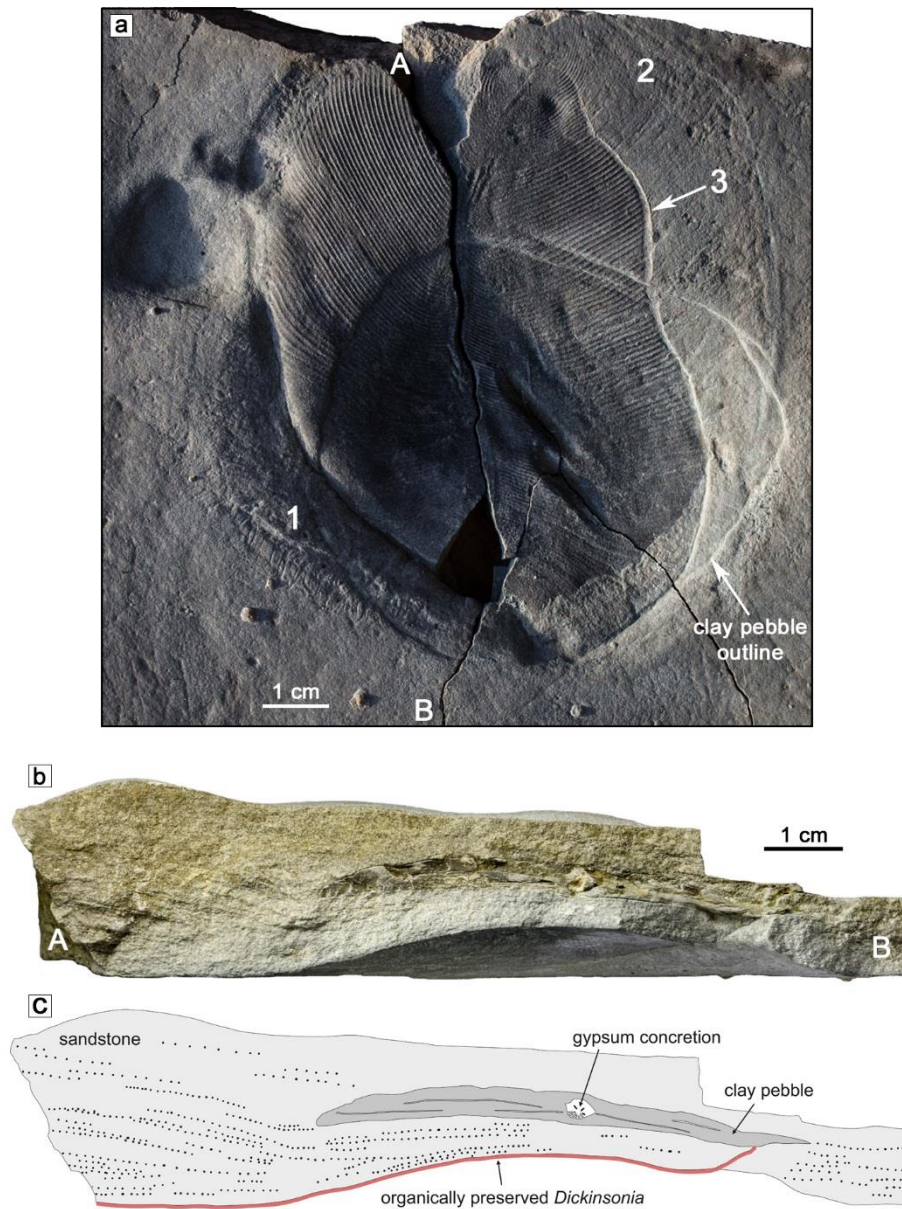


Fig. 5. *Dickinsonia* overlapping with a negative structure below a clay pebble within sandstone, a, sandstone base with negative hyporelief of *Dickinsonia*, A and B indicate the orientation of the cross section in (b); 1 – sand deposited under an edge of *Dickinsonia*; 2 – initial position of *Dickinsonia* preserved in negative hyporelief; 3 – a thin contraction rim preserved in negative hyporelief; b, cross-section view along the crack going through the specimen; c, interpretative drawing of the cross-section.

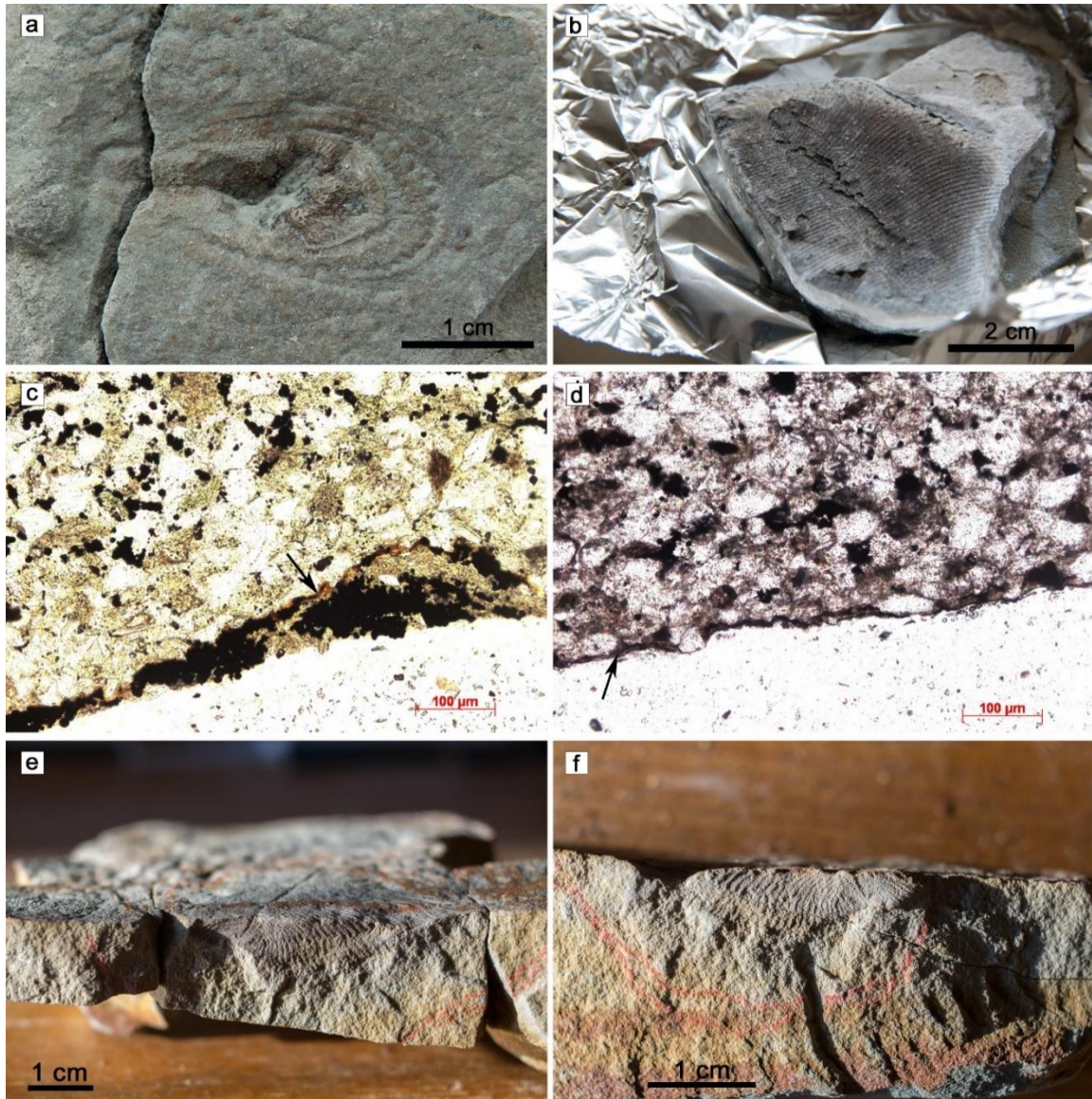


Fig. 6. Organically preserved Ediacaran fossils, and *Dickinsonia* transitional between Flinders- and Nama-style preservation; a, organically preserved *Kimberella* from the Zimnie Gory locality; note a brown layer of organic matter on *Kimberella* and a thinner layer on the entire MISS surface surrounding the fossil; **b**, organic matter flaking off from a *Dickinsonia* specimen from the Lyamtsa locality after treatment with hydrofluoric acid; **c**, arrow pointing to a thin layer of organic matter in a thin section through *Kimberella*; **d**, arrow pointing to a thin layer of organic matter in a thin section through *Dickinsonia*; **e**, *Dickinsonia* from the Zimnie Gory locality with an edge that is flipped and preserved within overlying sandstone; **f**, a cast of the flipped edge of the same *Dickinsonia* within the sandstone. In **c** and **d**, note that there is no cementation directly above the organic remains and in the overlying sandstone, where they should be present according to the cementation hypotheses; pyrite is concentrated within clay below the organic matter, indicating that it formed during and/or after decomposition of the organism, but did not take part in the fossil preservation.

Methods

Samples

Specimens were collected from the Lyamtsa and Zimnie Gory localities of the Ediacara biota in the White Sea region (Russia). Some specimens were collected by the authors during field work 2015 to 2018, the rest were studied at the collections of Ediacaran macrofossils of the Borissiak Paleontological Institute RAS (Moscow, Russia). To study fossils, clay covering the impressions from below was gently washed off with water. According to different early diagenetic cementation hypotheses, only the sediment overlying the Ediacaran organism became cemented^{19-21,23-25}. Thus, no relevant information about cementation is lost due to clay removal. Separation of organic matter from organically preserved specimens was performed only on some specimens using hydrofluoric acid as described elsewhere⁴⁵, and these specimens were not used further for any inorganic geochemical and thin section analyses in this study. Ediacaran fossils from South Australia were studied at the South Australian Museum (Adelaide, Australia).

Thin sections and electron microscopy

Polished thin sections were prepared through specimens of *Dickinsonia*, *Kimberella* and *Aspidella* perpendicular to the bedding plane and were studied under a polarizing microscope. Thin sections and hand specimens of fossils were studied using scanning electron microscopy for surface and mineral morphology and elemental composition. Images of uncoated specimens and specimens coated in Au-Pd were taken with a secondary electron and backscattered electron detector of a Tescan Vega (Czech Republic) scanning electron microscope operated in low vacuum or high vacuum modes respectively. EDX spectra were obtained with an INCA (Oxford Instruments, UK) microanalysis system.

Taphonomic experiments

To test the rheological hypothesis of negative hyporelief impressions, four taphonomic simulation experiments were conducted. In three experiments, a part of a 'Death Star'-shaped spherical ice cast (5 cm in diameter) represented an organism carcass, and a thin textured layer of cardboard (3 cm in diameter) placed horizontally into the middle of the ice cast simulated an internal organic 'skeleton' (Figs. 3a,b). By placing the cardboard into the

middle of the ice cast we do not imply that Ediacaran organisms must have possessed an internal structure, rather we intend to demonstrate that even an internal rigid structure, if it is more stable than the rest of the body, would be imprinted in negative hyporelief. One experiment was performed without cardboard. In each experiment, sediments above and below the ice cast were separated by a double layer of thin cellulose tissue (Kleenex) mimicking the presence of microbial mat. The goal of the experiments is to demonstrate the rheological behaviour of sediments during the decay of organisms of the Ediacara biota, and highlight the observation that sediment can fill a forming void from below without cementation of the overlying coarser sediment.

Three of the above experiments were performed to simulate the typical White Sea lithology with clay below and fine sand above the cast. In experiments 1 and 2, a quarter-sphere of the Death Star ice cast was placed against the transparent wall of a perspex container, underlain by water-saturated clay and covered with a layer of water-saturated fine-grained (0.1-0.18 mm) sand. Pressures of 4300 Pa (experiment 1) and 9800 Pa (experiment 2), roughly equal to the pressure created by 18 and 40 cm of sand respectively, were applied from above to mimic sediment pressure after initial burial and to provide the force to induce sediment flow. The third experiment, with no cardboard ('no cuticle'), was performed under the same conditions as experiment 2 but with an additional star-shaped ice cast placed on the clay-sand interface (Supplementary Fig. 1b). The fourth experiment ('South Australia simulation') was performed in a metal container. The ice cast was underlain by well-rounded coarse-grained (0.5-0.8 mm fraction) sand (artificial sand beads) and covered by angular coarse-grained (0.5-0.8 mm fraction) sand. The pressure applied in the experiment (22500 Pa) was equal to the pressure generated by a 90 cm thick sand layer.

In the first, low-pressure experiment, as the ice cast melted, clay expanding up from below reached the horizontal cardboard sheet in the middle of the ice cast and stopped there, while the space above the cardboard barrier was filled by sand from above creating an impression of the corrugated cardboard sheet (Supplementary Figs. 1c,d). In the second experiment with higher applied pressure, the cardboard was pushed by clay all the way up to the top of the cast, forming an impression of its corrugations in the overlying sand (Figs. 3c,d). In the third experiment, with no cardboard used, clay extruding from below filled all the space

vacated by the slowly melting ice cast (Supplementary Fig. 1b). However, even though the Death Star had considerable relief on its surface (e.g. a deep engineering bay around the superlaser focus lens, Fig. 3a), no relief was captured on sand. A star-shaped ice cast (Supplementary Fig. 1a), placed next to the Death Star in this experiment, left a star-shaped impression in the overlying sand albeit with little detail (Supplementary Fig. 1b). In experiment 4, the ‘South Australia simulation’, well-rounded sand from below protruded upwards all the way to the top of the ice cast (Figs. 3e,f).

All experiments were performed at 1°C in a temperature regulated chamber to cause slow melting of the ice casts. The initial temperature of the ice casts was -21°C. After the ice casts had melted, the entire experimental set up was frozen at -21°C and then cracked open with a hammer along the surface between the two lithologies.

Data availability

All materials are available within the main text and supporting documents. Palaeontological specimens from South Australia are stored at the South Australian Museum, specimens from the White Sea area are stored at the Borissiak Palaeontological Institute. Thin sections and higher quality images are available from the corresponding authors on request.

References

- 1 Fedonkin, M. A. & Waggoner, B. M. The Late Precambrian fossil *Kimberella* is a mollusc-like bilaterian organism. *Nature* **388**, 868, doi:10.1038/42242 (1997).
- 2 Ivantsov, A. Y. Paleontological evidence for the supposed precambrian occurrence of mollusks. *Paleontological Journal* **44**, 1552-1559, doi:10.1134/s0031030110120105 (2010).
- 3 Antcliffe, J. B., Gooday, A. J. & Brasier, M. D. Testing the protozoan hypothesis for Ediacaran fossils: a developmental analysis of *Palaeopascichnus*. *Palaeontology* **54**, 1157-1175, doi:10.1111/j.1475-4983.2011.01058.x (2011).
- 4 Seilacher, A., Grazhdankin, D. & Legouta, A. Ediacaran biota: The dawn of animal life in the shadow of giant protists. *Paleontological Research* **7**, 43-54, doi:10.2517/prpsj.7.43 (2003).
- 5 Kolesnikov, A. V. *et al.* The oldest skeletal macroscopic organism *Palaeopascichnus linearis*. *Precambrian Research* **316**, 24-37, doi:<https://doi.org/10.1016/j.precamres.2018.07.017> (2018).
- 6 Bobrovskiy, I., Hope, J. M., Krasnova, A., Ivantsov, A. & Brocks, J. J. Molecular fossils from organically preserved Ediacara biota reveal cyanobacterial origin for *Beltanelliformis*. *Nature Ecology & Evolution*, doi:10.1038/s41559-017-0438-6 (2018).

- 7 Ivantsov, A. Y., Gritsenko, V. P., Konstantinenko, L. I. & Zakrevskaya, M. A. Revision of the problematic Vendian macrofossil *Beltanelliformis* (=Beltanelloides, Nemiana). *Paleontological Journal* **48**, 1415-1440, doi:10.1134/s0031030114130036 (2014).
- 8 Xiao, S. & Laflamme, M. On the eve of animal radiation: phylogeny, ecology and evolution of the Ediacara biota. *Trends Ecol Evol* **24**, 31-40, doi:10.1016/j.tree.2008.07.015 (2009).
- 9 Budd, G. E. & Jensen, S. The origin of the animals and a 'Savannah' hypothesis for early bilaterian evolution. *Biological Reviews* **92**, 446-473, doi:doi:10.1111/brv.12239 (2017).
- 10 Brasier, M. D. & Antcliffe, J. B. Dickinsonia from Ediacara: A new look at morphology and body construction. *Palaeogeography, Palaeoclimatology, Palaeoecology* **270**, 311-323, doi:<http://dx.doi.org/10.1016/j.palaeo.2008.07.018> (2008).
- 11 Droser, M. L., Gehling, J. G. & Jensen, S. R. Assemblage palaeoecology of the Ediacara biota: The unabridged edition? *Palaeogeography, Palaeoclimatology, Palaeoecology* **232**, 131-147, doi:10.1016/j.palaeo.2005.12.015 (2006).
- 12 Dzik, J. Organic membranous skeleton of the Precambrian metazoans from Namibia. *Geology* **27**, 519-522 (1999).
- 13 Parry, L. A. *et al.* Soft-Bodied Fossils Are Not Simply Rotten Carcasses – Toward a Holistic Understanding of Exceptional Fossil Preservation. *BioEssays* **40**, 1700167, doi:doi:10.1002/bies.201700167 (2018).
- 14 Narbonne, G. M. The Ediacara Biota: Neoproterozoic Origin of Animals and Their Ecosystems. *Annual Review of Earth and Planetary Sciences* **33**, 421-442, doi:10.1146/annurev.earth.33.092203.122519 (2005).
- 15 Waggoner, B. The Ediacaran Biotas in Space and Time. *Integrative and Comparative Biology* **43**, 104-113, doi:10.1093/icb/43.1.104 (2003).
- 16 Grazhdankin, D. Patterns of distribution in the Ediacaran biotas: facies versus biogeography and evolution. *Paleobiology* **30**, 203-221, doi:10.1666/0094-8373(2004)030<0203:PODITE>2.0.CO;2 (2004).
- 17 Boag, T. H., Darroch, S. A. F. & Laflamme, M. Ediacaran distributions in space and time: testing assemblage concepts of earliest macroscopic body fossils. *Paleobiology* **42**, 574-594, doi:10.1017/pab.2016.20 (2016).
- 18 Wade, M. Preservation of Soft-Bodied Animals in Precambrian Sandstones at Ediacara, South Australia. *Lethaia* **1**, 238-267, doi:10.1111/j.1502-3931.1968.tb01740.x (1968).
- 19 Gehling, J. G. Microbial mats in terminal Proterozoic siliciclastics; Ediacaran death masks. *PALAIOS* **14**, 40-57, doi:10.2307/3515360 (1999).
- 20 Liu, A. G. Framboidal Pyrite Shroud Confirms the 'Death Mask' Model for Moldic Preservation of Ediacaran Soft-Bodied Organisms. *Palaaios* **31**, 259-274, doi:10.2110/palo.2015.095 (2016).
- 21 Gibson, B. M., Schiffbauer, J. D. & Darroch, S. A. F. Ediacaran-style Decay Experiments using Mollusks and Sea Anemones. *Palaaios* **33**, 185-203, doi:10.2110/palo.2017.091 (2018).
- 22 Liu, A. G., McMahon, S., Matthews, J. J., Still, J. W. & Brasier, A. T. Petrological evidence supports the death mask model for the preservation of Ediacaran soft-bodied organisms in South Australia. *Geology* (in press).
- 23 Serezhnikova, E. A. Microbial Binding as a Probable Cause of Taphonomic Variability of Vendian Fossils: Carbonate Casting? **131**, 525-535, doi:10.1007/978-3-642-10415-2_31 (2011).
- 24 Tarhan, L. G., Hood, A. v. S., Droser, M. L., Gehling, J. G. & Briggs, D. E. G. Exceptional preservation of soft-bodied Ediacara Biota promoted by silica-rich oceans. *Geology* **44**, 951-954, doi:10.1130/g38542.1 (2016).
- 25 Callow, R. H. T. & Brasier, M. D. Remarkable preservation of microbial mats in Neoproterozoic siliciclastic settings: Implications for Ediacaran taphonomic models. *Earth-Science Reviews* **96**, 207-219, doi:10.1016/j.earscirev.2009.07.002 (2009).

- 26 Gehling, J. G. & Droser, M. L. Textured organic surfaces associated with the Ediacara biota in South Australia. *Earth-Science Reviews* **96**, 196-206, doi:10.1016/j.earscirev.2009.03.002 (2009).
- 27 Seilacher, A. Biomat-related lifestyles in the Precambrian. *Palaios* **14**, 86-93 (1999).
- 28 Dzik, J. Anatomical information content in the Ediacaran fossils and their possible zoological affinities. *Integrative and Comparative Biology* **43**, 114-126 (2003).
- 29 Fedonkin, M. A. in *Origin and Early Evolution of the Metazoa* (eds Jere H. Lipps & Philip W. Signor) 87-129 (Springer US, 1992).
- 30 Cai, Y., Schiffbauer, J. D., Hua, H. & Xiao, S. Preservational modes in the Ediacaran Gaojiashan Lagerstätte: Pyritization, aluminosilicification, and carbonaceous compression. *Palaeogeography, Palaeoclimatology, Palaeoecology* **326-328**, 109-117, doi:10.1016/j.palaeo.2012.02.009 (2012).
- 31 Orr, P. J., Briggs, D. E. G. & Kearns, S. L. Cambrian Burgess Shale Animals Replicated in Clay Minerals. *Science* **281**, 1173-1175, doi:10.1126/science.281.5380.1173 (1998).
- 32 Gehling, J., Droser, M., Jensen, S., Runnegar, B. & Briggs, D. in *Evolving form and function: fossils and development; Proceedings of a Symposium Honouring Adolf Seilacher for His Contributions to Paleontology, in Celebration of His 80th Birthday*. (ed DEG Briggs) 43-66 (Yale University Press, 2005).
- 33 Ivantsov, A. Y. Feeding traces of proarticulata—the Vendian metazoa. *Paleontological Journal* **45**, 237-248, doi:10.1134/s0031030111030063 (2011).
- 34 Seilacher, A. Vendozoa: Organismic construction in the Proterozoic biosphere. *Lethaia* **22**, 229-239, doi:doi:10.1111/j.1502-3931.1989.tb01332.x (1989).
- 35 Evans, S. D., Droser, M. L. & Gehling, J. G. Dickinsonia liftoff: Evidence of current derived morphologies. *Palaeogeography, Palaeoclimatology, Palaeoecology* **434**, 28-33, doi:<https://doi.org/10.1016/j.palaeo.2015.02.006> (2015).
- 36 Retallack, G. J. Were the Ediacaran fossils lichens? *Paleobiology* **20**, 523-544 (1994).
- 37 Jeong, S. W., Locat, J., Leroueil, S. & Malet, J.-P. Rheological properties of fine-grained sediment: the roles of texture and mineralogy. *Canadian Geotechnical Journal* **47**, 1085-1100, doi:10.1139/T10-012 (2010).
- 38 Darroch, S. A. F., Laflamme, M., Schiffbauer, J. D. & Briggs, D. E. G. Experimental Formation of a Microbial Death Mask. *Palaios* **27**, 293-303, doi:10.2110/palo.2011.p11-059r (2012).
- 39 Verruijt, A. *An Introduction to Soil Mechanics*. Vol. 30 (VSSD, 2018).
- 40 Panagiotopoulos, I., Voulgaris, G. & Collins, M. B. The influence of clay on the threshold of movement of fine sandy beds. *Coastal Engineering* **32**, 19-43, doi:[https://doi.org/10.1016/S0378-3839\(97\)00013-6](https://doi.org/10.1016/S0378-3839(97)00013-6) (1997).
- 41 Tarhan, L. G., Droser, M. L., Gehling, J. G. & Dzaugis, M. P. Taphonomy and morphology of the Ediacara form genus *Aspidella*. *Precambrian Research* **257**, 124-136, doi:<https://doi.org/10.1016/j.precamres.2014.11.026> (2015).
- 42 Burzynski, G., Narbonne, G. M., Alexander Dececchi, T. & Dalrymple, R. W. The ins and outs of Ediacaran discs. *Precambrian Research* **300**, 246-260, doi:<https://doi.org/10.1016/j.precamres.2017.08.012> (2017).
- 43 Ivantsov, A. Y. Reconstruction of Charniodiscus yorgensis (Macrobiota from the Vendian of the White Sea). *Paleontological Journal* **50**, 1-12, doi:10.1134/s0031030116010032 (2016).
- 44 Noffke, N. The criteria for the biogenicity of microbially induced sedimentary structures (MISS) in Archean and younger, sandy deposits. *Earth-Science Reviews* **96**, 173-180, doi:<https://doi.org/10.1016/j.earscirev.2008.08.002> (2009).
- 45 Bobrovskiy, I. et al. Ancient steroids establish the Ediacaran fossil *Dickinsonia* as one of the earliest animals. *Science* **361**, 1246-1249, doi:10.1126/science.aat7228 (2018).

- 46 Steiner, M. & Reitner, J. Evidence of organic structures in Ediacara-type fossils and associated microbial mats. *Geology* **29**, 1119-1122, doi:10.1130/0091-7613(2001)029<1119:eoosie>2.0.co;2 (2001).
- 47 Kenchington, C. G. & Wilby, P. R. in *Reading and Writing of the Fossil Record: Preservation Pathways to Exceptional Fossilization The Paleontological Society Papers* (eds M. Laflamme, S. A. F. Darroch, & J. D. Schiffbauer) 101-122 (Cambridge University Press, 2017).
- 48 Liu, A. G., McIlroy, D., Antcliffe, J. B. & Brasier, M. D. Effaced preservation in the Ediacara biota and its implications for the early macrofossil record. *Palaeontology* **54**, 607-630, doi:doi:10.1111/j.1475-4983.2010.01024.x (2011).
- 49 Fedonkin, M. A., Simonetta, A. & Ivantsov, A. Y. New data on *Kimberella*, the Vendian mollusc-like organism (White Sea region, Russia): palaeoecological and evolutionary implications. *Geological Society, London, Special Publications* **286**, 157-179, doi:10.1144/sp286.12 (2007).
- 50 Dzik, J. & Ivantsov, A. Y. Internal anatomy of a new Precambrian dickinsoniid dipleurozoan from northern Russia. *Neues Jahrbuch für Geologie und Paläontologie Monatshefte*, 385-396 (2002).

Simple sediment rheology explains the Ediacara biota preservation

Supplementary Figures

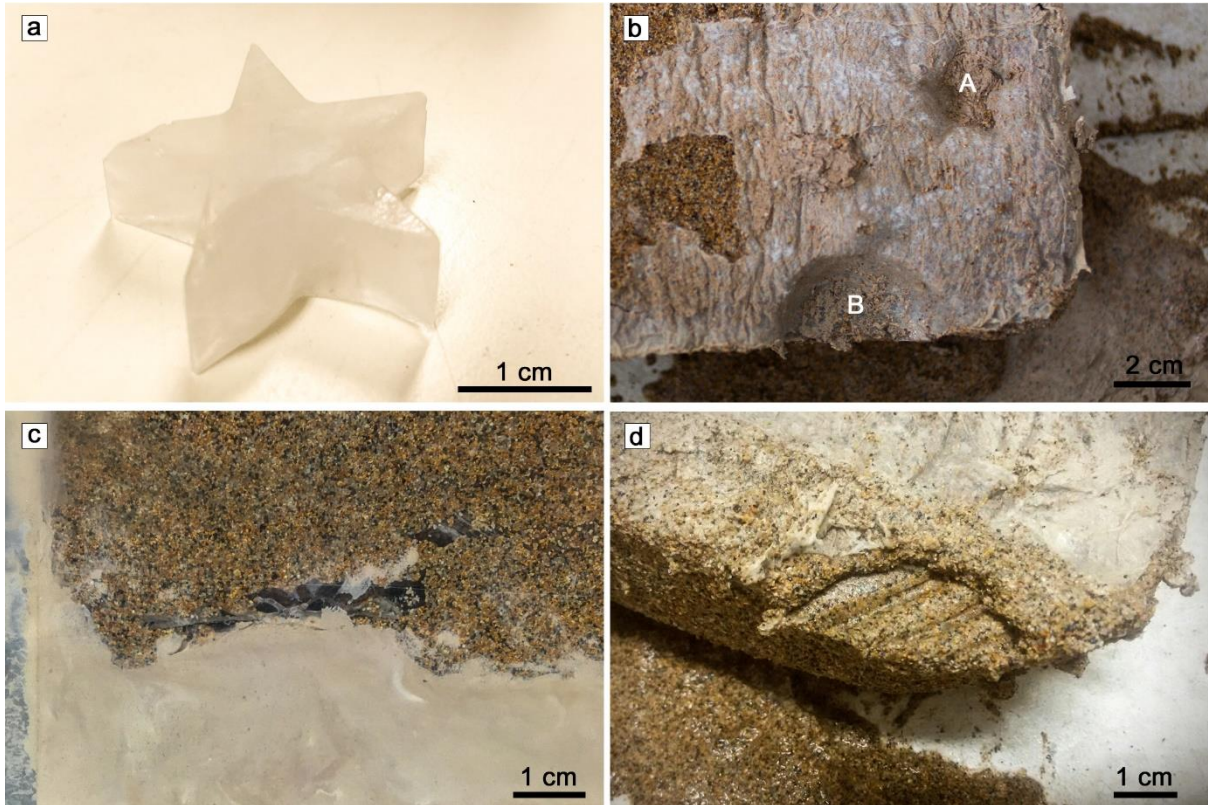
Ilya Bobrovskiy^{1*}, Anna Krasnova^{2,3}, Andrey Ivantsov², Ekaterina Luzhnaya (Serezhnikova)², Jochen J. Brocks^{1*}

¹Research School of Earth Sciences, Australian National University, Canberra, ACT 2601, Australia

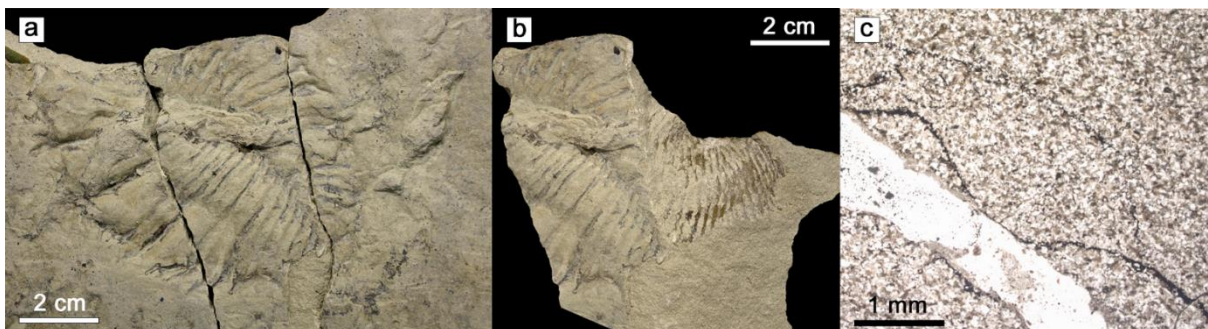
²Borissiak Paleontological Institute, Russian Academy of Sciences, Moscow 117997, Russia

³Faculty of Geology, Lomonosov Moscow State University, Moscow 119991, Russia

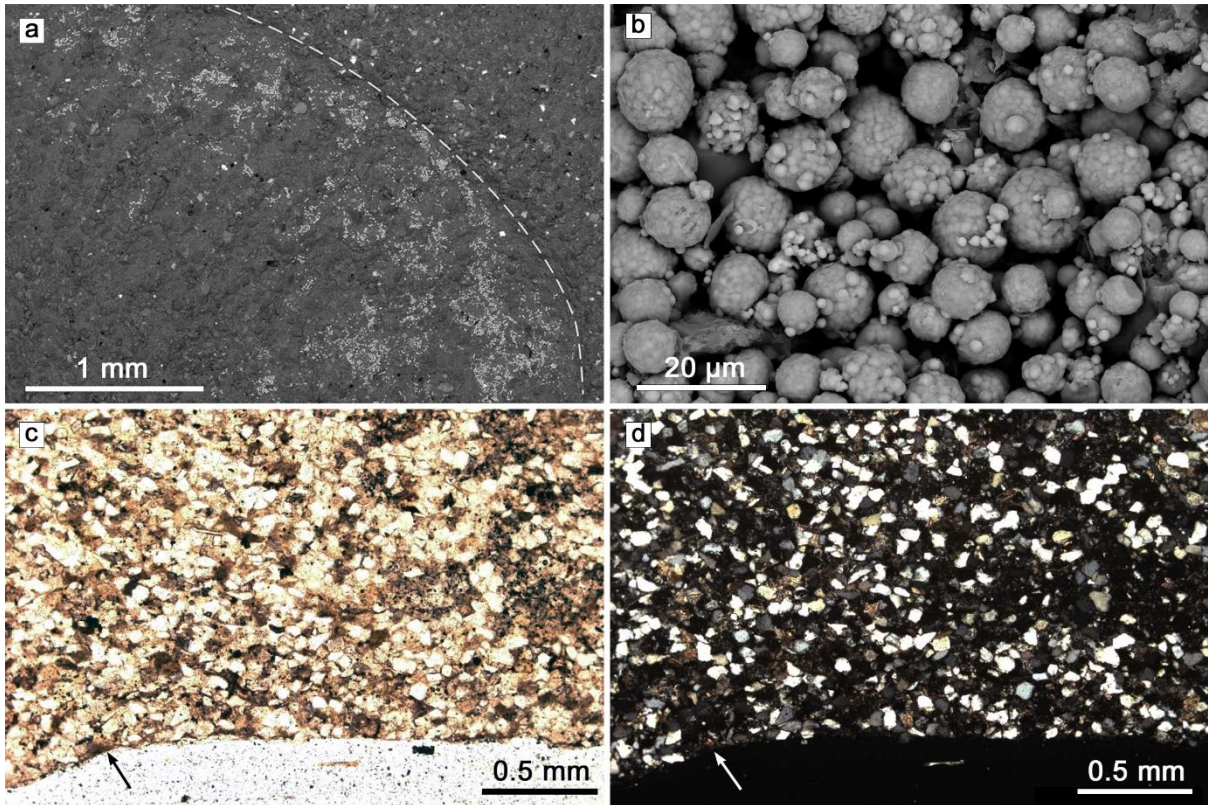
*Correspondence to: ilya.bobrovskiy@anu.edu.au, jochen.brocks@anu.edu.au



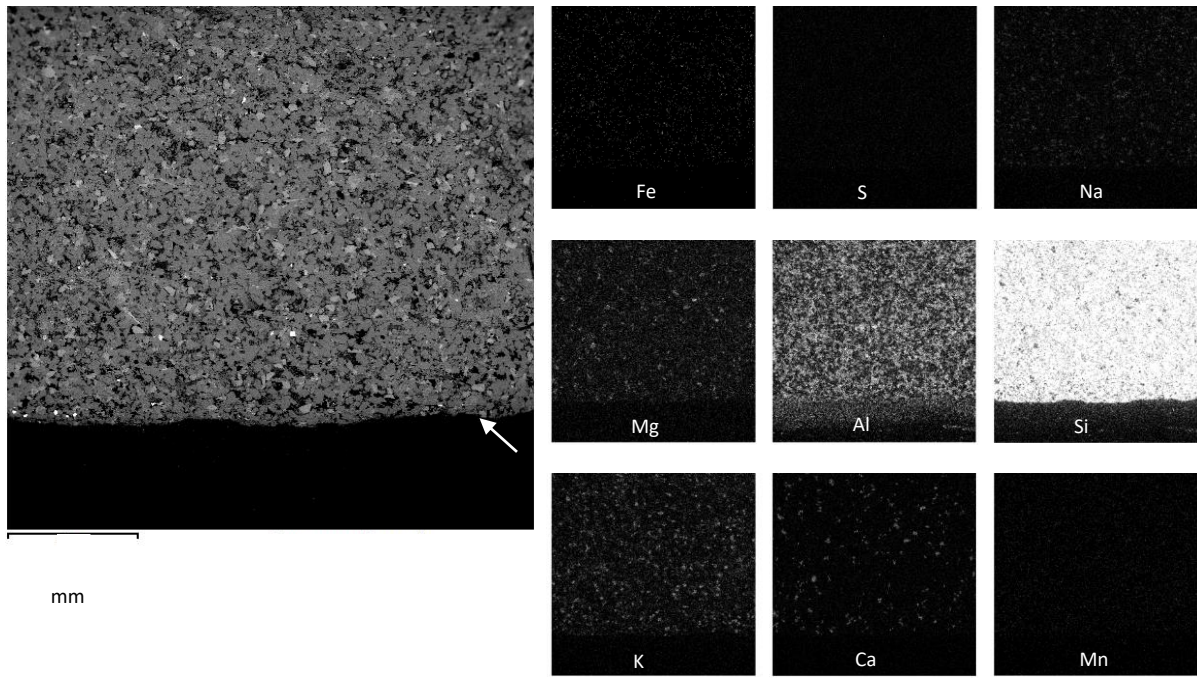
Supplementary Fig. 1. Taphonomic laboratory simulations, a, star-shaped ice mould used in experiment 3; **b**, experiment 3, negative hyporelief impression on sand base; A – impression of the star-shaped ice mould; B – impression of the Death Star ice mould; **c**, **d** – experiment 1, negative hyporelief impression on sand base. The diameter of the impressions is 5 cm in all experiments.



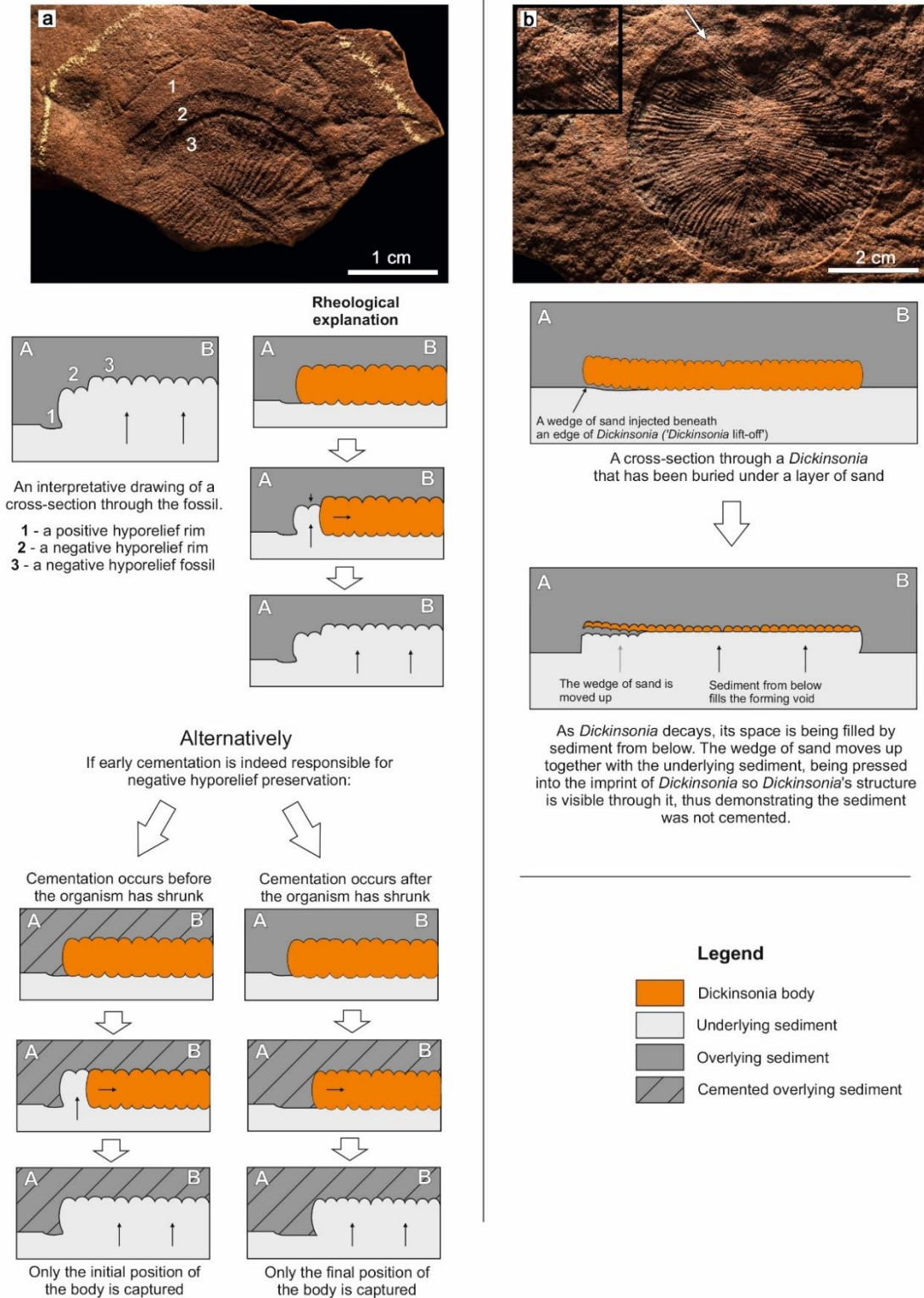
Supplementary Fig. 2. *Dickinsonia* with its middle part dragged into overlying sandstone, a, impression at the base of sandstone; **b**, part of impression at the base of sandstone and the part of *Dickinsonia* dragged into sandstone (Nama-style preservation); **c**, thin section through this *Dickinsonia*; note how pyrite (black) forms a thin line, replacing residual organic matter of *Dickinsonia*.



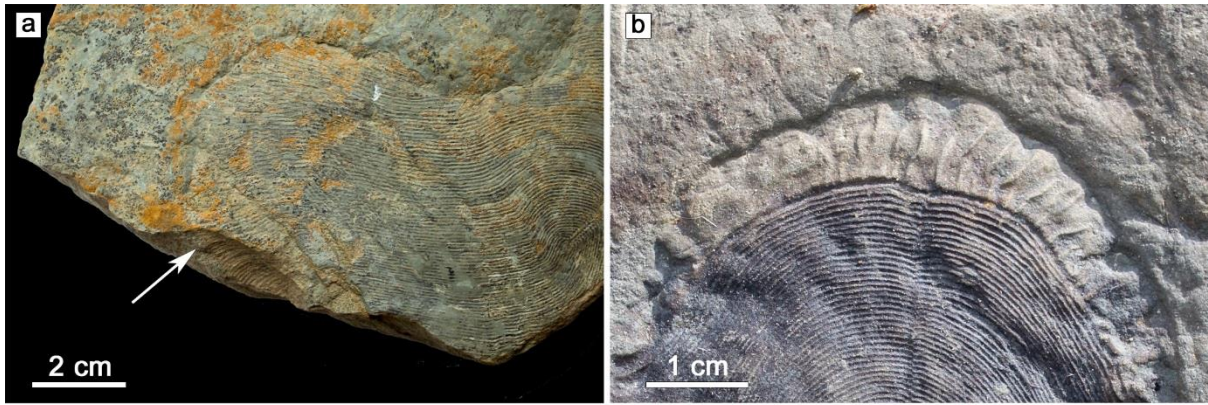
Supplementary Fig. 3. Tracking early diagenetic mineralization. **a**, SEM image of *Dickinsonia*; dashed line outlines the fossil, light-grey tone represents pyrite; note that large areas of the fossil lack pyrite, but *Dickinsonia*'s preservation is not affected by this; **b**, – magnified SEM image of the same surface on the area where pyrite is concentrated, demonstrating perfect preservation of pyrite framboids; **c**, photomicrograph of a thin section through *Dickinsonia*, Nichols parallel and **d**, Nichols crossed. In **c** and **d**, arrows point at the surface of the fossil; note that the pore space is filled with clay, not pyrite, silica or carbonate material.



Supplementary Fig. 4. SEM elemental mapping of a cross section through a *Dickinsonia*. Note the distribution of Fe and S, reflecting virtual absence of pyrite and the distribution of Ca and Mg, reflecting low abundance of dolomite. Arrow points at the surface of the fossil.

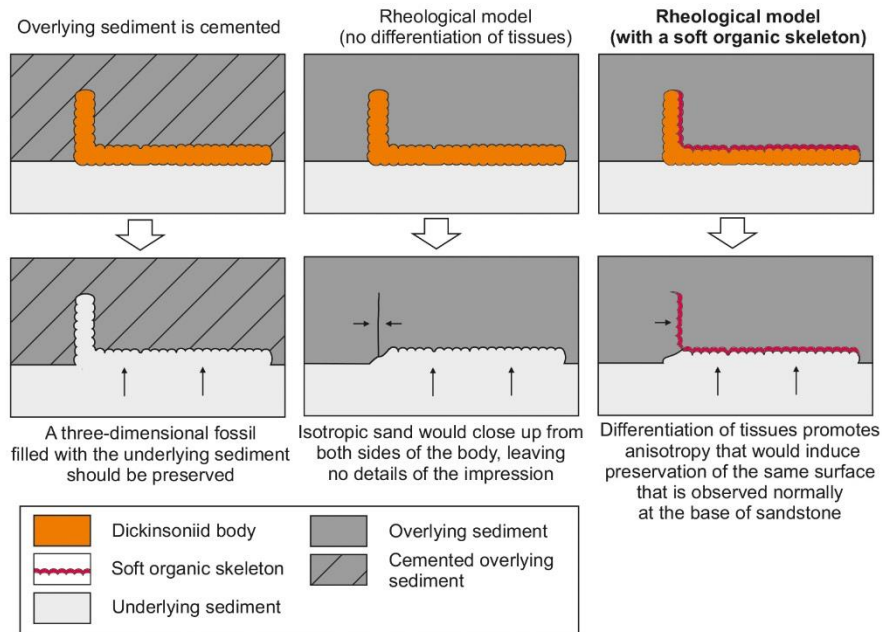


Supplementary Fig. 5. Schematic explanation for contraction rims around *Dickinsonia* and sand wedges taphonomy (compare Fig. 2). **a**, Contraction rims around *Dickinsonia* from South Australia (South Australian Museum, sample P40944) and their formation mechanism; **b**, *Dickinsonia* from South Australia with a thin wedge of sand material intruded beneath its edge (South Australian Museum, sample P12557), arrow points at *Dickinsonia*'s isomers visible through the wedge (also shown in magnification in the insert).



c

Possible explanations for Nama-style dickinsoniid preservation



Supplementary Fig. 6. Evidence for differentiation of tissues in dickinsoniids. **a**, *Andiva* from the White Sea Area, partially preserved in both Flinders and Nama-style preservation (the arrow points at the area preserved in Nama-style); **b**, *Andiva* from the White Sea Area that demonstrates differential preservation of tissues: the metameric central part of the fossil is preserved organically, while the surrounding smoother area is not; **c**, a scheme that illustrates three alternative scenarios of Nama-style preservation of dickinsoniids, showing they must have relatively more and less resistant tissues to form the fossils that we observe.

CHAPTER 5. FOOD SOURCES FOR THE EDIACARA BIOTA

Understanding the environments inhabited by the Ediacara biota is an integral part of building our knowledge on connections and distinctions between Ediacaran and Phanerozoic macroorganisms. Unlike Chapters 1-3, this part of the thesis applies a more classical way of using biomarkers and reconstructs the composition of primary producers in the environments that were inhabited by Ediacaran macroorganisms. It shows that, in contrast to earlier predictions, the Ediacara biota inhabited nutrient replete environments with an abundance of algal food sources comparable to Phanerozoic ecosystems.

Statement of Contribution

This thesis is submitted as a Thesis by Compilation in accordance with https://policies.anu.edu.au/ppl/document/ANUP_003405

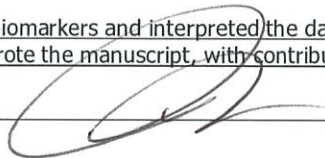
I declare that the research presented in this Thesis represents original work that I carried out during my candidature at the Australian National University, except for contributions to multi-author papers incorporated in the Thesis where my contributions are specified in this Statement of Contribution.

Title and authors: Bobrovskiy, I., Hope, J. M., Golubkova, E., Brocks, J. J. Food sources for the Ediacara biota communities. _____

Current status of paper: Not Yet Submitted/**Submitted**/Under Revision/Accepted/Published

Contribution to paper: I.B. designed the study, analyzed biomarkers and interpreted the data; J.M.H. helped with biomarker analysis; I.B. and E.G. collected samples; I.B. and J.J.B. wrote the manuscript, with contributions from all authors. _____

Senior author or collaborating authors endorsement: _____



Ilya Bobrovskiy

Candidate – Print Name



Signature

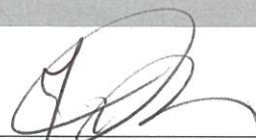
18/04/2019

Date

Endorsed

Jochen Brocks

Chair of Supervisory Panel – Print Name



Signature

18/04/2019

Date

Stewart Fallon

Delegated Authority – Print Name



Signature

29/04/2019

Date

Food sources for the Ediacara biota communities

Ilya Bobrovskiy^{1*}, Janet M. Hope¹, Elena Golubkova², Jochen J. Brocks^{1*}

¹Research School of Earth Sciences, Australian National University, Canberra, Australia

² Institute of Precambrian Geology and Geochronology, Russian Academy of Sciences, St. Petersburg, Russia

*Correspondence to: ilya.bobrovskiy@anu.edu.au, jochen.brocks@anu.edu.au

The Ediacara biota represents the first complex macroscopic organisms in the geological record, foreshadowing the radiation of eumetazoan animals in the Cambrian explosion. However, little is known about the contingencies that lead to their emergence, including the possible roles of nutrient availability and the quality of food sources. With the proliferation of algae in planktonic and benthic marine environments, food availability and quality must have radically changed at the beginning of the Ediacaran period. Yet it remains unclear whether Ediacaran macroorganisms inhabited oligotrophic environments with dissolved organic matter and bacterial picoplankton as main nutrient sources, or were part of a new Ediacaran ecology where eukaryotic algae were the predominant food source. Here we present information on primary producers in the Ediacaran based on biomarker molecules that were extracted from sediments hosting Ediacaran microfossils. High relative abundances of algal steranes over bacterial hopanes suggest that the Ediacara biota inhabited nutrient replete environments with an abundance of algal food sources comparable to Phanerozoic ecosystems. Thus, organisms of the Ediacara biota inhabited nutrient-rich environments akin to those that later fuelled the Cambrian explosion.

The appearance of the first macroscopic, morphologically complex organisms in the late Ediacaran (~571 to 541 million years [Ma] ago) was the onset of one of the most important biological transitions in Earth's history. However, it remains unclear which environmental, ecological and evolutionary factors accompanied the emergence of large animal-like organisms, and how these various factors interacted. The most popular models connect the

appearance and ecological success of animals with rising atmospheric oxygen concentrations in the Neoproterozoic¹⁻³. Yet, molecular oxygen as a limiting resource faces several challenges. While increasing oxygenation of deep marine waters in the Neoproterozoic broadly coincides with the appearance of macroorganisms in such environments⁴, suitably oxic conditions were probably established in well aerated surface environments hundreds of millions of years earlier⁵⁻⁹. Moreover, cyanobacterial mats are ubiquitous in shallow-marine environments in the Proterozoic and would have provided stable ecospace with elevated oxygen concentrations for organisms with mat-related lifestyles far back in Earth history^{10,11}.

An alternative environmental factor that may have constrained the timing of eumetazoan emergence and radiation is nutrient availability, including bio-limiting elements and efficient carbon sources supplied by primary producers. The abundance of different classes of primary producers in Precambrian oceans can be tracked using molecular fossils, or biomarkers¹²⁻¹⁴. The most common biomarkers are alteration products of membrane lipids such as hopanols found in numerous aerobic bacteria, including cyanobacteria, and sterols produced by algae and other eukaryotes. During sedimentary diagenesis, hopanols are transformed into hydrocarbon hopanes, while sterols yield fossil steranes. Hopanes and steranes are extracted from ancient sedimentary rocks using organic solvents and quantified using gas chromatograph-mass spectroscopy. The proportion of hopanes (H) over steranes (S), the H/S ratio, can be used as an estimate for the relative flux of bacterial versus eukaryotic organic matter to bottom sediments, and thus as a first-order approximation for the relative importance of algal versus cyanobacterial biomass, among both benthos and plankton¹²⁻¹⁴. The transition from bacteria- to eukaryote-dominated primary production in the oceans, recorded by biomarkers, occurred ~650-635 Ma¹⁵ ago and may have been crucial for the success of most macroscopic heterotrophs (Supplementary Information)^{15,16}.

The Ediacara biota represents the first global appearance of large heterotrophic organisms, including animals, in the fossil record, and thus reflects aspects of the ecology and evolution of early animals. Recent studies have reported biomarkers from Ediacaran sediments of the East European Platform (EEP) with H/S ratios that are high relative to typical Phanerozoic marine conditions^{17,18}. Consequently, it has been suggested that Ediacaran macro-organisms preferentially inhabited oligotrophic environments and used bacteria as

their main energy source, as either food or symbionts^{17,19-21}. It is notable, however, that none of the biomarker data came from localities that preserve Ediacaran macrofossils (Fig. 1), and it remains to be seen whether they usefully reflect ecological circumstances across the whole of the EEP. In order to resolve the particular circumstances under which Ediacaran macro-organisms lived, we analysed biomarkers from sediments with Ediacaran macrofossils from the White Sea area of the EEP.

Geological context of Ediacaran deposits of the White Sea area

Due to the mild thermal history of Ediacaran deposits in the White Sea area, Ediacaran macrofossils co-occur there with extremely well preserved biomarkers^{22,23}, offering a unique opportunity to assess the habitat and ecological preferences of these problematic organisms. The White Sea area offers localities with the most diverse and abundant Ediacara biota in the world, including various members of the White Sea, Avalon and Nama assemblages²⁴⁻²⁷. All sediments from the Lyamtsa and Zimnie Gory localities (Fig. 1) were originally deposited in shallow marine environments and preserve evidence for persistent and pervasive microbial mats²⁸. The distribution of Ediacaran macrofossils within the White Sea area sections is largely controlled by taphonomy – the fossils are best preserved at the soles of sandstone layers, but less abundant fossils of poorer quality are scattered throughout the entire sedimentary succession^{25,27}.

The distribution of Ediacaran macrofossils within the White Sea area sections is largely controlled by taphonomy – the fossils are best preserved at the soles of sandstone layers, but less abundant fossils of poorer quality are scattered throughout the entire sedimentary succession^{25,27}. To get a full picture about the distribution of primary producers in environments inhabited by the Ediacara biota, samples collected from the entire section exposed in the studied localities were analysed for biomarkers. Most organic geochemical studies analyse centimetre-scale sedimentary rock samples, thus averaging ecological signals across substantial periods of time, and potentially missing ecologically distinct endmembers. To ensure that we indeed capture the exact ecological environment of organisms of the Ediacara biota, we analysed sediments immediately beneath and above surfaces with Ediacara biota fossils at millimetre resolution. As organisms of the Ediacara biota are

preserved *in situ*, biomarkers extracted from clay underneath the fossils represent the substrate they were living on. Sandstones above fossils normally represent storm deposited material²⁸; biomarkers extracted from these sandstones presumably average the biomass of the local environment, but may also contain material transported from adjacent settings. Specifically, we analysed two surfaces in the Lyamtsa locality that contain abundant *Dickinsonia*, *Parvancorina* and *Palaeopascichnus* fossils, and well-studied surfaces in the Zimnie Gory, known as Z1(I) and Z11(XXII), which contain *Andiva*, *Archaeaspinus*, *Armillifera*, *Aspidella*, *Brachina*, *Charniodiscus*, *Cyanorus*, *Cyclomedusa*, *Dickinsonia*, *Inaria*, *Ivovicia*, *Kimberella*, *Onega*, *Ovatoscutum*, *Paleophragmodictya*, *Paravendia*, *Parvancorina*, *Tamga*, *Temnoxa*, *Tribrachidium* and *Yorgia*²⁷. Thus, this study looks at biomarkers representative of environments for a broad range of species of the Ediacara biota, including burrowers (e.g. *Sabellidita*, *Calyptrina*)^{29,30}, mat-scrapers (e.g. *Andiva*, *Dickinsonia*, *Kimberella*) and potentially filter- or osmotroph-feeding mat-stickers (Arborea, e.g. *Charniodiscus*). The collected data thus provide information about the ecological environment of representative organisms of all three existing Ediacara biota assemblages, which otherwise occur in a wider temporal and palaeogeographic context²⁴.

Hopane/Sterane ratios and primary producers from the Tonian to Phanerozoic

To place the Ediacaran biomarkers from the White Sea area into a broad temporal context, Figure 2 summarizes data for bacterial hopanes and algal steranes from the Tonian to the present. Based on biomarkers, bacteria were the only notable primary producers in Paleo- and Mesoproterozoic oceans³¹. Primitive eukaryotic sterane signatures emerged ~900 to 800 Ma ago^{15,32}, although the overall H/S ratio remained high (70% of values are H/S >29.5, and steranes are below detection limits in 43% of samples that contain hopanes). Moreover, it is unclear whether steranes in Tonian sediments are derived from algae or other organisms¹⁵. The first signs of unambiguous algal productivity occurred in a single sample assigned to the Cryogenian, around 650 Ma, and started to be a dominating signal from the very beginning of the Ediacaran, close to 635 Ma^{15,33}. This 'Rise of Algae' was marked by an order-of-magnitude drop in H/S ratios and the emergence of a near-modern sterane diversity (Fig. 2a,b). Phanerozoic sediments, in contrast to the Tonian, mainly demonstrate

continuously low H/S values, (H/S = 0.5-5 range accounts for 70% percentile with the mode at 1.3), indicating that algae have been key primary producers for the past 541 million years.

The Ediacaran, however, yields bitumens with H/S signatures resembling both the Tonian and Phanerozoic. Sediments from the Oman Salt Basin and the Siberian platform demonstrate H/S values similar to the Phanerozoic (Fig. 2c,d) (H/S = 0.75-1.4 range accounts for 70% percentile with the mode value 1.3). By contrast, bitumens from the Ediacaran interior seaway of the EEP¹⁷ include numerous elevated H/S values up to 119 (H/S = 1.5-12.5 range accounts for 70% percentile with several modes, and median value 7.7), values otherwise typical for the Tonian (Fig. 2f). It has been suggested¹⁷ that the elevated H/S values in the interior seaway of the EEP, just as those from the Tonian^{15,16}, might reflect a strong predominance of bacteria among primary producers, potentially due to regionally oligotrophic conditions, thus highlighting a high spatial heterogeneity in primary producer communities in Ediacaran marine environments (though see Supplementary Information)¹⁷.

Based on the H/S data from global Ediacaran sediments, the Ediacara biota might have either inhabited newly established algae-rich environments^{15,16} or, conversely, thrived in nutrient-depleted ecosystems dominated by bacterial primary productivity akin to the Tonian or Mesoproterozoic^{17,20}. If latter hypothesis is correct, then the diet and ecology of organisms of the Ediacara biota must have been very distinct from most Phanerozoic animals^{17,19,20}, and it would invalidate the premise that the emergence of abundant algal food sources was crucial for the ecological success of eumetazoan animals. Biomarker data from sediments directly associated with Ediacara biota fossils can shed light on this dispute.

Primary producers at the Ediacara biota localities

The clay and sandstone material directly surrounding Ediacara biota fossils in the White Sea sections demonstrate low H/S ratios (H/S = 2.5-5) (Fig. 3). The overall H/S values from the whole set of White Sea area sediments vary slightly more broadly (H/S = 1-7 range accounts for 70% percentile with the mode value 3.3, n = 59; Fig. 2e). These H/S values suggest that the Ediacara biota inhabited environments with near-modern fluxes of bacterial versus eukaryotic biomass (Fig. 3). Moreover, steranes of the White Sea area are strongly dominated by stigmastanes (C_{29} (%) = $75 \pm 9\%$ of C_{27} to C_{29} sterane homologues; n = 59). The C_{29}

predominance among steranes in the White Sea area is characteristic of Ediacaran biomarker signatures and likely reflects predominance of green algae among eukaryotes³⁴. The mode of H/S value in the White Sea area is somewhat elevated in comparison to the Phanerozoic (Fig. 2c and e). This elevation may reflect a stronger relative contribution of planktonic cyanobacterial biomass than the average Phanerozoic, but is more likely associated with benthic cyanobacterial mats that are widespread in White Sea sediments and generally abundant in Ediacaran shallow water environments^{35,36}. Regardless, Ediacaran macroorganisms of the White Sea area inhabited environments that were orders of magnitude enriched in algal relative to bacterial food sources when compared to the Tonian, and in this respect similar to Phanerozoic marine habitats.

Primary producers and early animal evolution

The Rise of Algae 650-635 Ma has changed the ecosystems on our planet forever, although the trigger for this phenomenon is unclear. It has been proposed that a potential increase in nutrient levels in the oceans at that time could have made algae more competitive relative to photosynthetic bacteria^{15,16}, or alternatively that protistan eukaryotes or bacteriovorous sponge-grade animals effectively reduced bacterial biomass, thus providing ecospace for algae^{6,7,33,37-39}. Whatever the causes for the proliferation of planktonic algae, their biomass may have fuelled the radiation of eumetazoan animals by increasing the efficiency of nutrient and energy transfer to higher trophic levels based on larger cells sizes compared to bacterial phytoplankton, and by supplying fast sinking food particles to benthic animal communities at the sea floor^{15,16}. However, this is to ignore that microbial mats were present in the oceans long before algal food became available. With the discovery of a motile lifestyle among the earliest branching Eumetazoa (Placozoa and Ctenophora⁴⁰), pervasive cyanobacterial mat coverage in well-oxygenated shallow water environments would have provided ample resources for metazoan proliferation. Yet, the vast majority of extant eumetazoan animals prefers a eukaryote-dominated diet; with rare exceptions, eumetazoans are not sustained by purely bacterial food sources^{41,42}. A preference for a eukaryotic diet may thus be the ancestral state of Eumetazoa, possible due to the high nutritional quality of algal biomass.

Based on sedimentological evidence²⁸ and biomarker data presented here, the Ediacara biota of the EEP inhabited well-mixed oxygenated shallow-water environments with levels of potential algal food supply comparable to the Phanerozoic. This observation in the White Sea area is consistent with a recent spatial analyses of ~570 Ma old Ediacaran ecosystems on the Avalon Peninsula, overlapping with the White Sea area taxonomically, that showed that competition for resources was not the driving factor for local Ediacaran communities⁴³. Unlike previously predicted^{17,19,20}, bacteria-dominated ecosystems in Ediacaran marine basins were generally not a cause of the unusual appearance and ecology of the Ediacara biota. Rather, the ecological and evolutionary bridge leading from a mid-Proterozoic bacteria-dominated world to the appearance of Phanerozoic animal-dominated ecosystems was paved with algae-rich environments akin to those preferred by modern eumetazoan animals. Although morphologically and possibly phylogenetically distinct from Phanerozoic animals, the large organisms of the Ediacara biota were a part of newly established nutrient and energy-rich environments that later hosted the Cambrian diversification of animal life.

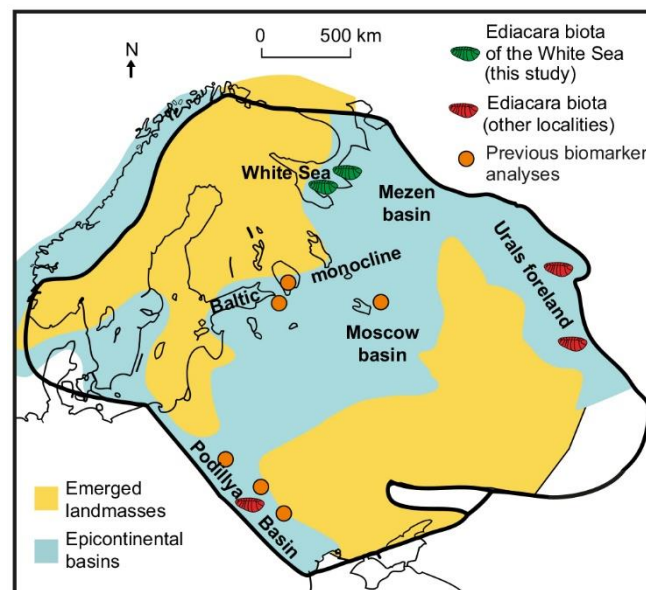


Fig. 1 – Map contrasting the fossil and biomarker localities of this (green) and previous (orange)¹⁷ studies; modified after Pehr, et al. ¹⁷ and Sliapura, et al. ⁴⁴

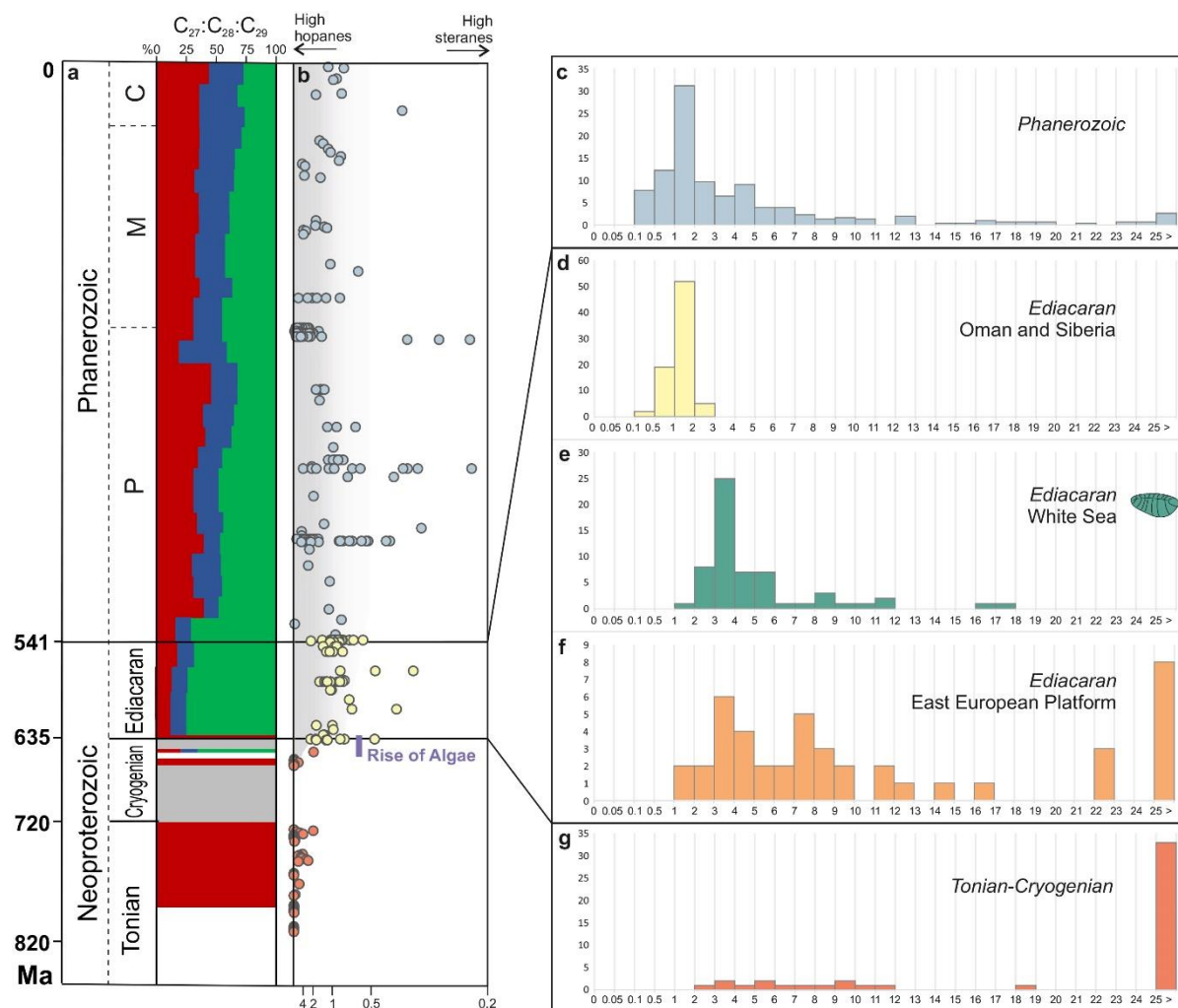


Fig. 2 – Timeline through the Neoproterozoic and Phanerozoic and abundance information for hopanes and steranes. **(a)** The relative abundance of the sterane homologues cholestane (C₂₇, green), ergostane (C₂₈, blue) and stigmastane (C₂₉, green). Size of the coloured areas reflects relative sterane abundances. **(b)** Evolution of the relative abundance of bacterial hopanes over eukaryotic steranes (H/S) through time (orange = Tonian and Cryogenian; yellow – Ediacaran (data from Oman and Siberia); blue = Phanerozoic); the scale goes from H/S ~ ∞ (with no steranes detected) to H/S = 0.25, converted from the S/H ratio values from 0 to 4 in Brocks et al.¹⁵ **(c)** to **(g)** Histograms showing the abundance distribution of H/S values for different periods and locations. Data from the EEP from Pehr, et al.¹⁷, data for the White Sea this study, all other data recalculated from Brocks, et al.¹⁵.

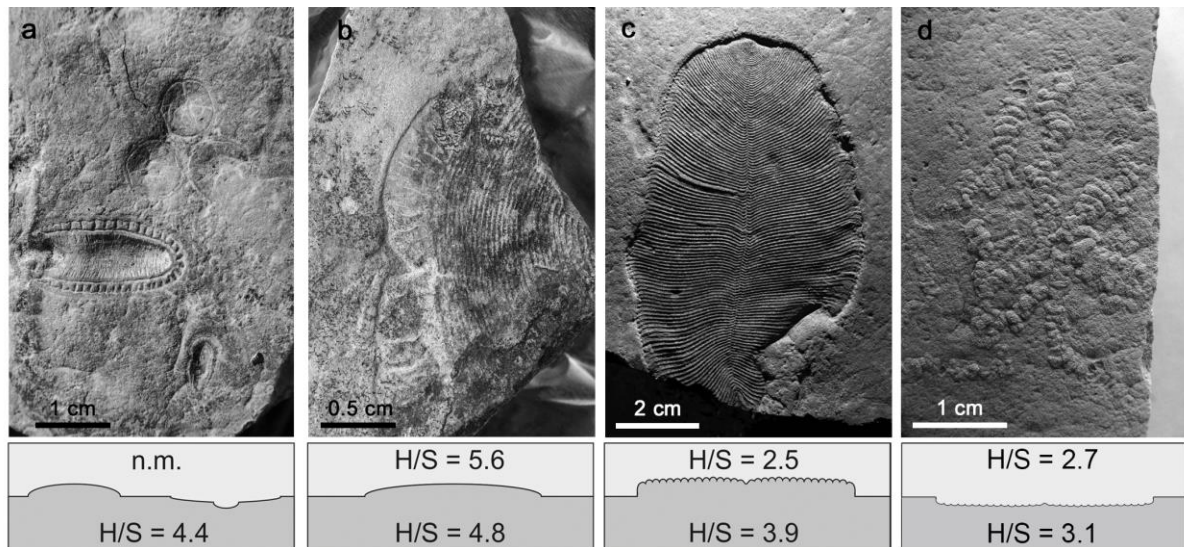


Figure 3 – Examples of Ediacaran macrofossils from the White Sea Area and associated H/S ratios from sediments immediately over- and underlying the fossils. **a**, *Aspidella* and *Kimberella* from the Z11(XXII) surface (Zimnie Gory, photo by E. Uryvaeva); **b**, *Andiva* from the Z1(1) surface (Zimnie Gory), the surface also contains *Archaeaspinus*, *Armilifera*, *Brachina*, *Charniodiscus*, *Cyanorus*, *Cyclomedusa*, *Dickinsonia*, *Inaria*, *Ivovicia*, *Kimberella*, *Onega*, *Paravendia*, *Parvancorina*, *Temnoxa*, *Tribrachidium*, *Yorgia*²⁷; **c**, *Dickinsonia* (Lyamtsa); **d**, *Palaeopascichnus* (Lyamtsa).

Methods

Sample collection

Samples were collected during fieldworks in the White Sea Region (Russia) in 2015-2017 specifically for biomarker analysis. Samples are coming from around 40 m thick stratigraphic interval of Lyamtsa and Arkhangelsk Beds (Ust-Pinega Formation, Redkino Regional Stage) in the Lyamtsa Ediacara biota locality, and from around 120 m thick interval of Vaysitsa, Zimnie Gory (Ust-Pinega Formation, Redkino Regional Stage) and Erga Beds (Mezen Formation, Kotlin Regional Stage) in the Zimnie Gory locality. Samples were collected avoiding weathered zones and cracks and were immediately wrapped in pre-baked aluminium foil (300°C, 9h) and packed in calico bags under strict avoidance of contamination.

Deposits in the Lyamtsa and Zimnie Gory localities of the Ediacara biota are mainly represented by clay and mm-scale heterolithic interlamination of clay, siltstone and sandstone, with occasional 0.5-10 cm, sometimes up to 60 cm thick sandstone lenses and layers. In the Zimnie Gory locality, nearly every siltstone and sandstone, including mm-thick lenses in the interlamination, has a microbial mat impression at the base; in Lyamtsa, these impressions are relatively rarer, and some surfaces are erosional. Fossils are typically preserved at the base of sandstone layers with microbial mat impressions, however some species are also sometimes found within clay^{23,45}. Samples include sediments immediately (within the first millimetres) underlying (clay) and overlying (typically sandstone) surfaces with Ediacara biota fossils, as well as 59 samples from sedimentary layers throughout the exposed sections that are not known to contain fossils. Ediacaran macroorganisms are found *in situ*, therefore biomarker composition of clays they were living on was taken as the closest approximation of environments the Ediacara biota inhabited. Sandstones overlying the fossils are mostly of storm origin²⁸ and would contain reworked organic matter deposited in the environments with the Ediacara biota, but might also contain material transported from other environments.

Sample preparation and extraction

Samples were prepared in an ultra-clean facility dedicated to trace biomarker analysis at the ANU. To identify and eliminate any surficial trace contaminants, the clay was analysed using the so-called Exterior-Interior protocol described in detail elsewhere⁴⁶⁻⁴⁸. Briefly, exterior ('E') 3-4 mm of the clay sample were removed using a micro drill (Dremel® 400 Series Digital, Mexico) with a combusted (290°C, 9 h) and solvent cleaned saw nozzle. Analysis of the last saw-blade solvent rinse confirmed that it was free of detectable contaminants. The exterior and the interior portions of the clay sample were ground to powder (>240 mesh) using a steel puck mill (Rocklabs Ltd., Onehunga, New Zealand). The mill was cleaned using dichloromethane and methanol, and by grinding combusted (600°C, 9 h) quartz sand. As the samples were collected from outcrops into aluminium foil and cotton bags, which has been proven to prevent contamination²³, for 10 samples both interior and exterior portions were analysed as control; for the rest, we analysed only interior portions, but exterior portions were kept in case there is any contamination in the analysed exterior portions or increased maturity parameters in these samples.

Bitumen was extracted from rock powder using an Accelerated Solvent Extractor (ASE 200, Dionex, USA) with DCM : methanol (9:1), reduced to 100 µl under a stream of nitrogen gas. All solvents used in the study were 99.9% grade (UltimAR®; Mallinckrodt Chemicals, St. Louis, MO, USA); all glassware was cleaned by combustion at 300°C for 9 h. An extract was then fractionated into saturated, aromatic and polar fractions using micro-column chromatography over annealed (300°C; 12 h) and dry packed silica gel (Silica Gel 60; 230– 600 mesh; EM Science). Saturated hydrocarbons were eluted with 1 dead volume (DV) of *n*-hexane, aromatic hydrocarbons with 4.5 DV of *n*-hexane : DCM (1 : 1) and the polar fraction with 3 ml DCM : methanol (1 : 1). An internal standard, 18-MEAME (18-methyleicosanoic acid methylester; Chiron Laboratories AS), was added to the saturated and aromatic fractions for quantification. The samples were analysed and quantified by GC–MS.

Gas chromatography–mass spectrometry (GC-MS)

GC-MS analyses were carried out on an Agilent 6890 gas chromatograph coupled to a Micromass Autospec Premier double sector mass spectrometer (Waters Corporation,

Milford, MA, USA). The GC was equipped with a 60 m DB-5 MS capillary column (0.25 mm i.d., 0.25 μm film thickness; Agilent JW Scientific, Agilent Technologies, Santa Clara, CA, USA), and helium was used as the carrier gas at a constant flow of 1 mL min⁻¹. Samples were injected in splitless mode into a Gerstel PTV injector at 60°C (held for 0.1 min) and heated at 260°C min⁻¹ to 300°C. For full-scan, selected ion recording (SIR) and metastable reaction monitoring (MRM) analyses, the GC oven was programmed from 60°C (held for 4 min) to 315°C at 4°C min⁻¹, with total run time of 100 min. All samples were injected in *n*-hexane to avoid deterioration of chromatographic signals by FeCl₂ build-up in the MS ion source through use of halogenated solvents⁴⁹. Steranes were quantified in MRM mode in M⁺ \rightarrow 217 and hopanes in M⁺ \rightarrow 191 transitions relative to the C₂₇ Tm hopane isomer content. The C₂₇ Tm hopane isomer content was quantified in a full-scan mode (*m/z* 191) relative to the 18-MEAME internal standard (*m/z* 340). Peak areas are uncorrected for differences in GC-MS response. Quantification errors were calculated as a function of a peak area established for the GC-MS used in this study²².

Laboratory system blanks

A comprehensive, accumulatory system blanks were performed covering all analytical steps including extraction, fractionation and instrumental analysis. For this purpose, a combusted (600°C, 9 h) sand was ground to powder and extracted using the methodologies and identical tools described above.

Supplementary Information

Syngeneity of biomarkers

GC-MS MRM, SIR and full-scan analyses of the comprehensive accumulatory laboratory system blanks confirmed that the detected hydrocarbons were not introduced by laboratory processes. Monitoring of the blanks yielded no *n*-alkanes, hopanes or steranes, even when measured using the most sensitive GC-MS MRM methods. The only contaminants detected in the blanks are trace amounts of phthalates—plasticizers present in small amounts in solvents used for extraction of biomarkers.

The high $\beta\alpha/(\beta\alpha + \alpha\beta)$ and low $T_s/(T_s + T_m)$ hopane isomer ratios, virtual absence of diasteranes and $\alpha\beta\beta$ sterane isomers^{22,23}, which are only found in the most immature sediments, indicate that the hydrocarbons in the Ediacaran deposits in the White Sea area are significantly below the oil-generative window, which means that the kerogen never thermally generated and expelled liquid hydrocarbons¹³. Such a low thermal maturity is never observed in contaminant petroleum products and migrated oils, which by their very nature must have a maturity within the oil generative window. This makes it very easy to track contamination by simply assessing the maturity parameters^{18,23}.

The results of Exterior/Interior (E/I) experiment for all analysed samples show nearly identical concentrations of all biomarkers in exterior and interior rock portions, with E/I values ranging from 0.75 to 2.35 for different compounds (Supplementary Table 2), which is within the range on natural variability within samples and indicates that the precombusted aluminium foil and clean calico bags prevented contamination of samples during transportation and storage, and confirm that all detected compounds are indigenous²³.

High hopane/sterane ratio values in the Ediacaran of the EEP

The unusually high H/S ratios reported from the interior of EEP have been interpreted as reflecting a strong predominance of bacteria among primary producers in the basin¹⁷, thus providing evidence for high heterogeneity in the distribution of major groups of photosynthetic organisms in the Ediacaran. However, while steroids and hopanoids have similar preservation potential in the sedimentary record due to the similarity of their structure⁵⁰, it cannot be completely excluded that these high H/S values may have been caused by severe bacterial degradation of eukaryotic biomass, causing replacement of algal sterols with hopanols from heterotrophic bacteria. An extreme case of such severe degradation in modern environments is, for instance, observed in soils, where primary plant debris may become so severely recycled by the soil microbiome that H/S rises to $\gg 10^{13,51,52}$. If this is the case, the local differences in H/S in the EEP are caused by different taphonomic conditions; if true, this would indicate that algae were already prevailing primary producers in the Late Ediacaran across the globe.

Locality	Regional stage	Beds	EB ¹	Sample	Lithology	H/S ²	C ₂₇ (%) ³	C ₂₈ (%) ⁴	C ₂₉ (%) ⁵	
Zimnie Gory	Kotlin	Erga		z2-16-5	thin interlamination ⁶	16.9 (0.0) ⁷	35.1 (0.4)	10.5 (0.2)	54.4 (0.7)	
				2-14-15	clay	2.6 (0.0)	28.5 (1.0)	13.8 (0.8)	57.8 (3.2)	
				z2-14-4	thin interlamination	5.4 (0.8)	15.4 (3.0)	11.7 (1.2)	72.9 (4.4)	
				z2-13-6	thin interlamination	3.5 (0.2)	20.4 (0.9)	13.1 (0.7)	66.5 (3.2)	
				z2-13-4	thin interlamination	4.9 (0.0)	23.6 (0.3)	11.1 (0.2)	65.3 (0.8)	
				z2-13-1	sandstone	11.2 (0.0)	23.7 (0.2)	14.5 (0.1)	61.7 (0.5)	
				z2-12-2	thin interlamination	5.0 (0.3)	21.5 (1.1)	12.5 (0.8)	65.9 (2.4)	
				z4-2-3	sandstone	5.6 (0.0)	38.0 (0.3)	9.7 (0.2)	52.3 (0.6)	
				z4-1-2	clay	4.8 (0.0)	23.4 (0.4)	9.6 (0.2)	67.0 (1.1)	
				z4-1-4	clay	5.6 (0.0)	27.7 (0.4)	8.7 (0.2)	63.5 (0.7)	
				z4-1-1	clay	4.8 (0.1)	23.4 (0.7)	9.6 (0.3)	67.0 (1.3)	
				z2-9-4	thin interlamination	4.4 (0.1)	19.2 (0.7)	8.9 (0.2)	72.0 (1.2)	
	z2-9-2	thin interlamination		5.5 (0.0)	29.8 (0.3)	10.8 (0.2)	59.4 (0.9)			
	z2-7-4B	thin interlamination		8.3 (0.0)	27.6 (0.1)	9 (0.0)	63.3 (0.6)			
	z2-7-4A	thin interlamination		8.8 (0.0)	27.3 (0.2)	8.2 (0.1)	64.5 (0.6)			
	z2-6-10	thin interlamination		4.3 (0.1)	21.0 (0.6)	8.6 (0.4)	70.4 (1.3)			
	z2-6-7	clay		3.5 (0.5)	11.8 (1.4)	9.4 (0.6)	78.8 (2.1)			
	z2-6-6	thin interlamination		4.5 (0.2)	22.6 (1.0)	10.2 (0.4)	67.2 (1.8)			
	z2-6-5	sandstone		8.6 (0.1)	22.0 (0.4)	12.7 (0.2)	65.3 (1.0)			
	z2-5-4	clay		17.5 (0.1)	32.6 (0.5)	13.1 (0.3)	54.3 (1.2)			
	z2-5-1	clay		8.0 (0.0)	28.2 (0.2)	9.0 (0.1)	62.8 (0.6)			
	z2-3-6	thin interlamination		10.1 (0.1)	22.2 (0.5)	10 (0.3)	67.8 (1.2)			
	z2-3-3	sandstone		11.6 (0.1)	21.3 (0.2)	11.2 (0.1)	67.5 (1.1)			
	z2-3-2	thin interlamination		3.9 (0.1)	19.5 (0.4)	10.8 (0.3)	69.7 (1.6)			
	z2-3-1	thin interlamination		5.8 (0.0)	21.7 (0.3)	11.1 (0.2)	67.1 (1.2)			
	z2-2-1	clay		5.9 (0.1)	9.9 (1.0)	5.7 (0.3)	84.4 (1.3)			
	z2-1-8	sandstone		3.3 (0.0)	12.7 (0.3)	10.3 (0.1)	76.9 (0.6)			
	z2-1-5	clay		3 (0.1)	11.1 (0.5)	7.7 (0.3)	81.2 (1.3)			
	z6-8-1	thin interlamination		6.8 (0.0)	36.2 (0.3)	10.5 (0.1)	53.3 (0.8)			
	z6-6-2	clay		1.7 (0.2)	18.5 (0.9)	9.7 (0.5)	71.9 (1.8)			
	z6-4-3	thin interlamination		3.3 (0.0)	13.3 (0.2)	10.3 (0.1)	76.4 (0.6)			
	z6-4-2	clay		3.6 (0.0)	11.9 (0.5)	9.4 (0.3)	78.7 (1.3)			
z6-1-1	clay	3.2 (0.0)	21.5 (0.3)	17.7 (0.2)	60.8 (1.2)					
Vaysitsa			z5-k1	sandstone	9.9 (0.1)	27.2 (0.8)	11.7 (0.2)	61.1 (2.5)		
Lyamtsa	Redkino	Lyamtsa		Arkhangelsk	31-3-3	clay	4.1 (0.0)	9.8 (0.0)	8.0 (0.0)	82.3 (0.0)
				31-1-6m	thin interlamination	3.7 (0.1)	11.2 (0.4)	7.7 (0.3)	81.1 (2.0)	
				31-1-5m	thin interlamination	3.0 (0.0)	13.1 (0.2)	9.1 (0.2)	77.9 (1.0)	
				35-4-3	clay	3.3 (0.0)	8.4 (0.2)	7.3 (0.2)	84.3 (0.9)	
				35-2-9m	sandstone	2.7 (0.0)	10.2 (0.2)	8.3 (0.2)	81.5 (1.4)	
				35-2-8m	thin interlamination	3.1 (0.0)	10.0 (0.2)	8.0 (0.2)	82.0 (1.1)	
				35-1-5m	thin interlamination	3.1 (0.0)	10.4 (0.2)	7.9 (0.1)	81.7 (0.9)	
				35-1-3m	thin interlamination	3.1 (0.0)	10.9 (0.2)	7.1 (0.2)	82.0 (1.1)	
				35-02-1m	thin interlamination	3.3 (0.0)	11 (0.2)	8.1 (0.1)	81.0 (1.0)	
				35-01-2m S	sandstone	2.3 (0.0)	11.3 (0.3)	8.6 (0.2)	80.1 (1.2)	
				35-01-1m	clay	3.3 (0.0)	10.8 (0.2)	8.1 (0.2)	81.2 (1.0)	
				D-Ly S	sandstone	2.5 (0.0)	11.7 (0.2)	8.6 (0.1)	79.7 (0.9)	
				D-Ly C	clay	3.9 (0.0)	9.7 (0.2)	7.9 (0.2)	82.4 (1.1)	
				34-5-4m	thin interlamination	3.1 (0.0)	10.3 (0.2)	8.0 (0.1)	81.7 (0.9)	
				34-4-4m	thin interlamination	3.1 (0.0)	10.6 (0.3)	8.1 (0.2)	81.3 (1.3)	
				34-4-2m	thin interlamination	3.4 (0.1)	12.2 (0.4)	8.2 (0.3)	79.6 (2.2)	
				34-5-2 in	clay	3.3 (0.0)	10.6 (0.3)	7.7 (0.2)	81.7 (1.2)	
				34-3-4m	thin interlamination	3.2 (0.0)	11.6 (0.3)	8.4 (0.2)	80.0 (1.4)	
				34-2-3m	thin interlamination	3.2 (0.0)	10.1 (0.3)	8.1 (0.2)	81.8 (1.2)	
				34-2-2m	sandstone	2.9 (0.0)	11.3 (0.2)	8.6 (0.2)	80.1 (1.1)	
34-01-MN in	thin interlamination	2.9 (0.0)	11.1 (0.3)	7.5 (0.2)	81.3 (1.5)					
34-01-2	clay	3.3 (0.0)	9.1 (0.2)	7.1 (0.1)	83.8 (0.8)					
34-01-7m	thin interlamination	2.5 (0.0)	11.2 (0.2)	8.3 (0.1)	80.5 (0.9)					

		34-01-6m	thin interlamination	3.0 (0.0)	9.9 (0.0)	7.7 (0.0)	82.4 (0.0)
--	--	----------	----------------------	-----------	-----------	-----------	------------

Supplementary Table 1. Relative distribution of hopanes and steranes in the White Sea area

Ediacaran deposits in stratigraphic order, ¹EB – intervals with the Ediacara biota; ²H/S = $\Sigma(C_{27-35} \text{ hopanes}) / \Sigma(C_{27-29} \text{ steranes})$, hopanes: $C_{27} = \Sigma(Ts, Tm, \beta)$, $C_{29} = \Sigma(\alpha\beta, Ts, \beta\alpha)$, $C_{30} = \Sigma(\alpha\beta, \beta\alpha)$, $C_{31-35} = \Sigma(\alpha\beta-22(S+R), \beta\alpha)$, $\alpha\beta = 17\alpha(H)21\beta(H)$, $\beta\alpha = 17\beta(H)21\alpha(H)$; steranes: $C_{27} = \Sigma(\beta\alpha-20(S+R)\text{-diacholestane, } \alpha\alpha\alpha\text{- and } \beta\alpha\alpha\text{-}20(S+R)\text{-cholestane})$, $C_{28} = \Sigma(\beta\alpha-20(S+R)\text{-diaergostane, } \alpha\alpha\alpha\text{- and } \beta\alpha\alpha\text{-}20(S+R)\text{-ergostane})$, $C_{29} = \Sigma(\beta\alpha-20(S+R)\text{-diastigmastane, } \alpha\alpha\alpha\text{- and } \beta\alpha\alpha\text{-}20(S+R)\text{-stigmastane})$, $\alpha\alpha\alpha = 5\alpha(H), 14\alpha(H), 17\alpha(H)$, $\beta\alpha\alpha = 5\beta(H), 14\alpha(H), 17\alpha(H)$; ³ $C_{27} (\%) = 100 * C_{27} \text{ steranes} / \Sigma(C_{27-29} \text{ steranes})$; ⁴ $C_{28} (\%) = 100 * C_{28} \text{ steranes} / \Sigma(C_{27-29} \text{ steranes})$; ⁵ $C_{29} (\%) = 100 * C_{29} \text{ steranes} / \Sigma(C_{27-29} \text{ steranes})$; ⁶thin interlamination of clay, siltstone and sandstone; ⁷numbers in parentheses are standard deviation values, value 0.0 indicates that the standard deviation is less than 0.05; light-green colour highlights samples immediately above and below horizons with fossils (marked with dark-green horizontal lines).

Sample	E/I ¹				Maturity parameters			
	Hopanes	C ₂₇ steranes	C ₂₈ steranes	C ₂₉ steranes	Dia/Reg I ²	Dia/Reg E ³	Mor/Hop I ⁴	Mor/Hop E ⁵
z4-1-2	1.04 (0.01)	0.97 (0.03)	1.13 (0.04)	0.92 (0.02)	0.04 (0.00)	0.05 (0.00)	0.33 (0.01)	0.33 (0.01)
z6-4-2	0.75 (0.01)	0.76 (0.03)	0.79 (0.04)	0.78 (0.03)	0.04 (0.00)	0.05 (0.01)	0.33 (0.01)	0.32 (0.02)
z6-8-1	1.54 (0.02)	2.35 (0.07)	1.56 (0.05)	1.6 (0.03)	0.21 (0.00)	0.14 (0.00)	0.23 (0.01)	0.31 (0.01)
z6-4-3	1.07 (0.03)	1.35 (0.12)	1.33 (0.12)	1.14 (0.06)	0.20 (0.00)	0.18 (0.00)	0.23 (0.01)	0.22 (0.01)
31-3-3	0.90 (0.02)	1.37 (0.09)	1.19 (0.08)	1.05 (0.04)	0.05 (0.02)	0.05 (0.01)	0.27 (0.02)	0.26 (0.02)
35-01-2m	0.83 (0.01)	0.82 (0.02)	0.79 (0.02)	0.71 (0.01)	0.05 (0.00)	0.05 (0.00)	0.26 (0.01)	0.25 (0.01)
34-5-2	1.12 (0.02)	1.90 (0.12)	2.04 (0.14)	1.28 (0.05)	0.04 (0.01)	0.06 (0.00)	0.30 (0.01)	0.26 (0.01)
34-2-3m	0.67 (0.01)	0.80 (0.02)	0.77 (0.02)	0.71 (0.01)	0.05 (0.00)	0.06 (0.00)	0.31 (0.01)	0.26 (0.02)
34-01-MN	0.94 (0.01)	1.05 (0.05)	1.04 (0.04)	1.05 (0.02)	0.05 (0.00)	0.05 (0.00)	0.25 (0.01)	0.25 (0.01)

Supplementary Table 2. Results of the ‘Exterior/Interior’ experiments for hopanes and steranes in selected samples, ¹relative proportion of a compound concentrations in the exterior and the interior portions of a sample; ²Dia/Reg I – proportion of diastigmastanes of the total stigmastanes in the interior portions; ³Dia/Reg E – proportion of diastigmastanes of the total stigmastanes in the exterior portions; ⁴Mor/Hop I - proportion of $\beta\alpha$ (moretan) of the total C₂₇ hopanes in the interior portions; ⁵Mor/Hop E - proportion of $\beta\alpha$ (moretan) of the total C₂₇ hopanes in the exterior portions.

References

- 1 Nursall, J. Oxygen as a prerequisite to the origin of the Metazoa. *Nature* **183**, 1170 (1959).
- 2 Reinhard, C. T., Planavsky, N. J., Olson, S. L., Lyons, T. W. & Erwin, D. H. Earth's oxygen cycle and the evolution of animal life. *Proceedings of the National Academy of Sciences* **113**, 8933-8938, doi:10.1073/pnas.1521544113 (2016).
- 3 Knoll, A. H. in *Origin and Early Evolution of the Metazoa* (eds Jere H. Lipps & Philip W. Signor) 53-84 (Springer US, 1992).
- 4 Canfield, D. E., Poulton, S. W. & Narbonne, G. M. Late-Neoproterozoic deep-ocean oxygenation and the rise of animal life. *Science* **315**, 92-95 (2007).
- 5 Mills, D. B. & Canfield, D. E. Oxygen and animal evolution: Did a rise of atmospheric oxygen "trigger" the origin of animals? *BioEssays* **36**, 1145-1155 (2014).
- 6 Butterfield, N. J. Animals and the invention of the Phanerozoic Earth system. *Trends in Ecology & Evolution* **26**, 81-87, doi:<https://doi.org/10.1016/j.tree.2010.11.012> (2011).
- 7 Butterfield, N. J. Oxygen, animals and oceanic ventilation: an alternative view. *Geobiology* **7**, 1-7, doi:doi:10.1111/j.1472-4669.2009.00188.x (2009).
- 8 Lyons, T. W., Reinhard, C. T. & Planavsky, N. J. The rise of oxygen in Earth's early ocean and atmosphere. *Nature* **506**, 307-315, doi:10.1038/nature13068 (2014).
- 9 Mills, D. B. *et al.* Oxygen requirements of the earliest animals. *Proceedings of the National Academy of Sciences* **111**, 4168-4172 (2014).
- 10 Gingras, M. *et al.* Possible evolution of mobile animals in association with microbial mats. *Nat. Geosci.* **4**, 372 (2011).
- 11 Olson, S. L., Kump, L. R. & Kasting, J. F. Quantifying the areal extent and dissolved oxygen concentrations of Archean oxygen oases. *Chemical Geology* **362**, 35-43 (2013).
- 12 Brocks, J. J. *et al.* Early sponges and toxic protists: possible sources of cryostane, an age diagnostic biomarker antedating Sturtian Snowball Earth. *Geobiology* **14**, 129-149, doi:10.1111/gbi.12165 (2016).
- 13 Peters, K. E., Walters, C. C. & Moldowan, J. M. *The biomarker guide*. Vol. 2 (Cambridge University Press, 2005).
- 14 Knoll, A. H., Summons, R. E., Waldbauer, J. R. & Zumberge, J. E. The Geological Succession of Primary Producers in the Oceans. 133-163, doi:10.1016/b978-012370518-1/50009-6 (2007).
- 15 Brocks, J. J. *et al.* The rise of algae in Cryogenian oceans and the emergence of animals. *Nature* **548**, 578 (2017).
- 16 Brocks, J. J. The transition from a cyanobacterial to algal world and the emergence of animals. *Emerging Topics in Life Sciences* **2**, 181-190 (2018).
- 17 Pehr, K. *et al.* Ediacara biota flourished in oligotrophic and bacterially dominated marine environments across Baltica. *Nature communications* **9**, 1807 (2018).
- 18 Goryl, M., Marynowski, L., Brocks, J. J., Bobrovskiy, I. & Derkowski, A. Exceptional preservation of hopanoid and steroid biomarkers in Ediacaran sedimentary rocks of the East European Craton. *Precambrian Research* **316**, 38-47, doi:<https://doi.org/10.1016/j.precamres.2018.07.026> (2018).
- 19 Kaufman, A. J. in *Chemostratigraphy Across Major Chronological Boundaries* Vol. 240 (eds A.N. Sial, C. Gaucher, Muthuvairavasamy Ramkumar, & V.P. Ferreira) 115-142 (2018).

- 20 Sperling, E. A. & Stockey, R. G. The Temporal and Environmental Context of Early Animal Evolution: Considering All the Ingredients of an “Explosion”. *Integrative and Comparative Biology* **58**, 605-622 (2018).
- 21 Dufour, S. C. & McIlroy, D. Ediacaran pre-placozoan diploblasts in the Avalonian biota: the role of chemosynthesis in the evolution of early animal life. *Geological Society, London, Special Publications* **448**, 211-219 (2017).
- 22 Bobrovskiy, I. *et al.* Ancient steroids establish the Ediacaran fossil *Dickinsonia* as one of the earliest animals. *Science* **361**, 1246-1249, doi:10.1126/science.aat7228 (2018).
- 23 Bobrovskiy, I., Hope, J. M., Krasnova, A., Ivantsov, A. & Brocks, J. J. Molecular fossils from organically preserved Ediacara biota reveal cyanobacterial origin for *Beltanelliformis*. *Nature Ecology & Evolution*, doi:10.1038/s41559-017-0438-6 (2018).
- 24 Grazhdankin, D. Patterns of distribution in the Ediacaran biotas: facies versus biogeography and evolution. *Paleobiology* **30**, 203-221, doi:10.1666/0094-8373(2004)030<0203:PODITE>2.0.CO;2 (2004).
- 25 Fedonkin, M., Ivantsov, A. Y., Leonov, M. & Serezhnikova, E. in *The rise and fall of the Vendian (Ediacaran) biota. Origin of the modern biosphere. Transact. Int. Conf. on the IGCP project.* 6-9.
- 26 Martin, M. W. *et al.* Age of Neoproterozoic bilaterian body and trace fossils, White Sea, Russia: Implications for metazoan evolution. *Science* **288**, 841-845 (2000).
- 27 Ivantsov, A. Y. Unique natural world heritage - Zimnie Gory locality of the impressions of the Vendian multicellular animals. *Geolog Ukrainy*, 89-98 (2011).
- 28 Grazhdankin, D. Structure and depositional environment of the Vendian Complex in the southeastern White Sea area. *Stratigraphy and Geological Correlation* **11**, 313-331 (2003).
- 29 Sokolov, B. in *Proceedings of the IPU, International Geological Congress.* 79-86.
- 30 Moczyłowska, M., Westall, F. & Foucher, F. Microstructure and biogeochemistry of the organically preserved Ediacaran metazoan Sabellidites. *Journal of Paleontology* **88**, 224-239 (2014).
- 31 Gueneli, N. *et al.* 1.1-billion-year-old porphyrins establish a marine ecosystem dominated by bacterial primary producers. *Proceedings of the National Academy of Sciences* **115**, E6978-E6986 (2018).
- 32 Hoshino, Y. *et al.* Cryogenian evolution of stigmasteroid biosynthesis. *Science advances* **3**, e1700887 (2017).
- 33 van Maldegem, L. M. *et al.* Bisnorgammacerane traces predatory pressure and the persistent rise of algal ecosystems after Snowball Earth. *Nature Communications* **10**, 476, doi:10.1038/s41467-019-08306-x (2019).
- 34 Kodner, R. B., Pearson, A., Summons, R. E. & Knoll, A. H. Sterols in red and green algae: quantification, phylogeny, and relevance for the interpretation of geologic steranes. *Geobiology* **6**, 411-420, doi:10.1111/j.1472-4669.2008.00167.x (2008).
- 35 Seilacher, A. Biomat-related lifestyles in the Precambrian. *Palaios* **14**, 86-93 (1999).
- 36 Gehling, J. G. & Droser, M. L. Textured organic surfaces associated with the Ediacara biota in South Australia. *Earth-Science Reviews* **96**, 196-206, doi:10.1016/j.earscirev.2009.03.002 (2009).
- 37 Butterfield, N. J. Oxygen, animals and aquatic bioturbation: An updated account. *Geobiology* **16**, 3-16 (2018).

- 38 Lenton, T. M. & Daines, S. J. The effects of marine eukaryote evolution on phosphorus, carbon and oxygen cycling across the Proterozoic–Phanerozoic transition. *Emerging Topics in Life Sciences*, ETLS20170156, doi:10.1042/etls20170156 (2018).
- 39 Nettersheim, B. J., Brocks, J.J., Schwelm, A., Hope, J.M., Not, F., Lomas, M., Schmidt, C., Schiebel, R., Nowack, E.C.M., De Deckker, P., Pawlowski, J., Bowser, S.S., Bobrovskiy, I., Zonneveld, K., Kucera, M., Stuhr, M., Hallmann, C. . Putative sponge biomarkers in unicellular Rhizaria question an early rise of animals. *Nature Ecology & Evolution* (in press).
- 40 Simion, P. *et al.* A large and consistent phylogenomic dataset supports sponges as the sister group to all other animals. *Current Biology* **27**, 958-967 (2017).
- 41 Cruz-Rivera, E. & Paul, V. J. Feeding by coral reef mesograzers: algae or cyanobacteria? *Coral Reefs* **25**, 617-627 (2006).
- 42 Cruz-Rivera, E. & Paul, V. in *Proc 9th Int Coral Reef Symp.* 515-520.
- 43 Mitchell, E. G. & Kenchington, C. G. The utility of height for the Ediacaran organisms of Mistaken Point. *Nature Ecology and Evolution* (2018). DOI: 10.1038/s41559-018-0591 6 (2018).
- 44 Sliupa, S., Fokin, P., Lazauskiene, J. & Stephenson, R. A. The Vendian-Early Palaeozoic sedimentary basins of the East European Craton. *Geological Society, London, Memoirs* **32**, 449-462 (2006).
- 45 Ivantsov, A. Y., Gritsenko, V. P., Konstantinenko, L. I. & Zakrevskaya, M. A. Revision of the problematic Vendian macrofossil Beltanelliformis (=Beltanelloides, Nemiana). *Paleontological Journal* **48**, 1415-1440, doi:10.1134/s0031030114130036 (2014).
- 46 Brocks, J. J., Grosjean, E. & Logan, G. A. Assessing biomarker syngeneity using branched alkanes with quaternary carbon (BAQCs) and other plastic contaminants. *Geochimica et Cosmochimica Acta* **72**, 871-888, doi:10.1016/j.gca.2007.11.028 (2008).
- 47 Schinteie, R. & Brocks, J. J. Evidence for ancient halophiles? Testing biomarker syngeneity of evaporites from Neoproterozoic and Cambrian strata. *Organic Geochemistry* **72**, 46-58, doi:10.1016/j.orggeochem.2014.04.009 (2014).
- 48 Jarrett, A. J. M., Schinteie, R., Hope, J. M. & Brocks, J. J. Micro-ablation, a new technique to remove drilling fluids and other contaminants from fragmented and fissile rock material. *Organic Geochemistry* **61**, 57-65, doi:10.1016/j.orggeochem.2013.06.005 (2013).
- 49 Brocks, J. J. & Hope, J. M. Tailing of Chromatographic Peaks in GC–MS Caused by Interaction of Halogenated Solvents with the Ion Source. *Journal of Chromatographic Science* **52**, 471-475, doi:10.1093/chromsci/bmt068 (2014).
- 50 Peters, K., Walters, C. & Moldowan, J. *The Biomarker Guide. Volume 2. Biomarkers and Isotopes in Petroleum Systems and Earth History.* 2nd edn, (Cambridge University Press, 2005).
- 51 Ries-Kautt, M. & Albrecht, P. Hopane-derived triterpenoids in soils. *Chemical Geology* **76**, 143-151 (1989).
- 52 Moldowan, J. M., Seifert, W. K. & Gallegos, E. J. Relationship between petroleum composition and depositional environment of petroleum source rocks. *AAPG bulletin* **69**, 1255-1268 (1985).

CONCLUSIONS

THESIS ACHIEVEMENTS

The thesis presents an entirely new approach to studying the enigmatic Ediacara biota, using biomarkers extracted from organically preserved macrofossils. While morphology alone had not been sufficient to make the final decision on the phylogenetic position of many Ediacaran organisms, biomarkers may provide in some cases the deciding information. Thus, *Beltanelliformis* produced hopanoids and long-chain *n*-alkanes with odd-over-even predominance, revealing that they were large spherical colonies of cyanobacteria. *Dickinsonia* and its morphological relatives solely produced cholesteroloids, which places these iconic members of the Ediacara biota among the oldest confirmed macroscopic animals in the rock record. Analysis of the lipid gut content of *Kimberella* and *Calyptrina* showed that they shared a diet of green algae and bacteria, contradicting previous suggestions that Ediacaran tube worms were chemosymbiotic. At the same time, lack of traces of dietary molecules in *Dickinsonia* indicates that these organisms did not possess a digestive system, and instead fed on microbial mats using external digestion.

The thesis shows that fossilization of Ediacaran organisms was promoted by unusually prolonged conservation of organic matter, coupled with differences in rheological behaviour of the over- and underlying sediments. In contrast to accepted models, cementation of overlying sand was not critical for fossil preservation, which is supported by the absence of cement in unweathered White Sea specimens and observations of soft sediment deformation in South Australian specimens. The rheological model implies that Ediacaran fossils do not necessarily reflect the external shape of the organism, but the morphology of a soft external or internal organic 'skeleton'. This model does not only explain all features observed in the Ediacara biota fossils, but also has been confirmed by laboratory simulations, which created Ediacaran-like impressions for the first time. The rheological mechanism provides new constraints on biological interpretations of the Ediacara biota.

Analysis of biomarkers from the Ediacaran deposits in the White Sea Area revealed high relative abundances of algal steranes over bacterial hopanes, suggesting that the Ediacara biota

inhabited nutrient replete environments with an abundance of algal food sources comparable to Phanerozoic ecosystems. Thus, organisms of the Ediacara biota inhabited nutrient and carbon-rich environments akin to those fuelling the Cambrian explosion.

Analysis of variations of biomarker parameters in Ediacaran deposits, Ediacaran macroalgae and modern algae showed that they can be strongly altered during microbial degradation.

FUTURE RESEARCH

The new technique of analysing biomarkers from individual fossils developed as part of my PhD is quite revolutionary for the studies of ancient life, bringing together palaeontology and biomarker research. The two discoveries, published in *Nature Ecology & Evolution* and *Science* in one year, highlight the breakthrough nature of this approach. Yet, there are more organically preserved strange Ediacaran creatures to be uncovered, such as fractal-shaped rangeomorphs.

The method goes further than the biological origins of ancient organisms. For example, biomarkers are able to detect the presence of a gut in some of these organisms, and allow to see the lipid composition not only of the organism, but also of its gut content. When combined with carbon stable isotope data, biomarkers can in theory not only distinguish dietary preferences of ancient animals, but also establish which trophic levels the animals occupied in their ecosystem. Thus, the method opens an entirely new dimension in the study of ancient macroscopic life, starting in the Ediacaran where it used to be notoriously difficult to distinguish organisms even at the domain level.

The new preservation model for the Ediacara biota has an enormous impact on our understanding of both biology and ecology of the oldest macroscopic organisms in the fossil record. It constrains our understanding of the morphology of these organism, and it helps to predict where and under what conditions Ediacaran organism become preserved. Thus, this model provides a new baseline for future studies of the Ediacara biota. New findings on the taphonomy of biomarkers presented in this thesis provide constrains on how biomarkers can be applied as a tool in the future.

CHAPTER 6. RECONSIDERING THE USE OF MOLECULAR FOSSILS AS A PALAEOECOLOGICAL INDICATOR

The White Sea area in Russia records a range of depositional palaeoenvironments that contain fossils of the Ediacara biota. It also records variable communities of Ediacaran macroorganisms, and it has been suggested that different communities preferentially inhabited different environments. Finally, throughout the entire section and across environments, it records biomarkers with large-scale variabilities in parameters that are classically interpreted as ecological proxies, such as the sterane/hopane ratio. In principle, correlations between biomarkers, fossils and environments could provide additional information on the palaeoecology of different Ediacara biota communities. However, a close statistical examination of these phenomena shows that variations of biomarker parameters are mainly controlled by the extent of heterotrophic microbial reworking of organic matter. Looking deeper into the processes of microbial alteration of biomarker parameters, this chapter presents new constraints on the general use of biomarkers as palaeoecological indicators, and an outlook how taphonomic and ecological constraints of biomarker ratios may eventually be resolved.



Australian
National
University

Statement of Contribution

This thesis is submitted as a Thesis by Compilation in accordance with https://policies.anu.edu.au/ppl/document/ANUP_003405

I declare that the research presented in this Thesis represents original work that I carried out during my candidature at the Australian National University, except for contributions to multi-author papers incorporated in the Thesis where my contributions are specified in this Statement of Contribution.

Title and authors: Bobrovskiy, I., Poulton, S. W., Hope, J. M., Brocks, J. J. Reconsidering the use of steroids and hopanoids as a palaeoecological indicator

Current status of paper: **Not Yet Submitted**/Submitted/Under Revision/Accepted/Published

Contribution to paper: _____

Senior author or collaborating authors endorsement: I.B. conceived the study, collected samples, did experiments and analyses, and interpreted the data; S.P. provided facilities for inorganic geochemistry analyses and advise on interpretations, J.M.H. helped with biomarker analysis; I.B. wrote the manuscript, with contributions from all authors.

Ilya Bobrovskiy

Candidate – Print Name

[Signature]

Signature

18/04/2019

Date

Endorsed

Jochen Brocks

Chair of Supervisory Panel – Print Name

[Signature]

Signature

18/04/2019

Date

Stewart Falla

Delegated Authority – Print Name

[Signature]

Signature

29/04/2019

Date

A new understanding of sterane and hopane biomarker parameters for ecological reconstructions

Ilya Bobrovskiy^{1*}, Simon W. Poulton², Janet M. Hope¹, Jochen J. Brocks^{1*}

¹Research School of Earth Sciences, Australian National University, Canberra, ACT 2601, Australia

²School of Earth and Environment, University of Leeds, Leeds, LS2 9JT, UK

*Correspondence to: ilya.bobrovskiy@anu.edu.au, jochen.brocks@anu.edu.au

Biomarkers are the remains of organic molecules of biological origin that are stable over geological timescales. They comprise a unique tool for palaeoecological reconstructions throughout Earth history. Two of the most commonly used biomarker parameters are the relative proportion of steranes and hopanes ($S/(S+H)$), which has been used to quantify the relative input of eukaryotic versus bacterial biomass into sediments, and the sterane tritacta ratio (the relative abundance of C_{27} , C_{28} and C_{29} steranes), which depends on the most prominent groups of eukaryotes in an environment. Here we show that the $S/(S+H)$ ratio, sterane distributions and the majority of sterane and hopane based maturity parameters are closely interlinked with the extent of degradation and oxygen exposure. Based on both modern and ancient examples, we show that even in normal marine environments, these parameters may be affected by microbial degradation to the extent that ecological information is nearly obliterated. These results provide a major constraint on the interpretation of steroids and hopanoids for palaeoecological reconstruction, but provide an opportunity to evaluate degradation effects on biomarker distributions in both recent and ancient environments.

INTRODUCTION

Most of our knowledge of the history of life on Earth has been obtained from body fossils that yield a continuous record of the evolution and diversification of some groups of organisms. However, this record is incomplete, as only a fraction of lifeforms are preserved as fossils. Particularly limited is our understanding of the base of the marine foodweb, the evolutionary trajectory, and the ecological importance of different photosynthetic primary producers in the oceans through time (1). Algae and phototrophic bacteria without external skeleton are rarely fossilized, and even if they are, their relative abundance in the rock record does not reflect their contribution to primary production. This is due to an extreme taphonomic bias that affects the relative preservation of different types of organisms. However, there is a complementary record that is used to extract at least semi-quantitative information about biological sources in modern and ancient sedimentary settings: molecular fossils, or biomarkers.

Biomarkers are organic molecules that have a specific biological origin and can be preserved in sedimentary rocks going back to the Palaeoproterozoic. They include biological lipids, pigments, fragments of macromolecules such as algal cell wall material, and diagenetic products of these compounds. Some of the most commonly employed biomarkers derive from sterols, which are membrane lipids of most eukaryotes, and hopanols produced by many bacteria. Alteration of sterols and hopanols by biological and chemical processes starts at the moment of death of an organism and continues throughout the history of the molecules, from transition through the water column and deposition in sediments, to deep burial in the rock record (2, 3). During these processes, biological sterols and hopanols are transformed into saturated hydrocarbon steranes (S) and hopanes (H), and aromatic steroids and hopanoids. The relative abundance of steranes and hopanes, expressed as the ratio $S/(S+H)$, is regarded as a measure of the relative flux of eukaryotic versus bacterial organic matter to bottom sediments, while the proportion of steranes with different side chain alkylation, such as the relative abundance of C_{27} , C_{28} and C_{29} steranes, is commonly used as an indicator of changes in the organic matter flux from different groups of eukaryotes (1, 3-5).

Sterane and hopane abundances, and those of their alteration products, including different stereo- and structural isomers, are also routinely used in petroleum studies to obtain information about source rock characteristics when analysing oils from reservoirs, seeps and spills. For instance, sterane trifecta and $S/(S+H)$ ratios are used to estimate the age of oils, allowing assignment to Palaeozoic, Mesozoic and Cenozoic sources, as well as for oil-source correlations (3, 6). Maturity parameters based on ratios between more and less thermally stable isomers, are used to establish the thermal history of source rocks and to estimate their oil generation potential (3). Some isomer ratios in oils yield further information about source rock properties, such as the proportion of diasteranes to regular steranes, which depends on the clay and carbonate content (3).

However, it has also been noted that most biomarker proxies are affected by more than one factor. For example, sterols in primary plant debris in soil may become so extensively recycled by the soil microbiome that $S/(S+H)$ may drop from 1.0 to $\ll 0.1$ (3, 7, 8). By contrast, this effect is commonly considered minimal in marine environments, where both $S/(S+H)$ and the relative abundance of C_{27} , C_{28} and C_{29} steranes are believed to be a robust reflection of the primary product. However, there has been little study of the extent, and under what conditions, these ratios are affected by microbial degradation and diagenesis (9).

It is also known that traditional maturity indicators may be driven by factors other than thermal history (10-14). In some instances, stronger isomerisation of steroids and hopanoids has been reported in apparently more oxic environments (10), while in other cases isomerisation appears to be elevated in anoxic, organic-rich samples (13). However, the conditions that drive sterane and hopane isomerisation in such instances are poorly constrained.

To elucidate the control of redox and degradation on sterane and hopane biomarker parameters, we chose a system where the thermal maturity and source of primary organic matter remained constant: 14 specimens of organically preserved macroalgae from thermally immature siliciclastic rocks of late Ediacaran age (558 Ma) in the White Sea area. The Ediacaran age ensures the absence of a significant terrestrial biomarker component, as well as an absence of bioturbation, as complicating factors. To place the results into context, we

also performed a series of laboratory degradation experiments on extant macroalgae and higher plants under varying conditions.

RESULTS

Biomarker composition of Ediacaran macroalgae

The White Sea area in Russia preserves thermally immature Ediacaran deposits (15) that formed in shallow-water marine environments at the edge of an intracratonic sea (16). Although the sea waters were well-mixed and sufficiently oxygenated to sustain macroscopic benthic bilaterians (17), biomarkers are well-preserved throughout the entire section, including storm-deposited sandstone layers (18). This can be attributed to anoxic conditions that quickly developed in the sediments, likely owing to the rapid growth of microbial mats that sealed the sediments from oxidant diffusion from the overlying water column. These conditions allowed for organic preservation of Ediacaran macrofossils (19, 20) and, in some layers, abundant macroalgae as carbonaceous compressions (15, 21).

We analysed biomarkers extracted with organic solvents from 14 macroalgae, all derived from a single 2 m-thick layer, which included one specimen of the genus *Archyfasma* (Fig. S1A), two specimens of bush-like bifurcating ex.gr. *Vendotaenides* (Fig. S1B), and eleven unidentifiable organic films that are identical in thickness and colour to macroalgae, but distinct from organic films derived from bacterial colonies and Ediacara biota fossils from the same locality (15, 18, 19). Correlations between different biomarker parameters of the macroalgae extracts are summarized in Fig. 1 and Table S1. The macroalgae demonstrate continuous distribution of sterane trifacta values with stigmastanes (C₂₉) comprising 47% to 91% of total trifacta steranes. Similarly, S/(S+H) ranges from 0.19 to 0.98 and 5 β /5 α sterane isomer values from 0.49 to 3.93 (Fig. 1, Table S2). Notably, all these parameters strongly correlate with each other. As 5 β /5 α changes from 3.93 to 0.49, the proportion of steranes over hopanes drops by a factor of 40, and the proportion of C₂₉ steranes in the steroid trifacta by a factor of ~2 (Fig. 1B, Table S2). At the same time, the overall yield of steranes and hopanes extracted from the algal biomass ([S+H] in μ g/g OM) decreases by a factor of 80 (Fig. 1B, Table S2). The only macroalga that does not follow this relationship is *Archifasma*, which demonstrates high S/(S+H) and 5 β /5 α values, but a relatively low stigmasteroid proportion (C₂₇ : C₂₈ : C₂₉ = 37% : 2% : 61%).

The strong correlations between biomarker concentrations from algal organic matter ([S+H]), sterane 5 β /5 α ratios, S/(S+H), and sterane trifacta ratios in the Ediacaran macroalgae implies that there is a single dominant factor controlling all these parameters. Thermal maturity can be excluded as a factor as all algae were collected from the same layer, and changes in primary biological input are unlikely because of the homogenous sample set of algal macrofossils and the continuous variations of ecological and diagenetic parameters. Also excluded are mineral surface effects, such as clay catalysis, as the biomarkers were extracted from organically preserved fossils. A strong contender, however, are redox conditions. Sterane 5 β /5 α ratios, which are at the centre of the network diagram (Fig. 1) are known to be controlled by redox (22-24), and the wide range of 5 β /5 α values reflects that the macroalgae had different diagenetic histories. Usually, the 'abiological' mechanism for the formation of 5 β and 5 α sterane isomers from sterol precursors goes through Δ^5 sterenes, which isomerise into Δ^4 sterenes at a constant proportion of $\Delta^5 / \Delta^4 = 0.64$ (22). As Δ^5 sterenes are the

precursors of 5β steranes, and Δ^4 yield 5α isomers, the most common $5\beta/5\alpha$ value in sedimentary rocks is ~ 0.6 (22). This is also the value characteristic of the Ediacaran White Sea area deposits (18), and is close to the lowest ratio observed in the analysed macroalgae (Fig. 1). The $5\beta/5\alpha$ values > 0.6 in most macroalgae indicate that there was an additional source of 5β steroids, derived through microbially-mediated conversion of sterols into 5β -stanols, and this process only proceeds under anoxic conditions (22-24). Consequently, elevated $5\beta/5\alpha$ values are indicative of anoxic diagenetic conditions such as those that developed in the decomposing bodies of the Ediacaran animal *Dickinsonia* (18). Thus, those macroalgae that demonstrate the highest $5\beta/5\alpha$ values must have experienced the lowest exposure to oxygen, for instance through quick burial and rapid onset of anoxic conditions, while the macroalgae with the lowest $5\beta/5\alpha$ values experienced maximal oxygen exposure during degradation.

Based on their strong correlation with the $5\beta/5\alpha$ ratio, both $S/(S+H)$ and the sterane tritacta ratio in the macroalgae are likely also controlled by the extent of oxygen exposure during degradation, shifting $S/(S+H)$ and C_{29} sterane proportions towards lower values. The oxic degradation of macroalgae was also accompanied by a massive loss of lipids, which can be observed in the drop of $[S+H]$ by a factor of 80 from the least to the most degraded alga (Fig. 1B). All analysed macroalgae, except *Archifasma*, initially contained little or no hopanoids and had similar steroid compositions, close to those in the specimens with highest $S/(S+H)$ and $5\beta/5\alpha$ values ($C_{27} : C_{28} : C_{29} = 6\% : 3\% : 91\%$). During oxic degradation, as the $S/(S+H)$ dropped, the sterane tritacta ratio changed towards $C_{27} : C_{28} : C_{29} = 49\% : 4\% : 47\%$ (Fig. 2C).

Oxic degradation effects on maturity parameters and other biomarker ratios

We further looked at relationships between a wider range of biomarker parameters in the macroalgae extracts. To quantify how the variability of these parameters is connected, we build a correlation matrix with 37 ratios that provides a measure of correlation between each biomarker parameter pair (Table S1). A network diagram visualizes these relationships (Fig. 1A). The edges (the connecting lines) in the network show individual correlations between the parameters, and the thickness of the edges, as well as the spacing of the nodes, reflects how strong the relationships are (quantified as Spearman's ρ). The network includes parameters that are traditionally interpreted as biological or ecological proxies (green nodes), thermal maturity indicators (red), redox proxies (yellow), and others that are often employed in palaeoecological and petroleum studies with various interpretations (grey). The network diagram shows that variations in 23 biomarker ratios in the Ediacaran macroalgae extracts are significantly interlinked (Fig. 1, Table S1), implying that there is a single factor that dominantly controls their distributions. The observation that $5\beta/5\alpha$ ratios form the core of the network suggests that this factor is likely the extent of oxygen exposure.

Overall, some biomarker parameters conventionally interpreted as maturity proxies show positive correlations with each other but also with sterane $5\beta/5\alpha$ ratios, $S/(S+H)$ and sterane $C_{29}\%$. Isomerisation of steroids and hopanoids to thermodynamically more stable structures, and thus higher apparent 'thermal maturity', is greatest in specimens that have seen least oxygen exposure (Fig. 1). As isomerization reactions often depend on the presence of double bonds, it is possible that initial oxygen exposure selectively removes compounds with unsaturations, or directly attacks and eliminates double bonds. Thus, with faster onset of anaerobic conditions, a greater proportion of lipids with double bonds survive and will

isomerize into thermodynamically more favourable configurations (11). Based on the network analysis, proxies that trend towards higher 'maturity' with decreasing oxygen exposure (earlier onset of reducing conditions) include Ts/Tm hopanes, moretanes/hopanes, $\alpha\beta\beta/\alpha\alpha\alpha$ steranes, 20S/R steranes as well as the proportion of aromatic steroids over saturated steranes (MAS/S and TAS/S) (note that the value of moretanes/hopanes generally decreases with increasing maturity and thus shows negative correlations).

Although the analysed Ediacaran macroalgae show a wide range in values of conventional 'thermal maturity' parameters, the highest apparent maturity values in the Ediacaran sections of the White Sea area are observed in one *Dickinsonia* fossil specimen. *Dickinsonia* was an animal that produced cholesterol as its main sterol, which was normally hydrogenated by a distinct microbial community within the decomposing animal carcass, transforming cholesterol mainly into 5 β -cholestane (18). Cholesterol in one of the *Dickinsonia* specimens, however, followed an exceptional taphonomic pathway: instead of being hydrogenated to the 5 β form, it was strongly isomerised into $\alpha\beta\beta$ cholestanes (Fig. S2). At the same time, no other isomerisation products (e.g. diasteranes or $\alpha\alpha\alpha$ 20S) were elevated, indicating that the process was microbially-mediated rather than related to particular steroid precursors, hypersaline environments, or double bond migration, as has been suggested previously (12, 14). Likewise, the isomerisation of organic molecules of the Ediacaran macroalgae might not have been a purely abiogenic chemical process, but mediated through microbial activity.

A second class of conventional maturity and source parameters in the macroalgae shows the opposite trend, i.e. their apparent maturity decreases under more reducing conditions. The proportion of steranes with a cleaved side chain (C₂₀ and C₂₁ pregnanes) relative to intact C₂₇-C₂₉ steranes (S Preg%), and the proportion of short-chain homologs among *n*-alkanes (*n*-alk long/short) and cheilanthanes ('Cheil C₁₉/C₂₃' and 'Cheil C₂₀/C₂₄') show positive correlations with 5 β /5 α ratios in macroalgae. Cleavage of C-C bonds in all these compounds may be related to degradation under elevated oxygen exposure. Cheilanthanes are ubiquitous components of oils and bitumens, although their biological source is unknown (4, 25). C₁₉/C₂₃ and C₂₀/C₂₄ cheilanthane ratios have been found to be highest in terrestrial environments, and elevated values have been used to trace terrestrial input to marine sediments (3, 26, 27). Terrestrial organic matter indeed suffers long oxygen exposure times within soil and during riverine transport; however, this also implies that C₁₉/C₂₃ and C₂₀/C₂₄ cheilanthane ratios may become elevated in oxic marine environments, and the ratios should thus only be applied in conjunction with other terrestrial markers.

The 3-methylhopane index (3MHI) and gammacerane index (GI) are also a part of the network. 3-methylhopanoids are thought to be mainly derived from methanotrophic bacteria (28, 29), while gammacerane is a likely diagenetic product of tetrahymanol (30), a membrane lipid found abundantly in some protozoa (31, 32) and in a wide range of bacteria (33). However, as both the 3MHI and GI ratios are normalised to hopanes, in our sample set these ratios are most likely primarily affected by the variation in hopane abundances, and might be connected to the network via S/(S+H). In other words, a small increase of 3MHI and GI in transitions from oxygenated to more reducing depositional conditions may simply imply a reduced flux of hopanoids from aerobic heterotrophic bacteria and not necessarily greater activity of methanotrophs and ciliates.

Sterol degradation in extant macroalgae and plants

To investigate whether the control of oxygen exposure on biomarkers in Ediacaran macroalgae is also applicable to modern organisms, we performed a series of degradation experiments on extant macroalgae and plants, and investigated the behaviour of sterols during their degradation in natural environments. In the experiments, the green macroalga *Ulva lactuca*, and the higher plant *Lactuca sativa* (lettuce) were degraded under oxic and dysoxic to anoxic conditions (see Methods). Oxygen limited degradation conditions were created either in water, reached by decomposition of large amounts of organic matter, or within sediments, where plants were sealed from the overlying water by a layer of clay (Methods). *U. lactuca* and *L. sativa* have a strong C₂₉ predominance among sterols, but the particular sterols are different (Fig. 3): *U. lactuca* contains almost solely isofucosterol (C₂₉ Δ^{5,24(28)}, 99% of total sterols, Fig. 4C), and *L. sativa* plant-typical stigmasterol (C₂₉ Δ^{5,22}, 35%), sitosterol (C₂₉ Δ⁵, 57%), and campesterol (C₂₉ Δ⁵, 8%; Fig. 5D). Additionally, *L. sativa* contains a small proportion of C₃₀ terpenoids (T) with an unsaturated ring system (S/(S+T) = 0.90). Anoxic decomposition was accompanied by the formation of black iron monosulphides, while oxic decomposition resulted in partial discolouration, disintegration and decrease in the amount of plant material. One of the *L. sativa* leaves accidentally floated to the water-air interface and became surrounded by a 2-3 mm thick, brown microbial mat (Fig. S3); different parts of the floated leaf were analysed for lipids as separate samples (Figs. 5A, S3).

After degradation of *U. lactuca* and *L. sativa* in the dark for five months at room temperature, there was a major contrast between oxic and anoxic experiments. Under anoxic conditions, the proportion between steroids and hopanoids (S/(S+H)) or C₃₀ terpenoids (S/(S+T)) in the algae and plants did not change, and the sterane trifterta ratios stayed very close to the initial sterol composition of the specimens (Figs. 2A,B, 4B, 5C). During oxic degradation, however, the reduction of detectable steroids in macroalgae was accompanied by a rise of GC-amenable hopanoids, presumably produced by aerobic heterotrophic bacteria, driving the S/(S+H) ratio to lower values (down to 0.88) (Fig. 2A). At the same time, the oxic degradation of sterols in both plants was accompanied by changes in the relative content of C₂₇, C₂₈ and C₂₉ sterols, with the proportion of C₂₉ sterols dropping by a factor of up to 5.5 (from 99% to 14-36% in *U. lactuca* (Figs. 2A, 4A), and from 92% to 36-85% in *L. sativa*; Figs. 2A,B, 4A, 5B). C₃₀ terpenoids present in *L. sativa* were initially S/(S+T) = 0.90, and these same compounds became enriched during oxic degradation (S/(S+T) = 0.27, Fig. 2B).

In addition to the relative abundance of sterols with different carbon numbers, particular sterol species changed their structure with the extent of oxic degradation. Isofucosterol, the major sterol in living *U. sativa* and possessing Δ⁵ and Δ²⁴⁽²⁸⁾ double bonds, was nearly absent after oxic degradation, and C₂₉ sterols were instead represented by sitosterol (Δ⁵) and stigmasterol (Δ^{5,22}) (Fig. 4A). In *L. sativa*, the proportion of stigmasterol to sitosterol increased, which was accompanied by the appearance of a double unsaturated Δ^{5,22} C₂₈ sterol (brassicasterol), absent in living *L. sativa* (Figs. 5B, S2). The increase in stigmasterol/sitosterol and brassicasterol/campesterol ratios progressed with the extent of oxic degradation along with a general decrease in C₂₉ sterols relative to other sterols, but were most pronounced in the leaf that floated at the water-air interface, even though the C₂₉ sterol proportion in this leaf (88-95%) stayed close to the initial value (Figs. 5A, S2). It is most likely that the pronounced dehydrogenation of sterols specifically at the 22 position has enzymatic control and is largely dependent on specific heterotrophic microorganisms.

To test whether the notable changes in sterol distributions during the laboratory degradation experiments are applicable to natural environments, we also analysed extant algae that had been degraded in natural shallow-marine environments. To achieve this, we collected fresh and degraded brown macroalgae *Ecklonia radiata* from the coast. Being physically more resistant than green algae, brown algae can be identified even at high levels of degradation; we collected discoloured specimens that had started to become slimy and to lose their integrity. Both fresh and degraded *E. radiata* were entangled in red macroalgae *Gracilaria edulis*, which we also analysed to account for possible epiphyte lipids.

The fresh red macroalga *G. edulis* displayed a strong cholesterol predominance among sterols (99.7%, Fig. S4D). However, in the *G. edulis* specimen entangling the degraded *E. radiata*, most of cholesterol (over 85%) was dehydrogenated at 22 position, mimicking the alteration of sterols observed in our laboratory degradation experiments. At the same time, only traces of C₂₈ (3.7%) and C₂₉ (0.7%) sterols were found, indicating that only small amounts of alien lipids, i.e. potentially not belonging to the macroalga, were present (Fig. S4C). The fresh brown macroalga *E. radiata* yielded 95.7% fucosterol ($\Delta^{5,24(28)}$ C₂₉ sterol; Fig. S4B), but the fucosterol content in the degraded specimens dropped to 54.3-65%, accompanied by a rise of C₂₇ and C₂₈ sterols, following the same trend as observed in our degradation experiments (Fig. S4A). With little contribution of exogenous sterols from epiphytes or heterotrophs, as evident from the content of red algae entangling *E. radiata*, the decrease of C₂₉ content relative to other sterols during degradation is likely caused by dealkylation to form lower sterols.

In summary, under both natural and laboratory conditions, sterol distributions and abundances in macroalgae change significantly during oxic degradation, and relative C₂₉ sterol contents drop, likely due to dealkylation of C₂₉ sterols. This pattern mirrors the results for the Ediacaran macroalgae, where relative C₂₉ sterane contents decrease with the extent of oxic degradation of algal lipids (Fig. 2).

DISCUSSION

Combined evidence from extant plants and Ediacaran macroalgae illustrate that the primary distributions of lipids can be severely altered during oxic degradation: aerobic heterotrophic microbial communities are apparently efficient in dehydrogenation, dealkylation, and destruction of lipids. Conversely, anoxic degradation may lead to the preservation of biomarker distributions that reflect the original lipid composition quite closely. Under oxic conditions, the proportion of steroids to hopanoids, and of C₂₉ steroids to other steroids, can decrease sharply, and the degree of organic matter degradation becomes the main control on these biomarker ratios. Core biomarker proxies such as the proportion of steranes and hopanes, and sterane homolog distributions can be altered by aerobic heterotrophic degradation to the extent of complete loss of primary ecological information. Furthermore, conventional 'thermal maturity' biomarker parameters can be affected during the early diagenesis by microbial and, possibly, chemical alteration of the biomarker precursors. While biomarkers may generally preserve information about the composition of primary producer communities, the heterotrophic overprint requires consideration before such information can be reliably extracted. Likely, sediments deposited under permanently anoxic waters retain biomarker distributions closest to the initial averaged biomass

composition, although any organic matter transported into the basin from terrestrial or shallow-water environments, or any slow-sinking biomass exported from the oxygenated mixed zone, may still have experienced significant oxygen exposure and aerobic alteration. Thus, in any palaeoenvironment, the effects of oxic degradation on biomarker distributions must be considered and tested.

The data presented here show that statistical analysis of biomarker distributions may be a powerful tool for identifying the effects of oxic degradation. Apart from correlations with other biomarker parameters, additional consideration of inorganic geochemistry, isotope systematics, and general understanding of the depositional environments and sources of organic matter may serve as indicators of degradation effects in each given situation. The major impact of aerobic degradation on lipid distributions observed in this study uncovers an underestimated control on biomarker parameters that have traditionally been interpreted as proxies for biological community composition, environmental settings, source rock lithology and thermal maturity. Redox control on such parameters may explain incongruent results between different proxies often observed in organic geochemical studies, and the correlations described here may eventually allow quantification and correction of oxic degradation effects. Future studies also need to explore how the affected biomarker ratios evolve with increasing maturity, and if other parameters such as mineralogy and organic matter type modify the response to oxic degradation.

MATERIALS AND METHODS

Ediacaran macroalgae

Biomarker analyses were conducted on 14 organically preserved macroalgae. Samples were collected specifically for biomarker analysis during fieldwork in 2015-2018, from the Lyamtsa locality of the Ediacara Biota in the White Sea area (Russia). Macroalgae were sampled from a 1.5 m thick layer of clay in the lower part of the Lyamtsa Beds (Ust-Pinega Formation, Redkino Regional Stage), exposed to the south of Lyamtsa Village. One specimen of *Dickinsonia* was collected in 2018 from a surface in the lower part of the Erga Beds (Mezen Formation, Kotlin Regional Stage) of the Zimnie Gory locality, the same fossiliferous surface from where specimens of organically preserved *Kimberella*, *Andiva* and *Yorgia* were found (18, 34). All samples were collected avoiding weathered zones and cracks and were immediately wrapped in pre-combusted aluminium foil (300°C, 9h) and packed in calico cotton bags under strict avoidance of contamination (15).

Extant plants and degradation experiments

Macroalgae for the analyses and experiments were collected on the south-eastern coast of Australia, New South Wales. Green macroalgae *Ulva lactuca* and ocean water for the experiments were collected from a tidal zone. Brown macroalgae *Ecklonia radiate* were collected from a shallow low-energy lagoon, formed in an area protected from waves by local coast configuration. We collected discoloured specimens that had started to become slimy and to lose their integrity. Freshly stranded *E. radiate* were collected from a nearby beach for comparison. Both fresh and degraded *E. radiate* were entangled in red macroalgae *Gracilaria edulis*, which we also analysed to account for any potential epiphyte lipids. *Lactuca sativa* (lettuce) specimens came from a supermarket. All specimens were washed with deionized (Millipore Elix 3UV, France) water, kept refrigerated overnight and further processed on the day after collection.

For degradation experiments, *Ulva* were organized into samples of around 0.6 g of wet weight and put into glass jars. For anoxic experiments, three samples were further covered with glass fibre filters, followed by around 5 mm of sand and around 1 cm of clay. The jars were then filled with ocean water and closed to avoid evaporation. Anoxic conditions were achieved in the sediment within days, as was visible by the production of black iron monosulphide, and these conditions persisted throughout the length of the experiments. For oxic experiments, three jars with algae were filled with ocean water, closed with lids, and were mixed with a metal spatula once a week to saturate water with oxygen; the spatula was sterilised with methanol and dichloromethane (DCM) before use on each sample.

For further analysis, samples covered with sediment were frozen, the bottoms of the jars were broken off and plant material was carefully separated from the overlying glass filters using tweezers and collected into sterile glass vials for extraction. For the analysis of oxic experiments, all water from the jars was filtered through a glass fibre filter, and these filters were extracted together with the captured plant material.

Lactuca experiments were set up the same way as *Ulva*, except that around 4 g of plant material (wet weight) were used for anoxic experiments without sediment cover as anoxic conditions in the water were sustained owing to decomposition of the larger amounts of organic matter (O_2 content < 0.05 $\mu\text{mol/L}$, measured with PreSens Microx 4 trace fiber optic oxygen meter, PreSens DP-PST7 factory-calibrated dipping probe). For all experiments, plant material was recovered with tweezers for subsequent extraction. Only one experiment with lettuce covered by sediment was analysed in this study. In this setup, a lettuce leaf escaped from the sediment during methane production in the first week of the experiment, and reached the top of the water layer. The leaf initiated rapid formation of a microbial mat around it. This leaf was separated into three samples: two samples came from within the floating mat, and one – from within the water column (Fig. S2). One of the oxic experiments on lettuce was excluded from the analysis as a lettuce leaf floated to the top of the water layer and became contaminated with mould.

Preparation and extraction of samples

Extant plant material was dried at 50°C overnight, extracted via ultrasonic agitation in solvents (methanol : dichloromethane (DCM) 3 : 2 for 15 min (x 2), DCM : *n*-hexane 2 : 3 for 15 min). The extract was fractionated into non-polar and polar fractions using micro-column chromatography over annealed (300°C; 12 h) and dry packed silica gel (Silica Gel 60; 230– 600 mesh; EM Science). Non-polar molecules were eluted with 1.5 ml of *n*-hexane : DCM (1 : 1) and the polar fraction with 1 ml DCM : methanol (1 : 1). The polar fractions were saponified in 1 ml of 5% KOH methanol : water 4 : 1 solution at 50°C overnight, 1 ml of water was added and a neutral fraction was extracted by vortexing for 1 min with 1 ml of DCM : *n*-hexane 1 : 4 (X 3). Sterols were further converted to the trimethylsilyl (TMS) derivatives for gas chromatography–mass spectrometry analysis.

All Ediacaran macroalgae were preserved as carbonaceous impressions within clay, so their organic matter could be gently removed from the rock surface with tweezers, sometimes additionally using a scalpel for initial separation. Hydrocarbons were extracted from the organic matter via ultrasonic agitation in solvents (methanol for 30 min, dichloromethane (DCM) for 15 min (x 2), DCM : *n*-hexane 1 : 1 for 15 min).

All solvents used in the study were 99.9% grade (UltimAR®; Mallinckrodt Chemicals, St. Louis, MO, USA). Glassware was cleaned by combustion at 300°C for 9 h, and metal appliances were washed with methanol and DCM before use.

Extracts of fossils were fractionated into saturated, aromatic and polar fractions using micro-column chromatography over annealed and dry packed silica gel. Saturated hydrocarbons were eluted with 1 dead volume (DV) of *n*-hexane, aromatic hydrocarbons with 4.5 DV of *n*-hexane : DCM (4 : 1) and the polar fraction with 3 ml DCM : methanol (1 : 1). Extracts from fossils with low hydrocarbon content were only fractionated into saturated+aromatic and polar fractions to reduce the loss of analytes. An internal standard, 18-MEAME (18-methyleicosanoic acid methylester; Chiron Laboratories AS), was added to the saturated and aromatic fractions, while D4 (d_4 -C₂₉- $\alpha\alpha\alpha$ R-ethylcholestane; Chiron Laboratories AS) was added to saturated and saturated+aromatic hydrocarbon fractions with low biomarker content. The samples were analysed and quantified by GC–MS.

Gas chromatography–mass spectrometry (GC-MS)

GC-MS analyses of biomarker extracts were carried out on an Agilent 6890 gas chromatograph coupled to a Micromass Autospec Premier double sector mass spectrometer (Waters Corporation, Milford, MA, USA) at the Australian National University. The GC was equipped with a 60 m DB-5 MS capillary column (0.25 mm i.d., 0.25 μm film thickness; Agilent JW Scientific, Agilent Technologies, Santa Clara, CA, USA), and helium was used as the carrier gas at a constant flow of 1 mL min^{-1} . Samples were injected in splitless mode into a Gerstel PTV injector at 60°C (held for 0.1 min) and heated at 260°C min^{-1} to 300°C. For full-scan, selected ion recording (SIR) and metastable reaction monitoring (MRM) analyses, the GC oven was programmed from 60°C (held for 4 min) to 315°C at 4°C min^{-1} , with total run time of 100 min. All samples were injected in *n*-hexane to avoid deterioration of chromatographic signals by FeCl_2 build-up in the MS ion source through use of halogenated solvents (35). *n*-Alkanes were quantified in full-scan mode in *m/z* 85 trace, and $\alpha\alpha\alpha$ 20R-stigmastane – in *m/z* 217 trace, relative to the 18-MEAME internal standard (*m/z* 340). Steranes and hopanes were quantified in MRM mode in $\text{M}^+ \rightarrow 217$ and $\text{M}^+ \rightarrow 191$ transitions respectively relative to $\alpha\alpha\alpha$ 20R-stigmastane. Aromatic steroids were quantified in SIR mode using the *m/z* 253 base ion. TMS-ethers from modern plants were quantified in full-scan using *m/z* 129 for sterols, *m/z* 191 and *m/z* 189 for hopanols; sterol and hopanol integrated areas were further corrected for differences in *m/z* response. Peak areas for saturated and aromatic molecules are uncorrected for differences in GC-MS response.

Error quantification

As repeat injections of fossil extracts were not possible due to the limited abundance of sample material, standard deviations for the concentration of each biomarker were externally determined based on the clear relationship between the peak area and coefficient of variation determined for the GC-MS system we used: $C_v = 186.18x^{0.31}$ ($R^2 = 0.82$), where *x* is the integrated peak area (18). The standard deviation was calculated as $\text{STD} = C_v \cdot \text{signal area}$. For biomarker ratios, error propagation followed standard root mean square error propagation formulae. As $\beta\alpha\alpha$ 20R-ergostane (5 β) coelutes with two other compounds, $\alpha\alpha\alpha$ 20S-ergostane and an unknown sterane (tentatively identified as a $\beta\alpha\alpha$ 20R-27-norsterane), its integration error should be expected to be much higher than the error for peaks that are not coeluting and are mainly controlled by signal/noise ratio. Thus, an integration error calculated on the whole dataset was used for the ergostane 5 β /5 α ratios, which was estimated to be $C_v = 0.34$ for the Ediacaran White Sea area extracts (18).

Laboratory system blanks

A comprehensive, accumulatory system blank was performed covering all analytical steps during extraction, fractionation to instrumental analysis. For this purpose, pre-extracted powdered clay was used to monitor background contamination.

Data processing

As many biomarker parameters do not have normal data distributions, the Spearman rank correlation coefficient was used instead of the more classically applied Pearson coefficient. A Spearman rank correlation matrix was built in PAST3 (36), and the correlation matrix-based network was built in Gephi (37) using the Force Atlas 2 layout algorithm.

Syngeneity of biomarkers

GC-MS MRM, SIR and full-scan analyses of the comprehensive accumulatory laboratory system blank confirmed that the detected hydrocarbons were not introduced by laboratory processes. Monitoring of the blank yielded no *n*-alkanes, hopanes or steranes, even when measured using the most sensitive GC-MS MRM methods. The only contaminants detected in the blank were trace amounts of phthalates — plasticizers present in small amounts in solvents used for extraction of biomarkers.

The results of exterior-interior analysis on samples with macroalgae showed that the surface of these samples was not contaminated with hydrocarbons (15). Macroalgae extracts demonstrate the same exceptionally low thermal maturity as other fossils from the White Sea area (15, 18). The high $\beta\alpha/\beta\alpha$ and low T_s/T_m hopane isomer ratios, virtual absence of diasteranes, $\alpha\beta\beta$ and $\alpha\alpha\alpha 20S$ sterane isomers, are characteristic of the most immature sediments, which demonstrates that the hydrocarbons are significantly below the so-called oil-generation window (i.e. the kerogen never thermally generated and expelled liquid hydrocarbons (3). Such a low thermal maturity is never observed in contaminant petroleum products and migrated oils, which by their very nature must have a maturity within the oil generative window. Thus, contamination of the samples with petroleum products or by migrated hydrocarbons did not occur.

References and Notes

1. A. H. Knoll, R. E. Summons, J. R. Waldbauer, J. E. Zumberge, The Geological Succession of Primary Producers in the Oceans. 133-163 (2007).
2. J. I. Hedges, R. G. Keil, Sedimentary organic matter preservation: an assessment and speculative synthesis. *Marine chemistry* **49**, 81-115 (1995).
3. K. Peters, C. Walters, J. Moldowan, *The Biomarker Guide. Volume 2. Biomarkers and Isotopes in Petroleum Systems and Earth History*. (Cambridge University Press, New York, ed. 2nd, 2005), pp. 634.
4. J. J. Brocks, A. Pearson, Building the Biomarker Tree of Life. *Reviews in Mineralogy and Geochemistry* **59**, 233-258 (2005).
5. J. K. Volkman, Sterols and other triterpenoids: source specificity and evolution of biosynthetic pathways. *Organic Geochemistry* **36**, 139-159 (2005).
6. P. Grantham, L. Wakefield, Variations in the sterane carbon number distributions of marine source rock derived crude oils through geological time. *Organic Geochemistry* **12**, 61-73 (1988).
7. J. M. Moldowan, W. K. Seifert, E. J. Gallegos, Relationship between petroleum composition and depositional environment of petroleum source rocks. *AAPG bulletin* **69**, 1255-1268 (1985).

8. M. Ries-Kautt, P. Albrecht, Hopane-derived triterpenoids in soils. *Chemical Geology* **76**, 143-151 (1989).
9. E. A. Canuel, C. S. Martens, Reactivity of recently deposited organic matter: Degradation of lipid compounds near the sediment-water interface. *Geochimica et Cosmochimica Acta* **60**, 1793-1806 (1996).
10. J. M. Moldowan, P. Sundararaman, M. Schoell, Sensitivity of biomarker properties to depositional environment and/or source input in the Lower Toarcian of SW-Germany. *Organic Geochemistry* **10**, 915-926 (1986).
11. S. Brassell *et al.*, Isomerisation, rearrangement and aromatisation of steroids in distinguishing early stages of diagenesis. *Organic Geochemistry* **6**, 11-23 (1984).
12. H. Ten Haven, J. De Leeuw, T. Peakman, J. Maxwell, Anomalies in steroid and hopanoid maturity indices. *Geochimica et Cosmochimica Acta* **50**, 853-855 (1986).
13. X. Sun, T. Zhang, Y. Sun, K. L. Milliken, D. Sun, Geochemical evidence of organic matter source input and depositional environments in the lower and upper Eagle Ford Formation, south Texas. *Organic Geochemistry* **98**, 66-81 (2016).
14. T. M. Peakman, H. L. T. Haven, J. R. Rechka, J. W. De Leeuw, J. R. Maxwell, Occurrence of (20R)- and (20S)- Δ 8(14) and Δ 14 5 α (H)-sterenes and the origin of 5 α (H),14 β (H),17 β (H)-steranes in an immature sediment. *Geochimica et Cosmochimica Acta* **53**, 2001-2009 (1989).
15. I. Bobrovskiy, J. M. Hope, A. Krasnova, A. Ivantsov, J. J. Brocks, Molecular fossils from organically preserved Ediacara biota reveal cyanobacterial origin for *Beltanelliformis*. *Nature Ecology & Evolution* **2**, 437-440 (2018).
16. D. Grahdankin, Structure and depositional environment of the Vendian Complex in the southeastern White Sea area. *Stratigraphy and Geological Correlation* **11**, 313-331 (2003).
17. M. A. Fedonkin, A. Simonetta, A. Y. Ivantsov, New data on *Kimberella*, the Vendian mollusc-like organism (White Sea region, Russia): palaeoecological and evolutionary implications. *Geological Society, London, Special Publications* **286**, 157-179 (2007).
18. I. Bobrovskiy *et al.*, Ancient steroids establish the Ediacaran fossil *Dickinsonia* as one of the earliest animals. *Science* **361**, 1246-1249 (2018).
19. I. Bobrovskiy, A. Krasnova, A. Ivantsov, E. Luzhnaya, J. J. Brocks, Simple sediment rheology explains the Ediacara biota preservation. *Nature Ecology & Evolution* **3**, 582-589 (2019).
20. J. G. Gehling, Microbial mats in terminal Proterozoic siliciclastics; Ediacaran death masks. *PALAIOS* **14**, 40-57 (1999).
21. M. V. Leonov, Macroscopic plant remains from the base of the Ust'-Pinega formation (Upper Vendian of the Arkhangelsk Region). *Paleontological Journal* **41**, 683-691 (2007).
22. T. M. Peakman, J. W. De Leeuw, W. I. C. Rijpstra, Identification and origin of Δ 8(14)5 α - and Δ 14 5 α -sterenes and related hydrocarbons in an immature bitumen from the Monterey Formation, California. *Geochimica et Cosmochimica Acta* **56**, 1223-1230 (1992).
23. I. Björkhem, J.-Å. Gustafsson, Mechanism of Microbial Transformation of Cholesterol into Coprostanol. *European Journal of Biochemistry* **21**, 428-432 (1971).
24. S. J. Gaskell, G. Eglinton, Sterols of a contemporary lacustrine sediment. *Geochimica et Cosmochimica Acta* **40**, 1221-1228 (1976).
25. G. Ourisson, in *Early life on earth. Nobel Symposium Vol. 84*, S. Bengtson, Ed. (Columbia University Press, New York, 1994), pp. 259-269.

26. R. A. Noble, R. Alexander, R. I. Kagi, J. K. Nox, Identification of some diterpenoid hydrocarbons in petroleum. *Organic Geochemistry* **10**, 825-829 (1986).
27. K. L. French, J. Sepulveda, J. Trabucho-Alexandre, D. Gröcke, R. E. Summons, Organic geochemistry of the early Toarcian oceanic anoxic event in Hawsker Bottoms, Yorkshire, England. *Earth and Planetary Science Letters* **390**, 116-127 (2014).
28. R. E. Summons, L. L. Jahnke, Z. Roksandic, Carbon isotopic fractionation in lipids from methanotrophic bacteria: relevance for interpretation of the geochemical record of biomarkers. *Geochimica et Cosmochimica Acta* **58**, 2853-2863 (1994).
29. M. Zundel, M. Rohmer, Prokaryotic triterpenoids: 1. 3 β -Methylhopanoids from *Acetobacter* species and *Methylococcus capsulatus*. *European Journal of Biochemistry* **150**, 23-27 (1985).
30. H. Ten Haven, M. Rohmer, J. Rullkötter, P. Bissere, Tetrahymanol, the most likely precursor of gammacerane, occurs ubiquitously in marine sediments. *Geochimica et Cosmochimica Acta* **53**, 3073-3079 (1989).
31. F. B. Mallory, J. T. Gordon, R. L. Conner, The isolation of a pentacyclic triterpenoid alcohol from a protozoan. *Journal of the American Chemical Society* **85**, 1362-1363 (1963).
32. K. Takishita *et al.*, Microbial eukaryotes that lack sterols. *Journal of Eukaryotic Microbiology* **64**, 897-900 (2017).
33. A. B. Banta, J. H. Wei, P. V. Welander, A distinct pathway for tetrahymanol synthesis in bacteria. *Proceedings of the National Academy of Sciences* **112**, 13478-13483 (2015).
34. I. Bobrovskiy, A. Nagovitsyn, J. M. Hope, E. Luzhnaya (Serezhnikova), J. J. Brocks, Biomarker evidence for guts, gut contents, and feeding strategies of Ediacaran animals. (in prep.).
35. J. J. Brocks, J. M. Hope, Tailing of Chromatographic Peaks in GC–MS Caused by Interaction of Halogenated Solvents with the Ion Source. *Journal of Chromatographic Science* **52**, 471-475 (2014).
36. Ø. Hammer, D. A. Harper, P. D. Ryan, PAST: paleontological statistics software package for education and data analysis. *Palaeontologia electronica* **4**, 9 (2001).
37. M. Bastian, S. Heymann, M. Jacomy, in *Third international AAAI conference on weblogs and social media*. (2009).

Acknowledgments: We thank E. Luzhnaya, A. Krasnova, A. Nagovitsyn, P. Rychkov, V. Rychkov and S. Rychkov for their help with collecting Ediacaran fossils. **Funding:** The study was funded by Australian Research Council grants DP160100607 and DP170100556 (to J.J.B.), Russian Foundation for Basic Research project No. 17-05-02212A (to I.B). I.B. gratefully acknowledges an Australian Government Research Training Program stipend scholarship. **Author contributions:** I.B. conceived the study, collected samples, did experiments and analyses; I.B. and J.J.B. interpreted the data; J.M.H. helped with biomarker analyses; I.B. wrote the manuscript, with contributions from all authors. **Competing interests:** Authors declare no competing interests. **Data and materials availability:** All data required to understand and assess the conclusions of this research are available in the main text and supplementary materials.

Supplementary Materials:

Figs. S1 to S4

Table S1

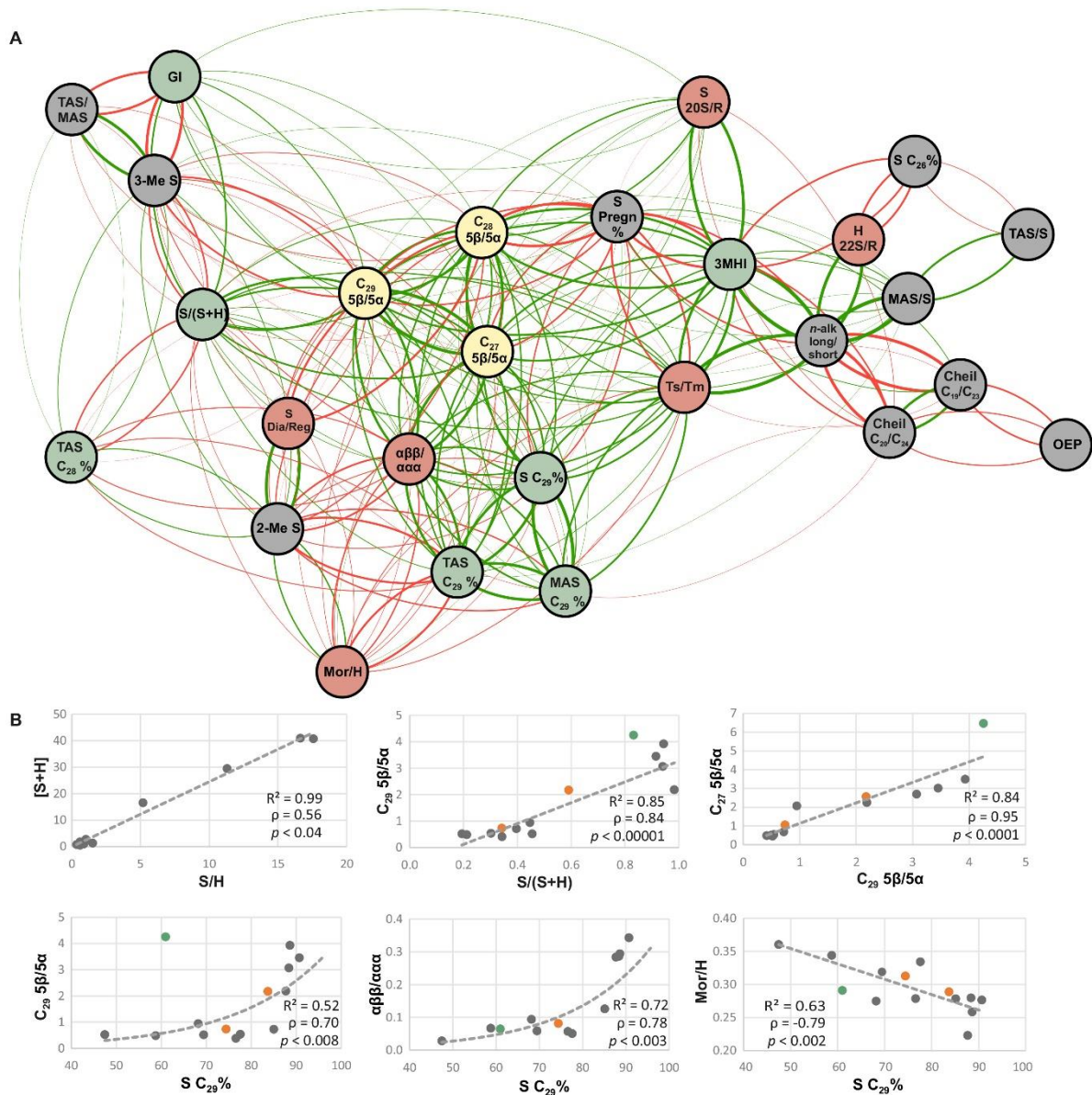


Fig. 1. Relationships between selected biomarker parameters in Ediacaran macroalgae. (A) Network analysis demonstrating the interlink between all major biomarker parameters. The structure is based on a Spearman's ρ correlation matrix, filtered by $p < 0.05$, $|\rho| > 0.6$; distance between nodes and edge line thickness reflect ρ correlation coefficient values between parameters, green edges show positive correlation, red – negative correlation; nodes are coloured according to traditional interpretations of biomarker parameters: yellow – $5\beta/5\alpha$ sterane ratios, reflecting diagenetic redox conditions; green – parameters traditionally interpreted as biological or ecological proxies; red – ratios traditionally interpreted as thermal maturity parameters; grey – unknown or mixed interpretations; (B) xy plots showing correlations between selected biomarker parameters in macroalgae, green – *Archifasma*, orange – ex. gr. Vendotaenides, grey – unidentifiable macroalgae. Abbreviations: TAS – triaromatic steroids, MAS – monoaromatic steroids, S – steranes, H – hopanes, Cheil – cheilanthanes, GI – gammacerane index, 3-Me S – 3-methylsteranes, 2-Me S – 2-methylsteranes, S Dia/Reg – diasteranes/regular steranes, Mor – moretane, S Pregn% - $(C_{21}+C_{22})/(C_{27}+C_{28}+C_{29})$ steranes, 3MHI – 3-methylhopane index, *n*-alk long/short – proportion

between long- and short-chain *n*-alkanes (C₂₅₋₂₇/C₂₉₋₃₁), OEP – odd-over-even predominance among *n*-alkanes; for the exact computations of the ratios see Table S1.

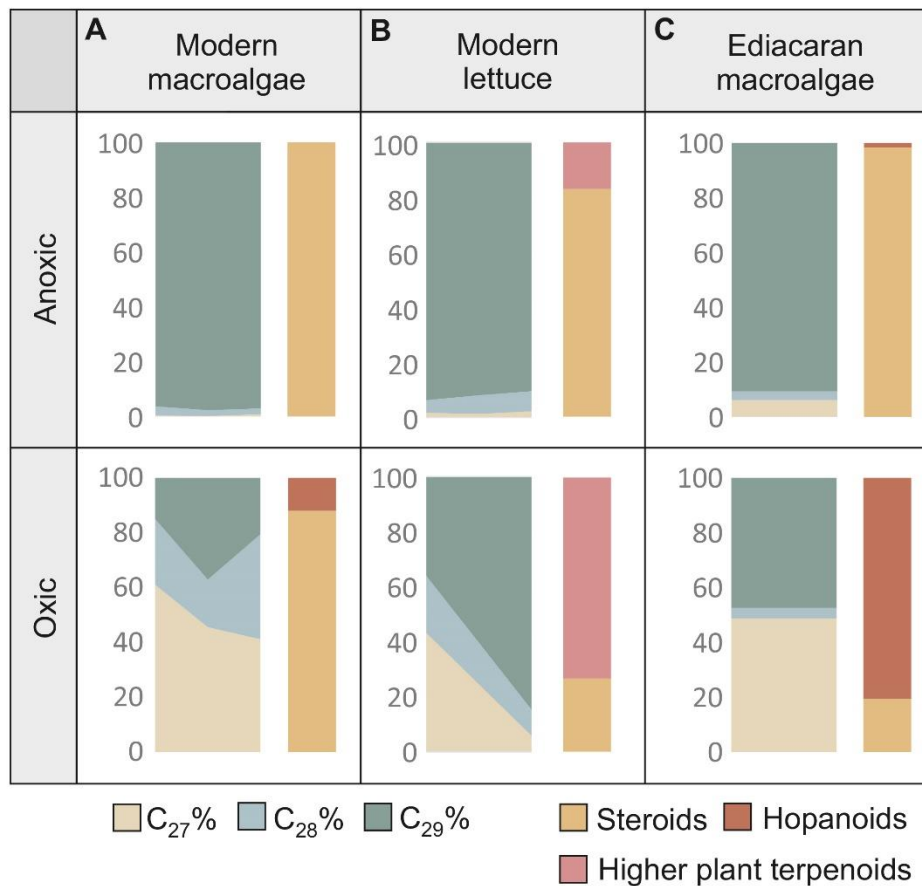


Fig. 2. Contrast between the biomarker distributions for organic matter degraded in more anoxic and oxic settings. (A) degradation of extant green macroalga *Ulva*; oxic and anoxic conditions are represented by three experiments each; **(B)** degradation of lettuce; anoxic conditions are represented by three experiments, oxic conditions by two experiments; **(C)** the end members of the correlations of the 5 β /5 α ratio with S/(S+H) and percentage of C₂₉ steranes in the Ediacaran macroalgae dataset (excluding *Archifasma*), representing algae degraded in most anoxic and most oxic conditions as inferred from 5 β /5 α ratios; note that the assignment of biomarker distributions to oxic and anoxic settings for the fossil algae is an interpretation.

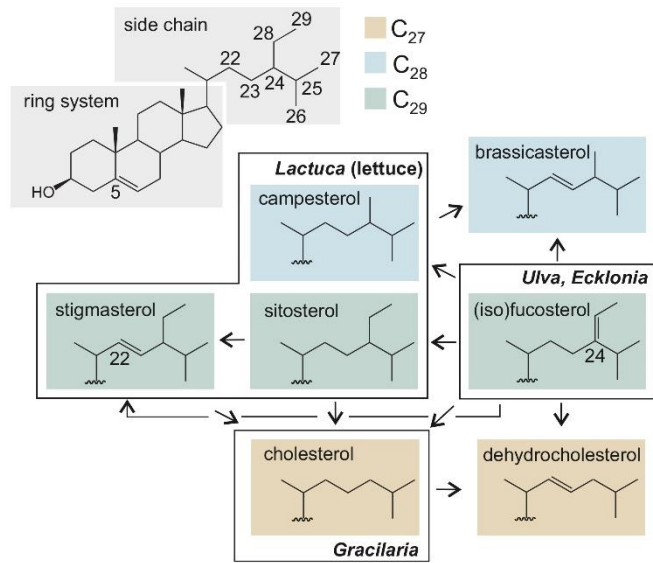


Fig. 3. Sterol nomenclature, initial sterol compositions of the analysed macroalgae *Ulva*, *Ecklonia*, and *Gracilaria*, and the plant *Lactuca* (lettuce), with common names of sterols where used in the text; arrows illustrate the main transformation pathways of sterols during oxic degradation.

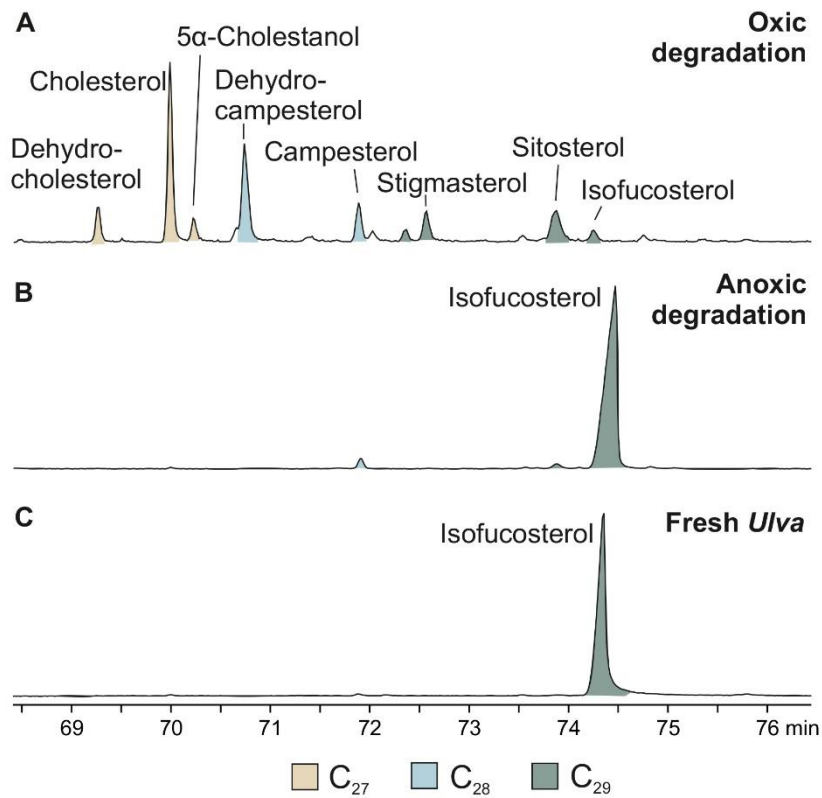


Fig. 4. Chromatograms showing the distribution of sterols in *Ulva* before and after degradation experiments (m/z 129). (A) Sterols of *Ulva* degraded in oxic environments; (B) sterols of *Ulva* degraded in anoxic environments; (C) initial sterol composition of *Ulva*.

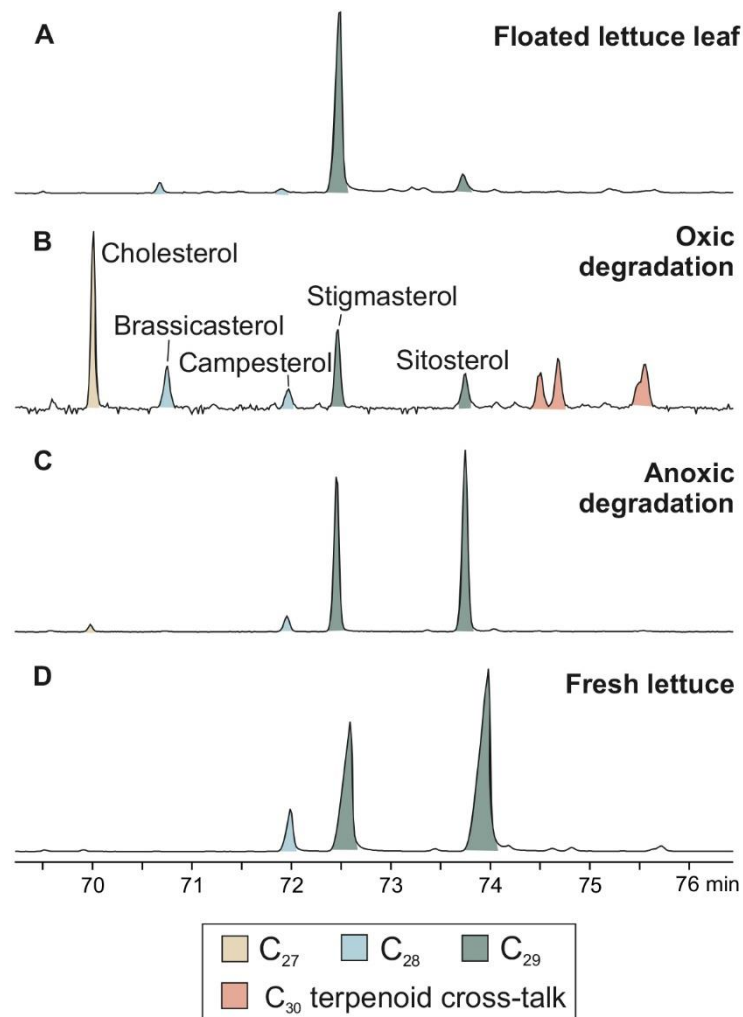


Fig. 5. Chromatograms showing the distribution of sterols in lettuce before and after degradation experiments (m/z 129). (A) Sterols of a lettuce leaf that floated to the top of the water layer (sample C in the Supplementary Fig. 3); (B) sterols of lettuce degraded in oxic environments; (C) sterols of lettuce degraded in anoxic environments; (D) initial sterol composition of lettuce.

SUPPLEMENTARY MATERIALS

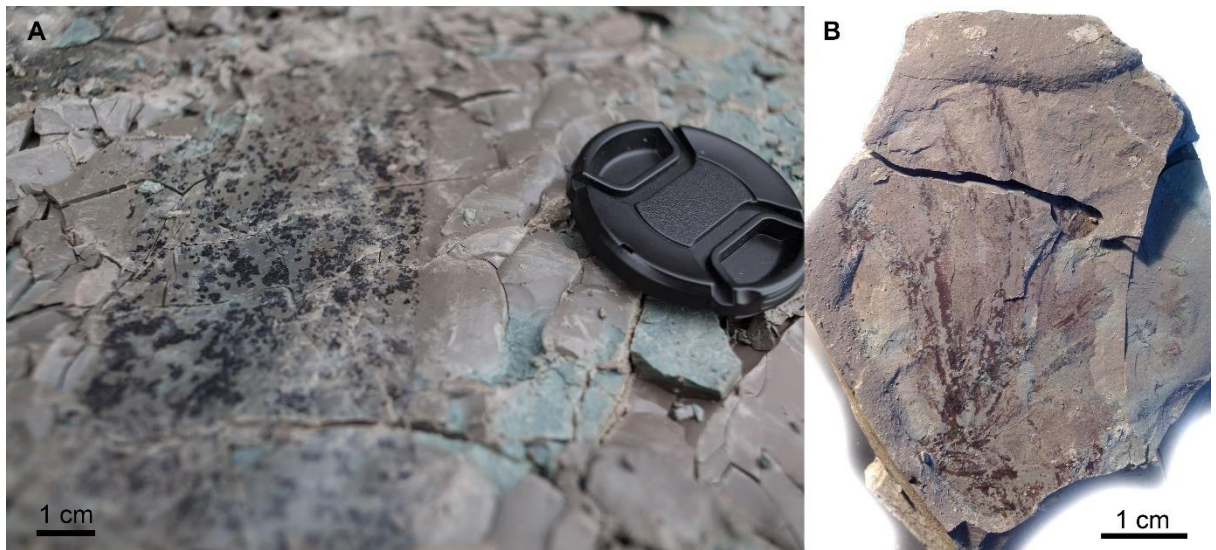


Fig. S1. Organically preserved Ediacaran macroalgae from the White Sea area. (A) *Archyfasma lamellata*; (B) ex gr. *Vendotaenides*.

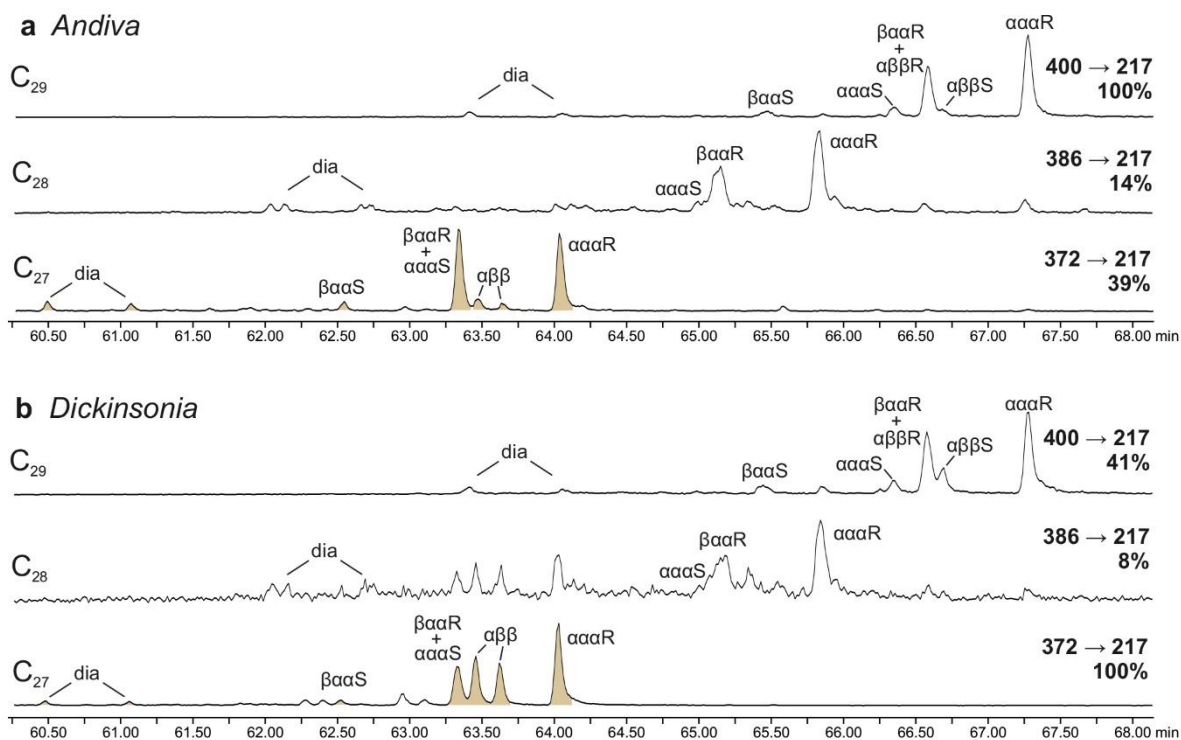


Fig. S2. Sterane distribution in *Andiva* (a), and *Dickinsonia* (b), preserved next to each other on the same surface; both extracts are largely represented by steranes from the underlying microbial mat plus cholestane from the animals. Cholesterol of these organisms was preferentially transformed into 5β (βαα) sterane isomers in *Andiva*, and into αββ isomers in *Dickinsonia*.

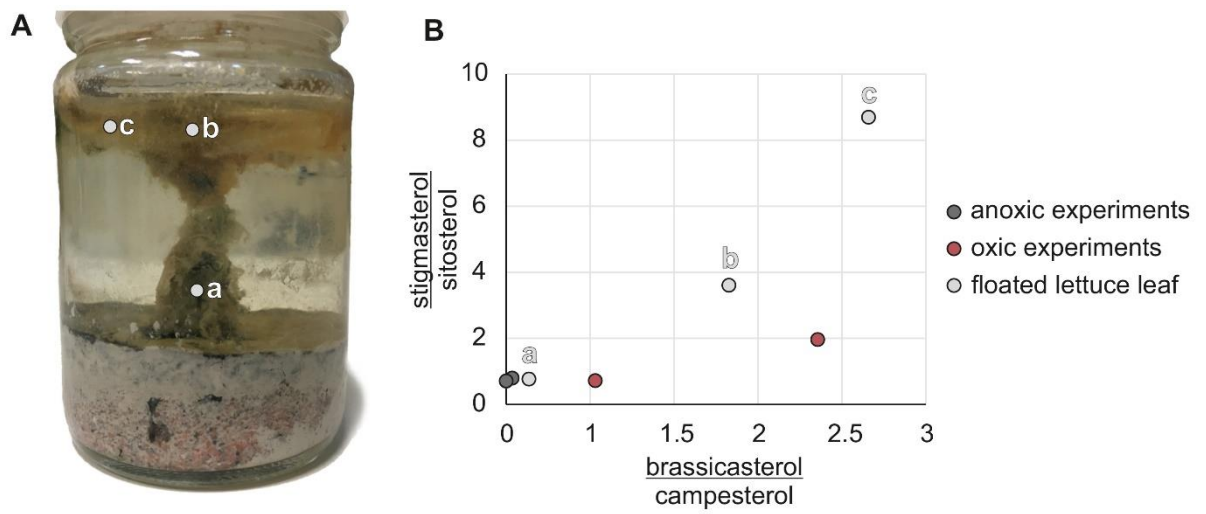


Fig. S3. A lettuce leaf that floated to the top of the water layer and is surrounded by a microbial mat, with sampling points (A), and (B) a plot of the proportion of sterols with and without unsaturation on the side chain between C₂₈ (brassicasterol/campesterol) and C₂₉ (stigmasterol/sitosterol) sterols in the floated lettuce leaf and other experiments.

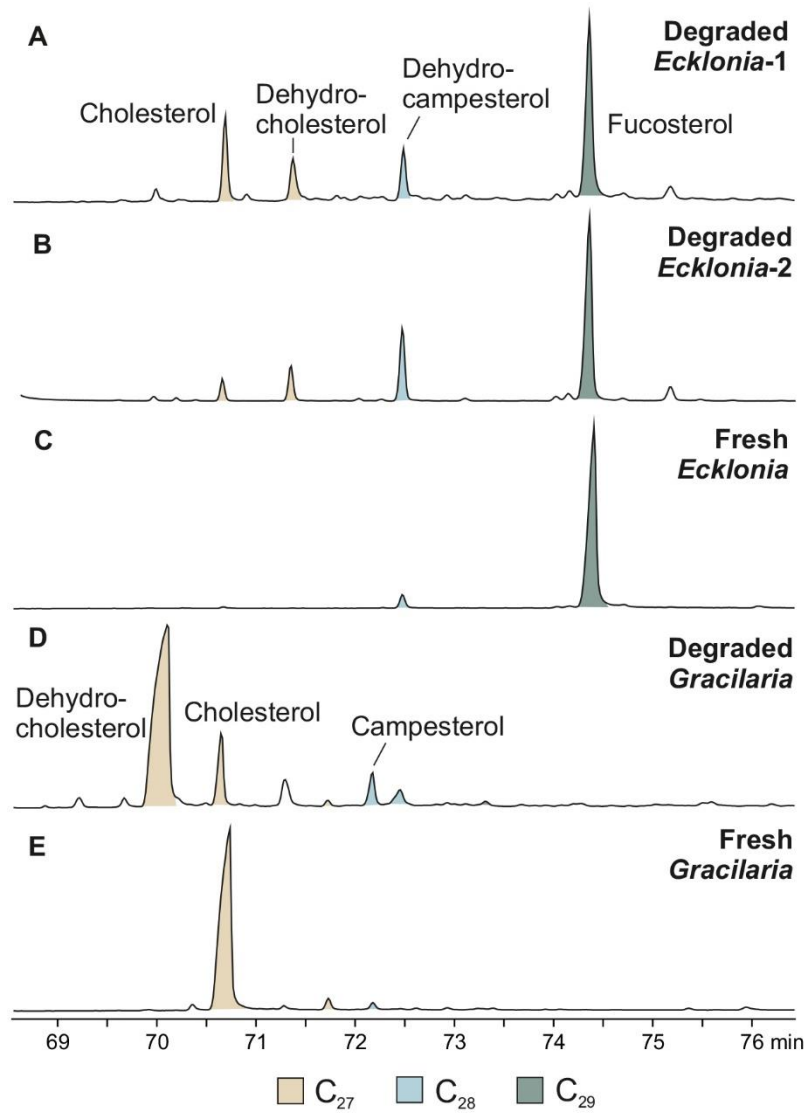


Fig. S4. Chromatograms showing the distribution of sterols in fresh and degraded brown (*Ecklonia*) and red algae (*Gracilaria*) (m/z 129).

← **Table S1. Spearman ρ correlation matrix on biomarker parameters of the macroalgae rearranged according to correlation with 5 β /5 α ratio for C₂₉ steranes.** Each value in the table is a correlation coefficient ρ between two biomarker parameters; the values are filtered by $p < 0.05$, $|\rho| > 0.6$, and *Archifasma* is excluded from the dataset; parameters marked with yellow – 5 β /5 α sterane ratios that reflect diagenetic redox conditions, green – parameters with assigned biological meanings, red – maturity parameters, grey – unknown interpretation; the light-grey parameters are those that were calculated but do not correlate with 5 β /5 α ratio or S/(S+H) ratio; green cells in the table are positive correlations with 5 β /5 α ratio, red are negative; values close to -1 indicate the strongest negative correlation, values close to +1 indicate the strongest positive correlation. Biomarker parameters: **5 β /5 α** = ($\beta\alpha\alpha$ 20R+ $\alpha\alpha\alpha$ 20S)/ $\alpha\alpha\alpha$ 20R; **$\alpha\beta\beta/\alpha\alpha\alpha$** = C₂₇ $\alpha\beta\beta$ (20S+20R)/ $\alpha\alpha\alpha$ 20R; **S/(S+H)** = Σ (C₂₇₋₂₉ steranes) / Σ (C₂₇₋₂₉ steranes, C₂₇₋₃₅ hopanes), steranes: C₂₇ = Σ ($\beta\alpha$ -20(S+R)-diacholestane, $\alpha\alpha\alpha$ - and $\beta\alpha\alpha$ -20(S+R)-cholestane), C₂₈ = Σ ($\beta\alpha$ -20(S+R)-diaergostane, $\alpha\alpha\alpha$ - and $\beta\alpha\alpha$ -20(S+R)-ergostane), C₂₉ = Σ ($\beta\alpha$ -20(S+R)-diastigmastane, $\alpha\alpha\alpha$ - and $\beta\alpha\alpha$ -20(S+R)-stigmastane), $\alpha\alpha\alpha$ = 5 α (H),14 α (H),17 α (H), $\beta\alpha\alpha$ = 5 β (H),14 α (H),17 α (H); hopanes: C₂₇ = Σ (Ts, Tm, β), C₂₉ = Σ ($\alpha\beta$, Ts, $\beta\alpha$), C₃₀ = Σ ($\alpha\beta$, $\beta\alpha$), C₃₁₋₃₅ = Σ ($\alpha\beta$ -22(S+R), $\beta\alpha$), $\alpha\beta$ = 17 α (H)21 β (H), $\beta\alpha$ = 17 β (H)21 α (H); C₂₉ = Σ ($\alpha\beta$, Ts, $\beta\alpha$), C₃₀ hopane = Σ ($\alpha\beta$, $\beta\alpha$), C₃₁₋₃₅ = Σ ($\alpha\beta$ -22(S+R), $\beta\alpha$); **3MHI** = 100*(Σ C₃₁ 3-methylhopane) / (Σ C₃₁ 3-methylhopane + Σ ($\alpha\beta$ -22(S+R), $\beta\alpha$) C₃₀ hopane); **S C29%** = 100*C₂₉ steranes / Σ (C₂₇₋₂₉ steranes); **TAS C29%** = 100*C₂₈ triaromatic steroids / Σ (C₂₆₋₂₈ triaromatic steroids); **Ts/Tm** = Ts/Tm C₂₇ hopanes; **GI** = gammacerane / C₃₀ hopanes; **MAS C29%** = 100*C₂₉ monoaromatic steroids / Σ (C₂₇₋₂₉ monoaromatic steroids); **S 20S/R** = $\alpha\alpha\alpha$ 20S/ $\alpha\alpha\alpha$ 20R C₂₉ steranes; **MAS/S** = Σ (C₂₇₋₂₉ monoaromatic steroids) / Σ (C₂₇₋₂₉ steranes); **S C28%** = 100*C₂₈ steranes / Σ (C₂₇₋₂₉ steranes); **TAS C28 %** = 100*C₂₇ triaromatic steroids / Σ (C₂₆₋₂₈ triaromatic steroids); **Mor/H** = $\beta\alpha/\alpha\beta$ C₃₀ hopane; **TAS/MAS** = Σ (C₂₆₋₂₈ triaromatic steroids) / Σ (C₂₇₋₂₉ monoaromatic steroids); **MAS C27%** = 100*C₂₇ monoaromatic steroids / Σ (C₂₇₋₂₉ monoaromatic steroids); **2-Me S** = $\alpha\alpha\alpha$ 20R 2-methylstigmastane / $\alpha\alpha\alpha$ 20R stigmastane; **Dia/Reg** = $\beta\alpha$ -20(S+R)-diacholestane / Σ ($\alpha\alpha\alpha$ - and $\beta\alpha\alpha$ -20(S+R)-cholestane); **TAS C27%** = 100*C₂₆ triaromatic steroids / Σ (C₂₆₋₂₈ triaromatic steroids); **S C27%** = 100*C₂₇ steranes / Σ (C₂₇₋₂₉ steranes); **S Pregn%** = Σ (C₂₁₋₂₂ steranes) / Σ (C₂₇₋₂₉ steranes); **3-Me S** = $\alpha\alpha\alpha$ 20R 3-methylstigmastane / $\alpha\alpha\alpha$ 20R stigmastane; **TAS Pregn%** = Σ (C₂₀₋₂₁ triaromatic steroids) / Σ (C₂₆₋₂₈ triaromatic steroids); **MAS Pregn%** = Σ (C₂₁₋₂₂ monoaromatic steroids) / Σ (C₂₇₋₂₉ monoaromatic steroids); **Pr/Ph** = pristane/phytane; **OEP** = (4C₁₉ + 4C₂₁) / (C₁₈ + 6C₂₀ + C₂₂) *n*-alkanes; **Ch C19/C23** = C₁₉/C₂₃ cheilanthanes; **Ch C20/C24** = C₂₀/C₂₄ cheilanthanes; **S C26%** = 100*C₂₆ steranes / Σ (C₂₆₋₂₉ steranes), C₂₆ steranes are only 27-norcholestanes; **H 22S/R** = $\alpha\beta$ 22S/ $\alpha\beta$ R C₃₁ hopanes; **H C27/C29** = C₂₇/C₂₉ hopanes; **H C30/C31** = C₃₀/C₃₁ hopanes; **2MHI** = 100*(Σ C₃₁ 2 α +2 β -methylhopane) / (Σ C₃₁ 2 α +2 β -methylhopane + Σ ($\alpha\beta$ -22(S+R), $\beta\alpha$) C₃₀ hopane); **MAS C28%** = 100*C₂₈ monoaromatic steroids / Σ (C₂₇₋₂₉ monoaromatic steroids); **TAS/S** = Σ (C₂₆₋₂₈ triaromatic steroids) / Σ (C₂₇₋₂₉ steranes).

Sample	Type	[S+H] (µg/l)	Pi/Ph	OEP	long/short	CH C19/C23	CH C20/C24	S/(S+H)	S Pregn%	S C26%	S C27%	S C28%	S C29%	MAS C27 %	MAS C28 %	MAS C29 %	TAS C27 %	TAS C28 %	TAS C29 %	C27 5b/5a	C28 5b/5a	C29 5b/5a	
OM5	Macroalgae*	0.78				0.672	0.212	0.173	5.18	35.30	5.95	58.74	47.45	3.90	2.94	85.10	5.63	3.89	67.25	0.498	0.738	0.487	
OM8	Macroalgae	2.67				0.709	0.983	0.040	7.23	7.73	4.59	87.68	17.63	6.17	76.20	6.83	6.83	89.57	3.60	89.57	2.254	2.752	2.189
BM1	Macroalgae	40.94	1.48	1.12	0.375	0.340	0.805	0.940	0.08	7.71	3.91	88.38	11.26	2.33	86.41	5.89	4.12	89.99	4.12	89.99	2.694	3.210	3.068
BM2	Macroalgae	40.76	0.68	1.30	0.962	0.300	0.803	0.943	0.05	7.71	3.91	88.38	11.26	2.33	86.41	5.89	4.12	89.99	4.12	89.99	2.694	3.210	3.068
OM12	Archifasma	16.59	0.89	0.92	0.090	0.402	0.760	0.832	0.07	36.73	2.28	60.98	38.15	3.00	58.85	28.74	3.48	67.78	3.48	67.78	3.499	4.324	3.928
OM13	Vendotaenides	1.31	0.86	1.27	0.972	0.292	0.747	0.590	0.051	13.55	2.75	83.70	47.45	3.90	2.94	85.10	5.63	3.89	67.25	0.498	0.738	0.487	
OM14	Macroalgae	2.74	1.07	1.07	0.066	0.728	0.932	0.455	0.186	48.67	3.87	47.45	45.75	3.90	2.94	85.10	5.63	3.89	67.25	0.498	0.738	0.487	
BM3	Macroalgae	29.48	1.66	1.09	0.122	0.306	0.805	0.915	0.050	6.15	3.17	90.68	11.96	2.94	85.10	5.63	3.89	90.48	3.016	3.559	3.452	3.452	3.452
OM16	Vendotaenides	0.50	0.42	1.06		0.523	0.855	0.342	0.117	1.02	21.66	3.94	74.40	26.28	3.33	70.38	16.52	5.90	77.58	1.062	0.899	0.739	
OM17	Macroalgae	1.01	1.36	1.05	0.094	0.497	0.827	0.446	0.074	0.60	28.06	3.75	68.18	29.49	3.59	66.93	16.13	6.72	77.15	2.072	1.041	0.949	
OM21	Macroalgae	1.79	1.48	1.14	0.076	0.434	0.825	0.342	0.125	0.83	18.60	4.80	76.60	21.11	4.32	74.57	12.47	7.56	79.96	0.494	0.762	0.415	
OM25	Macroalgae	3.91				0.682	0.896	0.396	0.141	12.60	2.28	85.12	18.61	2.26	79.13	13.23	5.74	81.03	5.74	81.03	0.690	0.725	0.719
OM26	Macroalgae	28.96				0.225	0.822	0.194	0.126	0.74	23.09	7.47	69.44	26.73	4.58	68.89	22.35	8.58	69.07	0.457	0.748	0.520	
OM27	Macroalgae	1.25				0.301	0.058	0.301	0.058	0.71	17.54	4.88	77.58	24.54	4.77	70.69	20.03	8.57	71.39	0.542	0.769	0.543	

Sample	Type	2-Me S	3-Me S	TAS/MAS	MAS Pregn%	TAS Pregn%	MAS/S	TAS/S	S 20S/R	eBβ/total	Dia/Reg	Is/Tm	Mor/H	H 22S/R	H C27/C29	H C30/C31	2MHI	3MHI	GI
OM5	Macroalgae*	0.343	0.040	0.040			0.15	0.19	0.134	0.067	0.036	0.042	0.344	0.456	0.735	0.656			
OM8	Macroalgae	0.018	0.002	0.58	0.13	0.02	0.15	0.10	0.281	0.284	0.147	0.220	0.283	0.450	0.610	0.646			
BM1	Macroalgae	0.018	0.002	0.30	0.10	0.03	2.45	0.78	0.243	0.287	0.012	0.078	0.280	0.504	0.693	0.706	0.678	1.05	0.06
BM2	Macroalgae	0.021	0.002	0.31	0.10	0.02	2.80	0.94	0.226	0.294	0.071	0.071	0.258	0.489	0.717	0.754	2.118	1.62	
OM12	Archifasma	0.057	0.009	0.28	0.11	0.03	2.33	0.71	0.126	0.065	0.026	0.068	0.291	0.472	0.718	0.740			0.02
OM13	Vendotaenides	0.098	0.015	0.015	0.04	0.04	0.04	0.43	0.125		0.079	0.079	0.289	0.504	0.671	0.727			0.03
OM14	Macroalgae	0.097	0.014	0.49	0.26	0.14	0.28	0.16	0.104	0.029		0.037	0.361	0.438	0.795	0.791	0.604	0.29	0.03
BM3	Macroalgae	0.020	0.004	0.28	0.09	0.03	0.60	0.18	0.221	0.343	0.010	0.070	0.276	0.483	0.657	0.704	0.493	0.75	0.04
OM16	Vendotaenides	0.090	0.032	0.99	0.16	0.12	0.51	0.52	0.129	0.082	0.015	0.038	0.313	0.466	0.671	0.747	0.397	0.41	0.02
OM17	Macroalgae	0.086	0.021	0.92	0.13	0.07	0.50	0.49	0.131	0.094	0.018	0.059	0.275	0.480	0.663	0.708	0.574	0.65	0.03
OM21	Macroalgae	0.094	0.028	1.19	0.17	0.12	0.48	0.62	0.113	0.057	0.025	0.051	0.279	0.472	0.702	0.714	0.544	0.30	0.02
OM25	Macroalgae	0.96	0.17	0.14	0.32	0.14	0.32	0.32	0.094	0.126	0.032	0.062	0.278	0.504	0.716	0.819			0.02
OM26	Macroalgae	0.085	0.021	0.66	0.23	0.19	0.18	0.12	0.127	0.059	0.016	0.046	0.319	0.504	0.680	0.778	0.945	0.32	0.02
OM27	Macroalgae	0.126	0.010	0.64	0.20	0.12	0.28	0.20	0.129	0.051	0.028	0.059	0.335	0.494	0.606	0.747	1.067	0.76	0.03

←**Table S2. Values for biomarker parameters measured for Ediacaran macroalgae.** For the colour legend and explanations of the biomarker parameters see Table S1. *more precise identification of macroalgae was not possible, blank fields indicate that one or more biomarkers in the ratio were below detection limit.

REFERENCES

- Alexander, R., Berwick, L., Pierce, K., 2011. Single carbon surface reactions of 1-octadecene and 2,3,6-trimethylphenol on activated carbon: Implications for methane formation in sediments. *Organic Geochemistry* 42, 540-547.
- Allard, B., Templier, J., 2001. High molecular weight lipids from the trilaminar outer wall (TLS)-containing microalgae *Chlorella emersonii*, *Scenedesmus communis* and *Tetraedron minimum*. *Phytochemistry* 57, 459-467.
- Antcliffe, J.B., Gooday, A.J., Brasier, M.D., 2011. Testing the protozoan hypothesis for Ediacaran fossils: a developmental analysis of *Palaeopascichnus*. *Palaeontology* 54, 1157-1175.
- Aseeva, E.A., 1988. Fossil remains of Vendian thallophytes, in: Ryabenko, V.A., Aseeva, E.A., Furtes, V.V. (Eds.), *Biostratigraphy and Paleogeographic Reconstructions of the Precambrian of Ukraine*. Naukova Dumka, Kiev, pp. 81-92.
- Banta, A.B., Wei, J.H., Welander, P.V., 2015. A distinct pathway for tetrahymanol synthesis in bacteria. *Proceedings of the National Academy of Sciences* 112, 13478-13483.
- Bastian, M., Heymann, S., Jacomy, M., 2009. Gephi: an open source software for exploring and manipulating networks, Third international AAAI conference on weblogs and social media.
- Bengtson, S., 2002. Origins and early evolution of predation. *The Paleontological Society Papers* 8, 289-318.
- Björkhem, I., Gustafsson, J.-Å., 1971. Mechanism of Microbial Transformation of Cholesterol into Coprostanol. *European Journal of Biochemistry* 21, 428-432.
- Blumenberg, M., Kruger, M., Nauhaus, K., Talbot, H.M., Oppermann, B.I., Seifert, R., Pape, T., Michaelis, W., 2006. Biosynthesis of hopanoids by sulfate-reducing bacteria (genus *Desulfovibrio*). *Environmental Microbiology* 8, 1220-1227.
- Boag, T.H., Darroch, S.A.F., Laflamme, M., 2016. Ediacaran distributions in space and time: testing assemblage concepts of earliest macroscopic body fossils. *Paleobiology* 42, 574-594.
- Bobrovskiy, I., Hope, J.M., Golubkova, E., Brocks, J.J., in review. Food sources for the Ediacara biota communities. *Nature Communications*.
- Bobrovskiy, I., Hope, J.M., Ivantsov, A., Nettersheim, B.J., Hallmann, C., Brocks, J.J., 2018a. Ancient steroids establish the Ediacaran fossil *Dickinsonia* as one of the earliest animals. *Science* 361, 1246-1249.
- Bobrovskiy, I., Hope, J.M., Krasnova, A., Ivantsov, A., Brocks, J.J., 2018b. Molecular fossils from organically preserved Ediacara biota reveal cyanobacterial origin for *Beltanelliformis*. *Nature Ecology & Evolution*.
- Bobrovskiy, I., Krasnova, A., Ivantsov, A., (Serezhnikova), E.L., Brocks, J.J., in press. Simple sediment rheology explains the Ediacara biota preservation. *Nature Ecology & Evolution*.
- Bobrovskiy, I., Krasnova, A., Ivantsov, A., Luzhnaya, E., Brocks, J.J., 2019. Simple sediment rheology explains the Ediacara biota preservation. *Nature Ecology & Evolution* 3, 582-589.
- Bobrovskiy, I., Nagovitsyn, A., Hope, J.M., Luzhnaya (Serezhnikova), E., Brocks, J.J., in prep. Biomarker evidence for guts, gut contents, and feeding strategies of Ediacaran animals.
- Bradshaw, S.A., Eglinton, G., 1993. Marine Invertebrate Feeding and the Sedimentary Lipid Record, in: Engel, M.H., Macko, S.A. (Eds.), *Organic Geochemistry: Principles and Applications*. Springer US, Boston, MA, pp. 225-235.

- Bradshaw, S.A., O'Hara, S.C., Corner, E.D., Eglinton, G., 1989. Assimilation of dietary sterols and faecal contribution of lipids by the marine invertebrates *Neomysis integer*, *Scrobicularia plana* and *Nereis diversicolor*. *Journal of the Marine Biological Association of the United Kingdom* 69, 891-911.
- Bradshaw, S.A., O'Hara, S.C.M., Corner, E.D.S., Eglinton, G., 1990a. Dietary lipid changes during herbivory and coprophagy by the marine invertebrate *Nereis diversicolor*. *Journal of the Marine Biological Association of the United Kingdom* 70, 771-787.
- Bradshaw, S.A., O'Hara, S.C.M., Corner, E.D.S., Eglinton, G., 1991. Effects on Dietary Lipids of the Marine Bivalve *Scrobicularia Plana* Feeding in Different Modes. *Journal of the Marine Biological Association of the United Kingdom* 71, 635-653.
- Bradshaw, S.A., O'Hara, S.C.M., Cornert, E.D.S., Eglinton, G., 1990b. Changes in lipids during simulated herbivorous feeding by the marine crustacean *Neomysis integer*. *Journal of the Marine Biological Association of the United Kingdom* 70, 225-243.
- Brasier, M.D., Antcliffe, J.B., 2008. Dickinsonia from Ediacara: A new look at morphology and body construction. *Palaeogeography, Palaeoclimatology, Palaeoecology* 270, 311-323.
- Brassell, S., McEvoy, J., Hoffmann, C., Lamb, N., Peakman, T., Maxwell, J., 1984. Isomerisation, rearrangement and aromatisation of steroids in distinguishing early stages of diagenesis. *Organic Geochemistry* 6, 11-23.
- Brocks, J.J., 2018. The transition from a cyanobacterial to algal world and the emergence of animals. *Emerging Topics in Life Sciences* 2, 181-190.
- Brocks, J.J., Buick, R., Logan, G.A., Summons, R.E., 2003. Composition and syngeneity of molecular fossils from the 2.78 to 2.45 billion-year-old Mount Bruce Supergroup, Pilbara Craton, Western Australia. *Geochimica et Cosmochimica Acta* 67, 4289-4319.
- Brocks, J.J., Grosjean, E., Logan, G.A., 2008. Assessing biomarker syngeneity using branched alkanes with quaternary carbon (BAQCs) and other plastic contaminants. *Geochimica et Cosmochimica Acta* 72, 871-888.
- Brocks, J.J., Hope, J.M., 2014. Tailing of Chromatographic Peaks in GC-MS Caused by Interaction of Halogenated Solvents with the Ion Source. *Journal of Chromatographic Science* 52, 471-475.
- Brocks, J.J., Jarrett, A.J., Sirantoine, E., Hallmann, C., Hoshino, Y., Liyanage, T., 2017. The rise of algae in Cryogenian oceans and the emergence of animals. *Nature* 548, 578.
- Brocks, J.J., Jarrett, A.J., Sirantoine, E., Kenig, F., Moczydlowska, M., Porter, S., Hope, J., 2016. Early sponges and toxic protists: possible sources of cryostane, an age diagnostic biomarker antedating Sturtian Snowball Earth. *Geobiology* 14, 129-149.
- Brocks, J.J., Pearson, A., 2005. Building the Biomarker Tree of Life. *Reviews in Mineralogy and Geochemistry* 59, 233-258.
- Buatois, L.A., Mángano, M.G., 2016. Ediacaran Ecosystems and the Dawn of Animals, in: Mángano, M.G., Buatois, L.A. (Eds.), *The Trace-Fossil Record of Major Evolutionary Events: Volume 1: Precambrian and Paleozoic*. Springer Netherlands, Dordrecht, pp. 27-72.
- Budd, G.E., Jensen, S., 2017. The origin of the animals and a 'Savannah' hypothesis for early bilaterian evolution. *Biological Reviews* 92, 446-473.
- Bull, I.D., Lockheart, M.J., Elhmmali, M.M., Roberts, D.J., Evershed, R.P., 2002. The origin of faeces by means of biomarker detection. *Environment international* 27, 647-654.
- Burzynski, G., Narbonne, G.M., Alexander Decechi, T., Dalrymple, R.W., 2017. The ins and outs of Ediacaran discs. *Precambrian Research* 300, 246-260.

- Butler, A.D., Cunningham, J.A., Budd, G.E., Donoghue, P.C.J., 2015. Experimental taphonomy of *Artemia* reveals the role of endogenous microbes in mediating decay and fossilization. *Proceedings of the Royal Society B: Biological Sciences* 282.
- Butterfield, N.J., 2009. Oxygen, animals and oceanic ventilation: an alternative view. *Geobiology* 7, 1-7.
- Butterfield, N.J., 2011. Animals and the invention of the Phanerozoic Earth system. *Trends in Ecology & Evolution* 26, 81-87.
- Butterfield, N.J., 2018. Oxygen, animals and aquatic bioturbation: An updated account. *Geobiology* 16, 3-16.
- Cai, Y., Schiffbauer, J.D., Hua, H., Xiao, S., 2012. Preservational modes in the Ediacaran Gaojiashan Lagerstätte: Pyritization, aluminosilicification, and carbonaceous compression. *Palaeogeography, Palaeoclimatology, Palaeoecology* 326-328, 109-117.
- Callow, R.H.T., Brasier, M.D., 2009. Remarkable preservation of microbial mats in Neoproterozoic siliciclastic settings: Implications for Ediacaran taphonomic models. *Earth-Science Reviews* 96, 207-219.
- Canfield, D.E., Poulton, S.W., Narbonne, G.M., 2007. Late-Neoproterozoic deep-ocean oxygenation and the rise of animal life. *Science* 315, 92-95.
- Canuel, E.A., Martens, C.S., 1996. Reactivity of recently deposited organic matter: Degradation of lipid compounds near the sediment-water interface. *Geochimica et cosmochimica acta* 60, 1793-1806.
- Carbone, C.A., Narbonne, G.M., Macdonald, F.A., Boag, T.H., 2015. New Ediacaran fossils from the uppermost Blueflower Formation, northwest Canada: disentangling biostratigraphy and paleoecology. *Journal of Paleontology* 89, 281-291.
- Chistyakov, V.G., Kalmykova, N.A., Nessonov, L.A., Suslov, G.A., 1984. On the presence of the Vendian deposits in the mid-stream of Onega River and on the possible existence of tunicates (Tunicata: Chordata) in the Precambrian. *Vestnik Leningradskogo Universiteta* 6, 11-19.
- Colombo, J., Silverberg, N., Gearing, J., 1997. Lipid biogeochemistry in the Laurentian trough—II. Changes in composition of fatty acids, sterols and aliphatic hydrocarbons during early diagenesis. *Organic Geochemistry* 26, 257-274.
- Cruz-Rivera, E., Paul, V., 2002. Coral reef benthic cyanobacteria as food and refuge: diversity, chemistry and complex interactions, *Proc 9th Int Coral Reef Symp*, pp. 515-520.
- Cruz-Rivera, E., Paul, V.J., 2006. Feeding by coral reef mesograzers: algae or cyanobacteria? *Coral Reefs* 25, 617-627.
- Darroch, S.A.F., Laflamme, M., Schiffbauer, J.D., Briggs, D.E.G., 2012. Experimental Formation of a Microbial Death Mask. *Palaios* 27, 293-303.
- Droser, M.L., Gehling, J.G., 2015. The advent of animals: The view from the Ediacaran. *Proceedings of the National Academy of Sciences* 112, 4865-4870.
- Droser, M.L., Gehling, J.G., Jensen, S.R., 2006. Assemblage palaeoecology of the Ediacara biota: The unabridged edition? *Palaeogeography, Palaeoclimatology, Palaeoecology* 232, 131-147.
- Dunn, F.S., Liu, A.G., Donoghue, P.C., 2018. Ediacaran developmental biology. *Biological Reviews* 93, 914-932.
- Dzik, J., 1999. Organic membranous skeleton of the Precambrian metazoans from Namibia. *Geology* 27, 519-522.

- Dzik, J., 2003. Anatomical information content in the Ediacaran fossils and their possible zoological affinities. *Integrative and Comparative Biology* 43, 114-126.
- Dzik, J., Ivantsov, A.Y., 2002. Internal anatomy of a new Precambrian dickinsoniid dipleurozoan from northern Russia. *Neues Jahrbuch für Geologie und Paläontologie Monatshefte*, 385-396.
- Erwin, D.H., Laflamme, M., Tweedt, S.M., Sperling, E.A., Pisani, D., Peterson, K.J., 2011. The Cambrian Conundrum: Early Divergence and Later Ecological Success in the Early History of Animals. *Science* 334, 1091-1097.
- Evans, S.D., Droser, M.L., Gehling, J.G., 2015. Dickinsonia liftoff: Evidence of current derived morphologies. *Palaeogeography, Palaeoclimatology, Palaeoecology* 434, 28-33.
- Evans, S.D., Droser, M.L., Gehling, J.G., 2017. Highly regulated growth and development of the Ediacara macrofossil Dickinsonia costata. *PLOS ONE* 12, e0176874.
- Fauchald, K., Jumars, P.A., 1979. The diet of worms: a study of polychaete feeding guilds.
- Fedonkin, M., Ivantsov, A.Y., Leonov, M., Serezhnikova, E., 2007a. Dynamics of evolution and biodiversity in Late Vendian: a view from the White Sea, The rise and fall of the Vendian (Ediacaran) biota. *Origin of the modern biosphere. Transact. Int. Conf. on the IGCP project*, pp. 6-9.
- Fedonkin, M.A., 1992. Vendian Faunas and the Early Evolution of Metazoa, in: Lipps, J.H., Signor, P.W. (Eds.), *Origin and Early Evolution of the Metazoa*. Springer US, Boston, MA, pp. 87-129.
- Fedonkin, M.A., Simonetta, A., Ivantsov, A.Y., 2007b. New data on Kimberella, the Vendian mollusc-like organism (White Sea region, Russia): palaeoecological and evolutionary implications. *Geological Society, London, Special Publications* 286, 157-179.
- Fedonkin, M.A., Waggoner, B.M., 1997. The Late Precambrian fossil Kimberella is a mollusc-like bilaterian organism. *Nature* 388, 868.
- Fontaine, J., Grandmougin-Ferjani, A., Hartmann, M.-A., Sancholle, M., 2001. Sterol biosynthesis by the arbuscular mycorrhizal fungus *Glomus intraradices*. *Lipids* 36, 1357-1363.
- French, K.L., Sepulveda, J., Trabucho-Alexandre, J., Gröcke, D., Summons, R.E., 2014. Organic geochemistry of the early Toarcian oceanic anoxic event in Hawsker Bottoms, Yorkshire, England. *Earth and Planetary Science Letters* 390, 116-127.
- Gaskell, S.J., Eglinton, G., 1976. Sterols of a contemporary lacustrine sediment. *Geochimica et Cosmochimica Acta* 40, 1221-1228.
- Gehling, J., Droser, M., Jensen, S., Runnegar, B., Briggs, D., 2005. Ediacara organisms: relating form to function, in: Briggs, D. (Ed.), *Evolving form and function: fossils and development; Proceedings of a Symposium Honouring Adolf Seilacher for His Contributions to Paleontology, in Celebration of His 80th Birthday*. Yale University Press, New Haven, pp. 43-66.
- Gehling, J.G., 1999. Microbial mats in terminal Proterozoic siliciclastics; Ediacaran death masks. *PALAIOS* 14, 40-57.
- Gehling, J.G., Droser, M.L., 2009. Textured organic surfaces associated with the Ediacara biota in South Australia. *Earth-Science Reviews* 96, 196-206.
- Gehling, J.G., Rigby, J.K., 2016. Long expected sponges from the Neoproterozoic Ediacara fauna of South Australia. *Journal of Paleontology* 70, 185-195.
- Gehling, J.G., Runnegar, B.N., Droser, M.L., 2014. Scratch Traces of Large Ediacara Bilaterian Animals Ediacara Bilaterian Traces. *Journal of Paleontology* 88, 284-298.

- Geider, R.J., La Roche, J., 2002. Redfield revisited: variability of C : N : P in marine microalgae and its biochemical basis. *European Journal of Phycology* 37, 1-17.
- Gelpi, E., Oró, J., Schneider, H.J., Bennett, E.O., 1968. Olefins of High Molecular Weight in Two Microscopic Algae. *Science* 161, 700-701.
- Georgieva, M.N., Little, C.T., Watson, J.S., Sephton, M.A., Ball, A.D., Glover, A.G., 2019. Identification of fossil worm tubes from Phanerozoic hydrothermal vents and cold seeps. *Journal of Systematic Palaeontology* 17, 287-329.
- Gibson, B.M., Schiffbauer, J.D., Darroch, S.A.F., 2018. Ediacaran-style Decay Experiments using Mollusks and Sea Anemones. *Palaios* 33, 185-203.
- Gill-King, H., 1997. Chemical and ultrastructural aspects of decomposition. *Forensic taphonomy: The postmortem fate of human remains*, 93-108.
- Gingras, M., Hagadorn, J.W., Seilacher, A., Lalonde, S.V., Pecoits, E., Petrash, D., Konhauser, K.O., 2011. Possible evolution of mobile animals in association with microbial mats. *Nat. Geosci.* 4, 372.
- Glaessner, M.F., 1984. *The dawn of animal life: a biohistorical study*. Cambridge University Press, Cambridge, UK.
- Gnilovskaya, M., Ishchenko, Kolesnikov, C., Korenchuk, L., Udaltsov, A., 1988. *Vendotenidy Vostochno-Evropeskoi platformy (Vendotenids of the East-European Platform)*. Nauka, Leningrad.
- Gold, D.A., Grabenstatter, J., de Mendoza, A., Riesgo, A., Ruiz-Trillo, I., Summons, R.E., 2016. Sterol and genomic analyses validate the sponge biomarker hypothesis. *Proceedings of the National Academy of Sciences* 113, 2684-2689.
- Gold, D.A., Runnegar, B., Gehling, J.G., Jacobs, D.K., 2015. Ancestral state reconstruction of ontogeny supports a bilaterian affinity for Dickinsonia. *Evolution & Development* 17, 315-324.
- Gooday, A.J., Holzmann, M., Caille, C., Goineau, A., Kamenskaya, O., Weber, A.A.T., Pawlowski, J., 2017. Giant protists (xenophyophores, Foraminifera) are exceptionally diverse in parts of the abyssal eastern Pacific licensed for polymetallic nodule exploration. *Biological Conservation* 207, 106-116.
- Goryl, M., Marynowski, L., Brocks, J.J., Bobrovskiy, I., Derkowski, A., 2018. Exceptional preservation of hopanoid and steroid biomarkers in Ediacaran sedimentary rocks of the East European Craton. *Precambrian Research* 316, 38-47.
- Grabenstatter, J., Méhay, S., McIntyre-Wressnig, A., Giner, J.-L., Edgcomb, V.P., Beaudoin, D.J., Bernhard, J.M., Summons, R.E., 2013. Identification of 24-n-propylidenecholesterol in a member of the Foraminifera. *Organic geochemistry* 63, 145-151.
- Grazhdankin, D., 2003. Structure and depositional environment of the Vendian Complex in the southeastern White Sea area. *Stratigraphy and Geological Correlation* 11, 313-331.
- Grazhdankin, D., 2004. Patterns of distribution in the Ediacaran biotas: facies versus biogeography and evolution. *Paleobiology* 30, 203-221.
- Grazhdankin, D., 2011. Ediacaran Biota, in: Reitner, J., Thiel, V. (Eds.), *Encyclopedia of Geobiology*. Springer Netherlands, Dordrecht, pp. 342-348.
- Grazhdankin, D., 2014. Patterns of Evolution of the Ediacaran Soft-Bodied Biota. *Journal of Paleontology* 88, 269-283.
- Grazhdankin, D., Gerdes, G., 2007. Ediacaran microbial colonies. *Lethaia* 40, 201-210.

- Grazhdankin, D., Nagovitsin, K., Maslov, A., 2007. Late Vendian Miaohe-type ecological assemblage of the east European platform, *Doklady Earth Sciences*. Springer, pp. 1183-1187.
- Gueneli, N., McKenna, A., Ohkouchi, N., Boreham, C., Beghin, J., Javaux, E., Brocks, J., 2018. 1.1-billion-year-old porphyrins establish a marine ecosystem dominated by bacterial primary producers. *Proceedings of the National Academy of Sciences* 115, E6978-E6986.
- Hammer, Ø., Harper, D.A., Ryan, P.D., 2001. PAST: paleontological statistics software package for education and data analysis. *Palaeontologia electronica* 4, 9.
- Hedges, J.I., Keil, R.G., 1995. Sedimentary organic matter preservation: an assessment and speculative synthesis. *Marine chemistry* 49, 81-115.
- Hoefs, M.J., Rijpstra, W.I.C., Damsté, J.S.S., 2002. The influence of oxic degradation on the sedimentary biomarker record I: Evidence from Madeira Abyssal Plain turbidites. *Geochimica et Cosmochimica Acta* 66, 2719-2735.
- Hoekzema, R.S., Brasier, M.D., Dunn, F.S., Liu, A.G., 2017. Quantitative study of developmental biology confirms Dickinsonia as a metazoan. *Proceedings of the Royal Society B: Biological Sciences* 284, 20171348.
- Hoshino, Y., Poshibaeva, A., Meredith, W., Snape, C., Poshibaev, V., Versteegh, G.J., Kuznetsov, N., Leider, A., van Maldegem, L., Neumann, M., 2017. Cryogenian evolution of stigmasteroid biosynthesis. *Science advances* 3, e1700887.
- Hoyal Cuthill, J.F., Han, J., 2018. Cambrian petalonamid Stromatoveris phylogenetically links Ediacaran biota to later animals. *Palaeontology* 61, 813-823.
- Hua, H., Pratt, B.R., Zhang, L.-Y., 2003. Borings in Cloudina shells: complex predator-prey dynamics in the terminal Neoproterozoic. *Palaios* 18, 454-459.
- Ingall, E.D., Cappellen, P.V., 1990. Relation between sedimentation rate and burial of organic phosphorus and organic carbon in marine sediments. *Geochimica et Cosmochimica Acta* 54, 373-386.
- Innes, H.E., Bishop, A.N., Fox, P.A., Head, I.M., Farrimond, P., 1998. Early diagenesis of bacteriohopanoids in Recent sediments of Lake Pollen, Norway. *Organic Geochemistry* 29, 1285-1295.
- Ivantsov, A.Y., 2010. Paleontological evidence for the supposed precambrian occurrence of mollusks. *Paleontological Journal* 44, 1552-1559.
- Ivantsov, A.Y., 2011a. Feeding traces of proarticulata—the Vendian metazoa. *Paleontological Journal* 45, 237-248.
- Ivantsov, A.Y., 2011b. Unique natural world heritage - Zimnie Gory locality of the impressions of the Vendian multicellular animals. *Geolog Ukrainy*, 89-98.
- Ivantsov, A.Y., 2013. Trace fossils of precambrian metazoans “Vendobionta” and “Mollusks”. *Stratigraphy and Geological Correlation* 21, 252-264.
- Ivantsov, A.Y., 2016. Reconstruction of Charniodiscus yorgensis (Macrobionta from the Vendian of the White Sea). *Paleontological Journal* 50, 1-12.
- Ivantsov, A.Y., Gritsenko, V.P., Konstantinenko, L.I., Zakrevskaya, M.A., 2014. Revision of the problematic Vendian macrofossil Beltanelliformis (=Beltanelloides, Nemiana). *Paleontological Journal* 48, 1415-1440.
- Janaway, R.C., Percival, S.L., Wilson, A.S., 2009. Decomposition of Human Remains, in: Percival, S.L. (Ed.), *Microbiology and Aging: Clinical Manifestations*. Humana Press, Totowa, NJ, pp. 313-334.

- Jarrett, A.J.M., Schinteie, R., Hope, J.M., Brocks, J.J., 2013. Micro-ablation, a new technique to remove drilling fluids and other contaminants from fragmented and fissile rock material. *Organic Geochemistry* 61, 57-65.
- Jenkins, R., 1996. Aspects of the geological setting and palaeobiology of the Ediacara assemblage. *Natural history of the flinders ranges* 7, 33-45.
- Jenkins, R.J., 1995. The problems and potential of using animal fossils and trace fossils in terminal Proterozoic biostratigraphy. *Precambrian Research* 73, 51-69.
- Jenner, R.A., 2004. When molecules and morphology clash: reconciling conflicting phylogenies of the Metazoa by considering secondary character loss. *Evolution & Development* 6, 372-378.
- Jeong, S.W., Locat, J., Leroueil, S., Malet, J.-P., 2010. Rheological properties of fine-grained sediment: the roles of texture and mineralogy. *Canadian Geotechnical Journal* 47, 1085-1100.
- Jones, J.G., 1969. Studies on Lipids of Soil Micro-organisms with Particular Reference to Hydrocarbons. *Microbiology* 59, 145-152.
- Jumars, P.A., Dorgan, K.M., Lindsay, S.M., 2015. Diet of Worms Emended: An Update of Polychaete Feeding Guilds. *Annual Review of Marine Science* 7, 497-520.
- Kanazawa, A., 2001. Sterols in marine invertebrates. *Fisheries Science* 67, 997-1007.
- Kaufman, A.J., 2018. The Ediacaran-Cambrian Transition: A Resource-Based Hypothesis for the Rise and Fall of the Ediacara Biota, in: Sial, A.N., Gaucher, C., Ramkumar, M., Ferreira, V.P. (Eds.), *Chemostratigraphy Across Major Chronological Boundaries*, pp. 115-142.
- Kennington, C.G., Wilby, P.R., 2017. Of Time and Taphonomy: Preservation in the Ediacaran, in: Laflamme, M., Darroch, S.A.F., Schiffbauer, J.D. (Eds.), *Reading and Writing of the Fossil Record: Preservational Pathways to Exceptional Fossilization*, 07/21 ed. Cambridge University Press, Cambridge, pp. 101-122.
- Kerr, R.G., Baker, B.J., 1991. Marine sterols. *Natural Product Reports* 8, 465-497.
- Kicklighter, C.E., Hay, M.E., 2007. To avoid or deter: interactions among defensive and escape strategies in sabellid worms. *Oecologia* 151, 161-173.
- Kissin, Y.V., 1987. Catagenesis and composition of petroleum: Origin of n-alkanes and isoalkanes in petroleum crudes. *Geochimica et Cosmochimica Acta* 51, 2445-2457.
- Knoll, A.H., 1992. Biological and Biogeochemical Preludes to the Ediacaran Radiation, in: Lipps, J.H., Signor, P.W. (Eds.), *Origin and Early Evolution of the Metazoa*. Springer US, Boston, MA, pp. 53-84.
- Knoll, A.H., Summons, R.E., Waldbauer, J.R., Zumberge, J.E., 2007a. The Geological Succession of Primary Producers in the Oceans. 133-163.
- Knoll, A.H., Summons, R.E., Waldbauer, J.R., Zumberge, J.E., 2007b. The geological succession of primary producers in the oceans, in: Falkowski, P., Knoll, A.H. (Eds.), *Evolution of Primary Producers in the Sea*. Academic Press, Boston, pp. 133-163.
- Kodner, R.B., Pearson, A., Summons, R.E., Knoll, A.H., 2008a. Sterols in red and green algae: quantification, phylogeny, and relevance for the interpretation of geologic steranes. *Geobiology* 6, 411-420.
- Kodner, R.B., Summons, R.E., Pearson, A., King, N., Knoll, A.H., 2008b. Sterols in a unicellular relative of the metazoans. *Proc Natl Acad Sci U S A* 105, 9897-9902.
- Kolesnikov, A.V., Rogov, V.I., Bykova, N.V., Danelian, T., Clausen, S., Maslov, A.V., Grazhdankin, D.V., 2018. The oldest skeletal macroscopic organism *Palaeopascichnus linearis*. *Precambrian Research* 316, 24-37.

- Krom, M.D., Berner, R.A., 1981. The diagenesis of phosphorus in a nearshore marine sediment. *Geochimica et Cosmochimica Acta* 45, 207-216.
- Lenton, T.M., Daines, S.J., 2018. The effects of marine eukaryote evolution on phosphorus, carbon and oxygen cycling across the Proterozoic–Phanerozoic transition. *Emerging Topics in Life Sciences*, ETL20170156.
- Leonov, M.V., 2007a. Comparative taphonomy of Vendian genera *Beltanelloides* and *Nemiana*: taxonomy and lifestyle. Geological Society, London, Special Publications 286, 259-267.
- Leonov, M.V., 2007b. Macroscopic plant remains from the base of the Ust'-Pinega formation (Upper Vendian of the Arkhangelsk Region). *Paleontological Journal* 41, 683-691.
- Littlewood, D.T.J., 2017. Animal Evolution: Last Word on Sponges-First? *Current Biology* 27, R259-R261.
- Liu, A.G., 2016. Framboidal Pyrite Shroud Confirms the 'Death Mask' Model for Moldic Preservation of Ediacaran Soft-Bodied Organisms. *Palaios* 31, 259-274.
- Liu, A.G., McIlroy, D., Antcliffe, J.B., Brasier, M.D., 2011. Effaced preservation in the Ediacara biota and its implications for the early microfossil record. *Palaeontology* 54, 607-630.
- Liu, A.G., McMahon, S., Matthews, J.J., Still, J.W., Brasier, A.T., in press. Petrological evidence supports the death mask model for the preservation of Ediacaran soft-bodied organisms in South Australia. *Geology*.
- Love, G.D., Grosjean, E., Stalvies, C., Fike, D.A., Grotzinger, J.P., Bradley, A.S., Kelly, A.E., Bhatia, M., Meredith, W., Snape, C.E., Bowring, S.A., Condon, D.J., Summons, R.E., 2009. Fossil steroids record the appearance of Demospongiae during the Cryogenian period. *Nature* 457, 718-721.
- Lyons, T.W., Reinhard, C.T., Planavsky, N.J., 2014. The rise of oxygen in Earth's early ocean and atmosphere. *Nature* 506, 307-315.
- MacNaughton, R.B., Narbonne, G.M., 1999. Evolution and ecology of Neoproterozoic-Lower Cambrian trace fossils, NW Canada. *Palaios*, 97-115.
- Mallory, F.B., Gordon, J.T., Conner, R.L., 1963. The isolation of a pentacyclic triterpenoid alcohol from a protozoan. *Journal of the American Chemical Society* 85, 1362-1363.
- Martin, M.W., Grazhdankin, D.V., Bowring, S.A., Evans, D.A.D., Fedonkin, M., Kirschvink, J., 2000. Age of Neoproterozoic bilaterian body and trace fossils, White Sea, Russia: Implications for metazoan evolution. *Science* 288, 841-845.
- Matsumoto, G.I., Yamada, S., Ohtani, S., Broady, P.A., NAGASHIMA, H., 1996. BIOGEOCHEMICAL FEATURES OF HYDROCARBONS IN CULTURED CYANOBACTERIA AND GREEN ALGAE FROM ANTARCTICA (17th Symposium on Polar Biology), Proceedings of the NIPR Symposium on Polar Biology, pp. 275-282.
- Matz, M.V., Frank, T.M., Marshall, N.J., Widder, E.A., Johnsen, S., 2008. Giant Deep-Sea Protist Produces Bilaterian-like Traces. *Current Biology* 18, 1849-1854.
- McCaffrey, M.A., Moldowan, J.M., Lipton, P.A., Summons, R.E., Peters, K.E., Jeganathan, A., Watt, D.S., 1994. Paleoenvironmental implications of novel C 30 steranes in Precambrian to Cenozoic age petroleum and bitumen. *Geochimica et Cosmochimica Acta* 58, 529-532.
- McMenamin, M.A., 1986. The Garden of Ediacara. *Palaios*, 178-182.
- Mcmenamin, M.A., 2003. Origin and Early Evolution of Predators, Predator—Prey Interactions in the Fossil Record. Springer, pp. 379-400.
- Milkova, T.S., Popov, S.S., Marekov, N.L., Andreev, S.N., 1980. Sterols from black sea invertebrates—I. Sterols from Scyphozoa and Anthozoa (Coelenterata). *Comparative Biochemistry and Physiology Part B: Comparative Biochemistry* 67, 633-638.

- Mills, D.B., Canfield, D.E., 2014. Oxygen and animal evolution: Did a rise of atmospheric oxygen “trigger” the origin of animals? *BioEssays* 36, 1145-1155.
- Mills, D.B., Ward, L.M., Jones, C., Sweeten, B., Forth, M., Treusch, A.H., Canfield, D.E., 2014. Oxygen requirements of the earliest animals. *Proceedings of the National Academy of Sciences* 111, 4168-4172.
- Mitchell, E.G., Kenchington, C.G., 2018. The utility of height for the Ediacaran organisms of Mistaken Point. *Nature Ecology and Evolution* (2018). DOI: 10.1038/s41559-018-0591 6.
- Moczyłowska, M., Westall, F., Foucher, F., 2014. Microstructure and biogeochemistry of the organically preserved Ediacaran metazoan Sabellidites. *Journal of Paleontology* 88, 224-239.
- Moldowan, J.M., Seifert, W.K., Gallegos, E.J., 1985. Relationship between petroleum composition and depositional environment of petroleum source rocks. *AAPG bulletin* 69, 1255-1268.
- Moldowan, J.M., Sundararaman, P., Schoell, M., 1986. Sensitivity of biomarker properties to depositional environment and/or source input in the Lower Toarcian of SW-Germany. *Organic Geochemistry* 10, 915-926.
- Müller, P., 1977. CN ratios in Pacific deep-sea sediments: Effect of inorganic ammonium and organic nitrogen compounds sorbed by clays. *Geochimica et Cosmochimica Acta* 41, 765-776.
- Nagovitsyn, A., 2015a. New ichnofossils of a Cambrian look from the Vendian of Arkhangelsk Region, in: Alekseev, A.S. (Ed.), *PALEOSTRAT-2015*. PIN RAS, Moscow, pp. 57-58.
- Nagovitsyn, A., 2015b. New ichnofossils of the Cambrian guise from the Vendian of the Arkhangelsk Region, in: Alekseev, A.S. (Ed.), *PALEOSTRAT-2015*. PIN RAS, Moscow.
- Najle, S.R., Molina, M.C., Ruiz-Trillo, I., Uttaro, A.D., 2016. Sterol metabolism in the filasterean *Capsaspora owczarzaki* has features that resemble both fungi and animals. *Open Biology* 6.
- Narbonne, G.M., 2004. Modular Construction of Early Ediacaran Complex Life Forms. *Science* 305, 1141-1144.
- Narbonne, G.M., 2005. The Ediacara Biota: Neoproterozoic Origin of Animals and Their Ecosystems. *Annual Review of Earth and Planetary Sciences* 33, 421-442.
- Narbonne, G.M., Hofmann, H.J., 1987. Ediacaran biota of the Wernecke Mountains, Yukon, Canada. *Palaeontology* 30, 647-676.
- Nettersheim, B.J., Brocks, J.J., Schwelm, A., Hope, J.M., Not, F., Lomas, M., Schmidt, C., Schiebel, R., Nowack, E.C.M., De Deckker, P., Pawlowski, J., Bowser, S.S., Bobrovskiy, I., Zonneveld, K., Kucera, M., Stuhr, M., Hallmann, C., in press. Putative sponge biomarkers in unicellular Rhizaria question an early rise of animals. *Nature Ecology & Evolution*.
- Nishimura, M., Koyama, T., 1977. The occurrence of stanols in various living organisms and the behavior of sterols in contemporary sediments. *Geochimica et cosmochimica acta* 41, 379-385.
- Noble, R.A., Alexander, R., Kagi, R.I., Nox, J.K., 1986. Identification of some diterpenoid hydrocarbons in petroleum. *Organic Geochemistry* 10, 825-829.
- Noffke, N., 2009. The criteria for the biogenicity of microbially induced sedimentary structures (MISS) in Archean and younger, sandy deposits. *Earth-Science Reviews* 96, 173-180.
- Nursall, J., 1959. Oxygen as a prerequisite to the origin of the Metazoa. *Nature* 183, 1170.
- Olson, S.L., Kump, L.R., Kasting, J.F., 2013. Quantifying the areal extent and dissolved oxygen concentrations of Archean oxygen oases. *Chemical Geology* 362, 35-43.

- Orr, P.J., Briggs, D.E.G., Kearns, S.L., 1998. Cambrian Burgess Shale Animals Replicated in Clay Minerals. *Science* 281, 1173-1175.
- Ourisson, G., 1994. Biomarkers in the Proterozoic record, in: Bengtson, S. (Ed.), *Early life on earth. Nobel Symposium Vol. 84.* Columbia University Press, New York, pp. 259-269.
- Panagiotopoulos, I., Voulgaris, G., Collins, M.B., 1997. The influence of clay on the threshold of movement of fine sandy beds. *Coastal Engineering* 32, 19-43.
- Parry, L.A., Smithwick, F., Nordén, K.K., Saitta, E.T., Lozano-Fernandez, J., Tanner, A.R., Caron, J.-B., Edgecombe, G.D., Briggs, D.E.G., Vinther, J., 2018. Soft-Bodied Fossils Are Not Simply Rotten Carcasses – Toward a Holistic Understanding of Exceptional Fossil Preservation. *BioEssays* 40, 1700167.
- Peakman, T.M., De Leeuw, J.W., Rijpstra, W.I.C., 1992. Identification and origin of $\Delta 8(14)5\alpha$ - and $\Delta 14 5\alpha$ -sterenes and related hydrocarbons in an immature bitumen from the Monterey Formation, California. *Geochimica et Cosmochimica Acta* 56, 1223-1230.
- Peakman, T.M., Haven, H.L.T., Rechka, J.R., De Leeuw, J.W., Maxwell, J.R., 1989. Occurrence of (20R)- and (20S)- $\Delta 8(14)$ and $\Delta 14 5\alpha(H)$ -sterenes and the origin of $5\alpha(H)$, $14\beta(H)$, $17\beta(H)$ -steranes in an immature sediment. *Geochimica et Cosmochimica Acta* 53, 2001-2009.
- Pehr, K., Love, G.D., Kuznetsov, A., Podkovyrov, V., Junium, C.K., Shumlyanskyy, L., Sokur, T., Bekker, A., 2018. Ediacara biota flourished in oligotrophic and bacterially dominated marine environments across Baltica. *Nature communications* 9, 1807.
- Peters, K., Walters, C., Moldowan, J., 2005a. *The Biomarker Guide. Volume 2. Biomarkers and Isotopes in Petroleum Systems and Earth History*, 2nd ed. Cambridge University Press, New York.
- Peters, K.E., Walters, C.C., Moldowan, J.M., 2005b. *The biomarker guide.* Cambridge University Press.
- Peterson, K.J., Waggoner, B., Hagadorn, J.W., 2003. A Fungal Analog for Newfoundland Ediacaran Fossils? *Integrative and Comparative Biology* 43, 127-136.
- Phleger, C.F., Nichols, P.D., Virtue, P., 1998. Lipids and trophodynamics of Antarctic zooplankton. *Comparative Biochemistry and Physiology Part B: Biochemistry and Molecular Biology* 120, 311-323.
- Presnell, Jason S., Vandepas, Lauren E., Warren, Kaitlyn J., Swalla, Billie J., Amemiya, Chris T., Browne, William E., 2016. The Presence of a Functionally Tripartite Through-Gut in Ctenophora Has Implications for Metazoan Character Trait Evolution. *Current Biology* 26, 2814-2820.
- Ragozina, A.L., 2001. Fruticose Algae of the Genus *Eoholynia* and Tubular Calyptrina in the Upper Vendian of Arkhangelsk Region, in *Proceedings of the 2nd International Symposium "Evolution of Life on Earth"*. Izd. Nauchno-Tekh. Lit-ry, Tomsk, pp. 133-137.
- Reinhard, C.T., Planavsky, N.J., Olson, S.L., Lyons, T.W., Erwin, D.H., 2016. Earth's oxygen cycle and the evolution of animal life. *Proceedings of the National Academy of Sciences* 113, 8933-8938.
- Retallack, G.J., 1994. Were the Ediacaran fossils lichens? *Paleobiology* 20, 523-544.
- Retallack, G.J., 2013. Ediacaran life on land. *Nature* 493, 89-92.
- Retallack, G.J., 2016. Ediacaran fossils in thin-section. *Alcheringa: An Australasian Journal of Palaeontology* 40, 583-600.
- Retallack, G.J., 2019. Interflag sandstone laminae, a novel sedimentary structure, with implications for Ediacaran paleoenvironments. *Sedimentary Geology* 379, 60-76.

- Ricci, J.N., Coleman, M.L., Welander, P.V., Sessions, A.L., Summons, R.E., Spear, J.R., Newman, D.K., 2014. Diverse capacity for 2-methylhopanoid production correlates with a specific ecological niche. *ISME J* 8, 675-684.
- Ricci, J.N., Morton, R., Kulkarni, G., Summers, M.L., Newman, D.K., 2016. Hopanoids play a role in stress tolerance and nutrient storage in the cyanobacterium *Nostoc punctiforme*. *Geobiology*, n/a-n/a.
- Ries-Kautt, M., Albrecht, P., 1989. Hopane-derived triterpenoids in soils. *Chemical Geology* 76, 143-151.
- Roeselers, G., Newton, I.L.G., 2012. On the evolutionary ecology of symbioses between chemosynthetic bacteria and bivalves. *Applied Microbiology and Biotechnology* 94, 1-10.
- Rohmer, M., Bouvier-Nave, P., Ourisson, G., 1984. Distribution of Hopanoid Triterpenes in Prokaryotes. *Microbiology* 130, 1137-1150.
- Runnegar, B., Fedonkin, M., 1992. Proterozoic metazoan body fossils, in: Schopf, J.W., Klein, C. (Eds.), *The Proterozoic biosphere: a multidisciplinary study*. Cambridge University Press, New York, pp. 369-388.
- Safe, S., Safe, L.M., Maass, W.S.G., 1975. Sterols of three lichen species: *Lobaria pulmonaria*, *Lobaria Scrobiculata* and *Usnea Longissima*. *Phytochemistry* 14, 1821-1823.
- Schinteie, R., Brocks, J.J., 2014. Evidence for ancient halophiles? Testing biomarker syngeneity of evaporites from Neoproterozoic and Cambrian strata. *Organic Geochemistry* 72, 46-58.
- Schouten, S., Klein Breteler, W.C.M., Blokker, P., Schogt, N., Rijpstra, W.I.C., Grice, K., Baas, M., Sinninghe Damsté, J.S., 1998. Biosynthetic effects on the stable carbon isotopic compositions of algal lipids: implications for deciphering the carbon isotopic biomarker record. *Geochimica et Cosmochimica Acta* 62, 1397-1406.
- Seidel, S.B., Proudfoot, J.R., Djerassi, C., Sica, D., Sodano, G., 1986. Minor and trace sterols from marine invertebrates 56. Novel coprostanols from the marine sponge *Petrosia ficiformis*. *Steroids* 47, 49-62.
- Seilacher, A., 1989. Vendozoa: Organismic construction in the Proterozoic biosphere. *Lethaia* 22, 229-239.
- Seilacher, A., 1992. Vendobionta and Psammocorallia: lost constructions of Precambrian evolution. *Journal of the Geological Society* 149, 607-613.
- Seilacher, A., 1999. Biomat-related lifestyles in the Precambrian. *Palaaios* 14, 86-93.
- Seilacher, A., 2007a. The nature of vendobionts. Geological Society, London, Special Publications 286, 387-397.
- Seilacher, A., 2007b. Trace fossil analysis. Springer Berlin Heidelberg, Berlin.
- Seilacher, A., Buatois, L.A., Gabriela Mángano, M., 2005. Trace fossils in the Ediacaran–Cambrian transition: Behavioral diversification, ecological turnover and environmental shift. *Palaeogeography, Palaeoclimatology, Palaeoecology* 227, 323-356.
- Seilacher, A., Grazhdankin, D., Legouta, A., 2003. Ediacaran biota: The dawn of animal life in the shadow of giant protists. *Paleontological Research* 7, 43-54.
- Serezhnikova, E.A., 2011. Microbial Binding as a Probable Cause of Taphonomic Variability of Vendian Fossils: Carbonate Casting? 131, 525-535.
- Shaw, D.G., Wiggs, J.N., 1979. Hydrocarbons in alaskan marine intertidal algae. *Phytochemistry* 18, 2025-2027.
- Simion, P., Philippe, H., Baurain, D., Jager, M., Richter, D.J., Di Franco, A., Roure, B., Satoh, N., Queinnee, E., Ereskovsky, A., 2017a. A large and consistent phylogenomic dataset supports sponges as the sister group to all other animals. *Current Biology* 27, 958-967.

- Simion, P., Philippe, H., Baurain, D., Jager, M., Richter, D.J., Di Franco, A., Roure, B., Satoh, N., Quéinnec, É., Ereskovsky, A., Lapébie, P., Corre, E., Delsuc, F., King, N., Wörheide, G., Manuel, M., 2017b. A Large and Consistent Phylogenomic Dataset Supports Sponges as the Sister Group to All Other Animals. *Current Biology* 27, 958-967.
- Sliaupa, S., Fokin, P., Lazauskiene, J., Stephenson, R.A., 2006. The Vendian-Early Palaeozoic sedimentary basins of the East European Craton. Geological Society, London, *Memoirs* 32, 449-462.
- Sokolov, B., 1967. The oldest Pogonophora. *Doklady Akademii Nauk SSSR* 177, 201-204.
- Sokolov, B., 1968. Vendian and Early Cambrian sabelliditida (Pogonophora) of the USSR, Proceedings of the IPU, International Geological Congress, pp. 79-86.
- Sokolov, B., 1997. Essays on the Advent of the Vendian System. KMK Scientific, Moscow.
- Sokolov, B.S., 1965. Ancient deposits of the Early Cambrian and sabelliditids, in: Sokolov, B.S. (Ed.), Proceedings of All-Union Symposium on Precambrian and Cambrian Paleontology, Institute of Geology and Geophysics, Siberian Branch, USSR Academy of Sciences, Novosibirsk, USSR, pp. pp. 78–91.
- Sperling, E.A., Frieder, C.A., Raman, A.V., Girguis, P.R., Levin, L.A., Knoll, A.H., 2013. Oxygen, ecology, and the Cambrian radiation of animals. *Proceedings of the National Academy of Sciences* 110, 13446-13451.
- Sperling, E.A., Stockey, R.G., 2018. The Temporal and Environmental Context of Early Animal Evolution: Considering All the Ingredients of an “Explosion”. *Integrative and Comparative Biology* 58, 605-622.
- Sperling, E.A., Vinther, J., 2010. A placozoan affinity for Dickinsonia and the evolution of late Proterozoic metazoan feeding modes. *Evolution & Development* 12, 201-209.
- Sprigg, R.C., 1947. Early Cambrian (?) jellyfishes from the Flinders Ranges, South Australia. *Transactions of the Royal Society of South Australia* 71, 212-224.
- Steiner, M., 1996. *Chuar*ia Circularis WALCOTT 1899 - "Megasphaeromorph Acritarch" or Prokaryotic Colony? *Acta Universitatis Carolinae Geologica* 40, 645-665.
- Steiner, M., Reitner, J., 2001. Evidence of organic structures in Ediacara-type fossils and associated microbial mats. *Geology* 29, 1119-1122.
- Summons, R.E., Jahnke, L.L., Hope, J.M., Logan, G.A., 1999. 2-Methylhopanoids as biomarkers for cyanobacterial oxygenic photosynthesis. *Nature* 400, 554-557.
- Summons, R.E., Jahnke, L.L., Roksandic, Z., 1994. Carbon isotopic fractionation in lipids from methanotrophic bacteria: relevance for interpretation of the geochemical record of biomarkers. *Geochimica et Cosmochimica Acta* 58, 2853-2863.
- Sun, M.-Y., Wakeham, S., 1998. A study of oxic/anoxic effects on degradation of sterols at the simulated sediment–water interface of coastal sediments. *Organic geochemistry* 28, 773-784.
- Sun, X., Zhang, T., Sun, Y., Milliken, K.L., Sun, D., 2016. Geochemical evidence of organic matter source input and depositional environments in the lower and upper Eagle Ford Formation, south Texas. *Organic Geochemistry* 98, 66-81.
- Takishita, K., Chikaraishi, Y., Tanifuji, G., Ohkouchi, N., Hashimoto, T., Fujikura, K., Roger, A.J., 2017. Microbial eukaryotes that lack sterols. *Journal of Eukaryotic Microbiology* 64, 897-900.
- Talbot, H.M., Summons, R.E., Jahnke, L.L., Cockell, C.S., Rohmer, M., Farrimond, P., 2008. Cyanobacterial bacteriohopanepolyol signatures from cultures and natural environmental settings. *Organic Geochemistry* 39, 232-263.

- Tarhan, L.G., Droser, M.L., Gehling, J.G., Dzaugis, M.P., 2015. Taphonomy and morphology of the Ediacara form genus *Aspidella*. *Precambrian Research* 257, 124-136.
- Tarhan, L.G., Hood, A.v.S., Droser, M.L., Gehling, J.G., Briggs, D.E.G., 2016. Exceptional preservation of soft-bodied Ediacara Biota promoted by silica-rich oceans. *Geology* 44, 951-954.
- Taylor, M.W., Radax, R., Steger, D., Wagner, M., 2007. Sponge-Associated Microorganisms: Evolution, Ecology, and Biotechnological Potential. *Microbiology and Molecular Biology Reviews* 71, 295-347.
- Telford, Maximilian J., Budd, Graham E., Philippe, H., 2015. Phylogenomic Insights into Animal Evolution. *Current Biology* 25, R876-R887.
- Ten Haven, H., De Leeuw, J., Peakman, T., Maxwell, J., 1986. Anomalies in steroid and hopanoid maturity indices. *Geochimica et Cosmochimica Acta* 50, 853-855.
- Ten Haven, H., Rohmer, M., Rullkötter, J., Bisserset, P., 1989. Tetrahymanol, the most likely precursor of gammacerane, occurs ubiquitously in marine sediments. *Geochimica et Cosmochimica Acta* 53, 3073-3079.
- Tribovillard, N., Algeo, T.J., Lyons, T., Riboulleau, A., 2006. Trace metals as paleoredox and paleoproductivity proxies: An update. *Chemical Geology* 232, 12-32.
- Urbanek, A., Mierzejewska, G., 1977. The Fine Structure of Zooidal tubes in Sabellidita and Pogonophora with reference to their affinity. *Acta Palaeontologica Polonica* 22, 223-240.
- van Maldegem, L.M., Sansjofre, P., Weijers, J.W.H., Wolkenstein, K., Strother, P.K., Wörmer, L., Hefter, J., Nettersheim, B.J., Hoshino, Y., Schouten, S., Sinninghe Damsté, J.S., Nath, N., Griesinger, C., Kuznetsov, N.B., Elie, M., Elvert, M., Tegelaar, E., Gleixner, G., Hallmann, C., 2019. Bisnorgammacerane traces predatory pressure and the persistent rise of algal ecosystems after Snowball Earth. *Nature Communications* 10, 476.
- Vannier, J., 2012. Gut Contents as Direct Indicators for Trophic Relationships in the Cambrian Marine Ecosystem. *PLOS ONE* 7, e52200.
- Verruijt, A., 2018. An Introduction to Soil Mechanics. VSSD, Delft.
- Versteegh, G.J.M., Blokker, P., 2004. Resistant macromolecules of extant and fossil microalgae. *Phycological Research* 52, 325-339.
- Volkman, J.K., 2005. Sterols and other triterpenoids: source specificity and evolution of biosynthetic pathways. *Organic Geochemistry* 36, 139-159.
- Volkman, J.K., Barrett, S.M., Blackburn, S.I., Mansour, M.P., Sikes, E.L., Gelin, F., 1998. Microalgal biomarkers: A review of recent research developments. *Organic Geochemistry* 29, 1163-1179.
- Vrijenhoek, R.C., 2013. On the instability and evolutionary age of deep-sea chemosynthetic communities. *Deep Sea Research Part II: Topical Studies in Oceanography* 92, 189-200.
- Wade, M., 1968. Preservation of Soft-Bodied Animals in Precambrian Sandstones at Ediacara, South Australia. *Lethaia* 1, 238-267.
- Waggoner, B., 2003. The Ediacaran Biotas in Space and Time. *Integrative and Comparative Biology* 43, 104-113.
- Weete, J.D., Abril, M., Blackwell, M., 2010. Phylogenetic distribution of fungal sterols. *PLoS One* 5, e10899.
- Welander, P.V., Coleman, M.L., Sessions, A.L., Summons, R.E., Newman, D.K., 2010. Identification of a methylase required for 2-methylhopanoid production and implications for the interpretation of sedimentary hopanes. *Proceedings of the National Academy of Sciences* 107, 8537-8542.

- Xiao, S., Dong, L., 2006. On the Morphological and Ecological History of Proterozoic Macroalgae, in: Xiao, S., Kaufman, A.J. (Eds.), *Neoproterozoic Geobiology and Paleobiology*. Springer Netherlands, Dordrecht, pp. 57-90.
- Xiao, S., Droser, M., Gehling, J.G., Hughes, I.V., Wan, B., Chen, Z., Yuan, X., 2013. Affirming life aquatic for the Ediacara biota in China and Australia. *Geology* 41, 1095-1098.
- Xiao, S., Knauth, L.P., 2013. Palaeontology: Fossils come in to land. *Nature* 493, 28-29.
- Xiao, S., Laflamme, M., 2009. On the eve of animal radiation: phylogeny, ecology and evolution of the Ediacara biota. *Trends Ecol Evol* 24, 31-40.
- Xiao, S., Yuan, X., Steiner, M., Knoll, A.H., 2002. Macroscopic carbonaceous compressions in a terminal Proterozoic shale: a systematic reassessment of the Miaohu biota, South China. *Journal of Paleontology* 76, 347-376.
- Zaika Novatsky, V., Palij, V., 1974. Most ancient fossil organisms in the deposits of Vendian complex of the Dniester Region. *Paleontol. Sb.* 11, 59-65.
- Zhao, N., Berova, N., Nakanishi, K., Rohmer, M., Mougnot, P., Jürgens, U.J., 1996. Structures of two bacteriohopanoids with acyclic pentol side-chains from the cyanobacterium *Nostoc* PCC 6720. *Tetrahedron* 52, 2777-2788.
- Zhao, Y., Vinther, J., Parry, L.A., Wei, F., Green, E., Pisani, D., Hou, X., Edgecombe, G.D., Cong, P., 2019. Cambrian Sessile, Suspension Feeding Stem-Group Ctenophores and Evolution of the Comb Jelly Body Plan. *Current Biology* 29, 1112-1125.e1112.
- Zhuravlev, A.Y., 1993. Were Ediacaran Vendobionta multicellulars? *Neues Jahrbuch für Geologie und Paläontologie, Abhandlungen* 190, 299-314.
- Zollo, F., Finamore, E., Gargiulo, D., Riccio, R., Minale, L., 1986. Marine sterols. Coprostanols and 4 α -methyl sterols from mediterranean tunicates. *Comparative Biochemistry and Physiology Part B: Comparative Biochemistry* 85, 559-560.
- Zundel, M., Rohmer, M., 1985a. Hopanoids of the methylotrophic bacteria *Methylococcus capsulatus* and *Methylomonas* sp. as possible precursors of C29 and C30 hopanoid chemical fossils. *FEMS microbiology letters* 28, 61-64.
- Zundel, M., Rohmer, M., 1985b. Prokaryotic triterpenoids: 1. 3 β -Methylhopanoids from *Acetobacter* species and *Methylococcus capsulatus*. *European Journal of Biochemistry* 150, 23-27.